frontiers
RESEARCH TOPICS

STRUCTURE, FUNCTION, AND PLASTICITY OF HIPPOCAMPAL DENTATE GYRUS MICROCIRCUITS

Topic Editors
Peter Jonas and John Lisman

frontiers in
NEURAL CIRCUITS

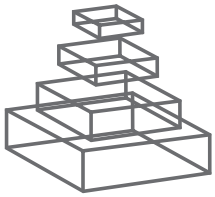

frontiers

ISSN 1664-8714
ISBN 978-2-88919-387-5
DOI 10.3389/978-2-88919-387-5

ABOUT FRONTIERS

Frontiers is more than just an open-access publisher of scholarly articles: it is a pioneering approach to the world of academia, radically improving the way scholarly research is managed. The grand vision of Frontiers is a world where all people have an equal opportunity to seek, share and generate knowledge. Frontiers provides immediate and permanent online open access to all its publications, but this alone is not enough to realize our grand goals.

FRONTIERS JOURNAL SERIES

The Frontiers Journal Series is a multi-tier and interdisciplinary set of open-access, online journals, promising a paradigm shift from the current review, selection and dissemination processes in academic publishing.
All Frontiers journals are driven by researchers for researchers; therefore, they constitute a service to the scholarly community. At the same time, the Frontiers Journal Series operates on a revolutionary invention, the tiered publishing system, initially addressing specific communities of scholars, and gradually climbing up to broader public understanding, thus serving the interests of the lay society, too.

DEDICATION TO QUALITY

Each Frontiers article is a landmark of the highest quality, thanks to genuinely collaborative interactions between authors and review editors, who include some of the world's best academicians. Research must be certified by peers before entering a stream of knowledge that may eventually reach the public - and shape society; therefore, Frontiers only applies the most rigorous and unbiased reviews.
Frontiers revolutionizes research publishing by freely delivering the most outstanding research, evaluated with no bias from both the academic and social point of view.
By applying the most advanced information technologies, Frontiers is catapulting scholarly publishing into a new generation.

WHAT ARE FRONTIERS RESEARCH TOPICS?

Frontiers Research Topics are very popular trademarks of the Frontiers Journals Series: they are collections of at least ten articles, all centered on a particular subject. With their unique mix of varied contributions from Original Research to Review Articles, Frontiers Research Topics unify the most influential researchers, the latest key findings and historical advances in a hot research area!
Find out more on how to host your own Frontiers Research Topic or contribute to one as an author by contacting the Frontiers Editorial Office: researchtopics@frontiersin.org

STRUCTURE, FUNCTION, AND PLASTICITY OF HIPPOCAMPAL DENTATE GYRUS MICROCIRCUITS

Topic Editors:
Peter Jonas, Institute of Science and Technology, Austria
John Lisman, Brandeis University, USA

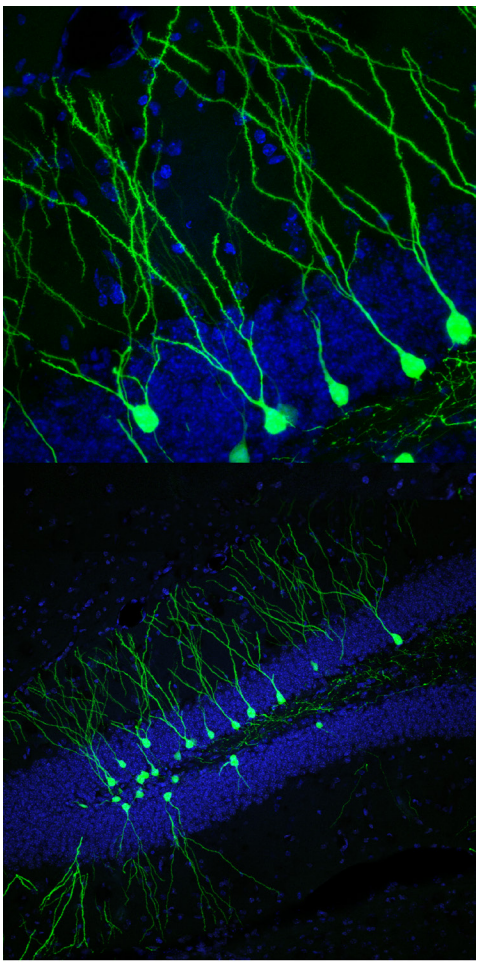

Images were taken as part of work performed at the National Institute on Aging / National Institutes of Health

The hippocampus mediates several higher brain functions, such as learning, memory, and spatial coding. The input region of the hippocampus, the dentate gyrus, plays a critical role in these processes. Several lines of evidence suggest that the dentate gyrus acts as a preprocessor of incoming information, preparing it for subsequent processing in CA3. For example, the dentate gyrus converts input from the entorhinal cortex, where cells have multiple spatial fields, into the spatially more specific place cell activity characteristic of the CA3 region. Furthermore, the dentate gyrus is involved in pattern separation, transforming relatively similar input patterns into substantially different output patterns. Finally, the dentate gyrus produces a very sparse coding scheme in which only a very small fraction of neurons are active at any one time.

How are these unique functions implemented at the level of cells and synapses? Dentate gyrus granule cells receive excitatory neuron input from the entorhinal cortex and send excitatory output to the hippocampal CA3 region via the mossy fibers. Furthermore, several types of GABAergic interneurons are present in this region, providing inhibitory control over granule cell activity via feedback and feedforward inhibition. Additionally, hilar mossy cells mediate an excitatory loop, receiving powerful input from a small number of granule cells and providing highly distributed excitatory output to a large number of granule cells. Finally, the dentate gyrus is one of the few brain regions exhibiting adult neurogenesis. Thus, new neurons are generated and functionally integrated throughout life. How these specific cellular and synaptic properties contribute to higher brain functions remains unclear.

One way to understand these properties of the dentate gyrus is to try to integrate experimental data into models, following the famous Hopfield quote: "Build it, and you understand it." However, when trying this, one faces two major challenges. First, hard quantitative data about cellular properties, structural connectivity, and functional properties of synapses are lacking. Second, the number of individual neurons and synapses to be represented in the model is huge. For example, the dentate gyrus contains ~1 million granule cells in rodents, and ~10 million in humans. Thus, full scale models will be complex and computationally demanding.

In this Frontiers Research Topic, we collect important information about cells, synapses, and microcircuit elements of the dentate gyrus. We have put together a combination of original research articles, review articles, and a methods article.

We hope that the collected information will be useful for both experimentalists and modelers. We also hope that the papers will be interesting beyond the small world of "dentology," i.e., for scientists working on other brain areas. Ideally, the dentate gyrus may serve as a blueprint, helping neuroscientists to define strategies to analyze network organization of other brain regions.

Table of Contents

frontiers in
NEURAL CIRCUITS

EDITORIAL
published: 10 September 2014
doi: 10.3389/fncir.2014.00107

Structure, function, and plasticity of hippocampal dentate gyrus microcircuits

***Peter Jonas*[1]* and *John Lisman*[2]**

[1] *IST Austria (Institute of Science and Technology Austria), Klosterneuburg, Austria*
[2] *Biology, Volen National Center for Complex Systems, Brandeis University, Waltham, MA, USA*
**Correspondence: peter.jonas@ist.ac.at*

Edited and reviewed by:
Dmitri B. Chklovskii, Howard Hughes Medical Institute, USA

Keywords: hippocampus, dentate gyrus, granule cells, mossy cells, mossy fibers, mossy fiber synapses, adult neurogenesis

The hippocampus mediates several higher brain functions, such as learning, memory, and spatial coding. The input region of the hippocampus, the dentate gyrus, plays a critical role in these processes. Several lines of evidence suggest that the dentate gyrus acts as a preprocessor of incoming information, preparing it for subsequent processing in CA3. For example, the dentate gyrus converts input from the entorhinal cortex, where cells have multiple spatial fields, into the spatially more specific place cell activity characteristic of the CA3 region. Furthermore, the dentate gyrus is involved in pattern separation, transforming relatively similar input patterns into substantially different output patterns. Finally, the dentate gyrus produces a very sparse coding scheme in which only a very small fraction of neurons are active at any one time.

How are these unique functions implemented at the level of cells and synapses? Dentate gyrus granule cells receive excitatory neuron input from the entorhinal cortex and send excitatory output to the hippocampal CA3 region via the mossy fibers. Furthermore, several types of GABAergic interneurons are present in this region, providing inhibitory control over granule cell activity via feedback and feedforward inhibition. Additionally, hilar mossy cells mediate an excitatory loop, receiving powerful input from a small number of granule cells and providing highly distributed excitatory output to a large number of granule cells. Finally, the dentate gyrus is one of the few brain regions exhibiting adult neurogenesis. Thus, new neurons are generated and functionally integrated throughout life. How these specific cellular and synaptic properties contribute to higher brain functions remains unclear.

One way to understand these properties of the dentate gyrus is to try to integrate experimental data into models, following the famous Hopfield quote: "Build it, and you understand it." However, when trying this, one faces two major challenges. First, hard quantitative data about cellular properties, structural connectivity, and functional properties of synapses are lacking. Second, the number of individual neurons and synapses to be represented in the model is huge. For example, the dentate gyrus contains ∼1 million granule cells in rodents, and ∼10 million in humans. Thus, full scale models will be complex and computationally demanding.

In this Frontiers Research Topic series of papers, we collect important information about cells, synapses, and microcircuit elements of the dentate gyrus. We have put together a combination of original research articles, review articles, and a Methods article. The collection includes contributions on:

- Connectomics and lamellar organization of the dentate gyrus (Sloviter and Lømo, 2012).
- Role of hilar mossy cells in dentate gyrus microcircuits (Jinde et al., 2013; Scharfman and Myers, 2013).
- Structural and functional properties of granule cell axons and mossy fiber output synapses (Zhao et al., 2012; Ruiz and Kullmann, 2013).
- Adult neurogenesis, with focus on integration of new granule cells into the dentate network (Lopez et al., 2012; Dieni et al., 2013; Vivar and van Praag, 2013).
- Analysis of coding mechanisms by full-scale computational models and theoretical approaches (Schneider et al., 2012; Stella et al., 2013).
- Plasticity of the dentate gyrus during injury (Perederiy and Westbrook, 2013).

We hope that the collected information will be useful for both experimentalists and modelers. We also hope that the papers will be interesting beyond the small world of "dentology," i.e., for scientists working on other brain areas. Ideally, the dentate gyrus may serve as a blueprint, helping neuroscientists to define strategies to analyze network organization of other brain regions.

REFERENCES

Dieni, C. V., Chancey, J. H., and Overstreet-Wadiche, L. S. (2013). Dynamic functions of GABA signaling during granule cell maturation. *Front. Neural Circuits* 6:113. doi: 10.3389/fncir.2012.00113

Jinde, S., Zsiros, V., and Nakazawa, K. (2013). Hilar mossy cell circuitry controlling dentate granule cell excitability. *Front. Neural Circuits* 7:14. doi: 10.3389/fncir.2013.00014

Lopez, C. M., Pelkey, K. A., Chittajallu, R., Nakashiba, T., Tóth, K., Tonegawa, S., et al. (2012). Competition from newborn granule cells does not drive axonal retraction of silenced old granule cells in the adult hippocampus. *Front. Neural Circuits* 6:85. doi: 10.3389/fncir.2012.00085

Perederiy, J. V., and Westbrook, G. L. (2013). Structural plasticity in the dentate gyrus- revisiting a classic injury model. *Front. Neural Circuits* 7:17. doi: 10.3389/fncir.2013.00017

Ruiz, A. J., and Kullmann, D. M. (2013). Ionotropic receptors at hippocampal mossy fibers: roles in axonal excitability, synaptic transmission, and plasticity. *Front. Neural Circuits* 6:112. doi: 10.3389/fncir.2012.00112

Scharfman, H. E., and Myers, C. E. (2013). Hilar mossy cells of the dentate gyrus: a historical perspective. *Front. Neural Circuits* 6:106. doi: 10.3389/fncir.2012.00106

Schneider, C. J., Bezaire, M., and Soltesz, I. (2012). Toward a full-scale computational model of the rat dentate gyrus. *Front. Neural Circuits* 6:83. doi: 10.3389/fncir.2012.00083

Sloviter, R. S., and Lømo, T. (2012). Updating the lamellar hypothesis of hippocampal organization. *Front. Neural Circuits* 6:102. doi: 10.3389/fncir.2012.00102

Stella, F., Cerasti, E., and Treves, A. (2013). Unveiling the metric structure of internal representations of space. *Front. Neural Circuits* 7:81. doi: 10.3389/fncir.2013.00081

Vivar, C., and van Praag, H. (2013). Functional circuits of new neurons in the dentate gyrus. *Front. Neural Circuits* 7:15. doi: 10.3389/fncir.2013.00015

Zhao, S., Studer, D., Chai, X., Graber, W., Brose, N., Nestel, S., et al. (2012). Structural plasticity of spines at giant mossy fiber synapses. *Front. Neural Circuits* 6:103. doi: 10.3389/fncir.2012.00103

Conflict of Interest Statement: The authors declare that the research was conducted in the absence of any commercial or financial relationships that could be construed as a potential conflict of interest.

Received: 15 July 2014; accepted: 18 August 2014; published online: 10 September 2014.
Citation: Jonas P and Lisman J (2014) Structure, function, and plasticity of hippocampal dentate gyrus microcircuits. Front. Neural Circuits ***8****:107. doi: 10.3389/fncir.2014.00107*
This article was submitted to the journal Frontiers in Neural Circuits.

frontiers in
NEURAL CIRCUITS

REVIEW ARTICLE
published: 10 December 2012
doi: 10.3389/fncir.2012.00102

Updating the lamellar hypothesis of hippocampal organization

Robert S. Sloviter*[1] *and* ***Terje Lømo*[2]**

[1] *Department of Neurobiology, Morehouse School of Medicine, Atlanta, GA, USA*
[2] *Department of Physiology, Institute of Basic Medical Sciences, University of Oslo, Oslo, Norway*

Edited by:
Peter Jonas, Institute of Science and Technology, Austria

Reviewed by:
Joachim H. Lübke, Research Centre Jülich GmbH, Germany
Richard Miles, Institut Pour le Cerveau et la Moëlle Epinière, France

***Correspondence:**
Robert S. Sloviter, Department of Neurobiology, Morehouse School of Medicine, 720 Westview Drive SW, Atlanta, GA 30310, USA.
e-mail: rssloviter@yahoo.com

Andersen et al. (1971) proposed that excitatory activity in the entorhinal cortex propagates topographically to the dentate gyrus, and on through a "trisynaptic circuit" lying within transverse hippocampal "slices" or "lamellae." In this way, a relatively simple structure might mediate complex functions in a manner analogous to the way independent piano keys can produce a nearly infinite variety of unique outputs. The lamellar hypothesis derives primary support from the "lamellar" distribution of dentate granule cell axons (the mossy fibers), which innervate dentate hilar neurons and area CA3 pyramidal cells and interneurons within the confines of a thin transverse hippocampal segment. Following the initial formulation of the lamellar hypothesis, anatomical studies revealed that unlike granule cells, hilar mossy cells, CA3 pyramidal cells, and Layer II entorhinal cells all form axonal projections that are more divergent along the longitudinal axis than the clearly "lamellar" mossy fiber pathway. The existence of pathways with "translamellar" distribution patterns has been interpreted, incorrectly in our view, as justifying outright rejection of the lamellar hypothesis (Amaral and Witter, 1989). We suggest that the functional implications of longitudinally projecting axons depend not on whether they exist, but on what they do. The observation that focal granule cell layer discharges normally inhibit, rather than excite, distant granule cells suggests that longitudinal axons in the dentate gyrus may mediate "lateral" inhibition and define lamellar function, rather than undermine it. In this review, we attempt a reconsideration of the evidence that most directly impacts the physiological concept of hippocampal lamellar organization.

Keywords: hippocampus, hippocampal formation, dentate gyrus, entorhinal cortex, lamellar organization, lateral inhibition, mossy cells, inhibitory interneurons

ORIGINS OF THE LAMELLAR HYPOTHESIS

The anatomical features of the mammalian hippocampal formation are well described, and the importance of the hippocampus to memory formation and spatial navigation is undisputed, but exactly how the three-dimensional structural organization of the hippocampal formation governs its behavior at the network level, and how a relatively simple structure differentiates and encodes so many distinct memories and locations remains incompletely understood (O'Keefe and Nadel, 1978; Treves and Rolls, 1992; McNaughton et al., 1996; Leutgeb et al., 2007; Morris, 2007; Rolls, 2010). The lamellar hypothesis of hippocampal function in its simplest original form posited that excitatory activity travels from the entorhinal cortex and through the hippocampus via a "trisynaptic circuit" lying within a series of parallel hippocampal "slices" or "lamellae" (Andersen et al., 1969, 1971). In this way, it was envisaged that temporal lobe interactions between the entorhinal cortex and the hippocampus were organized topographically, and that "lamellae" might operate independently, permitting a relatively simple structure to mediate complex behaviors.

The lamellar hypothesis as originally conceived (Andersen et al., 1969) was greatly influenced by the still unpublished anatomical findings of Blackstad and his colleagues in Århus, Denmark, who had made two observations based on the distribution of degenerating fibers after focal injury in the dentate gyrus or entorhinal cortex. First, Blackstad et al. (1970) reported that after small lesions of the dentate gyrus, degenerating mossy fibers exhibited a "lamellar" pattern in the transverse plane, and they also noted that "very narrow bands were seen in a few animals with particularly small lesions." Second, Andersen and colleagues cited as a personal communication from Jeune the subsequently published finding that, "each specific level of the entorhinal area distributes fibers to a restricted segment of the hippocampus" (Hjorth-Simonsen and Jeune, 1972). On the basis of these anatomical features, and the electrophysiological responses to afferent stimulation (Lømo, 1971), Andersen and colleagues suggested that entorhinal neurons topographically excite a thin strip of granule cells, which then topographically excites CA3 neurons, and so on, through the serial elements of the trisynaptic pathway lying within a transverse hippocampal "slice" (Andersen et al., 1969, 1971; Lømo, 1971). Unsurprisingly, anatomical studies have clearly demonstrated that the structural organization of the hippocampal trisynaptic circuit is far more intricate than originally appreciated.

The original lamellar hypothesis (Andersen et al., 1971) did not anticipate all of the implications of the longitudinal axonal distributions of Layer II entorhinal neurons, dentate hilar mossy cells and CA3 pyramidal cells, and because these structural features can be

interpreted as being either consistent (Andersen et al., 2000; Lømo, 2009) or inconsistent (Amaral and Witter, 1989) with the lamellar hypothesis, we believe that the hypothesis merits discussion and updating in a way that takes all of the relevant information into account. In the original publication that introduced the lamellar hypothesis, Andersen et al. (1971) did not state or imply that lamellae are spatially rigid "hardware" units that function independently under all conditions, or that excitatory neurotransmission through the "trisynaptic circuit" must remain wholly within individual transverse "slices." To the contrary, Andersen and colleagues stated that, *"the functional independence of neighboring lamellae suggests that the hippocampus, despite its stereotyped structure, may be capable of considerable operational flexibility,"* and noted that, *"the total output from the hippocampus would derive from a series of lamellae, the number and size of which would largely depend on the pattern of afferent impulses passing along the perforant path fibers from the entorhinal area."* Perhaps most importantly, Andersen and colleagues also wrote that they had not directly examined, *"...the possible defocusing effect of the longitudinal associational fibers, which are collaterals of CA3 cells running parallel to the long axis of the hippocampus and making synaptic contact with other CA3 cells (Lorente De Nó, 1934)."* Thus, Andersen and colleagues proposed the lamellar hypothesis with the recognition and understanding that the longitudinal CA3 pathway existed, and that translamellar facilitation and inhibition mediated by longitudinal excitatory and inhibitory pathways would sculpt excitatory signals and govern the parameters of lamellar function (Andersen et al., 1971).

Following the earliest anatomical studies cited by Andersen and colleagues in their initial proposal of the lamellar hypothesis, tracer studies concluded that the entorhinal cortex forms a topographic, but somewhat divergent innervation of the dentate gyrus (Wyss, 1981; Ruth et al., 1982, 1988; Witter et al., 1989), and that both CA3 pyramidal cells (Lorente De Nó, 1934; Swanson et al., 1981) and dentate hilar neurons (Zimmer, 1971; Swanson et al., 1978; Berger et al., 1981; Laurberg and Sørensen, 1981) also form extensive longitudinal associational axonal projections. The relevance of longitudinally extensive afferent and associational pathways to the concept of lamellar organization was addressed in a commentary article by Amaral and Witter (1989), who concluded that the existence of pathways that travel in the septo-temporal plane was incompatible with *"a strict interpretation of the lamellar hypothesis,"* and stated that, *"clinging to the lamellar concept of hippocampal function is fast becoming detrimental to further advances in understanding structure/function relationships in this system."* The outright rejection by Amaral and Witter of a "strict" version of the lamellar hypothesis that was neither stated nor implied by the original hypothesis (Andersen et al., 2000) has been so influential that only limited discussion of the lamellar hypothesis has subsequently appeared, and virtually no mention of the hypothesis is made in the recently published encyclopedic compendium of all things hippocampal (Andersen et al., 2007).

REVISITING THE LAMELLAR HYPOTHESIS

In our view, the lamellar hypothesis has much to recommend it, and its appeal involves no attraction to outdated or obsolete concepts. To the contrary, we think it would be imprudent to discard a useful hypothesis unless its value has been irretrievably diminished. We suggest that the significance of longitudinally projecting axons depends not on whether they exist, but on what they do, and that the data from tracing studies can be just as readily interpreted as supporting the lamellar hypothesis as undermining it. In this review, we attempt a reconsideration of the evidence that most directly impacts the lamellar hypothesis. Our position is not that the hypothesis as originally formulated anticipated all subsequent findings, or that it should remain unmodified. Rather, we suggest that a reappraisal of all of the relevant data is warranted and compelling, and that the implications of the lamellar hypothesis for understanding hippocampal function need to be reconsidered in light of several issues that have not informed previous discussions of the subject.

The structural organization and function of the hippocampus can be viewed from different perspectives, and we do not pretend to know how to determine objectively which perspective might most closely approximate the truth. From the most fundamental biological article of faith that structure governs function, we assume that hippocampal "lamellar" function, if it is an operative physiological process that can be defined, is established and governed by the three-dimensional organization of the hippocampal formation, and also by other brain regions that influence hippocampal events. Before considering the connectivity of each hippocampal cell population in greater detail, we will examine the entorhinal input to the dentate gyrus by perforant path fibers because hippocampal information flow apparently starts there, and our understanding of how information in the entorhinal cortex reaches the hippocampus will facilitate an understanding of what the dentate gyrus might do and how it might do it.

HOW "LAMELLAR" OR "NON-LAMELLAR" IS THE ENTORHINAL CORTEX INPUT TO THE DENTATE GYRUS?

A primary piece of anatomical evidence supporting the initial formulation of the lamellar hypothesis was the finding that the entorhinal fibers, *"...spread out in the septo-temporal direction..."* and that, *"each specific level of the entorhinal area distributes fibers to a restricted segment of the hippocampus"* (Hjorth-Simonsen and Jeune, 1972). The longitudinal spread of entorhinal fibers was understandable within a "lamellar" context, as noted by Hjorth-Simonsen and Jeune, because the entorhinal cortex is smaller than the hippocampus, and therefore, the outputs must fan out naturally to some extent to form a topographical "lamellar" innervation of the larger hippocampus. However, numerous studies using tracer injections reported that although the entorhinal cortex input to the dentate gyrus has clear topographic features, with different parts of the entorhinal cortex projecting to different segments of the dentate gyrus along the septo-temporal axis, it is nonetheless more divergent longitudinally than expected for a "lamellar" input (Ruth et al., 1982, 1988; Witter et al., 1989; Dolorfo and Amaral, 1998; van Groen et al., 2003; Witter, 2007). The conclusion that entorhinal cells form longitudinally extensive axonal terminations in the molecular layers of the dentate gyrus derives mainly from the observation that when an anterograde tracer is injected into the entorhinal cortex, the tracer is subsequently found to distribute along a significant expanse of the dentate gyrus (Witter, 2007). This finding seems to contradict the

argument made by Andersen et al. (1971) that *"a point source of entorhinal activity projects its impulses. . . along a slice, or lamella, of hippocampal tissue."* The tracer data appear similarly inconsistent with the observation that local stimulation of perforant path fibers near their entry to the dentate gyrus excites granule cells within a narrow transverse plane of the dentate gyrus, with the extracellular EPSP falling off sharply on either side (Lømo, 1971, 2009). However, no inconsistency arises if the entorhinal cortex contains separate columns that process incoming information similarly across the region, as do columns for individual parts of the visual field, the body surface, or composite sounds in primary visual, somatosensory, or auditory cortices (Kandel et al., 2000). In this scenario, co-mingled neurons that send longitudinally restricted axons to different portions of the dentate gyrus would appear, after injection of anterograde tracer into one site, to form highly divergent projections. Therefore, we hypothesize that cells in one such column (represented by Cell 1 in **Figure 1**) project their axons to one transverse lamella, while neighboring cells in the same column (Cell 2) project their axons to a different lamella, and so on for other neurons (Cell n) within the column. In addition, we suggest that cells with properties similar to Cell 1 in Columns 2 and 3 project their axons into the same lamella as Cell 1 in Column 1, and that cells with properties similar to Cell 2 project into the lamella of Cell 2, and so on (**Figure 1**). With such an organization, the results of both the tracer studies and the electrophysiological studies would be completely compatible. There is anatomical evidence that the entorhinal cortex, like other neocortical regions, is organized into a mosaic of similar columns (Witter and Moser, 2006). Intermingling of neurons that target spatially separated targets occurs in other parts of the cortex, for example in the primary motor cortex where adjacent neurons project to motor neurons that innervate different muscles (Andersen et al., 1975), and would give the appearance, after focal tracer injection, that all cells have divergent axonal projections.

HOW DIVERGENT ARE THE AXONS OF LAYER II ENTORHINAL NEURONS ALONG THE SEPTO-TEMPORAL AXIS?

Uncertainty regarding the extent of divergence of perforant path fiber input to the dentate gyrus makes two studies particularly relevant. First, if most or all Layer II entorhinal cortex neurons innervate wide expanses of the dentate gyrus, then two different retrograde tracers injected into two widely separated segments of the dentate gyrus should be transported and co-localized by most or all Layer II cells. This study was performed in the monkey, and although some co-localization of tracer was noted in some cells in the transitional area between the two cortical regions that project to the two tracer injection sites, individual cells containing both tracers were relatively rare (Witter et al., 1989). This finding suggests that most entorhinal neurons probably do not innervate a large expanse of the dentate molecular layer.

Second, if a small injection of anterograde tracer into the entorhinal cortex can label a broad expanse of the dentate gyrus because individual Layer II entorhinal neurons reliably innervate that same longitudinal expanse, then individual entorhinal neurons filled with dye should exhibit axons that span that large expanse. However, that does not appear to be the case (Tamamaki and Nojyo, 1993). Although reviews emphasizing the divergence of the entorhinal projection to the dentate gyrus cite 2.0 mm

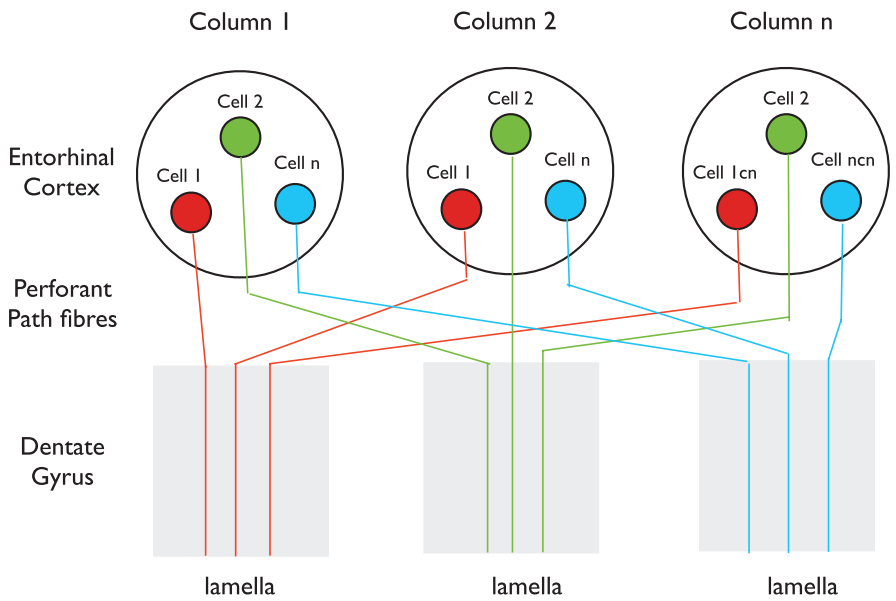

FIGURE 1 | A possible organization of the entorhinal input to the dentate gyrus. The entorhinal cortex in this perspective consists of a mosaic of vertical columns. Each column contains subsets of cells of similar properties (red, green, or blue) present in each column. Cells in each subset project their perforant path axons into the same lamella. Tracers injected locally into either the entorhinal cortex or the dentate gyrus, after anterograde or retrograde transport, respectively, will label extensive regions of the dentate gyrus or entorhinal cortex, even though individual axons enter only one lamella. This scenario is consistent with both the longitudinally restricted axonal projections of single Layer II cells described by Tamamaki and Nojyo (1993), the divergent spread of tracers after focal injection into the entorhinal cortex (Witter, 2007) and the lamellar excitation of dentate granule cells by stimulation of perforant path fibers where they enter the dentate gyrus (Lømo, 2009).

(∼20% of the length of the rat dentate gyrus) as the approximate longitudinal extent of the terminal arbors of individual Layer II entorhinal neuron axons (Amaral and Lavenex, 2007; Witter, 2007), we note the following points in the study by Tamamaki and Nojyo (1993), in which the axons of six individual Layer II neurons were described. Five of the six cells analyzed exhibited axons that extended <1.5 mm along the longitudinal axis, and the sixth cell did not reach 2.0 mm in its longitudinal extent. The average longitudinal spread of single axon terminals may therefore be <1.5 mm. Functionally, the width of the transverse strip, the size of the cluster of granule cells, or the spatial extent of the granule cells brought to firing by perforant path input in the normal state may be narrower still. This is likely to occur predominantly along the midline of the axon's terminal field because that is where the efficiency or density of terminals is probably highest. That is also where EPSPs will summate most effectively and where repetitive impulse activity will cause the greatest "frequency potentiation," as observed during repetitive stimulation at 10–20 Hz (Andersen et al., 1966; Bliss and Lømo, 1973), which corresponds to frequencies recorded *in vivo* from entorhinal cortex layer II cells projecting to the dentate gyrus during exploration (Fyhn et al., 2007).

Several methodological factors make it difficult to be certain about the axonal distribution of the six cells described by Tamamaki and Nojyo (1993). Of the 16 cells that were initially labeled, 10 cells were too inadequately filled for the authors to give any description of their axonal distribution. Thus, it remains a possibility that the remaining six cells that were reconstructed and described may have been only partially filled, and the longitudinal extent of their axonal projections underestimated, although the extensive cell-filling in the transverse plane suggests that the longitudinal axon distribution estimates of most cells may well be accurate (∼1.4 mm). These authors also stated that the somata of all six Layer II cells were from a dorsolateral subregion of the entorhinal cortex that specifically innervates the septal dentate gyrus, and that technical factors may have biased cell selection for large neurons. Therefore, these six cells may be a non-representative subset of all Layer II neurons (Tamamaki and Nojyo, 1993).

Thus, we are left with uncertainty about several anatomical features that have unknown significance for the functional issue being discussed. But regardless of whether an "anatomical lamella" or granule cell "cluster" is only as wide as the narrowest part of the mossy fiber pathway (∼0.2 mm), or is the width of the entorhinal input to the dentate gyrus and most inhibitory interneurons (∼1.0–1.5 mm), we do not think that these anatomical features can be assumed to have linear control of lamellar physiology. That is, we do not see the transverse strips or clusters of active granule cells as "hard-wired" anatomical lamellae of a fixed width, but rather, as narrow functional strips or clusters of activity, one strip or cluster flowing into others, shifting position and width as events unfold, and interacting via longitudinal connections. Assuming that most entorhinal neurons have a ∼1.0–1.4 mm axonal divergence along the septo-temporal axis, the available data support the lamellar hypothesis in the sense that individual entorhinal neurons apparently send their axons to a relatively narrow transverse segment of the dentate gyrus (Tamamaki and Nojyo, 1993), as originally stated by Hjorth-Simonsen and Jeune (1972).

Although the available anatomical data can be cited to support opposite perspectives, and the scheme in **Figure 1** above may be wrong, it is nonetheless difficult to reconcile the observed activation of a narrow transverse strip of dentate granule cells in the rabbit (Lømo, 1971, 2009), or the idea of pattern separation (McNaughton, 1989; Leutgeb et al., 2007), with the idea of a uniformly diffuse non-lamellar input to the dentate gyrus. Clearly, should future studies demonstrate that most or all Layer II neurons possess axons that target granule cells along most or all of the dorsal dentate gyrus (∼4.0 mm), as concluded by Amaral and Witter (1989), our suggested scheme would be incorrect. Regardless, the issue of the longitudinal divergence of the entorhinal input to the dentate gyrus may be a moot point with regard to lamellar function because it is clear that even if the entorhinal input to the dentate gyrus is only 1.0–1.5 mm along the longitudinal axis (Tamamaki and Nojyo, 1993), it is still more extensive longitudinally than the clearly "lamellar" mossy fiber pathway, which may be as limited as ∼0.2 mm in the septo-temporal plane (Blackstad et al., 1970; Claiborne et al., 1986).

FUNCTIONAL IMPLICATIONS OF A POSSIBLY DIVERGENT ENTORHINAL INPUT TO THE DENTATE GYRUS

How does the recognition that the entorhinal input to the dentate gyrus is more extensive longitudinally than the mossy fiber pathway impact the concept of lamellar function? Very little, in our view, for several reasons. First, since we have argued that the existence of longitudinal associational pathways is not, in and of itself, evidence against the concept of lamellar function, we view the anatomical features of the entorhinal input to the hippocampus similarly. That is, we would argue that the existence of a somewhat divergent afferent pathway has no obvious implications for lamellar function because the physiological implications of anatomical features cannot be easily inferred. Second, it is now clear that the perforant path input to the dentate gyrus directly innervates molecular layer dendrites of granule cells (McNaughton et al., 1981), basket cells, and axo-axonic cells (Soriano and Frotscher, 1989; Zipp et al., 1989), as well as the dendrites of hilar mossy cells (Figure 7C of Sloviter, 1983) and hilar somatostatin-positive neurons that send dendrites into the molecular layer (Sloviter, 1983; Leranth et al., 1990; Soltesz et al., 1993; Frotscher et al., 1994; Buckmaster, 2012). Thus, the perforant path input to the dentate gyrus could evoke feed-forward inhibition in granule cells (Buzsáki, 1984; Sloviter, 1991a), thereby inhibiting weakly excited granule cells and resulting in a highly focused excitation of granule cells, perhaps at the center of a somewhat divergent entorhinal axonal plexus. In addition, strong recurrent inhibition of dentate granule cells, as demonstrated in the rabbit (Lømo, 2009), might similarly "sharpen" the input message, as might an inhibitory component included in the entorhinal input to the dentate gyrus (Germroth et al., 1989). Regardless, it seems highly doubtful that the net physiological influence of any axonal pathway can be inferred solely, or even secondarily, from its structural dimensions.

THE LONGITUDINAL EXTENT OF THE ASSOCIATIONAL AXONS OF HIPPOCAMPAL NEURONS: AN OVERVIEW

Before discussing the features of the different hippocampal neuron subpopulations, we summarize here (**Table 1**) the main

Table 1 | Comparative lengths of longitudinal associational axon projections of different hippocampal neuron subpopulations.

Cell type	Axon plexus longitudinal length	Reference
Entorhinal layer II pyramidal neurons	∼1.4–1.9 mm	Tamamaki and Nojyo (1993)
Dentate granule cells[+]	∼0.2–1.3 mm	Blackstad et al. (1970), Claiborne et al. (1986), Acsády et al. (1998), and Ropireddy and Ascoli (2011)
Dentate mossy cells [periodicity of axonal distribution (Soltesz et al., 1993) : ∼900 μm]	∼6.6 mm	Amaral and Witter (1989), Soltesz et al. (1993), and Buckmaster et al. (1996)
Dentate basket cells	∼1.0–1.5 mm	Struble et al. (1978), Amaral and Lavenex (2007), Freund and Buzsáki (1996), and Sík et al. (1997)
Dentate hilar dendritically projecting cells[#]	∼1.0–1.5 mm	Buckmaster and Schwartzkroin (1995), Freund and Buzsáki (1996), and Sík et al. (1997)
CA3 pyramidal cells [periodicity of axonal distribution and HSP72 expression after ischemic injury (Hsu and Buzsáki, 1993; Li et al., 1994) : ∼300–600 μm]	∼4–7 mm	Ishizuka et al. (1990), Li et al. (1994), and Tamamaki and Nojyo (1991)
CA1 pyramidal cells (associational fibers)	Negligible	Amaral et al. (1991) and Amaral and Lavenex (2007)

[+] *Note that the longitudinal course taken by the mossy fibers at the end of their trajectory at particular septo-temporal levels (Swanson et al., 1978; Tamamaki and Nojyo, 1991; Acsády et al., 1998; Ropireddy and Ascoli, 2011) is not considered here.*

[#] *Note that the distances are those in which most axon length is sequestered, not the longest distance traversed by a single fiber.*

hippocampal cell types with reference to the relative extents of their longitudinal associational axon projections, because the existence of these projections has been cited as the primary evidence undermining the concept of lamellar function (Amaral and Witter, 1989).

Hippocampal neurons with longitudinally limited associational axon projections, i.e., neurons that form few associational axons, or keep most of their axons within ∼1.0–1.5 mm of their somata, include dentate granule cells (Blackstad et al., 1970; Gaarskjaer, 1978, 1981), most or virtually all hippocampal inhibitory interneurons (Struble et al., 1978; Buckmaster and Schwartzkroin, 1995; Freund and Buzsáki, 1996; Sík et al., 1997; Zappone and Sloviter, 2001, 2004; Gloveli et al., 2005; Amaral and Lavenex, 2007), and CA1 pyramidal cells, which form longitudinal projections to the subiculum, but few associational axons that interconnect CA1 pyramidal cells (Amaral et al., 1991; Amaral and Lavenex, 2007). Hippocampal neurons with extensive longitudinal associational axons (most axon length greater than ∼1.5 mm from the soma of origin) include only dentate hilar mossy cells (Soltesz et al., 1993; Buckmaster et al., 1996) and CA3 pyramidal cells (Ishizuka et al., 1990; Li et al., 1994). It should be noted that although hippocampal interneurons restrict most of their ipsilateral associational axon length to within ∼1 mm of their somata, many of the same interneurons form long-axon projections that innervate the contralateral hippocampus and the medial septum (Zappone and Sloviter, 2001, 2004).

In the discussion that follows, we address the question of whether the available anatomical evidence really negates the lamellar hypothesis, or whether longitudinal "translamellar" axons could be consistent with a model in which the granule cells are functionally separated from adjacent granule cells by lateral inhibition, and further, whether granule cell information transmitted to mossy cells and CA3 pyramidal cells via the undisputedly "lamellar" mossy fiber pathway is then conveyed topographically to targets at multiple levels throughout the longitudinal axis of the hippocampus, inhibiting some targets and exciting others. In this scenario, the net effect of "translamellar" axonal projections would depend on the net effects of longitudinally projecting mossy cells and CA3 pyramidal cells on principal cells or interneurons at different levels along their longitudinal trajectories (Gulyás et al., 1993; Sik et al., 1993; Bernard and Wheal, 1994; Wittner et al., 2006; Ropireddy et al., 2011). If these effects include excitation of distant inhibitory neurons, then the existence of longitudinally projecting axons could define lamellar function, rather than undermine it. After all, how could activity in spatially separated "lamellae" or "clusters" of pyramidal cells or granule cells be coordinated (Deadwyler and Hampson, 1999; Hampson et al., 1999; Small, 2002) without the involvement of longitudinal excitatory projections?

THREE-DIMENSIONAL ORGANIZATION OF THE DENTATE GYRUS

IS THE EXISTENCE OF LONGITUDINALLY PROJECTING MOSSY CELL AXONS NECESSARILY ANTITHETICAL TO THE CONCEPT OF LAMELLAR FUNCTION?

It is clear and undisputed that whereas the dentate granule cells send "lamellar" axons to their hilar and area CA3 target cells (Blackstad et al., 1970; Gaarskjaer, 1978, 1981; Claiborne et al., 1986; Acsády et al., 1998; Ropireddy and Ascoli, 2011), dentate hilar mossy cells form a complementary longitudinal axon system that preferentially innervates distant segments of the dentate gyrus along the septo-temporal axis. That is, mossy cells preferentially avoid innervating the inner molecular layer within the "lamella" in which they receive mossy fiber excitation, but instead, apparently innervate local interneurons in the hilus of their "home" lamella before their axons enter the molecular layer and travel longitudinally to preferentially innervate the inner molecular layer of distant segments of the dentate gyrus (Amaral and Witter, 1989; Soltesz et al., 1993; Buckmaster et al., 1996). Importantly, whereas

the convergence of granule cell input to inhibitory interneurons is high, convergence of mossy fibers onto mossy cells and CA3 pyramidal cells is low (Acsády et al., 1998), which is a structural feature consistent with a highly topographic ("lamellar") excitation of targeted principal cells by individual granule cells. That is, many granule cells contribute to the convergent activation of nearby inhibitory interneurons that presumably generates intralamellar inhibition, whereas the non-convergent innervation of mossy cells and CA3 pyramidal cells likely conserves the point-to-point lamellar nature of the transmission from granule cells to their excitatory target cells.

The "lamellar" pattern of mossy fiber distribution and the complementary "translamellar" pattern of mossy cell axon distribution prompt several questions. First, what purpose does it serve for granule cells to severely limit the longitudinal spread of their initial communication if that highly focused message is simply going to be extensively amplified and spread longitudinally to other granule cells by mossy cells, thereby "defocusing" the excitation of the initially targeted lamella by the entorhinal input? Second, is the existence of excitatory longitudinal associational fibers, in and of itself, antithetical to the concept of lamellar organization? The answers to these questions are apparent, but only if lamellar function is defined by "on-beam" excitation of granule cell target cells and "off-beam" translamellar lateral inhibition that spatially restricts granule cell excitation (Sloviter, 1994; Zappone and Sloviter, 2004). This hypothesized organization within the dentate gyrus may have significant similarities to the structural organization of the cerebellum, in which "on-beam" excitation of Purkinje cells by the parallel fibers is focused by lateral inhibition mediated via excitation of inhibitory interneurons (Eccles et al., 1967; Ito, 1984; Cohen and Yarom, 2000; Gao et al., 2006). Thus, if the mossy cell-derived longitudinal axon system activates distant dentate inhibitory interneurons, thereby producing lateral granule cell inhibition in distant granule cells, the "lamellar" pattern of granule cell axon distribution and the "translamellar" pattern of mossy cell axon distribution might establish lamellar function, rather than undermine it. Similarly, if two groups of spatially separated CA1 pyramidal cells must discharge synchronously to encode a particular memory or recognize a particular location in space (Deadwyler and Hampson, 1999; Hampson et al., 1999), transverse and longitudinal axon collaterals of CA3 pyramidal cells may be the primary means of synchronizing two or more spatially separated target populations. Of particular relevance to this issue are reports that both dentate mossy cells and CA3 pyramidal cells innervate their respective target regions unevenly, with periodic clusters of axon length occurring at intervals of ∼900 μm for mossy cells (Soltesz et al., 1993) and ∼300–600 μm for CA3 pyramidal cells (Hsu and Buzsáki, 1993; Li et al., 1994), respectively. This pattern of axon distribution by excitatory longitudinal fibers, which might form "bands" of excitation and inhibition via excitation of principal cells and inhibitory interneurons (Wittner et al., 2006), respectively, may be entirely consistent with lamellar organization (Li et al., 1994). That is, communication between spatially separated neurons or neuronal clusters (Deadwyler and Hampson, 1999; Hampson et al., 1999; Small, 2002) would require an excitatory longitudinal associational pathway to coordinate this spatially separated activity.

LATERAL INHIBITION IN THE DENTATE GYRUS AS A MECHANISM DEFINING LAMELLAR FUNCTION

The anatomical perspective that the "translamellar" distribution pattern of dentate mossy cell axons is, in and of itself, antithetical to the concept of lamellar function (Amaral and Witter, 1989) was the logical consequence of assuming that hilar mossy cells directly excite distant granule cells, thereby defocusing the entorhinal excitation of the granule cell layer. However, this does not appear to be the case. In studies performed *in vivo* before the features of the ipsilateral longitudinal associational projections of mossy cells were fully appreciated, Buzsáki and colleagues (Buzsáki and Czeh, 1981; Buzsáki and Eidelberg, 1981, 1982) and Goddard and colleagues (Douglas et al., 1983; Bilkey and Goddard, 1987) reported that stimulation of the excitatory dentate commissural pathway formed by glutamatergic mossy cells (Frotscher, 1992; Soriano and Frotscher, 1994) produced a paradoxical net inhibitory effect on contralateral granule cells because the commissural excitation of basket cells apparently predominated over "very weak" commissural excitation of granule cells (Douglas et al., 1983). The subsequent finding that mossy cells also form an extensive associational axon collateral system (Amaral and Witter, 1989) should have led to the hypothesis that mossy cells might also excite basket cells ipsilaterally, producing granule cell lateral inhibition, rather than lateral excitation, but that connection was not made at the time.

It was the discovery that the seizure-induced death of hilar mossy cells is closely associated with the immediate development of granule cell hyperexcitability (Sloviter, 1987, 1991b), taken together with the data indicating the translamellar pattern of mossy cell axon distribution (Amaral and Witter, 1989), that led us to propose the hypothesis that seizure-induced mossy cell death might denervate distant basket cells, resulting in translamellar granule cell disinhibition (Sloviter, 1994). The concept of translamellar granule cell disinhibition implied the existence of normal translamellar inhibition, and this implication led us to determine whether lateral inhibition exists in the normal dentate gyrus (Sloviter and Brisman, 1995), and whether it is abolished following extensive hilar neuron loss (Zappone and Sloviter, 2004).

To selectively activate a "lamella" or "cluster" of granule cells, and then determine the effect of that discharge on granule cell responses in a distant "lamella," is not a trivial undertaking because even highly localized electrical stimulation of the granule cell layer might produce ipsilateral effects a few millimeters along the longitudinal axis via unidentifiable pathways or mechanisms (Hetherington et al., 1994). Therefore, we developed a method of locally delivering the GABA-A receptor antagonist bicuculline to the granule cell layer to produce a highly localized and augmented granule cell layer discharge in response to afferent stimulation outside the hippocampus. During continuous perforant path stimulation *in vivo* at 0.3 Hz, passive diffusion of bicuculline methiodide from the tip of a recording microelectrode resulted in spatially restricted (<1 mm) granule cell layer discharges that caused powerful, long-lasting (>150 ms) lateral inhibition at distant granule cell layer recording sites up to 4.5 mm along the septo-temporal axis (Sloviter and Brisman, 1995; Zappone and Sloviter, 2004). Thus, "lamellar" granule cell layer discharges produce powerful

distant granule cell lateral inhibition, which apparently predominates over an underlying "associative" excitation of granule cells by mossy cells (Zappone and Sloviter, 2004).

Importantly, only *extensive* hilar neuron loss caused by prolonged perforant path stimulation abolished this translamellar inhibitory effect (Zappone and Sloviter, 2004). Minor mossy cell loss in kainate-treated rats (Zappone and Sloviter, 2004), or in hippocampal slices in which a small percentage of mossy cells were manually destroyed after being visually identified (Ratzliff et al., 2004), failed to replicate the granule cell hyperexcitability associated with extensive hilar neuron loss. The hypothesis that granule cell hyperexcitability is specifically caused by *extensive* mossy cell loss (Sloviter, 1994; Zappone and Sloviter, 2004) is supported by a recent study in a conditional knockout mouse that selectively expresses the diphtheria toxin receptor in hilar mossy cells. In these animals, diphtheria toxin triggers selective and extensive mossy cell loss, immediate granule cell hyperexcitability *in vitro*, as well as impaired pattern separation in the dentate gyrus (Jinde et al., in press).

Consistent with the studies in rats described above, strong stimulation of perforant path fibers where they enter the dentate gyrus causes dentate granule cells to discharge along a narrow transverse strip in the rabbit (Lømo, 2009). Stimulation of mossy fibers in area CA3 activates a similar transverse strip antidromically. Both activations are accompanied immediately afterward by lateral inhibition, which in the rabbit lasts up to 100 ms and spreads 4–5 mm to either side of the strip (Lømo, 2009). Evidently, impulses along collaterals of granule cell axons activate local interneurons (Acsády et al., 1998) that inhibit granule cells. Local inhibitory interneurons likely cause the inhibition within and immediately outside the lamella, whereas mossy cells may inhibit granule cells at greater longitudinal distances via excitation of inhibitory interneurons, as described in the preceding paragraphs. Signs of feed-forward inhibition did not appear under the conditions of these experiments (Lømo, 2009), but may well occur given that many inhibitory interneurons extend dendrites into the molecular layer, and may respond to volleys along the perforant path before the granule cells discharge (Buzsáki, 1984).

LONGITUDINAL INFLUENCES OF DENTATE GYRUS INHIBITORY INTERNEURONS

If individual lamellae of the dentate gyrus, spatially restricted clusters of granule cells, or individual granule cells function independently and form unique combinations of temporally associated activity with other granule cells in distant locations, then the inhibitory interneurons that mossy cells excite would be predicted to have longitudinally restricted axons that inhibit individual lamellae, rather than expansive axonal networks that inhibit large segments of the granule cell layer. That is, if different combinations of spatially separated granule cells need to discharge in unison under different conditions, it would be hypothetically unproductive for the activation of cells in one lamella to inhibit all other lamellae indiscriminately. Thus, mossy cell activation of distant interneurons having longitudinally restricted axonal projections might ideally permit control of individual lamellae, allowing distantly separated neurons to discharge in varying combinations, perhaps to encode specific memories (Small, 2002) or to register, remember, and locate particular spatial locations (Deadwyler and Hampson, 1999; Hampson et al., 1999).

The results of virtually all studies of the longitudinal axonal distributions of dye-filled and reconstructed interneurons appear consistent with lamellar organization because virtually all interneurons studied keep most of their axon length within ∼1 mm of their somata (Amaral and Lavenex, 2007). Although the method of filling individual neurons with a dye and then calculating the longitudinal extent of their axons from reconstructed consecutive sections is technically difficult and prone to underestimation when a cell is incompletely filled (Sík et al., 1997), the studies of the axonal fields of the few dentate gyrus interneurons that have been filled and reconstructed have consistently shown that most of the axon length of inhibitory interneurons remains close to the soma, with a sharp drop-off of axon length as the septo-temporal distance from the soma increases past ∼1 mm (Buckmaster and Schwartzkroin, 1995; Sík et al., 1997). Filled hilar interneurons that innervate the perforant path termination zone in the outer dentate molecular layer, and correspond to the hilar somatostatin-positive population (Bakst et al., 1986; Sloviter and Nilaver, 1987; Halasy and Somogyi, 1993), also concentrate most of their axonal length within their lamellae of origin (Amaral and Witter, 1989; Buckmaster and Schwartzkroin, 1995; Freund and Buzsáki, 1996; Sík et al., 1997), although a few axons extend farther (Buckmaster and Schwartzkroin, 1995), possibly on their way to the septum (Zappone and Sloviter, 2001). The few dentate basket cells that have been analyzed exhibit a similarly restricted axonal distribution (Sík et al., 1997), with axons extending ∼1.0–1.5 mm along the septo-temporal axis (Struble et al., 1978; Sík et al., 1997), which is, interestingly, the width of the septo-temporal expanse specifically avoided by the mossy cells (Amaral and Witter, 1989; Soltesz et al., 1993; Buckmaster et al., 1996).

The small body of data describing individual inhibitory interneurons that have been filled *in vivo* and reconstructed, and the complete lack of information about how generally extensive the longitudinal associational projections of most hippocampal interneuron subpopulations might be, led us to initiate retrograde tracer studies to identify the extent of both the commissurally- and associationally projecting interneuron subpopulations (Zappone and Sloviter, 2001, 2004). Although a retrograde tracer study cannot describe the projections of any given single cell, its strength lies in the ability of a tracer to label a large percentage of any neuronal population capable of transporting the tracer from a particular location. Thus, tracer studies give a more representative estimate of the extent of the axonal projections formed by entire cell populations, as opposed to the features of single cells that may not be representative of the larger cell population. The results of these retrograde tracer studies showed that a majority of dentate gyrus interneurons, and virtually all somatostatin-positive hilar interneurons, innervate the contralateral hippocampus, and that the somatostatin-positive interneurons of both the hippocampal stratum oriens and the dentate hilus are a unique population of long-axon-, septally projecting hippocampal interneurons (Zappone and Sloviter, 2001), a finding that has been confirmed by other laboratories (Jinno and Kosaka, 2002; Gulyás et al., 2003; Melzer et al., 2012; Quilichini et al., 2012). Most importantly, despite their ability to pick up and retrogradely transport tracer

from the distant septum or the distant contralateral hippocampus, these same somatostatin-positive interneurons consistently failed to take up and transport the same tracer when it was placed only ∼2.5 mm along the septo-temporal axis (Zappone and Sloviter, 2004). This finding is consistent with the observations in filled cells that somatostatin-positive hilar interneurons concentrate their axons within their "home" lamellae (Buckmaster and Schwartzkroin, 1995; Sík et al., 1997; Amaral and Lavenex, 2007), and with the results of anterograde tracer distribution to the outer dentate molecular layer mentioned in a footnote in the study by Amaral and Witter (1989).

All known interneuron populations of the dentate gyrus showed similarly minimal associational transport of retrograde tracer (Zappone and Sloviter, 2001, 2004). Immediately adjacent to the tracer injection site, all interneurons with the morphologies and locations of dentate basket cells, molecular layer axo-axonic cells, and hilar dendritically projecting interneurons contained tracer in their somata, indicating that all interneuron subpopulations studied have the capacity to take up and retain the tracer locally. Although many parvalbumin-positive dentate basket cells readily transported tracer from the distant contralateral hippocampus (Goodman and Sloviter, 1992; Zappone and Sloviter, 2001), the same cells did not transport tracer placed only ∼2 mm along the septo-temporal axis (Zappone and Sloviter, 2004). Similarly, the population of axo-axonic interneurons of the dentate molecular layer that innervate the axon initial segments of granule cells (Soriano and Frotscher, 1989) appeared to be exclusively short-axon cells because they did not transport tracer from the contralateral or ipsilateral hippocampus, or from the septum (although the possibility of long projections to other areas not studied cannot be excluded). Thus, no interneuron subpopulation appeared to possess significant, longitudinally extensive associational axonal projections despite often having much longer commissural and septal axon projections (Zappone and Sloviter, 2001). These results using a retrograde tracer are consistent with the findings of the single cell studies indicating that the longitudinal axonal projections of hippocampal interneurons are rarely significant more than ∼1 mm from the soma in the septo-temporal direction (Struble et al., 1978; Buckmaster and Schwartzkroin, 1995; Freund and Buzsáki, 1996; Sík et al., 1997; Gloveli et al., 2005; Amaral and Lavenex, 2007).

The finding that focal granule cell discharges caused powerful and long-lasting lateral inhibition in longitudinally distant granule cells (Zappone and Sloviter, 2004), taken together with the anatomical data on the longitudinal axonal projections of each cell type cited above, has led us to suggest that: (1) granule cells excite hilar mossy cells and interneurons "on-beam" via the "lamellar" mossy fiber projection (Acsády et al., 1998), (2) this lamellar excitation produces monosynaptic intralamellar granule cell inhibition via direct mossy fiber excitation of dentate inhibitory neurons, and disynaptic intralamellar granule cell inhibition via mossy fiber excitation of mossy cells that then excite inhibitory neurons, and (3) excitation of longitudinally distant inhibitory interneurons by mossy cells evokes distant disynaptic translamellar lateral inhibition (Sloviter, 1991b, 1994; Zappone and Sloviter, 2004). These three processes might collectively restrict granule cell excitation to the lamella most powerfully targeted by an entorhinal input.

IMPLICATIONS OF THE LAMELLAR HYPOTHESIS FOR UNDERSTANDING DENTATE GYRUS FUNCTION AND MALFUNCTION

It should be clearly understood that we regard the lamellar hypothesis to be a general perspective regarding the functional implications of a number of structural features, rather than a specific and rigid proposal that all granule cells within a transverse plane must discharge in synchrony in response to a perforant path input that is anatomically extensive in the transverse plane (Tamamaki and Nojyo, 1993), or that all activity within the trisynaptic circuit must remain within the transverse plane.

In the freely behaving rat, specific behavioral tasks apparently involve the discharge of very few granule cells (Alme et al., 2010), whereas the large-amplitude population spikes evoked by angular bundle stimulation reflect a mass discharge that is undoubtedly an artifact of the experimental condition (Andersen et al., 1966; Lømo, 1971; McNaughton et al., 1981). Therefore, a physiological "lamellar" discharge could involve very few granule cells, and an activation of a correspondingly small number of CA3 pyramidal cells (Deguchi et al., 2011), as long as the longitudinal spread of the granule cell excitation is restricted. It is perhaps surprising that so few granule cells discharge during normal behavior (Alme et al., 2010) and at such low firing frequencies (<0.2 Hz; Jung and McNaughton, 1993). More recent studies, however, report that higher spike frequencies (averaging about 1 Hz) normally occur (Leutgeb et al., 2007; Mistry et al., 2011). Moreover, during behavioral tasks, many perforant path axons conduct impulses at rates of 10–20 Hz or more (Fyhn et al., 2007), while granule cells may generate high frequency bursts of impulses (Mistry et al., 2011). Interestingly, such bursts occur primarily on a background of very low mean frequencies, and only stimulus patterns that mimic this pattern are capable of inducing long-term potentiation (LTP) at mossy fiber synapses with CA3 pyramidal cells. The LTP at mossy fiber synapses is presynaptic and NMDA receptor-independent (non-Hebbian), whereas the LTP at perforant path-granule cells synapses is associative (Hebbian) and requires NMDA receptor activation, for example through some stronger coincident input. Perforant path synapses are generally weak because substantial summation of perforant path evoked EPSPs is needed in order to discharge granule cells (Lømo, 1971; McNaughton et al., 1981). Yet they undergo LTP if additional perforant path or other inputs evoke sufficient coincident depolarization. LTP at both perforant path and mossy fiber synapses are commonly induced in narrow, transverse slices of the hippocampus, consistent with the lamellar hypothesis proposed here, and with the idea that storage and recall of information from the entorhinal cortex require persistent changes in synaptic efficiency. For example, in mice in which dentate granule cells specifically lack NMDA receptors, LTP at perforant path – granule cell synapses (but not at other synapses in the hippocampus) is abolished, together with the ability to retain memories that allow discrimination between similar environments in ways that are consistent with pattern separation (McHugh et al., 2007).

In contrast to the normal behavioral state in which few granule cells apparently discharge in response to physiological afferent input, we suggest that it is entirely possible that many or all

granule cells within a thin transverse plane might discharge synchronously when hilar neurons are extensively injured and granule cells become immediately disinhibited (Sloviter, 1991b, 1994). The recent observations that mature granule cells in normal rats are strongly inhibited, whereas newly born granule cells are unusually responsive because their axo-somatic inhibitory innervation is apparently still incomplete (Kempermann, 2012; Marin-Burgin et al., 2012), suggests that newly born, hyperexcitable granule cells constitute a disproportionate population of the granule cells that normally encode memories or locations, whereas mature granule cells are more inhibited and thereby perhaps held in "reserve" for specific tasks (Alme et al., 2010; Nakashiba et al., 2012). We suggest that the seizure-induced hilar neuron loss that produces immediate granule cell hyperexcitability (Sloviter, 1987, 1991b, 1994) may convert the inhibitory status of mature granule cells from "inhibited" to the "disinhibited" phenotype of newly born granule cells, thereby calling "reserve" granule cells to "active-duty." This possible recapitulation of ontogeny as a result of a disinhibiting and epileptogenic hippocampal injury might explain why weak afferent stimulation in these injured animals evokes massive granule cell population spikes (Sloviter, 1991b, 1994). That is, inhibited mature granule cells that are normally resistant to discharging (Alme et al., 2010) presumably become disinhibited and join the younger, already disinhibited granule cells (Marin-Burgin et al., 2012) in their response to entorhinal input. In this instance, when young and older granule cells become similarly disinhibited, a lamellar discharge might involve a full strip of granule cells discharging synchronously within a thin transverse lamella, or in multiple adjacent lamellae (Sloviter, 1994). Thus, normal "lamellar" function might involve very few granule cells discharging in the normal state, whereas "lamellar" dysfunction might involve full strips of granule cells discharging in a spontaneously epileptic hippocampus (Sloviter, 1994; Bumanglag and Sloviter, 2008).

Normally, however, the dentate gyrus appears to perform pattern separation of inputs coming from the entorhinal cortex (McNaughton, 1989; Leutgeb et al., 2007; McHugh et al., 2007; Nakashiba et al., 2012). That is, patterns representing similar information are separated and the small differences between them augmented to facilitate their later recall as different. The CA3 region is then thought to perform pattern completion by storing the separated patterns in such a way that when a partial version of one of them is presented later, a more complete version of it can be reactivated. One recent computational model able to perform some form of pattern separation, storage, and recall divides dentate gyrus and CA3 into lamellae, exploits known properties of excitatory mossy cells and hilar inhibitory interneurons, and adds back-propagation from CA3 to inhibit granule cells within lamellae (Myers and Scharfman, 2011). However, the model does not incorporate the possibility that mossy cells activate basket cells more powerfully than granule cells (Douglas et al., 1983; Misgeld et al., 1992a,b; Scharfman, 1995), or that the perforant path input may also be functionally lamellar. Nor do most other published models of dentate-CA3 processing take these factors into account. As long as these are real possibilities, we believe that these features need to be considered if a more complete understanding of dentate gyrus and CA3 function is to be reached. In particular, if the perforant path splits information from the entorhinal area into multiple lamellar units, this may be one of the mechanisms by which pattern separation is established in the dentate gyrus.

CA3 PYRAMIDAL CELLS AND THEIR EXTENSIVE ASSOCIATIONAL AXONS

In retrospect, it is easy to see how the longitudinal projections of dentate hilar mossy cells could have been viewed from a purely anatomical perspective as being antithetical to the idea of lamellar function (Amaral and Witter, 1989). Given the assumption that longitudinal excitatory axons of hilar mossy cells must excite distant granule cells (Amaral and Witter, 1989; Buckmaster and Schwartzkroin, 1994), despite it having never been demonstrated, it was possible to conclude that, "*. . .the extensive associational projections of the dentate gyrus have the potential of widely dispersing the inputs that come into any particular level*" (Witter et al., 1989). With regard to whether the excitation of CA3 and CA1 pyramidal cells by associational axonal projections of CA3 pyramidal cells should have been viewed as being similarly inconsistent with lamellar function (Amaral and Witter, 1989), it is interesting to note which cells are innervated or avoided by CA3 pyramidal cells. Like dentate granule cells, which only innervate ipsilateral hilar and area CA3 neurons, CA3 pyramidal cells have a limited number of targets. CA3 pyramidal cells form recurrent excitatory connections with other CA3 pyramidal cells (Miles and Wong, 1987), and also innervate CA1 pyramidal cells, axo-somatic inhibitory interneurons (Wittner et al., 2006), and the lateral septum (Swanson et al., 1981). CA3 pyramidal cells do not innervate the medial septum, subiculum, presubiculum, parasubiculum, or the entorhinal cortex (Amaral and Lavenex, 2007). Thus, CA3 pyramidal cells receive lamellar information from granule cells, and primarily convey that information topographically to other CA3 pyramidal cells, to axo-somatic inhibitory interneurons, and to CA1 pyramidal cells. CA1 pyramidal cells, in turn, topographically innervate the ipsilateral subiculum (Amaral et al., 1991). The topographic distribution of CA3 pyramidal cell axons (Ishizuka et al., 1990; Li et al., 1994), the selective innervation by CA3 pyramidal cells of the interneuron subpopulation that mediates powerful axo-somatic pyramidal cell inhibition (Wittner et al., 2006), and the lack of CA3 pyramidal cell innervation of the subiculum and entorhinal cortex, indicate that CA3 pyramidal cells primarily convey lamellar input information within the hippocampus "proper," and do not directly influence the entorhinal source of hippocampal input. Although CA3 pyramidal cell axons clearly do not restrict their axons to a transverse lamella, as acknowledged by Andersen et al. (1971), *the collective picture of the trisynaptic circuit, from our perspective, speaks to the preservation of topographic lamellar information within the trisynaptic circuit.*

POSSIBLE "LAMELLAR" INFLUENCES OF SEPTAL AND BRAINSTEM INPUTS TO INHIBITORY INTERNEURONS

The perspective that the mere existence of longitudinal pathways undermines the entire concept of lamellar function (Amaral and Witter, 1989) ignores the possible involvement of other influences that might impose lamellar function on a structure that includes longitudinal circuitry. Several external inputs to the dentate gyrus and hippocampus "proper" might serve such a role. A prominent reciprocal relationship exists between the hippocampus and the

medial septum/diagonal band of Broca (MSDB; Buzsáki et al., 1981; Nyakas et al., 1987; Freund and Antal, 1988; Leranth and Frotscher, 1989; Bland and Oddie, 1998; Takács et al., 2008). Virtually all hippocampal interneurons that innervate the septum belong to a single subpopulation of hippocampal interneurons: the somatostatin-positive cells of both the dentate gyrus and the hippocampus "proper" (Zappone and Sloviter, 2001, 2004). These hippocampal septally projecting (HS) cells directly innervate GABAergic and cholinergic neurons of the MSDB (Tóth et al., 1993; Gulyás et al., 2003; Takács et al., 2008). Thus, dentate hilar somatostatin-positive interneurons, which receive highly "lamellar" information from the granule cells, convey this topographically derived information directly to the medial septum. In turn, the cholinergic and GABAergic neurons of the septum/MSDB innervate hippocampal mossy cells, basket cells, and the somatostatin-positive hippocampo-septal cells (Freund and Antal, 1988; Freund and Buzsáki, 1996; Lübke et al., 1997; Deller et al., 1999; Takács et al., 2008). Thus, medial septal cells (both excitatory cholinergic and inhibitory GABAergic subtypes) appear ideally organized to regulate translamellar inhibition in the dentate gyrus by influencing mossy cells and inhibitory interneurons.

Perhaps most importantly, the medial septal projections to the hippocampus are topographically organized (Amaral and Kurz, 1985; Kiss et al., 1990), suggesting that lamellar information within the hippocampus is conveyed topographically to cells in the medial septum via the somatostatin-positive interneurons (because these cells receive lamellar input from the mossy fibers) and, in return, medial septal cells control basket cells and mossy cells in particular lamellae via topographical projections back to the hippocampus. *Therefore, we hypothesize that medial septal GABAergic neurons, by topographically inhibiting basket cells within a given lamella, convert perhaps multi-lamellar excitatory inputs from the entorhinal cortex into signals that selectively activate individually disinhibited lamellae.* By disinhibiting one granule cell layer "lamella" via inhibition of its basket cells (Bilkey and Goddard, 1987), medial septal GABAergic cells may establish lamellar function in the dentate gyrus without requiring that the entorhinal input to the dentate gyrus be as "lamellar" as the mossy fiber pathway. That is, *a divergent afferent pathway need not be viewed as being antithetical to the concept of lamellar function because a highly focused topographic inhibitory input to basket cells in one lamella could result in a highly restricted 'lamellar' response to a divergent excitatory input from the entorhinal cortex.* This control mechanism could be extraordinarily precise depending on the specificity of the topographical septal input to inhibitory interneurons in both the longitudinal and transverse planes. The hypothesis that the medial septum might regulate longitudinal transmission may be consistent with the conclusions of recent studies indicating that "theta waves" travel throughout the longitudinal hippocampal axis (Lubenov and Siapas, 2009; Patel et al., 2012).

A similar external (extrahippocampal) control mechanism may be exerted by the serotonergic input from the median raphe nucleus (Winson, 1980; Nitz and McNaughton, 1999), which selectively innervates several interneuron populations, but specifically avoids parvalbumin-positive basket cells that mediate axo-somatic inhibition (Halasy et al., 1992; Acsády et al., 1993). Thus, input from the brainstem median raphe nucleus may selectively influence several interneuron subpopulations that receive lamellar input from granule cells and convey that information to medial septal cells (Zappone and Sloviter, 2001) and other targets. In this way, the serotonergic input might influence lamellar function by modulating the inhibitory output of the somatostatin-positive HS cells, whereas the cholinergic and GABAergic medial septal cells may modulate lamellar function by topographically exciting or inhibiting mossy cells and basket cells. Under this scenario, external inputs to the hippocampus from the septum, brainstem, hypothalamus, and thalamus (Amaral and Lavenex, 2007) could conceivably impose "lamellar" function on a structure with both lamellar and longitudinal structural components, and serve as a switching mechanism that shifts the hippocampus from a "lamellar" to a "less lamellar-" or "non-lamellar" mode of function. Incorporating these features of hippocampal organization into the discussion brings an entirely different perspective to the assertion that the simple existence of any longitudinal pathways should be viewed as being inherently antithetical to the concept of lamellar function (Amaral and Witter, 1989).

ON THE POSSIBILITY OF LAMELLAR AND NON-LAMELLAR MODES OF HIPPOCAMPAL FUNCTION

It seems at least hypothetically conceivable that the hippocampus might normally alternate between "lamellar" and "non-lamellar" functional modes during different behavioral states, e.g., awake function vs. dreaming. A fully lamellar functional mode may be necessary during awake interaction with the real spatial and cognitive world, when mistakes in memory or spatial localization have severe consequences, whereas a non-lamellar mode of function may be operative during dreaming, when consequence-free interactions with the "intracranial" virtual version of the real world serve useful purposes, and when memory recall is impaired (De Gennaro et al., 2010). This hypothesized dual function for the hippocampus may be analogous to the dual function of the thalamus, which shifts from a topographically faithful sensory relay mode to a non-topographical rhythmic mode depending on the behavioral state and the activity of external ascending or descending influences (Steriade et al., 1969; McCormick and von Krosigk, 1992).

The obvious advantage of duality in hippocampal function lies in having one piece of hardware serving multiple purposes depending on the behavioral state, or running different "programs" or "spatial maps" under different conditional states. Because mossy cells innervate both granule cells and inhibitory interneurons (Sloviter et al., 2003), the granule cell layer might shift between lamellar- and non-lamellar modes of function depending on whether granule cell associative excitation- or translamellar lateral inhibition predominates (Sloviter et al., 2012). That is, when mossy cell excitation of granule cells and basket cells results in net inhibition of granule cells, lamellar function might be operative. Conversely, under unknown conditions in which mossy cells might predominantly excite granule cells, i.e., if and when basket cells and axo-axonic cells are powerfully inhibited, perhaps via septal input as described above, or via basket cell–basket cell interactions (Bartos et al., 2001), the granule cell layer might theoretically respond to entorhinal excitation as a functional "syncytium," with the hippocampus operating as a single giant cortical module (Wittner et al., 2007).

Just as "petit mal" seizures apparently involve a defective switching of the thalamic pacemaker that causes sleep-like rhythms to occur during the awake state (Beenhakker and Huguenard, 2009), a failure to switch correctly between lamellar and non-lamellar hippocampal states might give rise to psychotic ideation, which can occur during spontaneous temporal lobe seizures (Nadkarni et al., 2007; Elliott et al., 2009; Small et al., 2011). A complete or partial shift from a "lamellar" to a "non-lamellar" functional state (Paré and Llinás, 1994) could occur under different normal behavioral conditions (Winson and Abzug, 1977; Lapray et al., 2012), or in temporal lobe epilepsy, where the injury-induced loss of mossy cells may cause normally functionally separated granule cells to become disinhibited, to coalesce, and to discharge synchronously in response to entorhinal input (Sloviter et al., 2012). Lamellar malfunction could therefore theoretically underlie both psychiatric and epileptic phenomena in which the hippocampus is causally involved. If mossy cells do indeed establish pattern separation in the dentate gyrus (Jinde et al., in press), then any genetic or developmental abnormalities that affect the final innervation patterns that mossy cells form postnatally might produce abnormal lateral inhibitory "maps" that influence lamellar hippocampal function and underlie some psychiatric and/or neurological disorders (Small et al., 2011), although this is admittedly speculative.

HOW WIDE IS A "LAMELLA?"

Although few disagreements exist about any specific features of hippocampal anatomy, perspectives differ with regard to their possible physiological implications because each perspective is dependent on how the anatomical data are judged, included, excluded, weighted, and related to the physiology. For example, it is difficult to address the question of how "wide" a lamella might be because we view the maximum lengths of longitudinally projecting axons to be only superficially related to the parameters of lamellar physiology. In addition, the fact that very few granule cells discharge at any given time (Jung and McNaughton, 1993; Alme et al., 2010), and the observation that individual granule cells form non-convergent connections with a small number of CA3 pyramidal cells (Acsády et al., 1998), contrast with the simplistic idea that entorhinal input causes the discharge of all granule cells and CA3 pyramidal cells within a lamella. Thus, it should be recognized that a perforant path stimulus delivered in the laboratory, which massively excites many targeted granule cells, is likely to be far less selective than a perforant path volley that occurs physiologically in a freely moving animal. In addition, lamellar function may have significant transverse, as well as longitudinal, components. That is, some granule cells within a transverse lamella might selectively innervate a subpopulation of CA3a pyramidal cells, whereas other granule cells within the same lamella might preferentially target a subset of CA3b pyramidal cells (Deguchi et al., 2011; Moser, 2011). If this is the case, the discharges of individual granule cells within the same transverse plane could encode different memories or locations (Alme et al., 2010) based on differences in the targeting of each granule cell. Therefore, physiological pattern separation may occur on multiple levels (multiple locations and long both the longitudinal and transverse axes) in a far more complex manner than anything that can be adequately described by citing a particular anatomical distance along the septo-hippocampal axis. For these reasons, we hesitate to speculate further on the possibly irrelevant and unanswerable question of how "wide" a lamella might be, or how many "lamellae" a hippocampus might contain. However, the observations that both dentate mossy cells and CA3 pyramidal cells innervate their longitudinally distant targets unevenly, with periodicities of ∼900 μm for mossy cells (Soltesz et al., 1993) and ∼300–600 μm for CA3 pyramidal cells (Hsu and Buzsáki, 1993; Li et al., 1994), may be particularly relevant in this regard.

TESTING THE HYPOTHESES

The value of any hypothesis depends largely on how testable and falsifiable it is (Popper, 1959; Kuhn, 1962). We contend that many of the hypotheses we have addressed or suggested in this review are eminently testable. It is certainly feasible to describe the topographical details of the entorhinal and septal inputs to the hippocampus more definitively, and it is similarly possible to conduct *in vivo* studies to identify the conditions under which longitudinal pathways have net excitatory or inhibitory effects on distant principal cell excitability. The septal inputs to hippocampal principal cells and interneurons can be elucidated in terms of their topography in both the longitudinal and transverse axes, and selective elimination of septal and other neurons, as has been done successfully in the hippocampus (Martin and Sloviter, 2001), is a practical approach that might clarify the role of extrahippocampal inputs in hippocampal network function. Whether it is currently practical and feasible to definitively demonstrate dual modes of lamellar hippocampal function is unclear, but one purpose in raising these issues is to emphasize that a reconsideration of the possibilities will suggest practical strategies to others and facilitate alternate interpretations of results obtained in behavioral and electrophysiological studies. As always, a main obstacle to progress is the belief that the important issues have been "settled" and, therefore, continued discussion is unnecessary and maybe even detrimental to further advances in understanding. Our main point is that the structural and functional organization of the hippocampal formation is still incompletely understood, and that all possibilities should be considered undogmatically when the results of experiments are interpreted, or when the hippocampus is modeled under a particular set of assumptions.

SUMMARY AND CONCLUSION

If the lamellar hypothesis is strictly defined from an anatomical perspective to imply that all excitatory activity must be restricted to single transverse slices no wider than the mossy fiber pathway, then even a single axon traveling outside a thin transverse hippocampal "slice" might refute the entire hypothesis. In our view, there is little to be gained from such a restrictive definition of lamellar organization, which was neither stated nor implied in the original or subsequent discussions of the hypothesis (Andersen et al., 1971, 2000; Lømo, 1971, 2009). We suggest that modification of the original lamellar hypothesis to incorporate new data and evolving perspectives is the prudent course, and preferable to outright rejection of an unnecessarily strict interpretation of the hypothesis. With that in mind, we suggest that lamellar

organization is a likely design feature of the dentate gyrus in particular, and that the mossy cell-derived longitudinal fiber system in the dentate gyrus may subserve that function by mediating lateral inhibition (as well as underlying associative excitation) in the granule cell layer (Sloviter, 1994; Sloviter and Brisman, 1995; Zappone and Sloviter, 2004; Jinde et al., in press). Once the lamellar impulses reach the CA3 region via the mossy fiber pathway, recurrent excitatory connections between pyramidal cells (Miles and Wong, 1987), and the extensive transverse and longitudinal axons of CA3 pyramidal cells, presumably convey this lamellar information topographically to multiple targets, including inhibitory interneurons and CA1 pyramidal cells (Ishizuka et al., 1990; Tamamaki and Nojyo, 1991; Li et al., 1994; Wittner et al., 2006), which finally activate the subiculum and entorhinal areas topographically (Amaral and Lavenex, 2007) for purposes that we do not yet fully understand.

Based on the sum of the available anatomical information, and the stipulation that every general anatomical statement is a generalization for which exceptions can be made, we suggest the following perspective. First, there are significant similarities between dentate granule cells, the main "entrance gate" to the hippocampus (Winson and Abzug, 1977), and CA1 pyramidal cells, the main output population. Granule cells and CA1 pyramidal cells lack recurrent excitatory connections, and their axons form few commissural or associational collaterals (Amaral and Lavenex, 2007). Therefore, both granule cells and CA1 pyramidal cells appear designed to receive and faithfully transmit "lamellar" information to their specific targets, which are the area CA3 neurons and the subiculum, respectively. Second, the lamellar granule cell output excites CA3 pyramidal cells, which uniquely form recurrent excitatory connections with other CA3 pyramidal cells, and also innervate CA1 pyramidal cells (Ishizuka et al., 1990; Li et al., 1994), axo-somatic interneurons in particular (Wittner et al., 2006), and targets in the lateral septum (Swanson et al., 1981). If normal hippocampal function involves synchronized excitation of spatially separated CA1 pyramidal cells (Deadwyler and Hampson, 1999; Hampson et al., 1999; Senior et al., 2008), then longitudinal associational axons of CA3 pyramidal cells would presumably be required for lamellar function, rather than being antithetical to it.

The scenarios discussed above emphasize our clearly subjective judgments about which anatomical features might be functionally most important, and we have not highlighted other anatomical features, such as the mossy fibers that turn longitudinally at the end of their termination in area CA3a (Swanson et al., 1981; Tamamaki and Nojyo, 1991; Acsády et al., 1998; Ropireddy and Ascoli, 2011), the entorhinal input from Layer III that innervates stratum lacunosum-moleculare interneurons and the distal apical dendrites of CA1 pyramidal cells (Jones, 1993; Vinogradova, 2001), semilunar granule cells (Hyde and Strowbridge, 2012), the perforant path fibers that directly innervate the distal apical dendrites of CA3a and CA3b pyramidal cells, or the CA3c-mossy cell "back-projection" (Amaral and Lavenex, 2007). Neurons send axons in response to molecular guidance cues presumably related to concentration gradients (Kolodkin and Tessier-Lavigne, 2011), and it is possible that some minor anatomical features, such as the longitudinal turn of mossy fibers at the end of their trajectory, or the CA3c-mossy cell "back-projection," could be functionally insignificant developmental aberrations that unavoidably develop in response to nearby attractant gradients.

We do not pretend to know which of these and other anatomical features may have major, minor, or negligible functional importance, or how, and to what extent, each anatomical feature dictates or influences hippocampal encoding of memories, or creation of maps of the spatial environment (Vinogradova, 2001; Giocomo et al., 2011; Krupic et al., 2012). Multiple hypotheses exist regarding the relationship between the dentate gyrus and area CA3 in memory formation and storage (McNaughton and Morris, 1987; McNaughton, 1989; Treves and Rolls, 1992; Patton and McNaughton, 1995; Colgin et al., 2008; Rolls, 2010), and it is beyond the scope of this work to suggest a comprehensive model of hippocampal function that incorporates and assigns relative importance to every known structural and molecular feature. Here we are simply arguing in favor of being open to multiple possibilities, and being willing to consider all of the relevant data, regardless of whether they support or undermine a particular perspective. In addition, it is at least possible that studying anesthetized animals and tissue slices gives us an inherently inaccurate picture of hippocampal physiology in its natural state. From our perspective, the sum of the available data favors the view that: (1) the existence of excitatory, longitudinally projecting associational pathways of dentate mossy cells and CA3 pyramidal cells is in no way antithetical to the concept of lamellar function; it depends on what these pathways do, and; (2) that afferent activity from the septum and brainstem nuclei (Bland and Oddie, 1998), which topographically target mossy cells and inhibitory interneurons, might play a central role in defining lamellar function, and perhaps switching between "lamellar" and "non-lamellar" functional states.

Clearly, inputs from extrahippocampal brain regions, and other factors, including the spatio-temporal interactions between principal cells (Senior et al., 2008) and among inhibitory neuron subpopulations (Bartos et al., 2001) and principal cells (Klausberger and Somogyi, 2008; Lapray et al., 2012), may play crucial roles in establishing and regulating lamellar function. The recent finding that there may be parallel, target-specific "subpathways" within each trisynaptic circuit (Deguchi et al., 2011; Moser, 2011), which is suggestive of an even more "lamellar" functional separation of signals in the dentate gyrus than originally conceived by Andersen et al. (1971), emphasizes the importance of recognizing that all "pathways" or influences are not anatomically obvious, and therefore, it might be prudent to have a malleable definition of what constitutes, defines, and governs "lamellar" function. An awareness that current hypotheses need to leave room for new processes and principles of organization that are yet to be discovered might facilitate reaching a closer approximation of the "truth," whatever that might someday be understood to be.

ACKNOWLEDGMENTS

We thank Drs. Norman Bowery, György Buzsáki, Michael Frotscher, Daniel Lowenstein, Peter MacLeish, Bruce McNaughton, and Menno Witter for useful discussions and suggestions, and their constructive criticism of earlier versions of this manuscript.

REFERENCES

Acsády, L., Halasy, K., and Freund, T. F. (1993). Calretinin is present in non-pyramidal cells of the rat hippocampus – III. Their inputs from the median raphe and medial septal nuclei. *Neuroscience* 52, 829–841.

Acsády, L., Kamondi, A., Sík, A., Freund, T., and Buzsáki, G. (1998). GABAergic cells are the major postsynaptic targets of mossy fibers in the rat hippocampus. *J. Neurosci.* 18, 3386–3403.

Alme, C. B., Buzzetti, R. A., Marrone, D. F., Leutgeb, J. K., Chawla, M. K., Schaner, M. J., et al. (2010). Hippocampal granule cells opt for early retirement. *Hippocampus* 20, 1109–1123.

Amaral, D. G., Dolorfo, C., and Alvarez-Royo, P. (1991). Organization of CA1 projections to the subiculum: a PHA-L analysis in the rat. *Hippocampus* 1, 415–435.

Amaral, D. G., and Kurz, J. (1985). An analysis of the origins of the cholinergic and noncholinergic septal projections to the hippocampal formation of the rat. *J. Comp. Neurol.* 240, 37–59.

Amaral, D. G., and Witter, M. P. (1989). The three-dimensional organization of the hippocampal formation: a review of anatomical data. *Neuroscience* 31, 571–591.

Amaral, D. G., and Lavenex, P. (2007). "Hippocampal neuroanatomy," in *The Hippocampus Book*, eds. P. Andersen, R. Morris, D. Amaral, T. Bliss, and J. O'Keefe (Oxford: Oxford University Press), 37–114.

Andersen, P., Bliss, T. V., Lømo, T., Olsen, L. I., and Skrede, K. K. (1969). Lamellar organization of hippocampal excitatory pathways. *Acta Physiol. Scand.* 76, 4A–5A.

Andersen, P., Bliss, T. V., and Skrede, K. K. (1971). Lamellar organization of hippocampal pathways. *Exp. Brain Res.* 13, 222–238.

Andersen, P., Hagan, P. J., Phillips, C. G., and Powell, T. P. (1975). Mapping by microstimulation of overlapping projections from area 4 to motor units of the baboon's hand. *Proc. R. Soc. Lond. B Biol. Sci.* 188, 31–36.

Andersen, P., Holmqvist, B., and Voorhoeve, P. E. (1966). Entorhinal activation of dentate granule cells. *Acta Physiol. Scand.* 66, 448–460.

Andersen, P., Morris, R., Amaral, D., Bliss, T., and O'Keefe, J. (2007). *The Hippocampus Book*. Oxford: Oxford University Press.

Andersen, P., Soleng, A. F., and Raastad, M. (2000). The hippocampal lamella hypothesis revisited. *Brain Res.* 886, 165–171.

Bakst, I., Avendano, C., Morrison, J. H., and Amaral, D. G. (1986). An experimental analysis of the origins of somatostatin-like immunoreactivity in the dentate gyrus of the rat. *J. Neurosci.* 6, 1452–1462.

Bartos, M., Vida, I., Frotscher, M., Geiger, J. R., and Jonas, P. (2001). Rapid signaling at inhibitory synapses in a dentate gyrus interneuron network. *J. Neurosci.* 21, 2687–2698.

Beenhakker, M. P., and Huguenard, J. R. (2009). Neurons that fire together also conspire together: is normal sleep circuitry hijacked to generate epilepsy? *Neuron* 62, 612–632.

Berger, T. W., Semple-Rowland, S., and Bassett, J. L. (1981). Hippocampal polymorph neurons are the cells of origin for ipsilateral association and commissural afferents to the dentate gyrus. *Brain Res.* 224, 329–336.

Bernard, C., and Wheal, H. V. (1994). Model of local connectivity patterns in CA3 and CA1 areas of the hippocampus. *Hippocampus* 4, 497–529.

Bilkey, D. K., and Goddard, G. V. (1987). Septohippocampal and commissural pathways antagonistically control inhibitory interneurons in the dentate gyrus. *Brain Res.* 405, 320–325.

Blackstad, T. W., Brink, K., Hem, J., and Jeune, B. (1970). Distribution of hippocampal mossy fibers in the rat. An experimental study with silver impregnation methods. *J. Comp. Neurol.* 138, 433–449.

Bland, B. H., and Oddie, S. D. (1998). Anatomical, electrophysiological and pharmacological studies of ascending brainstem hippocampal synchronizing pathways. *Neurosci. Biobehav. Rev.* 22, 259–273.

Bliss, T. V., and Lømo, T. (1973). Long-lasting potentiation of synaptic transmission in the dentate area of the anaesthetized rabbit following stimulation of the perforant path. *J. Physiol. (Lond.)* 232, 331–356.

Buckmaster, P. S. (2012). Mossy cell dendritic structure quantified and compared with other hippocampal neurons labeled in rats in vivo. *Epilepsia* 53(Suppl 1), 9–17.

Buckmaster, P. S., and Schwartzkroin, P. A. (1994). Hippocampal mossy cell function: a speculative view. *Hippocampus* 4, 393–402.

Buckmaster, P. S., and Schwartzkroin, P. A. (1995). Interneurons and inhibition in the dentate gyrus of the rat in vivo. *J. Neurosci.* 15, 774–789.

Buckmaster, P. S., Wenzel, H. J., Kunkel, D. D., and Schwartzkroin, P. A. (1996). Axon arbors and synaptic connections of hippocampal mossy cells in the rat in vivo. *J. Comp. Neurol.* 366, 271–292.

Bumanglag, A. V., and Sloviter, R. S. (2008). Minimal latency to hippocampal epileptogenesis and clinical epilepsy after perforant pathway stimulation-induced status epilepticus in awake rats. *J. Comp. Neurol.* 510, 561–580.

Buzsáki, G. (1984). Feed-forward inhibition in the hippocampal formation. *Prog. Neurobiol.* 22, 131–153.

Buzsáki, G., and Czeh, G. (1981). Commissural and perforant path interactions in the rat hippocampus. Field potentials and unitary activity. *Exp. Brain Res.* 43, 429–438.

Buzsáki, G., and Eidelberg, E. (1981). Commissural projection to the dentate gyrus of the rat: evidence for feed-forward inhibition. *Brain Res.* 230, 346–350.

Buzsáki, G., and Eidelberg, E. (1982). Direct afferent excitation and long-term potentiation of hippocampal interneurons. *J. Neurophysiol.* 48, 597–607.

Buzsáki, G., Grastyan, E., Czopf, J., Kellenyi, L., and Prohaska, O. (1981). Changes in neuronal transmission in the rat hippocampus during behavior. *Brain Res.* 225, 235–247.

Claiborne, B. J., Amaral, D. G., and Cowan, W. M. (1986). A light and electron microscopic analysis of the mossy fibers of the rat dentate gyrus. *J. Comp. Neurol.* 246, 435–458.

Cohen, D., and Yarom, Y. (2000). Cerebellar on-beam and lateral inhibition: two functionally distinct circuits. *J. Neurophysiol.* 83, 1932–1940.

Colgin, L. L., Moser, E. I., and Moser, M. B. (2008). Understanding memory through hippocampal remapping. *Trends Neurosci.* 31, 469–477.

De Gennaro, L., Marzano, C., Moroni, F., Curcio, G., Ferrara, M., and Cipolli, C. (2010). Recovery sleep after sleep deprivation almost completely abolishes dream recall. *Behav. Brain Res.* 206, 293–298.

Deadwyler, S. A., and Hampson, R. E. (1999). Anatomic model of hippocampal encoding of spatial information. *Hippocampus* 9, 397–412.

Deguchi, Y., Donato, F., Galimberti, I., Cabuy, E., and Caroni, P. (2011). Temporally matched subpopulations of selectively interconnected principal neurons in the hippocampus. *Nat. Neurosci.* 14, 495–504.

Deller, T., Katona, I., Cozzari, C., Frotscher, M., and Freund, T. F. (1999). Cholinergic innervation of mossy cells in the rat fascia dentata. *Hippocampus* 9, 314–320.

Dolorfo, C. L., and Amaral, D. G. (1998). Entorhinal cortex of the rat: topographic organization of the cells of origin of the perforant path projection to the dentate gyrus. *J. Comp. Neurol.* 398, 25–48.

Douglas, R. M., McNaughton, B. L., and Goddard, G. V. (1983). Commissural inhibition and facilitation of granule cell discharge in fascia dentata. *J. Comp. Neurol.* 219, 285–294.

Eccles, J. C., Ito, M., and Szentagothai, J. (1967). *The Cerebellum as a Neuronal Machine*. Berlin: Springer-Verlag.

Elliott, B., Joyce, E., and Shorvon, S. (2009). Delusions, illusions and hallucinations in epilepsy: 2. Complex phenomena and psychosis. *Epilepsy Res.* 85, 172–186.

Freund, T. F., and Antal, M. (1988). GABA-containing neurons in the septum control inhibitory interneurons in the hippocampus. *Nature* 336, 170–173.

Freund, T. F., and Buzsáki, G. (1996). Interneurons of the hippocampus. *Hippocampus* 6, 347–470.

Frotscher, M. (1992). Application of the Golgi/electron microscopy technique for cell identification in immunocytochemical, retrograde labeling, and developmental studies of hippocampal neurons. *Microsc. Res. Tech.* 23, 306–323.

Frotscher, M., Soriano, E., and Misgeld, U. (1994). Divergence of hippocampal mossy fibers. *Synapse* 16, 148–160.

Fyhn, M., Hafting, T., Treves, A., Moser, M. B., and Moser, E. I. (2007). Hippocampal remapping and grid realignment in entorhinal cortex. *Nature* 446, 190–194.

Gaarskjaer, F. B. (1978). Organization of the mossy fiber system of the rat studied in extended hippocampi. II. Experimental analysis of fiber distribution with silver impregnation methods. *J. Comp. Neurol.* 178, 73–88.

Gaarskjaer, F. B. (1981). The hippocampal mossy fiber system of the rat studied with retrograde tracing techniques. Correlation between topographic organization and neurogenetic gradients. *J. Comp. Neurol.* 203, 717–735.

Gao, W., Chen, G., Reinert, K. C., and Ebner, T. J. (2006). Cerebellar cortical molecular layer inhibition is organized in parasagittal zones. *J. Neurosci.* 26, 8377–8387.

Germroth, P., Schwerdtfeger, W. K., and Buhl, E. H. (1989). GABAergic neurons in the entorhinal cortex project to the hippocampus. *Brain Res.* 494, 187–192.

Giocomo, L. M., Moser, M. B., and Moser, E. I. (2011). Computational models of grid cells. *Neuron* 71, 589–603.

Gloveli, T., Dugladze, T., Rotstein, H. G., Traub, R. D., Monyer, H., Heinemann, U., et al. (2005). Orthogonal arrangement of rhythm-generating microcircuits in the hippocampus. *Proc. Natl. Acad. Sci. U.S.A.* 102, 13295–13300.

Goodman, J. H., and Sloviter, R. S. (1992). Evidence for commissurally projecting parvalbumin-immunoreactive basket cells in the dentate gyrus of the rat. *Hippocampus* 2, 13–21.

Gulyás, A. I., Hájos, N., Katona, I., and Freund, T. F. (2003). Interneurons are the local targets of hippocampal inhibitory cells which project to the medial septum. *Eur. J. Neurosci.* 17, 1861–1872.

Gulyás, A. I., Miles, R., Sik, A., Toth, K., Tamamaki, N., and Freund, T. F. (1993). Hippocampal pyramidal cells excite inhibitory neurons through a single release site. *Nature* 366, 683–687.

Halasy, K., Miettinen, R., Szabat, E., and Freund, T. F. (1992). GABAergic interneurons are the major postsynaptic targets of median raphe afferents in the rat dentate gyrus. *Eur. J. Neurosci.* 4, 144–153.

Halasy, K., and Somogyi, P. (1993). Subdivisions in the multiple GABAergic innervation of granule cells in the dentate gyrus of the rat hippocampus. *Eur. J. Neurosci.* 5, 411–429.

Hampson, R. E., Simeral, J. D., and Deadwyler, S. A. (1999). Distribution of spatial and nonspatial information in dorsal hippocampus. *Nature* 402, 610–614.

Hetherington, P. A., Austin, K. B., and Shapiro, M. L. (1994). Ipsilateral associational pathway in the dentate gyrus: an excitatory feedback system that supports N-methyl-D-aspartate-dependent long-term potentiation. *Hippocampus* 4, 422–438.

Hjorth-Simonsen, A., and Jeune, B. (1972). Origin and termination of the hippocampal perforant path in the rat studied by silver impregnation. *J. Comp. Neurol.* 144, 215–232.

Hsu, M., and Buzsáki, G. (1993). Vulnerability of mossy fiber targets in the rat hippocampus to forebrain ischemia. *J. Neurosci.* 13, 3964–3979.

Hyde, R. A., and Strowbridge, B. W. (2012). Mnemonic representations of transient stimuli and temporal sequences in the rodent hippocampus in vitro. *Nat. Neurosci.* 15, 1430–1438.

Ishizuka, N., Weber, J., and Amaral, D. G. (1990). Organization of intrahippocampal projections originating from CA3 pyramidal cells in the rat. *J. Comp. Neurol.* 295, 580–623.

Ito, M. (1984). *The Cerebellum and Neural Control.* New York: Raven.

Jinde, S., Zsiros, V., Jiang, Z., Nakao, K., Kohno, K., Belforte, J. E., et al. (in press). Hilar mossy cell degeneration causes transient dentate granule cell hyperexcitability and impaired pattern separation. *Neuron.* doi:10.1016/j.neuron.2012.10.036

Jinno, S., and Kosaka, T. (2002). Immunocytochemical characterization of hippocamposeptal projecting GABAergic nonprincipal neurons in the mouse brain: a retrograde labeling study. *Brain Res.* 945, 219–231.

Jones, R. S. (1993). Entorhinal-hippocampal connections: a speculative view of their function. *Trends Neurosci.* 16, 58–64.

Jung, M. W., and McNaughton, B. L. (1993). Spatial selectivity of unit activity in the hippocampal granular layer. *Hippocampus* 3, 165–182.

Kandel, E. R., Schwartz, J. H., and Jessel, T. M. (2000). *Principles of Neural Science.* New York: McGraw Hill.

Kempermann, G. (2012). Neuroscience. Youth culture in the adult brain. *Science* 335, 1175–1176.

Kiss, J., Patel, A. J., and Freund, T. F. (1990). Distribution of septohippocampal neurons containing parvalbumin or choline acetyltransferase in the rat brain. *J. Comp. Neurol.* 298, 362–372.

Klausberger, T., and Somogyi, P. (2008). Neuronal diversity and temporal dynamics: the unity of hippocampal circuit operations. *Science* 321, 53–57.

Kolodkin, A. L., and Tessier-Lavigne, M. (2011). Mechanisms and molecules of neuronal wiring: a primer. *Cold Spring Harb. Perspect. Biol.* 3:a001727. doi:10.1101/cshperspect.a001727

Krupic, J., Burgess, N., and O'Keefe, J. (2012). Neural representations of location composed of spatially periodic bands. *Science* 337, 853–857.

Kuhn, T. S. (1962). *The Structure of Scientific Revolutions.* Chicago: University of Chicago Press.

Lapray, D., Lasztoczi, B., Lagler, M., Viney, T. J., Katona, L., Valenti, O., et al. (2012). Behavior-dependent specialization of identified hippocampal interneurons. *Nat. Neurosci.* 15, 1265–1271.

Laurberg, S., and Sørensen, K. E. (1981). Associational and commissural collaterals of neurons in the hippocampal formation (hilus fasciae dentatae and subfield CA3). *Brain Res.* 212, 287–300.

Leranth, C., and Frotscher, M. (1989). Organization of the septal region in the rat brain: cholinergic-GABAergic interconnections and the termination of hippocampo-septal fibers. *J. Comp. Neurol.* 289, 304–314.

Leranth, C., Malcolm, A. J., and Frotscher, M. (1990). Afferent and efferent synaptic connections of somatostatin-immunoreactive neurons in the rat fascia dentata. *J. Comp. Neurol.* 295, 111–122.

Leutgeb, J. K., Leutgeb, S., Moser, M. B., and Moser, E. I. (2007). Pattern separation in the dentate gyrus and CA3 of the hippocampus. *Science* 315, 961–966.

Li, X. G., Somogyi, P., Ylinen, A., and Buzsáki, G. (1994). The hippocampal CA3 network: an in vivo intracellular labeling study. *J. Comp. Neurol.* 339, 181–208.

Lømo, T. (1971). Patterns of activation in a monosynaptic cortical pathway: the perforant path input to the dentate area of the hippocampal formation. *Exp. Brain Res.* 12, 18–45.

Lømo, T. (2009). Excitability changes within transverse lamellae of dentate granule cells and their longitudinal spread following orthodromic or antidromic activation. *Hippocampus* 19, 633–648.

Lorente De Nó, R. (1934). Studies on the structure of the cerebral cortex. II. Continuation of the study of the ammonic system. *J. Psychol. Neurol.* 46, 113–177.

Lubenov, E. V., and Siapas, A. G. (2009). Hippocampal theta oscillations are travelling waves. *Nature* 459, 534–539.

Lübke, J., Deller, T., and Frotscher, M. (1997). Septal innervation of mossy cells in the hilus of the rat dentate gyrus: an anterograde tracing and intracellular labeling study. *Exp. Brain Res.* 114, 423–432.

Marin-Burgin, A., Mongiat, L. A., Pardi, M. B., and Schinder, A. F. (2012). Unique processing during a period of high excitation/inhibition balance in adult-born neurons. *Science* 335, 1238–1242.

Martin, J. L., and Sloviter, R. S. (2001). Focal inhibitory interneuron loss and principal cell hyperexcitability in the rat hippocampus after microinjection of a neurotoxic conjugate of saporin and a peptidase-resistant analog of Substance P. *J. Comp. Neurol.* 436, 127–152.

McCormick, D. A., and von Krosigk, M. (1992). Corticothalamic activation modulates thalamic firing through glutamate "metabotropic" receptors. *Proc. Natl. Acad. Sci. U.S.A.* 89, 2774–2778.

McHugh, T. J., Jones, M. W., Quinn, J. J., Balthasar, N., Coppari, R., Elmquist, J. K., et al. (2007). Dentate gyrus NMDA receptors mediate rapid pattern separation in the hippocampal network. *Science* 317, 94–99.

McNaughton, B. L. (1989). "Neuronal mechanisms for spatial computation and information storage," in *Neural Connections, Mental Computations*, eds. L. Nadel, L. A. Cooper, P. Culicover, and R. M. Harnish (Cambridge, MA: The MIT Press), 285–350.

McNaughton, B. L., Barnes, C. A., and Andersen, P. (1981). Synaptic efficacy and EPSP summation in granule cells of rat fascia dentata studied in vitro. *J. Neurophysiol.* 46, 952–966.

McNaughton, B. L., Barnes, C. A., Gerrard, J. L., Gothard, K., Jung, M. W., Knierim, J. J., et al. (1996). Deciphering the hippocampal polyglot: the hippocampus as a path integration system. *J. Exp. Biol.* 199, 173–185.

McNaughton, B. L., and Morris, R. G. M. (1987). Hippocampal synaptic enhancement and information-storage within a distributed memory system. *Trends Neurosci.* 10, 408–415.

Melzer, S., Michael, M., Caputi, A., Eliava, M., Fuchs, E. C., Whittington, M. A., et al. (2012). Long-range-projecting GABAergic neurons modulate inhibition in hippocampus and entorhinal cortex. *Science* 335, 1506–1510.

Miles, R., and Wong, R. K. (1987). Latent synaptic pathways revealed after tetanic stimulation in the hippocampus. *Nature* 329, 724–726.

Misgeld, U., Bijak, M., and Brunner, H. (1992a). Granule cell inhibition and the activity of hilar neurons. *Epilepsy Res. Suppl.* 7, 113–118.

Misgeld, U., Bijak, M., Brunner, H., and Dembowsky, K. (1992b). K-dependent inhibition in the dentate-CA3 network of guinea pig hippocampal slices. *J. Neurophysiol.* 68, 1548–1557.

Mistry, R., Dennis, S., Frerking, M., and Mellor, J. R. (2011). Dentate gyrus granule cell firing patterns can induce mossy fiber long-term potentiation in vitro. *Hippocampus* 21, 1157–1168.

Morris, R. G. M. (2007). "Theories of hippocampal function," in *The Hippocampus Book*, eds. P. Andersen, R. Morris, D. Amaral, T. Bliss, and J.

O'Keefe (Oxford: Oxford University Press), 581–713.
Moser, E. I. (2011). The multi-laned hippocampus. *Nat. Neurosci.* 14, 407–408.
Myers, C. E., and Scharfman, H. E. (2011). Pattern separation in the dentate gyrus: a role for the CA3 backprojection. *Hippocampus* 21, 1190–1215.
Nadkarni, S., Arnedo, V., and Devinsky, O. (2007). Psychosis in epilepsy patients. *Epilepsia* 48(Suppl 9), 17–19.
Nakashiba, T., Cushman, J. D., Pelkey, K. A., Renaudineau, S., Buhl, D. L., McHugh, T. J., et al. (2012). Young dentate granule cells mediate pattern separation, whereas old granule cells facilitate pattern completion. *Cell* 149, 188–201.
Nitz, D. A., and McNaughton, B. L. (1999). Hippocampal EEG and unit activity responses to modulation of serotonergic median raphe neurons in the freely behaving rat. *Learn. Mem.* 6, 153–167.
Nyakas, C., Luiten, P. G., Spencer, D. G., and Traber, J. (1987). Detailed projection patterns of septal and diagonal band efferents to the hippocampus in the rat with emphasis on innervation of CA1 and dentate gyrus. *Brain Res. Bull.* 18, 533–545.
O'Keefe, J., and Nadel, L. (1978). *The Hippocampus as a Cognitive Map*. Oxford: Clarendon.
Paré, D., and Llinás, R. (1994). Nonlamellar propagation of entorhinal influences in the hippocampal formation: multiple electrode recordings in the isolated guinea pig brain in vitro. *Hippocampus* 4, 403–409.
Patel, J., Fujisawa, S., Berenyi, A., Royer, S., and Buzsáki, G. (2012). Traveling theta waves along the entire septotemporal axis of the hippocampus. *Neuron* 75, 410–417.
Patton, P. E., and McNaughton, B. (1995). Connection matrix of the hippocampal formation: I. The dentate gyrus. *Hippocampus* 5, 245–286.
Popper, K. R. (1959). *The Logic of Scientific Discovery*. New York: Basic Books.
Quilichini, P. P., Le Van Quyen, M., Ivanov, A., Turner, D. A., Carabalona, A., Gozlan, H., et al. (2012). Hub GABA neurons mediate gamma-frequency oscillations at ictal-like event onset in the immature hippocampus. *Neuron* 74, 57–64.
Ratzliff, A. H., Howard, A. L., Santhakumar, V., Osapay, I., and Soltesz, I. (2004). Rapid deletion of mossy cells does not result in a hyperexcitable dentate gyrus: implications for epileptogenesis. *J. Neurosci.* 24, 2259–2269.
Rolls, E. T. (2010). A computational theory of episodic memory formation in the hippocampus. *Behav. Brain Res.* 215, 180–196.
Ropireddy, D., and Ascoli, G. A. (2011). Potential Synaptic Connectivity of Different Neurons onto Pyramidal Cells in a 3D Reconstruction of the Rat Hippocampus. *Front. Neuroinform.* 5:5. doi:10.3389/fninf.2011.00005
Ropireddy, D., Scorcioni, R., Lasher, B., Buzsáki, G., and Ascoli, G. A. (2011). Axonal morphometry of hippocampal pyramidal neurons semi-automatically reconstructed after in vivo labeling in different CA3 locations. *Brain Struct. Funct.* 216, 1–15.
Ruth, R. E., Collier, T. J., and Routtenberg, A. (1982). Topography between the entorhinal cortex and the dentate septotemporal axis in rats: I. Medial and intermediate entorhinal projecting cells. *J. Comp. Neurol.* 209, 69–78.
Ruth, R. E., Collier, T. J., and Routtenberg, A. (1988). Topographical relationship between the entorhinal cortex and the septotemporal axis of the dentate gyrus in rats: II. Cells projecting from lateral entorhinal subdivisions. *J. Comp. Neurol.* 270, 506–516.
Scharfman, H. E. (1995). Electrophysiological evidence that dentate hilar mossy cells are excitatory and innervate both granule cells and interneurons. *J. Neurophysiol.* 74, 179–194.
Senior, T. J., Huxter, J. R., Allen, K., O'Neill, J., and Csicsvari, J. (2008). Gamma oscillatory firing reveals distinct populations of pyramidal cells in the CA1 region of the hippocampus. *J. Neurosci.* 28, 2274–2286.
Sík, A., Penttonen, M., and Buzsáki, G. (1997). Interneurons in the hippocampal dentate gyrus: an in vivo intracellular study. *Eur. J. Neurosci.* 9, 573–588.
Sik, A., Tamamaki, N., and Freund, T. F. (1993). Complete axon arborization of a single CA3 pyramidal cell in the rat hippocampus, and its relationship with postsynaptic parvalbumin-containing interneurons. *Eur. J. Neurosci.* 5, 1719–1728.
Sloviter, R. S. (1983). "Epileptic" brain damage in rats induced by sustained electrical stimulation of the perforant path. I. Acute electrophysiological and light microscopic studies. *Brain Res. Bull.* 10, 675–697.
Sloviter, R. S. (1987). Decreased hippocampal inhibition and a selective loss of interneurons in experimental epilepsy. *Science* 235, 73–76.
Sloviter, R. S. (1991a). Feedforward and feedback inhibition of hippocampal principal cell activity evoked by perforant path stimulation: GABA-mediated mechanisms that regulate excitability in vivo. *Hippocampus* 1, 31–40.
Sloviter, R. S. (1991b). Permanently altered hippocampal structure, excitability, and inhibition after experimental status epilepticus in the rat: the "dormant basket cell" hypothesis and its possible relevance to temporal lobe epilepsy. *Hippocampus* 1, 41–66.
Sloviter, R. S. (1994). The functional organization of the hippocampal dentate gyrus and its relevance to the pathogenesis of temporal lobe epilepsy. *Ann. Neurol.* 35, 640–654.
Sloviter, R. S., and Brisman, J. L. (1995). Lateral inhibition and granule cell synchrony in the rat hippocampal dentate gyrus. *J. Neurosci.* 15, 811–820.
Sloviter, R. S., Bumanglag, A. V., Schwarcz, R., and Frotscher, M. (2012). "Abnormal dentate gyrus network circuitry in temporal lobe epilepsy," in *Jasper's Basic Mechanisms of the Epilepsies*, 4th Edn, eds. J. L. Noebels, M. Avoli, M. A. Rogawski, R. W. Olsen, and A. V. Delgado-Escueta (Oxford: Oxford University Press), 454–469.
Sloviter, R. S., and Nilaver, G. (1987). Immunocytochemical localization of GABA-, cholecystokinin-, vasoactive intestinal polypeptide-, and somatostatin-like immunoreactivity in the area dentata and hippocampus of the rat. *J. Comp. Neurol.* 256, 42–60.
Sloviter, R. S., Zappone, C. A., Harvey, B. D., Bumanglag, A. V., Bender, R. A., and Frotscher, M. (2003). "Dormant basket cell" hypothesis revisited: relative vulnerabilities of dentate gyrus mossy cells and inhibitory interneurons after hippocampal status epilepticus in the rat. *J. Comp. Neurol.* 459, 44–76.
Small, S. A. (2002). The longitudinal axis of the hippocampal formation: its anatomy, circuitry, and role in cognitive function. *Rev. Neurosci.* 13, 183–194.
Small, S. A., Schobel, S. A., Buxton, R. B., Witter, M. P., and Barnes, C. A. (2011). A pathophysiological framework of hippocampal dysfunction in ageing and disease. *Nat. Rev. Neurosci.* 12, 585–601.
Soltesz, I., Bourassa, J., and Deschenes, M. (1993). The behavior of mossy cells of the rat dentate gyrus during theta oscillations in vivo. *Neuroscience* 57, 555–564.
Soriano, E., and Frotscher, M. (1989). A GABAergic axo-axonic cell in the fascia dentata controls the main excitatory hippocampal pathway. *Brain Res.* 503, 170–174.
Soriano, E., and Frotscher, M. (1994). Mossy cells of the rat fascia dentata are glutamate-immunoreactive. *Hippocampus* 4, 65–69.
Steriade, M., Iosif, G., and Apostol, V. (1969). Responsiveness of thalamic and cortical motor relays during arousal and various stages of sleep. *J. Neurophysiol.* 32, 251–265.
Struble, R. G., Desmond, N. L., and Levy, W. B. (1978). Anatomical evidence for interlamellar inhibition in the fascia dentata. *Brain Res.* 152, 580–585.
Swanson, L. W., Sawchenko, P. E., and Cowan, W. M. (1981). Evidence for collateral projections by neurons in Ammon's horn, the dentate gyrus, and the subiculum: a multiple retrograde labeling study in the rat. *J. Neurosci.* 1, 548–559.
Swanson, L. W., Wyss, J. M., and Cowan, W. M. (1978). An autoradiographic study of the organization of intrahippocampal association pathways in the rat. *J. Comp. Neurol.* 181, 681–715.
Takács, V. T., Freund, T. F., and Gulyás, A. I. (2008). Types and synaptic connections of hippocampal inhibitory neurons reciprocally connected with the medial septum. *Eur. J. Neurosci.* 28, 148–164.
Tamamaki, N., and Nojyo, Y. (1991). Crossing fiber arrays in the rat hippocampus as demonstrated by three-dimensional reconstruction. *J. Comp. Neurol.* 303, 435–442.
Tamamaki, N., and Nojyo, Y. (1993). Projection of the entorhinal layer II neurons in the rat as revealed by intracellular pressure-injection of neurobiotin. *Hippocampus* 3, 471–480.
Tóth, K., Borhegyi, Z., and Freund, T. F. (1993). Postsynaptic targets of GABAergic hippocampal neurons in the medial septum-diagonal band of broca complex. *J. Neurosci.* 13, 3712–3724.
Treves, A., and Rolls, E. T. (1992). Computational constraints suggest the need for two distinct input systems to the hippocampal CA3 network. *Hippocampus* 2, 189–199.
van Groen, T., Miettinen, P., and Kadish, I. (2003). The entorhinal cortex of the mouse: organization of the projection to the hippocampal formation. *Hippocampus* 13, 133–149.

Vinogradova, O. S. (2001). Hippocampus as comparator: role of the two input and two output systems of the hippocampus in selection and registration of information. *Hippocampus* 11, 578–598.

Winson, J. (1980). Influence of raphe nuclei on neuronal transmission from perforant pathway through dentate gyrus. *J. Neurophysiol.* 44, 937–950.

Winson, J., and Abzug, C. (1977). Gating of neuronal transmission in the hippocampus: efficacy of transmission varies with behavioral state. *Science* 196, 1223–1225.

Witter, M. P. (2007). The perforant path: projections from the entorhinal cortex to the dentate gyrus. *Prog. Brain Res.* 163, 43–61.

Witter, M. P., and Moser, E. I. (2006). Spatial representation and the architecture of the entorhinal cortex. *Trends Neurosci.* 29, 671–678.

Witter, M. P., Van Hoesen, G. W., and Amaral, D. G. (1989). Topographical organization of the entorhinal projection to the dentate gyrus of the monkey. *J. Neurosci.* 9, 216–228.

Wittner, L., Henze, D. A., Zaborszky, L., and Buzsáki, G. (2006). Hippocampal CA3 pyramidal cells selectively innervate aspiny interneurons. *Eur. J. Neurosci.* 24, 1286–1298.

Wittner, L., Henze, D. A., Zaborszky, L., and Buzsáki, G. (2007). Three-dimensional reconstruction of the axon arbor of a CA3 pyramidal cell recorded and filled in vivo. *Brain Struct. Funct.* 212, 75–83.

Wyss, J. M. (1981). An autoradiographic study of the efferent connections of the entorhinal cortex in the rat. *J. Comp. Neurol.* 199, 495–512.

Zappone, C. A., and Sloviter, R. S. (2001). Commissurally projecting inhibitory interneurons of the rat hippocampal dentate gyrus: a colocalization study of neuronal markers and the retrograde tracer Fluorogold. *J. Comp. Neurol.* 441, 324–344.

Zappone, C. A., and Sloviter, R. S. (2004). Translamellar disinhibition in the rat hippocampal dentate gyrus after seizure-induced degeneration of vulnerable hilar neurons. *J. Neurosci.* 24, 853–864.

Zimmer, J. (1971). Ipsilateral afferents to the commissural zone of the fascia dentata, demonstrated in decommissurated rats by silver impregnation. *J. Comp. Neurol.* 142, 393–416.

Zipp, F., Nitsch, R., Soriano, E., and Frotscher, M. (1989). Entorhinal fibers form synaptic contacts on parvalbumin-immunoreactive neurons in the rat fascia dentata. *Brain Res.* 495, 161–166.

Conflict of Interest Statement: The authors declare that the research was conducted in the absence of any commercial or financial relationships that could be construed as a potential conflict of interest.

Received: 29 August 2012; accepted: 21 November 2012; published online: 10 December 2012.

Citation: Sloviter RS and Lømo T (2012) Updating the lamellar hypothesis of hippocampal organization. Front. Neural Circuits ***6****:102. doi: 10.3389/fncir.2012.00102*

frontiers in
NEURAL CIRCUITS

REVIEW ARTICLE
published: 12 February 2013
doi: 10.3389/fncir.2013.00014

Hilar mossy cell circuitry controlling dentate granule cell excitability

Seiichiro Jinde[1†], Veronika Zsiros[2†] and Kazu Nakazawa[2*]

[1] *Department of Neuropsychiatry, Graduate School of Medicine, The University of Tokyo, Tokyo, Japan*
[2] *Unit on Genetics of Cognition and Behavior, National Institute of Mental Health, National Institutes of Health, Department of Health and Human Services, Bethesda, MD, USA*

Edited by:
Peter Jonas, Institute of Science and Technology Austria, Austria

Reviewed by:
Robert S. Sloviter, Morehouse School of Medicine, USA
Rolf Sprengel, Max Planck Institute for Medical Research, Germany

****Correspondence:***
Kazu Nakazawa, Unit on Genetics of Cognition and Behavior, National Institute of Mental Health, National Institutes of Health, Department of Health and Human Services, 35 Convent Drive, Bethesda, MD 20892-3710, USA.
e-mail: nakazawk@mail.nih.gov
† These authors have contributed equally to this work.

Glutamatergic hilar mossy cells of the dentate gyrus can either excite or inhibit distant granule cells, depending on whether their direct excitatory projections to granule cells or their projections to local inhibitory interneurons dominate. However, it remains controversial whether the net effect of mossy cell loss is granule cell excitation or inhibition. Clarifying this controversy has particular relevance to temporal lobe epilepsy, which is marked by dentate granule cell hyperexcitability and extensive loss of dentate hilar mossy cells. Two diametrically opposed hypotheses have been advanced to explain this granule cell hyperexcitability—the "dormant basket cell" and the "irritable mossy cell" hypotheses. The "dormant basket cell" hypothesis proposes that mossy cells normally exert a net inhibitory effect on granule cells and therefore their loss causes dentate granule cell hyperexcitability. The "irritable mossy cell" hypothesis takes the opposite view that mossy cells normally excite granule cells and that the surviving mossy cells in epilepsy increase their activity, causing granule cell excitation. The inability to eliminate mossy cells selectively has made it difficult to test these two opposing hypotheses. To this end, we developed a transgenic toxin-mediated, mossy cell-ablation mouse line. Using these mutants, we demonstrated that the extensive elimination of hilar mossy cells causes granule cell hyperexcitability, although the mossy cell loss observed appeared insufficient to cause clinical epilepsy. In this review, we focus on this topic and also suggest that different interneuron populations may mediate mossy cell-induced translamellar lateral inhibition and intralamellar recurrent inhibition. These unique local circuits in the dentate hilar region may be centrally involved in the functional organization of the dentate gyrus.

Keywords: mossy cells, granule cells, excitability, epileptogenesis, lateral inhibition, hippocampal mossy fibers, pattern separation, temporal lobe epilepsy

INTRODUCTION

The hippocampal formation is critically involved in various brain functions such as spatial memory and navigation (Burgess et al., 2002; Nakazawa et al., 2004), episodic or autobiographical memory (Eichenbaum et al., 1999), and the response to stress (McEwen and Magarinos, 1997). Therefore, any hippocampal impairments potentially lead to cognitive dysfunction or abnormal sensitivity to stress. The hippocampal formation is also often the focus of post-traumatic epileptic seizures, and hippocampal sclerosis is the most common pathology associated with refractory temporal lobe epilepsy (Margerison and Corsellis, 1966). Among hippocampal subregions, the dentate gyrus is the first central information processor, in which granule cells receive sensory inputs from the entorhinal cortex through the perforant path. Granule cell excitation faithfully detonates CA3 pyramidal cells as well as interneurons by mossy fiber axons. Dentate granule cells also send axon collaterals to the dentate hilus (also called the polymorphic cell layer), a region enclosed by the granule cell layer between the upper and lower blades of the dentate gyrus (Amaral et al., 2007). This region has two main classes of neurons, GABAergic interneurons and glutamatergic mossy cells (Soriano and Frotscher, 1994; Wenzel et al., 1997). Importantly, both of these two neuronal cell types are often depleted in the temporal lobe epilepsy patient brains whereas granule cells are less affected. Thus, a long-standing debate has centered on whether hilar neuronal loss is the cause or the consequence of chronic, persistent epileptic activity. In this review, we focus on the function of one type of hilar neuron, mossy cells, and its relation to granule cell activity. In particular, we argue the functional consequence of selective mossy cell loss from our data obtained from an inducible toxin-mediated, mossy cell-ablation mouse line.

PHYSIOLOGY AND CONNECTIVITY OF MOSSY CELLS

Glutamatergic hilar mossy cells are known to be highly excitable, because they receive high-frequency large excitatory synaptic potentials (Livsey and Vicini, 1992; Ishizuka and Kosaka, 1998), while they receive 90% less inhibition, as measured by spontaneous inhibitory postsynaptic potentials (IPSPs), when compared with CA3 pyramidal cells (Buckmaster et al., 1993).

Other properties, such as their relatively high input resistance together with large anomalous rectifier currents and less spike frequency accommodation, also appear to make them more excitable (Buckmaster et al., 1993). Histological studies have revealed that most of the synaptic inputs to mossy cells arrive via mossy fibers of dentate granule cells (Amaral, 1978; Murakawa and Kosaka, 2001). While there are estimated to be a million granule cells but only ∼30,000 mossy cells in rats (Buckmaster and Jongen-Rêlo, 1999), the convergence of mossy fibers onto mossy cells as well as onto CA3 pyramidal cells may be relatively low because granule cells innervate substantially more inhibitory than excitatory cells (Acsády et al., 1998; Mori et al., 2007). Therefore, it is unlikely that the spontaneous activity of mossy cells *in vitro* (Scharfman and Schwartzkroin, 1988; Buckmaster et al., 1992) and *in vivo* (Henze and Buzsáki, 2007) is attributed to the granule cell activity. Alternatively, Williams et al. (2007) recently found that although spiny, granule-like neurons in the inner molecular layer (IML), termed "semilunar granule cells," project to granule cells, these cells' axon collaterals mono-synaptically excite mossy cells. Since semilunar granule cells receive the input from entorhinal cortex in the molecular layer, it is suggested that semilunar granule cells may provide an alternate pathway for entorhinal inputs to persistently drive hilar neurons and CA3 cells (Larimer and Strowbridge, 2010; Gupta et al., 2012). Interestingly, semilunar granule cells also appear to receive mono-synaptic excitatory input from mossy cells (Williams et al., 2007), potentially making "reverberatory circuits." As another alternative, mossy cells also receive several other inputs. For example, mossy cells are known to receive excitatory innervation from the CA3 pyramidal cells, which is called "back-projection." Ishizuka et al. (1990) and later, Li et al. (1994) histologically revealed that CA3 pyramidal cells have collaterals in the hilus, and, particularly, ventral portion of CA3c that was identified as the area with greatest collateralization in the hilus. Additionally, simultaneous recordings in slice preparation showed that immediately after the onset of bicuculline-induced spontaneous bursts in CA3 pyramidal cells, hilar mossy cells, and GABAergic interneurons also demonstrated bursts (Scharfman, 1994a). Because mossy cells send axon to dentate granule cells, these results demonstrated that CA3 pyramidal cells can indirectly activate dentate granule cells via mossy cells under disinhibited condition. A histological study revealed that cholinergic and GABAergic boutons are also abundant around mossy cell somata and on their proximal dendrites, suggesting a direct innervation of hilar mossy cells by GABAergic and cholinergic neurons in the medial septal diagonal band area (Freund and Buzsáki, 1996; Deller et al., 1999). The dentate hilar region also received a prominent noradrenergic input, serotonergic input, dopamine input, and the excitatory inputs from supramammillary area (Amaral et al., 2007) (**Figure 1A**).

Mossy cells send their associational and commissural axonal projections to the ipsi- and contralateral IML of the dentate gyrus along the extensive longitudinal (septo-temporal) axis (Seress and Ribak, 1984; Amaral and Witter, 1989; Deller et al., 1994; Buckmaster et al., 1996; Wenzel et al., 1997; Zappone and Sloviter, 2001). This raises an important question about how the mossy cells function normally. In 1971, Andersen et al. proposed that the major hippocampal principal cell axons are oriented parallel to each other and course nearly transversally to the long axis of the hippocampus, so that the hippocampal cells are activated in such a near-transverse band, called a lamella, which could represent a functional unit of the hippocampus (Andersen et al., 1971). While this lamella hypothesis was criticized because of a wide, fan-shaped distribution of Schaffer collaterals of CA3 pyramidal cell axons, Sloviter suggested that this idea may be still valid in the dentate gyrus, on the assumption that the net effect of the longitudinal information flow in the dentate gyrus is inhibitory (Sloviter, 1994). Since the mossy fiber projection is known to be longitudinally restricted, his proposal on mossy cell-mediated translamellar lateral inhibition of granule cells was based on the previous anatomical finding in rats that hilar mossy cells longitudinally project to distant lamellae spanning 6–7 mm (Amaral and Witter, 1989). While, alternatively, dentate interneurons receiving mossy cell axons could contribute to translamellar granule cell inhibition, associational projections of any inhibitory interneurons appear to be minimal beyond a longitudinal distance of 1 mm (Struble et al., 1978; Qiu and Han, 1995; Buckmaster and Jongen-Rêlo, 1999; Zappone and Sloviter, 2004; Sloviter and Lømo, 2012).

A central question has been whether translamellar projections of excitatory mossy cells directly excite or inhibit granule cells. Anatomically, over 90% of the axon cloud of mossy cells targets granule cell dendrites at IML more septal or temporal to the lamella where the projecting mossy cell soma is located (Buckmaster et al., 1992, 1996). Furthermore, of these synapses 99% are on dendritic spines belonging to granule cells (Buckmaster et al., 1996; Wenzel et al., 1997). However, the mossy cells also send axons to local interneurons in a translamellar manner, which could inhibit dentate granule cell excitability, thereby contributing to feed-forward inhibition (Misgeld et al., 1992; Scharfman, 1994a; Larimer and Strowbridge, 2008). Supporting this, *in vitro* paired recordings studies by Scharfman have demonstrated that mossy cells mono-synaptically excite both granule cells and interneurons (Scharfman, 1994a, 1995). In addition, she observed polysynaptic inhibition of granule cells in response to mossy cell activity. Therefore, the functional impact of mossy cells has been the subjects of recent controversy (Scharfman and Myers, 2012).

MOSSY CELL FUNCTION

Since mossy cells participate in the recurrent excitatory circuitries with granule cells and also have the potential of inhibiting granule cells via excitation of GABAergic interneurons as described above, it has been hypothesized that mossy cells actively regulate the function of the dentate gyrus (Buckmaster and Schwartzkroin, 1994). Early *in vivo* electrophysiological studies consistently suggested that the excitatory commissural fibers that originate from the mossy cells have a net inhibitory effect on granule cells via activation of inhibitory neurons (Buzsáki and Czéh, 1981; Buzsáki and Eidelberg, 1981, 1982; Douglas et al., 1983; Bilkey and Goddard, 1987). However, it has recently been suggested that there is an excitatory influence of mossy cells on the granule cells under normal conditions (Ratzliff et al., 2004; Myers and Scharfman, 2009). In the following sections, we briefly review the roles that mossy cells are predicted to play in the

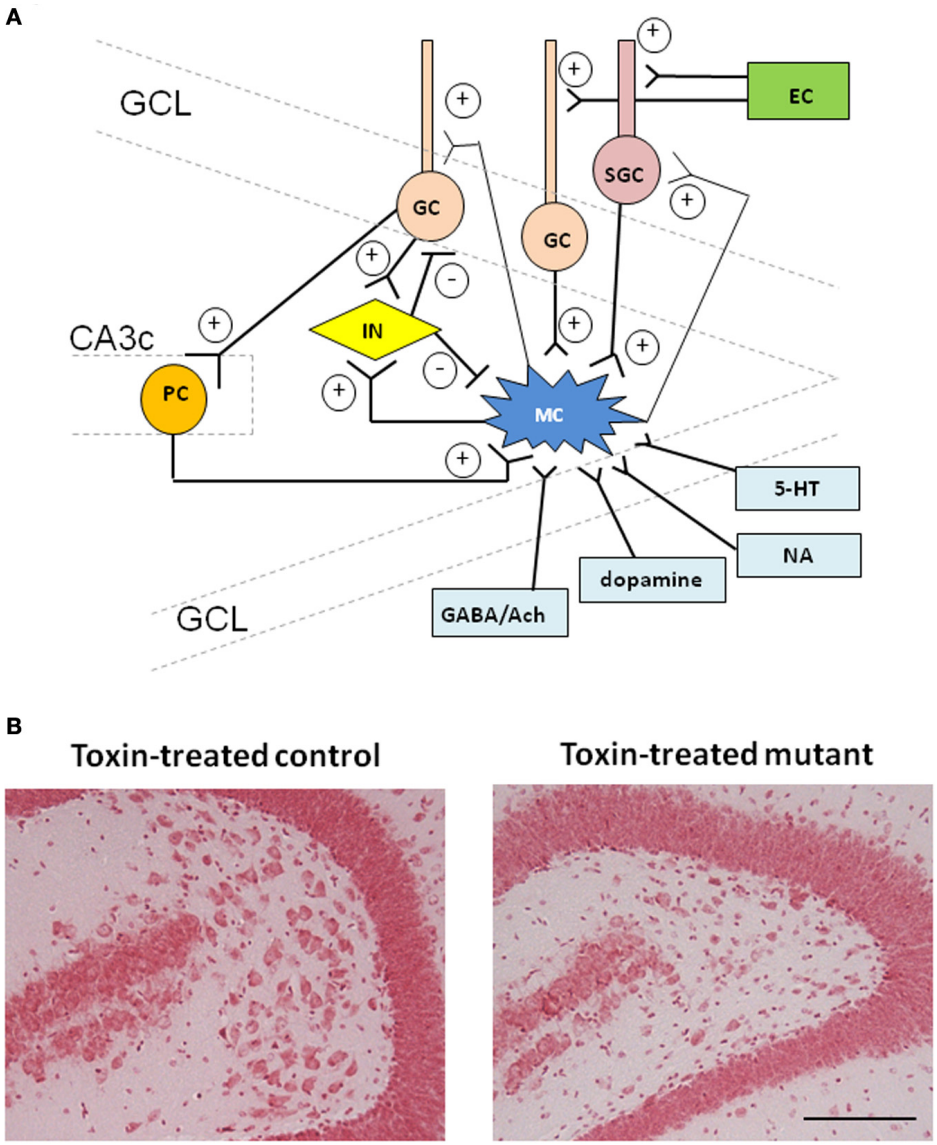

FIGURE 1 | Schematic of the connectivity of hilar mossy cells and toxin-induced mossy cell degeneration. (A) Mossy fiber axon collaterals of dentate granule cells are the main input to the mossy cells at their proximal dendrites, called "thorny excrescences." Mossy cells also receive strong excitatory inputs from semilunar granule cells at the relatively distal dendritic segments of mossy cells. A fraction of CA3 pyramidal cells "backproject" to mossy cells which also receive scarce input directly from the entorhinal cortex. Mossy cells also receive GABAergic inputs from hilar interneurons. Other inputs such as cholinergic and noradrenergic projections are known to modulate mossy cell activity. Mossy cell axons project to the dentate inner molecular layer (IML) along the septo-temporal axis and further contra-lateral hippocampus, where over 90% of asymmetric synaptic contacts are formed on granule cell proximal dendrites as well as semilunar granule cells. Mossy cells also send axon collaterals to dentate GABAergic interneurons in the different lamellae or in the contra-lateral hippocampus. Mutual connections between mossy cells are rare. For simplicity, not all the connections are shown. Ach, acetylcholine; EC, entorhinal cortex; GC, granule cell; GCL, granule cell layer; IN, interneuron; MC, mossy cell; NA, noradrenaline; PC, pyramidal cell; SGC, semilunar granule cell; 5-HT, serotonin. **(B)** Representative photographs of Nissl staining showing histological alterations in the hilar region in CA3c/mossy cell-cre/floxed-diphtheria toxin receptor mutant mouse (right) 4 weeks after diphtheria toxin (DT) administration. Compared to DT-treated control (left), mutant mouse showed the decreased cell number in the dentate hilus. Scale bar, 100 μm.

various dentate gyrus functions, especially memory processing and epileptogenesis.

MOSSY CELLS IN LEARNING AND MEMORY

Due to their unique connections, such as feedback excitatory connections to dentate granule cells and back projections from CA3 pyramidal cells, mossy cells have been suggested to play an important role in normal signal processing in learning and memory (Lisman, 1999). Among the dentate functions related to learning and memory, the dentate gyrus actively contributes to pattern separation, defined as the ability to transform a set of similar input patterns into a less similar set

of output patterns. An advanced hippocampal computational modeling including mossy cells and hilar interneurons demonstrated that mossy cells provide a mechanism for dynamic regulation of pattern separation (Myers and Scharfman, 2009). This modeling also suggests that pattern separation can be strongly diminished by decreasing mossy cell function and/or by increasing inhibitory hilar interneuron function, while pattern separation can be increased by the opposing manipulations. In support of this model, whole cell recoding of mossy cells *in vitro* by Lysetskiy et al. (2005) predicted that mossy cells can modulate information processing in the fascia dentate. Specifically, their study revealed that, following tetanic stimulation, the mossy fiber synapses on mossy cells showed significant NMDA receptor-independent long-term potentiation, associated with the increased amplitude of EPSCs and decreased failure rates. The mossy fiber synapses on mossy cells also showed activity-dependent short-term plasticity. Interestingly, Hyde and Strowbridge (2012) recently reported in the hippocampal slice preparation that dentate mossy cells reliably encode information as distinct patterns of spontaneous synaptic activity that persist for seconds, and these activities resemble the persistent activity patterns which were previously found in delay periods of working memory tasks. However, overall there are few reports evaluating functional roles of mossy cells in learning and memory, perhaps due to the technical difficulty of manipulating mossy cells *in vivo*.

TEMPORAL LOBE EPILEPSY AND MOSSY CELLS

Epilepsy is a neurological disorder characterized by recurrent seizures. There are many different types of epilepsy, which is mainly distinguished by "generalized or partial" and "idiopathic or symptomatic." Temporal lobe epilepsy, symptomatic partial epilepsy, is the most common type of epilepsy in adults, and is frequently associated with a typical pathological change of hippocampus, called hippocampal sclerosis. One of the pathological characteristics in the tissue of human hippocampal sclerosis is the remarkable neuronal loss in the dentate hilus. It is widely known that hilar cells, mainly glutamatergic mossy cells and GABAergic neuropeptide Y- or somatostatin-positive interneurons, are intrinsically vulnerable to excitotoxic damage (e.g., epilepsy, ischemia, and head trauma), while dentate granule cells appear to be relatively resistant (Sloviter, 1994; Blümcke et al., 1999). Another characteristic consequence of repeated seizures is synaptic reorganization called mossy fiber sprouting, which is an aberrant mossy fiber innervating to postsynaptic targets in abnormal locations, including the granule cell dendrites in the IML (Sutula et al., 1989). Since epilepsy-induced hilar cell loss and mossy fiber sprouting has been replicated in several kinds of animal models, such as pilocarpine-induced or kainic acid-induced epileptic rats (Mello et al., 1993; Buckmaster and Dudek, 1997), the underlying mechanism of hippocampal sclerosis has been extensively investigated for decades using these animal models. However, the exact relation between these pathological changes and epileptogenesis has not been fully understood yet.

While hilar mossy cells are known to be one of the most injury-prone hippocampal neurons, the functional consequence of mossy cell loss has not yet been clarified, regarding whether the net effect is to promote more or less excitability in the dentate gyrus. Therefore, the exact role of mossy cell death in epileptogenesis has long been a matter of debate among researchers. To that end, the following three hypotheses have been proposed and discussed: (1) "mossy cell loss-induced sprouting" hypothesis, (2) "dormant basket cell" hypothesis, and (3) "irritable mossy cell" hypothesis. The first theory, "mossy cell loss-induced sprouting" hypothesis, proposes that the epilepsy-induced loss of mossy cells triggers mossy fiber sprouting, which generates epileptogenesis (Nadler, 2003; Jiao and Nadler, 2007). However, there is no direct evidence that it is specifically the mossy cell loss, as opposed to hilar interneuronal loss, that triggers mossy fiber sprouting. Therefore, it has been questioned that mossy fiber sprouting is epileptogenic.

The second theory, the dormant basket cell hypothesis (Sloviter, 1991), seeks to explain functional consequences of missing excitatory hilar mossy cells. The loss of the mossy cells is thought to deprive interneurons of significant excitatory afferents, leading to a disinhibition of granule cells. In Sloviter's experiment, using the experimental epilepsy model of perforant path stimulation in the rat, an initial 24-h episode of intermittent stimulation-induced hippocampal discharges produced a decrease in the frequency-dependent, presumably feed-forward, inhibition of dentate granule cell discharge, and the development of permanent hyperexcitability in the granule cell populations. These permanent functional changes were replicated in normal rats by a subconvulsive dose of bicuculline, suggesting that the persistent seizure- and damage-associated functional changes may primarily reflect a permanent decrease in $GABA_A$ receptor-mediated inhibition of granule cells. In his model, physiological abnormality in dentate granule cell was seen only in animals that exhibited a loss of adjacent dentate hilar mossy cells and hilar somatostatin/neuropeptide Y-inimunoreactive neurons. GABA-immunoreactive dentate basket cells survived despite the extensive loss of adjacent hilar neurons. However, parvalbumin (PV) immunoreactivity, present normally in a subpopulation of GABA-immunoreactive dentate basket cells, was absent on the stimulated side. According to these results, he proposed the following hypothesis. After mossy cell loss, the excitatory synapses on interneurons (e.g., basket cells that inhibit granule cells) in the distant lamella are removed, making these translamellar interneurons hypoactive ("dormant") and thereby creating a seizure-prone dentate network. On the other hand, mossy cell-driven translamellar interneurons inhibit granule cells under normal condition, thereby dentate information flows only in a particular lamella to CA3 (Sloviter, 1994). Indeed, later Zappone and Sloviter (2004) demonstrated that the focally evoked granule cell activity suppressed distant evoked response ∼2.5–4.5 mm longitudinally, and this suppression effect was abolished after extensive hilar cell loss in kainate-treated epileptic rats, suggesting a translamellar lateral inhibition by hilar mossy cells. While this hypothesis triggered much debate, its validity has not been clarified yet (Bernard et al., 1998; Sloviter et al., 2003) because the exact *in vivo* effect of mossy cell-specific loss on dentate network cannot be evaluated by classical pharmacological techniques.

The third theory, named the "irritable mossy cell" hypothesis, proposed that it was not the loss but the survival of mossy cells that played a crucial role in dentate hyperexcitability (Ratzliff et al., 2002). Slice physiology experiment by Santhakumar et al. (2000) reported that, using fluid percussion head trauma model, the percentage decrease in the number of hilar interneurons labeled with either GAD67 or PV mRNA probes following trauma was not different from the decrease in the total population of hilar cells, indicating no preferential survival of interneurons with respect to the mossy cells. Dentate granule cells following trauma showed enhanced action potential discharges, and longer lasting depolarization's, in response to perforant path stimulation, in the presence of the $GABA_A$ receptor antagonist bicuculline. Hilar mossy cells in the traumatic dentate gyrus responded with significantly enhanced, prolonged trains of action potential discharges to perforant path stimulation suggesting that surviving mossy cells play a crucial role in the hyperexcitable responses of the posttraumatic dentate gyrus. Regarding the specific effect of mossy cell loss on dentate excitability, their recent experiment revealed that the rapid removal of hilar mossy cells from the dentate network invariably decreased (and not increased) granule cell excitability to perforant-path stimulation (Ratzliff et al., 2004), indicating that the loss of mossy cells in itself is unlikely to directly underlie dentate hyperexcitability. However, in this study, only a small subset (roughly 5–20%) of mossy cells were acutely ablated in slice preparation, which might have been insufficient to see some of the effect described by Zappone and Sloviter (2004).

The reason why little is known about mossy cells function could be due to the lack of specific marker which is commonly available between species, especially rat and mouse. Another reason for the difficulty could be that, unlike other principal excitatory cell types of the hippocampus, mossy cells do not form recognizable layers, and are scattered in the hilar region, which makes their *in vivo* accessibility for physiological studies difficult (Henze and Buzsáki, 2007). Therefore, to solve this question, an animal model in which mossy cells can be selectively manipulated, such as mossy cell-specific genetically-engineered mouse, has long been required.

MOSSY CELL-SPECIFIC ABLATION MICE

Recently we have generated a transgenic toxin-mediated, mossy cell-degeneration mouse line, by crossing the mossy cell/CA3-restricted Cre line with forebrain-restricted *loxP*-flanked diphtheria toxin receptor (fDTR) line (Jinde et al., 2012). Upon *i.p.* injection of diphtheria toxin (DT), immunostaining of GluA2/3 and calretinin (mossy cell markers) and Fluoro-Jade B staining for labeling neurodegeneration revealed that this mossy cell-restricted diphtheria toxin receptor expression line (mossy cell-DTR, hereafter referred to as mutant) showed an extensive mossy cell degeneration. The degree of degeneration was up to nearly 80% within a week and eventually 90% after 1 month, throughout the longitudinal axis of both dorsal and ventral hippocampus (**Figure 1B**). Whereas degeneration was also observed sparsely in area CA3c, subregion of area CA3 which is located close to the granule cell layer, there was no statistical difference in the cell number of CA3c between before and after DT administration and no other brain areas including dentate granule cells were affected. In contrast, DT-treated control mice, regardless of genotypes, showed no neurodegeneration. Therefore, using this mutant mouse, the impact of mossy cell-specific neuronal degeneration on dentate physiology and behavior can be evaluated. The major findings following toxin-induced mossy cell degeneration are summarized in **Table 1**.

EVALUATION OF EPILEPTOGENESIS THEORIES REGARDING MOSSY CELL FUNCTION

Our findings have several implications for the existing theories regarding the role of mossy cell loss in epileptogenesis. First, our results revealed that acute granule cell hyperexcitability follows the selective and extensive degeneration of mossy cells, which provides the first direct evidence for a net inhibitory role of mossy cells in the dentate gyrus. Thus, these results support the central tenet of the "dormant basket cell" hypothesis, which states that mossy cell loss reduces the excitatory drive onto the inhibitory basket cells, hence they become "dormant" and as a result, dentate granule cells become hyperexcitable (Sloviter, 1991; Sloviter et al., 2003). The "dormant basket cell" hypothesis postulates that reduction in GABAergic inhibition results in seizures, and this is consistent with the diminished GABAergic inhibition observed in models of temporal lobe epilepsy and during status epilepticus.

Second, despite of strong support for dormant basket cell hypothesis, our findings also indicate that the granule cell hyperexcitability caused by mossy cell loss in this mouse model is apparently not enough to cause spontaneous granule cell epileptiform discharges or spontaneous behavioral seizures. Granule cells are possibly powerful amplifiers of excitation, but the disinhibited granule cells alone may not generate spontaneous epileptiform discharges unless abnormal excitatory inputs elicit spontaneous epileptiform discharges in granule cells. One plausible explanation is the involvement of the entorhinal cortex and other related structures in temporal lobe epileptogenesis. Schwarcz and colleagues (Du et al., 1993) suggested that selective neuronal loss in the entorhinal cortex plays a pathophysiological role in epileptogenesis. Indeed, in perforant path-stimulated rats, spontaneous granule cell epileptiform discharges began immediately after stimulation, and preceded spontaneous behavioral seizures (Bumanglag and Sloviter, 2008). It is conceivable that generation of spontaneous epileptiform discharges requires aberrant excitatory input from the entorhinal cortex onto disinhibited dentate granule cells.

Third, we did not see any signature for "irritable" mossy cells, even if 10–20% of mossy cells survived in the mutants, because sEPSC frequency of granule cells in mutant mice was robustly reduced upon mossy cell degeneration. Accordingly, granule cell hyperexcitability in the mutants is unlikely due to the hyperexcitability of surviving mossy cells after DT treatment. However, we do not exclude a possibility that surviving mossy cells play a role in spreading excitability through their long-range direct connections to granule cells.

Fourth, our findings suggest that mossy cell loss alone is insufficient to trigger mossy fiber sprouting. As one of potential mechanisms of reverberating excitation in the dentate gyrus of epileptic

Table 1 | Summary findings after mossy cell-selective neurodegeneration.

	Acute phase (4–11 days)	Chronic phase (~6 weeks)	Comments
Morphology	No obvious change except mossy cell degeneration	No mossy fiber sprouting; GABAergic sprouting at IML	Mossy cell loss triggers no mossy fiber sprouting
sEPSC and sIPSC from granule cell	Frequencies both reduced	Back to normal level	Transient reduction of both excitatory and inhibitory input to granule cell
***In vitro* perforant path stimulation**	Hyperexcitable granule cell	Back to normal level	Net inhibitory role of mossy cell in granule cell activity
Kainate-induced IEG expression	Increase in c-Fos and Zif268	No change	Associated with hyper-excitable granule cell
Kainate-induced seizure	More susceptible	No change	Possibly due to hyper-excitable granule cell
***In vivo* LFP recording**	No epileptiform discharge	No epileptiform discharge	Mossy cell loss insufficient for spontaneous epilepsy
	Theta power enhanced during exploration	Back to normal level	Possibly due to hyper-excitable granule cell
Behavior	No behavioral seizure	No behavioral seizure	Mossy cell loss insufficient for spontaneous seizure
	Increased anxiety	Back to normal level	Possibly due to hyper-excitable granule cell
	Impaired contextual discrimination	Back to normal level	Possibly due to hyper-excitable granule cell

IEG, immediate early gene; IML, inner molecular layer; LFP, local field potential; sEPSC, spontaneous excitatory postsynaptic current; sIPSC, spontaneous inhibitory postsynaptic current.

brains, mossy fiber sprouting has been extensively studied since the original findings of Nadler and colleagues (Tauck and Nadler, 1985). However, it remains elusive as to what causes mossy fiber sprouting. One idea was that the sprouting is driven by the degeneration of and/or loss of innervation from mossy cells, because in the pilocarpine-induced status epilepticus rats, the extent of mossy fiber sprouting is correlated with the number of mossy cell loss (Jiao and Nadler, 2007). Contrary to this assumption, we did not observe any Timm staining-positive immunoreactivity in the IML even 6–8 weeks after DT treatment.

Finally, instead of mossy fiber sprouting, we observed compensatory GABAergic sprouting onto IML which began as early as 2 weeks after DT treatment and gradually progressed until 6–8 weeks after mossy cell degeneration. Concomitantly, the sIPSC frequency from the mutant granule cells, which was transiently decreased during the acute phase, returned back to the normal level by the chronic phase. This suggests that this slow process of synaptic reorganization may reverse the acute granule cell hyperexcitability.

EVALUATION OF MNEMONIC THEORY REGARDING MOSSY CELL FUNCTION

Our findings may also shed light on the mechanisms of dentate pattern separation. There are several possibilities that may explain the context discrimination deficits observed following mossy cell loss in the mutant mice. First, electrophysiological recordings from dentate gyrus of awake behaving rats demonstrated decorrelated firing patterns of the dentate granule cells in response to subtle changes in input as evidence for pattern separation (Leutgeb et al., 2007). Therefore, it is reasonable to assume that following mossy cell loss in the mutants the overall excitability increase in granule cells disrupts their ability to fire dissimilar to each other in the context discrimination tasks. A similar disruption may be elicited by cell-type specific ablation of functional NMDA receptors in the granule cells (McHugh et al., 2007).

Alternatively, mossy cell loss may disturb the feed-back regulation by CA3 cells of the pattern separation function, since mossy cells appear to be under direct modulation by CA3 axons, that back-project to the dentate gyrus (Scharfman, 2007). However, there must be some mechanisms that compensate for this potential disturbance by the chronic phase in the mutants, because contextual discrimination deficits were no longer observed in the chronic phase.

Finally, considering a likely role of newborn granule cells in the mnemonic processes (Aimone et al., 2011; Sahay et al., 2011), it is plausible that mossy cell loss may impair dentate neurogenesis, thereby disrupting pattern separation. However, in this mouse

model, contextual discrimination deficits are detected 1 week after toxin treatment, but not during the chronic phase when any possible effect of mossy cell loss in the neurogenesis should be seen. We also observed no detectable impact of mossy cell loss on adult neurogenesis as assessed during the chronic phase (Jinde et al., 2012). Further studies are necessary to delineate the pattern separation deficits in this mutant.

LIMITATION OF THIS MOUSE MODEL

There are a few limitations of the mossy cell deletion mouse model (Jinde et al., 2012) that need to be acknowledged and addressed. The first limitation is the extent to which the mossy cells were not quickly ablated. We found that toxin-treatment induces selective mossy cell degeneration up to over 75% of cells within a week and over 90% after 1 month throughout the longitudinal axis of both dorsal (septal) and ventral (temporal) hippocampus. This is quite extensive; however, it is still possible that the 10–20% of surviving mossy cells may play a role in epileptogenesis and pattern separation through their long-range direct connections to translamellar granule cells. Indeed, the longitudinal connections were cut in our horizontal slice preparation from ventral hippocampus in our study (Jinde et al., 2012). It is also noted that continuous EEG recordings across many days is required to detect any subtle epileptiform activity. There are also concerns about the mouse strain which we used. Our transgenic mouse model is in the C57BL/6 strain background. Systemic injection of pilocarpine results in robust mossy fiber sprouting in the C57BL/6 mice that survived status epilepticus (Shibley and Smith, 2002). However, after status epilepticus induced by kainic acid injection, the C57BL/6 strain of mice is also known to be more resistant to hilar cell loss and to mossy fiber sprouting as compared to other mouse strains (Schauwecker and Steward, 1997; Schauwecker et al., 2000; McKhann et al., 2003). The use of C57BL/6 strain in our study may reduce the vulnerability to spontaneous seizure, and may make these mice more resistant to mossy fiber sprouting. It will be interesting to genetically ablate the mossy cells in more seizure-prone strain background for seizure assessment and sprouting analysis.

TRANSLAMELLAR LATERAL INHIBITION BY BASKET CELL-LIKE INTERNEURONS

Our study using mossy cell degeneration mutant mice revealed that mossy cell-driven GABAergic interneurons play a crucial role in granule cell inhibition. Since mossy cells presumably project to virtually all types of interneurons across lamellae, except interneuron-selective cells (Zappone and Sloviter, 2004; Dyhrfjeld-Johnsen et al., 2007), most interneuron types could contribute to the granule cell lateral inhibition. Are there any specific types of interneurons involved in this inhibition? Spontaneous IPSC events from granule cells of mutants and controls in the presence and absence of glutamate receptor antagonists (NBQX and D-AP5) suggests that there are at least two sources of inhibition that can be found in the granule cells in the horizontal cut slices of dentate gyrus: 30% may originate from interneurons that receive intra-lamellar input from glutamatergic mossy cells, while the remaining (70%) may receive no contribution from mossy cells in slice preparation. Since sIPSC frequencies are nearly the same between control slice with the blockers and the mutants, we expect that only mossy cells, but not any other glutamatergic excitatory neurons, are driving interneurons in the same lamella in our slice preparation, thereby increasing the sIPSC events by 30% in the control mice.

Furthermore, analysis of granule cell-rise time separated in these preparation raises a possibility that two distinct types of interneurons that provide IPSCs of, project to the same granule cells, in relation to the location of mossy cells activating them (**Figure 2**). One group of interneurons target granule cells with IPSCs of slow-rise time kinetics, and they are located close to the mossy cells, e.g., they receive excitation from those mossy cells in an intra-lamellar manner. Another group is the interneurons with fast-rise time kinetics, which are located translamellar to the mossy cells, again receiving excitatory projection from those mossy cells. Since slow-rise time kinetics interneurons compose of only 30% of inhibition, we think mossy cell feed-forward inhibition is largely translamellar, which was first demonstrated by Zappone and Sloviter (2004).

It is widely accepted that properties of the presynaptic cells as well as the target cells determine the synaptic properties (Klausberger and Somogyi, 2008). Interestingly, there is some emerging evidence that $GABA_A$ receptor subunits inserted at the synapse also depend on the types of presynaptic interneurons. Kinetics of GABAergic transmission depends on the subunit composition of the $GABA_A$ receptors, and α subunits are particularly important among others. For example, GABAergic transmission involves α1 subunit at fast-spiking basket cell to CA1 pyramidal cell synapses (Thomson et al., 2000), and α2/3 subunits are expressed at much higher density at PV-negative basket cells synapses, and α2 or α2/3 often found in the receptors on the axon initial segments, while less present in somatic and dendritic synapses (Nusser et al., 1996; Loup et al., 1998; Pawelzik et al., 1999; Nyíri et al., 2001). Synapses with α1, α2, or α3 subunit containing $GABA_A$ receptors usually demonstrate fast-rise time kinetics, while α5 $GABA_A$ receptor subunits which are utilized for example, at the bitufted cell to pyramidal cell synapses in the somatosensory cortex display slower rise time kinetics (Ali and Thomson, 2008).

According to anatomical studies, we know that most interneuron types in the dentate gyrus receive inputs from mossy cells and that mossy cells are involved in translamellar lateral inhibition (Buckmaster et al., 1996; Zappone and Sloviter, 2004). Therefore, based on our results, we predict that a majority of translamellar lateral inhibition to granule cells with fast kinetics is derived from basket cell-type interneurons that display fast-rise time kinetics. In other words, mossy cells may preferentially project to basket cell-like interneurons in a translamellar manner, which exert a powerful synaptic inhibition onto granule cells. Therefore, it is plausible that hilar mossy cell loss results in a robust lateral or translamellar disinhibition of granule cells by the "dormant basket cells," which may contribute to the epileptogenesis after post-traumatic injury or prolonged febrile seizures (Sloviter, 1994). The types of interneurons with slow-rise time kinetics which are located in an intra-lamellar manner to mossy cells remain to be clarified. However, our finding that

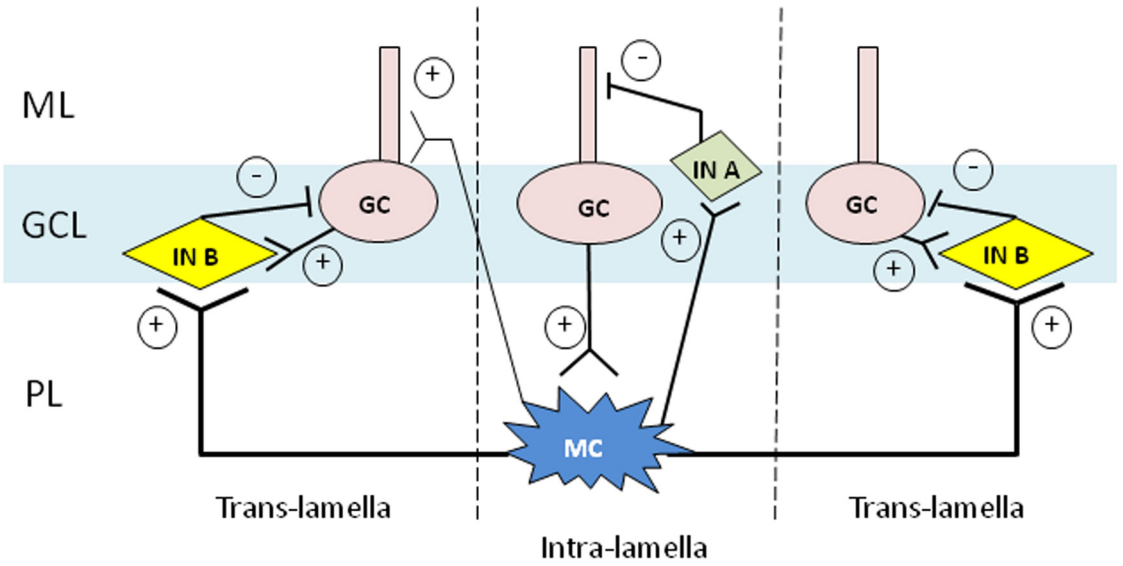

FIGURE 2 | Two hypothetical modes for mossy cell-driven feed-forward inhibition of granule cells. Based on our findings, dentate granule cells appear to be inhibited by two distinct categories of interneurons in light of fast- or slow-rise kinetics of postsynaptic $GABA_A$ receptors. We propose that granule cells located in the same lamellae receive inhibition from interneurons (In A; interneuron A) which display slow-rise time kinetics of sIPSCs at the granule cell dendrites. Conversely, granule cells translamellar to the mossy cells may receive perisomatic inhibition from interneurons (In B; interneuron B) that display fast-rise time kinetics. While the nature of those interneurons is uncertain, we suspect interneurons translamellar to the mossy cells are basket cell-like cells. For simplicity, the dendrites of mossy cells and interneurons are omitted. GC, granule cell; GCL, granule cell layer; MC, mossy cell; ML, molecular layer; PL, polymorphic layer.

IPSC fast-rise time from mutant granule cells is somehow similar to that of the control granule cells after glutamate receptor blockade suggests that glutamatergic mossy fiber projection to those interneurons has minimal impact on granule cell inhibition. It is possible that dentate molecular layer interneurons (so-called MOPP cells) play a role in intralamellar inhibition of granule cells because mossy fibers do not project to these MOPP cells (Halasy and Somogyi, 1993). Alternatively, mossy fiber input to the dentate interneurons may be negligible in slice preparation because the granule cells do not fire spontaneously. In this case, any types of interneurons, including HIPP (Hippocampal Interneurons of the Perforant Path) cells, may serve as type B interneuron ("In A" in **Figure 2**) in our model. Future study is necessary to assess our hypothesis presented here.

SUMMARY AND CONCLUSIONS

Here we presented an overview the characteristics of mossy cells, including connectivity, physiology and function. We described the involvement of mossy cells in temporal lobe epilepsy and mnemonic processes, reviewing several hypotheses addressing the effect of mossy cell loss. We further summarized the recent results from our transgenic mouse that exerts toxin-mediated mossy cell degeneration. The toxin-induced selective mossy cell degeneration resulted in acute granule cell hyperexcitability, which suggests a net inhibitory effect of mossy cells. Despite this, no epileptic seizure or mossy fiber sprouting was observed after mossy cell degeneration. Based on our *in vitro* slice recording using the mutant mice, we hypothesize that there are two distinct populations of mossy cell-driven interneurons which inhibit dentate granule cells. One is a type of interneurons with slow-rise time kinetics of sIPSCs at the granule cell synapse which receive inputs from mossy cells in an intra-lamellar manner. Another one is a basket cell-like interneuron-type with fast-rise time kinetics which receives excitatory input from mossy cells in a translamellar manner. Since our study as well as previous literature (Zappone and Sloviter, 2004) demonstrated that the translamellar lateral inhibition seems to be dominant, it is hypothesized that a majority of mossy cell-mediated granule cell inhibition is derived from basket cell-type interneurons with fast-rise time kinetics driven by mossy cells in a translamellar manner. These results may contribute to clarifying the underlying mechanism of epileptogenesis and the dentate function which is involved in learning and memory.

ACKNOWLEDGMENTS

We thank Stefan Kolata for his critical reading of this manuscript. This research was supported by the Intramural Research Programs of the NIMH. This research was partially supported by the Grant-in-Aid for Scientific Research of Ministry of Education, Culture, Sports, Science, and Technology, Japan (Grant number: 22591274). Seiichiro Jinde was supported in part by a Japan Society for the Promotion of Science (JSPS) fellowship.

REFERENCES

Aimone, J. B., Deng, W., and Gage, F. H. (2011). Resolving new memories: a critical look at the dentate gyrus, adult neurogenesis, and pattern separation. *Neuron* 70, 589–596.

Ali, A. B., and Thomson, A. M. (2008). Synaptic α5 subunit–containing GABAA receptors mediate IPSPs elicited by dendrite-preferring cells in rat neocortex. *Cereb. Cortex* 18, 1260–1271.

Amaral, D. G. (1978). A Golgi study of cell types in the hilar region of the hippocampus in the rat. *J. Comp. Neurol.* 182, 851–914.

Amaral, D. G., Scharfman, H. E., and Lavenex, P. (2007). The dentate gyrus: fundamental neuroanatomical organization (dentate gyrus for dummies). *Prog. Brain Res.* 163, 3–22.

Amaral, D. G., and Witter, M. P. (1989). The three-dimensional organization of the hippocampal formation: a review of anatomical data. *Neuroscience* 31, 571–591.

Andersen, P., Bliss, T. V., and Skrede, K. K. (1971). Unit analysis of hippocampal polulation spikes. *Exp. Brain Res.* 13, 208–221.

Acsády, L., Kamondi, A., Sík, A., Freund, T., and Buzsáki, G. (1998). GABAergic cells are the major postsynaptic targets of mossy fibers in the rat hippocampus. *J. Neurosci.* 18, 3386–3403.

Bernard, C., Esclapez, M., Hirsch, J. C., and Ben-Ari, Y. (1998). Interneurones are not so dormant in temporal lobe epilepsy: a critical reappraisal of the dormant basket cell hypothesis. *Epilepsy Res.* 32, 93–103.

Bilkey, D. K., and Goddard, G. V. (1987). Septohippocampal and commissural pathways antagonistically control inhibitory interneurons in the dentate gyrus. *Brain Res.* 405, 320–325.

Blümcke, I., Beck, H., Lie, A. A., and Wiestler, O. D. (1999). Molecular neuropathology of human mesial temporal lobe epilepsy. *Epilepsy Res.* 36, 205–223.

Buckmaster, P. S., and Dudek, F. E. (1997). Neuron loss, granule cell axon reorganization, and functional changes in the dentate gyrus of epileptic kainate-treated rats. *J. Comp. Neurol.* 385, 385–404.

Buckmaster, P. S., and Jongen-Rêlo, A. L. (1999). Highly specific neuron loss preserves lateral inhibitory circuits in the dentate gyrus of kainate-induced epileptic rats. *J. Neurosci.* 19, 9519–9529.

Buckmaster, P. S., and Schwartzkroin, P. A. (1994). Hippocampal mossy cell function: a speculative view. *Hippocampus* 4, 393–402.

Buckmaster, P. S., Strowbridge, B. W., Kunkel, D. D., Schmiege, D. L., and Schwartzkroin, P. A. (1992). Mossy cell axonal projections to the dentate gyrus molecular layer in the rat hippocampal slice. *Hippocampus* 2, 349–362.

Buckmaster, P. S., Strowbridge, B. W., and Schwartzkroin, P. A. (1993). A comparison of rat hippocampal mossy cells and CA3c pyramidal cells. *J. Neurophysiol.* 70, 1281–1299.

Buckmaster, P. S., Wenzel, H. J., Kunkel, D. D., and Schwartzkroin, P. A. (1996). Axon arbors and synaptic connections of hippocampal mossy cells in the rat *in vivo*. *J. Comp. Neurol.* 366, 270–292.

Bumanglag, A. V., and Sloviter, R. S. (2008). Minimal latency to hippocampal epileptogenesis and clinical epilepsy after perforant pathway stimulation-induced status epilepticus in awake rats. *J. Comp. Neurol.* 510, 561–580.

Burgess, N., Maguire, E. A., and O'Keefe, J. (2002). The human hippocampus and spatial and episodic memory. *Neuron* 35, 625–641.

Buzsáki, G., and Czéh, G. (1981). Commissural and perforant path interactions in the rat hippocampus. Field potentials and unitary activity. *Exp. Brain Res.* 43, 429–438.

Buzsáki, G., and Eidelberg, E. (1981). Commissural projection to the dentate gyrus of the rat: evidence for feed-forward inhibition. *Brain Res.* 230, 346–350.

Buzsáki, G., and Eidelberg, E. (1982). Direct afferent excitation and long-term potentiation of hippocampal interneurons. *J. Neurophysiol.* 48, 597–607.

Deller, T., Katona, I., Cozzari, C., Frotscher, M., and Freund, T. F. (1999). Cholinergic innervation of mossy cells in the rat fascia dentata. *Hippocampus* 9, 314–320.

Deller, T., Nitsch, R., and Frotscher, M. (1994). Associational and commissural afferents of parvalbumin-immunoreactive neurons in the rat hippocampus: a combined immunocytochemical and PHA-L study. *J. Comp. Neurol.* 350, 612–622.

Douglas, R. M., McNaughton, B. L., and Goddard, G. V. (1983). Commissural inhibition and facilitation of granule cell discharge in fascia dentata. *J. Comp. Neurol.* 219, 285–294.

Du, F., Whetsell, W. O. Jr., Abou-Khalil, B., Blumenkopf, B., Lothman, E. W., and Schwarcz, R. (1993). Preferential neuronal loss in layer III of the entorhinal cortex in patients with temporal lobe epilepsy. *Epilepsy Res.* 16, 223–233.

Dyhrfjeld-Johnsen, J., Santhakumar, V., Morgan, R. J., Huerta, R., Tsimring, L., and Soltesz, I. (2007). Topological determinants of epileptogenesis in large-scale structural and functional models of the dentate gyrus derived from experimental data. *J. Neurophysiol.* 97, 1566–1587.

Eichenbaum, H., Dudchenko, P., Wood, E., Shapiro, M., and Tanila, H. (1999). The hippocampus, memory, and place cells: is it spatial memory or a memory space? *Neuron* 23, 209–226.

Freund, T. F., and Buzsáki, G. (1996). Interneurons of the hippocampus. *Hippocampus* 6, 347–470.

Gupta, A., Elgammal, F. S., Proddutur, A., Shah, S., and Santhakumar, V. (2012). Decrease in tonic inhibition contributes to increase in dentate semilunar granule cell excitability after brain injury. *J. Neurosci.* 32, 2523–2537.

Halasy, K., and Somogyi, P. (1993). Subdivisions in the multiple GABAergic innervation of granule cells in the dentate gyrus of the rat hippocampus. *Eur. J. Neurosci.* 5, 411–429.

Henze, D. A., and Buzsáki, G. (2007). Hilar mossy cells: functional identification and activity *in vivo*. *Prog. Brain Res.* 163, 199–216.

Hyde, R. A., and Strowbridge, B. W. (2012). Mnemonic representations of transient stimuli and temporal sequences in the rodent hippocampus *in vitro*. *Nat. Neurosci.* 15, 1430–1438.

Ishizuka, N., Weber, J., and Amaral, D. G. (1990). Organization of intrahippocampal projections originating from CA3 pyramidal cells in the rat. *J. Comp. Neurol.* 295, 580–624.

Ishizuka, S., and Kosaka, T. (1998). Physiological properties of mouse hippocampal mossy cells. *Neuroreport* 9, 193–199.

Jiao, Y., and Nadler, J. V. (2007). Stereological analysis of GluR2-immunoreactive hilar neurons in the pilocarpine model of temporal lobe epilepsy: correlation of cell loss with mossy fiber sprouting. *Exp. Neurol.* 205, 569–582.

Jinde, S., Zsiros, V., Jiang, Z., Nakao, K., Kohno, K., Belforte, J. E., et al. (2012). Hilar mossy cell degeneration causes transient dentate granule cell hyperexcitability and impaired pattern separation. *Neuron* 76, 1189–1200.

Klausberger, T., and Somogyi, P. (2008). Neuronal diversity and temporal dynamics: the unity of hippocampal circuit operations. *Science* 321, 53–57.

Larimer, P., and Strowbridge, B. W. (2008). Nornrandom local circuits in the dentate gyrus. *J. Neurosci.* 28, 12212–12223.

Larimer, P., and Strowbridge, B. W. (2010). Representing information in cell assemblies: persistent activity mediated by semilunar granule cells. *Nat. Neurosci.* 13, 213–222.

Leutgeb, J. K., Leutgeb, S., Moser, M. B., and Moser, E. I. (2007). Pattern separation in the dentate gyrus and CA3 of the hippocampus. *Science* 315, 961–966.

Li, X. G., Somogyi, P., Ylinen, A., and Buzsáki, G. (1994). The hippocampal CA3 network: an *in vivo* intracellular labeling study. *J. Comp. Neurol.* 339, 181–208.

Lisman, J. E. (1999). Relating hippocampal circuitry to function: recall of memory sequences by reciprocal dentate-CA3 interactions. *Neuron* 22, 233–242.

Livsey, C. T., and Vicini, S. (1992). Slower spontaneous excitatory postsynaptic currents in spiny versus aspiny hilar neurons. *Neuron* 8, 745–755.

Loup, F., Weinmann, O., Yonekawa, Y., Aguzzi, A., Wieser, H. G., and Fritschy, J. M. (1998). A highly sensitive immunofluorescence procedure for analyzing the subcellular distribution of GABAA receptor subunits in the human brain. *J. Histochem. Cytochem.* 46, 1129–1139.

Lysetskiy, M., Földy, C., and Soltesz, I. (2005). Long- and short-term plasticity at mossy fiber synapses on mossy cells in the rat dentate gyrus. *Hippocampus* 15, 691–696.

Margerison, J. H., and Corsellis, J. A. (1966). Epilepsy and the temporal lobes. A clinical, electroencephalographic and neuropathological study of the brain in epilepsy, with particular reference to the temporal lobes. *Brain* 89, 499–530.

McEwen, B. S., and Magarinos, A. M. (1997). Stress effects on morphology and function of the hippocampus. *Ann. N.Y. Acad. Sci.* 821, 271–284.

McHugh, T. J., Jones, M. W., Quinn, J. J., Balthasar, N., Coppari, R., Elmquist, J. K., et al. (2007). Dentate gyrus NMDA receptors mediate rapid pattern separation in the hippocampal network. *Science* 317, 94–99.

McKhann, G. M. 2nd., Wenzel, H. J., Robbins, C. A., Sosunov, A. A., and Schwartzkroin, P. A. (2003). Mouse strain differences in kainic acid

sensitivity, seizure behavior, mortality, and hippocampal pathology. *Neuroscience* 122, 551–561.

Mello, L. E., Cavalheiro, E. A., Tan, A. M., Kupfer, W. R., Pretorius, J. K., Babb, T. L., et al. (1993). Circuit mechanisms of seizures in the pilocarpine model of chronic epilepsy: cell loss and mossy fiber sprouting. *Epilepsia* 34, 985–995.

Misgeld, U., Bijak, M., and Brunner, H. (1992). Granule cell inhibition and the activity of hilar neurons. *Epilepsy Res. Suppl.* 7, 113–118.

Mori, M., Gahwiler, B. H., and Gerber, U. (2007). Recruitment of an inhibitory hippocampal network after bursting in a single granule cell. *Proc. Natl. Acad. Sci. U.S.A.* 104, 7640–7645.

Murakawa, R., and Kosaka, T. (2001). Structural features of mossy cells in the hamster dentate gyrus, with special reference to somatic thorny excrescences. *J. Comp. Neurol.* 429, 113–126.

Myers, C. E., and Scharfman, H. E. (2009). A role for hilar cells in pattern separation in the dentate gyrus: a computational approach. *Hippocampus* 19, 321–337.

Nadler, J. V. (2003). The recurrent mossy fiber pathway of the epileptic brain. *Neurochem. Res.* 28, 1649–1658.

Nakazawa, K., McHugh, T. J., Wilson, M. A., and Tonegawa, S. (2004). NMDA receptors, place cells and hippocampal spatial memory. *Nat. Rev. Neurosci.* 5, 361–372.

Nusser, Z., Sieghart, W., Benke, D., Fritschy, J. M., and Somogyi, P. (1996). Differential synaptic localization of two major gamma-aminobutyric acid type A receptor alpha subunits on hippocampal pyramidal cells. *Proc. Natl. Acad. Sci. U.S.A.* 93, 11939–11944.

Nyíri, G., Freund, T. F., and Somogyi, P. (2001). Input-dependent synaptic targeting of alpha(2)-subunit-containing GABA(A) receptors in synapses of hippocampal pyramidal cells of the rat. *Eur. J. Neurosci.* 13, 428–442.

Pawelzik, H., Bannister, A. P., Deuchars, J., Ilia, M., and Thomson, A. M. (1999). Modulation of bistratified cell IPSPs and basket cell IPSPs by pentobarbitone sodium, diazepam and Zn2+: dual recordings in slices of adult rat hippocampus. *Eur. J. Neurosci.* 11, 3552–3564.

Qiu, K., and Han, Z. S. (1995). Local projections of GABAergic neurons in the dentate gyrus and CA1 region in the rat hippocampal formation. *Brain Res.* 702, 287–292.

Ratzliff, A. H., Howard, A. L., Santhakumar, V., Osapay, I., and Soltesz, I. (2004). Rapid deletion of mossy cells does not result in a hyperexcitable dentate gyrus: implications for epileptogenesis. *J. Neurosci.* 24, 2259–2269.

Ratzliff, A. H., Santhakumar, V., Howard, A., and Soltesz, I. (2002). Mossy cells in epilepsy: rigor mortis or vigor mortis? *Trends Neurosci.* 25, 140–144.

Sahay, A., Wilson, D. A., and Hen, R. (2011). Pattern separation: a common function for new neurons in hippocampus and olfactory bulb. *Neuron* 70, 582–588.

Santhakumar, V., Bender, R., Frotscher, M., Ross, S. T., Hollrigel, G. S., Toth, Z., et al. (2000). Granule cell hyperexcitability in the early post-traumatic rat dentate gyrus: the "irritable mossy cell" hypothesis. *J. Physiol.* 524, 117–134.

Scharfman, H. E. (1994a). EPSPs of dentate gyrus granule cells during epileptiform bursts of dentate hilar "mossy" cells and area CA3 pyramidal cells in disinhibited rat hippocampal slices. *J. Neurosci.* 14, 6041–6057.

Scharfman, H. E. (1994b). Evidence from simultaneous intracellular recordings in rat hippocampal slices that area CA3 pyramidal cells innervate dentate hilar mossy cells. *J. Neurophysiol.* 72, 2167–2180.

Scharfman, H. E. (1995). Electrophysiological evidence that dentate hilar mossy cells are excitatory and innervate both granule cells and interneurons. *J. Neurophysiol.* 74, 179–194.

Scharfman, H. E. (2007). The CA3 "backprojection" to the dentate gyrus. *Prog. Brain Res.* 163, 627–637.

Scharfman, H. E., and Myers, C. E. (2012). Hilar mossy cells: a historical perspective. *Front. Neural Circuits* 6:106. doi: 10.3389/fncir.2012.00106

Scharfman, H. E., and Schwartzkroin, P. A. (1988). Electrophysiology of morphologically identified mossy cells of the dentate hilus recorded in guinea pig hippocampal slices. *J. Neurosci.* 8, 3812–3821.

Schauwecker, P. E., Ramirez, J. J., and Steward, O. (2000). Genetic dissection of the signals that induce synaptic reorganization. *Exp. Neurol.* 161, 139–152.

Schauwecker, P. E., and Steward, O. (1997). Genetic determinants of susceptibility to excitotoxic cell death: implications for gene targeting approaches. *Proc. Natl. Acad. Sci. U.S.A.* 94, 4103–4108.

Shibley, H., and Smith, B. N. (2002). Pilocarpine-induced status epilepticus results in mossy fiber sprouting and spontaneous seizures in C57BL/6 and CD-1 mice. *Epilepsy Res.* 49, 109–120.

Seress, L., and Ribak, C. E. (1984). Direct commissural connections to the basket cells of the hippocampal dentate gyrus: anatomical evidence for feed-forward inhibition. *J. Neurocytol.* 13, 215–225.

Sloviter, R. S. (1991). Permanently altered hippocampal structure, excitability, and inhibition after experimental status epilepticus in the rat: the dormant basket cell hypothesis and its possible relevance to temporal lobe epilepsy. *Hippocampus* 1, 41–66.

Sloviter, R. S. (1994). The functional organization of the hippocampal dentate gyrus and its relevance to the pathogenesis of temporal lobe epilepsy. *Ann. Neurol.* 35, 640–654.

Sloviter, R. S., and Lømo, T. (2012). Updating the lamellar hypothesis of hippocampal organization. *Front. Neural Circuits* 6:102. doi: 10.3389/fncir.2012.00102

Sloviter, R. S., Zappone, C. A., Harvey, B. D., Bumanglag, A. V., Bender, R. A., and Frotscher, M. (2003). "Dormant basket cell" hypothesis revisited: relative vulnerabilities of dentate gyrus mossy cells and inhibitory interneurons after hippocampal status epilepticus in the rat. *J. Comp. Neurol.* 459, 44–76.

Soriano, E., and Frotscher, M. (1994). Mossy cells of the rat fascia dentata are glutamate-immunoreactive. *Hippocampus* 4, 65–69.

Struble, R. G., Desmond, N. L., and Levy, W. B. (1978). Anatomical evidence for interlamellar inhibition in the fascia dentata. *Brain Res.* 152, 580–585.

Sutula, T., Cascino, G., Cavazos, J., Parada, I., and Ramirez, L. (1989). Mossy fibers synaptic reorganization in the epileptic human temporal lobe. *Ann. Neurol.* 26, 321–330.

Tauck, D. L., and Nadler, J. V. (1985). Evidence of functional mossy fiber sprouting in hippocampal formation of kainic acid-treated rats. *J. Neurosci.* 5, 1016–1022.

Thomson, A. M., Bannister, A. P., Hughes, D. I., and Pawelzik, H. (2000). Differential sensitivity to Zolpidem of IPSPs activated by morphologically identified CA1 interneurons in slices of rat hippocampus. *Eur. J. Neurosci.* 12, 425–436.

Wenzel, H. J., Buckmaster, P. S., Anderson, N. L., Wenzel, M. E., and Schwartzkroin, P. A. (1997). Ultrastructural localization of neurotransmitter immunoreactivity in mossy cell axons and their synaptic targets in the rat dentate gyrus. *Hippocampus* 7, 559–570.

Williams, P. A., Larimer, P., Gao, Y., and Strowbridge, B. W. (2007). Semilunar granule cells: glutamatergic neurons in the rat dentate gyrus with axon collaterals in the inner molecular layer. *J. Neurosci.* 27, 13756–13761.

Zappone, C. A., and Sloviter, R. S. (2001). Commissurally projecting inhibitory interneurons of the rat hippocampal dentate gyrus: a colocalization study of neuronal markers and the retrograde tracer Fluoro-gold. *J. Comp. Neurol.* 441, 324–344.

Zappone, C. A., and Sloviter, R. S. (2004). Translamellar disinhibition in the rat hippocampal dentate gyrus after seizure-induced degeneration of vulnerable hilar neurons. *J. Neurosci.* 24, 853–864.

Conflict of Interest Statement: The authors declare that the research was conducted in the absence of any commercial or financial relationships that could be construed as a potential conflict of interest.

Received: 11 October 2012; accepted: 23 January 2013; published online: 12 February 2013.

Citation: Jinde S, Zsiros V and Nakazawa K (2013) Hilar mossy cell circuitry controlling dentate granule cell excitability. Front. Neural Circuits 7:14. doi: 10.3389/fncir.2013.00014

frontiers in
NEURAL CIRCUITS

REVIEW ARTICLE
published: 09 January 2013
doi: 10.3389/fncir.2012.00106

Hilar mossy cells of the dentate gyrus: a historical perspective

Helen E. Scharfman[1,2]* and Catherine E. Myers[3,4]

[1] *New York University Langone Medical Center, New York, NY, USA*
[2] *Center for Dementia Research, The Nathan Kline Institute for Psychiatric Research, Orangeburg, NY, USA*
[3] *Veterans Affairs Medical Center - New Jersey Healthcare System, East Orange, NY, USA*
[4] *New Jersey Medical School, University of Medicine and Dentistry of New Jersey, Newark, NJ, USA*

Edited by:
Peter Jonas, Institute of Science and Technology Austria, Austria

Reviewed by:
John Lisman, Brandeis University, USA
Michael Frotscher, Albert Ludwigs University, Germany

****Correspondence:***
Helen E. Scharfman, Center for Dementia Research, The Nathan Kline Institute for Psychiatric Research, 140 Old Orangeburg Rd., Bldg. 35, Orangeburg, NY 10962, USA.
e-mail: hscharfman@nki.rfmh.org; helen.scharfman@nyumc.org

The circuitry of the dentate gyrus (DG) of the hippocampus is unique compared to other hippocampal subfields because there are two glutamatergic principal cells instead of one: granule cells, which are the vast majority of the cells in the DG, and the so-called "mossy cells." The distinctive appearance of mossy cells, the extensive divergence of their axons, and their vulnerability to excitotoxicity relative to granule cells has led to a great deal of interest in mossy cells. Nevertheless, there is no consensus about the normal functions of mossy cells and the implications of their vulnerability. There even seems to be some ambiguity about exactly what mossy cells are. Here we review initial studies of mossy cells, characteristics that define them, and suggest a practical definition to allow investigators to distinguish mossy cells from other hilar neurons even if all morphological and physiological information is unavailable due to technical limitations of their experiments. In addition, hypotheses are discussed about the role of mossy cells in the DG network, reasons for their vulnerability and their implications for disease.

Keywords: dentate gyrus, hippocampus, interneuron, granule cell, mossy fibers, excitotoxicity, vulnerability

"MOSS" AND "MOSSY CELLS"

Ramon y Cajal was the first to describe the unusual large boutons of granule cell axons from his studies of the rabbit or guinea pig (Ramon y Cajal, 1911). He gave these axons the name "mossy fibers" because the giant terminals of granule cells, occurring periodically along the granule cell axons, gave the axons the appearance that they were covered in moss (Ramon y Cajal, 1911). The adjective "mossy" is also used for other fiber systems (e.g., cerebellar mossy fibers) but in the hippocampus the only cells with mossy fibers are granule cells.

Many decades later, electron microscopy was used to describe mossy fiber boutons in more detail, and showed that they are complex, large terminals, densely packed with synaptic vesicles (Blackstad and Kjaerheim, 1961; Laatsch and Cowan, 1966). These boutons innervate equally complex structures on the proximal apical dendrites of CA3 pyramidal cells, called "complex spines" or "thorny excrescences," a name that reflects the similarity to thorny excrescence of plants, which are complex protrusions that emerge from the main stem. The remarkable complexity of mossy fiber boutons and thorny excrescences—much more intricate than most pre- and postsynaptic structures—is not unique to area CA3, however. Complex, large mossy fiber boutons of granule cells are also abundant in the hilus, where they contact thorny excrescences on the proximal dendrites and somata of a subset of hilar neurons.

The neurons of the hilus with thorny excrescences were named "mossy cells" because their appearance resembles a cell covered in moss (Amaral, 1978) (**Figure 1**). Hilar mossy cells with these characteristics have now been described in numerous mammalian species besides rats and mice, including guinea pig (Scharfman and Schwartzkroin, 1988), gerbil (Kotti et al., 1996), hamster (Murakawa and Kosaka, 2001), and primates (Seress and Mrzljak, 1992; Seress and Ribak, 1995).

Before describing mossy cells in more detail, it is important to clarify nomenclature of the hilar region (see also, Amaral et al., 2007; Scharfman and Witter, 2007). Originally the hilus was described by other terms: area H5 (Rose, 1926), CA4 (Lorente De Nó, 1934), or the polymorphic zone, and it was debated if the area between the granule cell layer and area CA3 should be addressed as a single area or multiple subregions (discussed in Amaral, 1978). At the present time, "hilus" has replaced these terms for the most part, although the term "polymorphic zone" is still applicable to the dentate gyrus (DG) because the hilus is a polymorphic layer if one defines the DG as a structure composed of a molecular layer, cell layer, and polymorphic layer.

Another aspect of nomenclature that is important relates to the terms for the different parts of the hippocampus: septal vs. temporal poles. In the rodent, the septal pole is located in the dorsal part of the forebrain, and is more anterior than the rest of the hippocampus; the temporal pole is located in the ventral part of the forebrain and is more caudal or posterior (**Figure 2**). However, septal and dorsal hippocampus are not necessarily synonymous, because some of the hippocampus that is located in the dorsal part of the forebrain is relatively caudal and is not very close to the septum. Therefore, it is preferable to discuss the DG with terms such as septal or temporal rather than dorsal and ventral (Scharfman and Witter, 2007). On the other hand, a section cut in the horizontal plane in the dorsal part of the brain is best

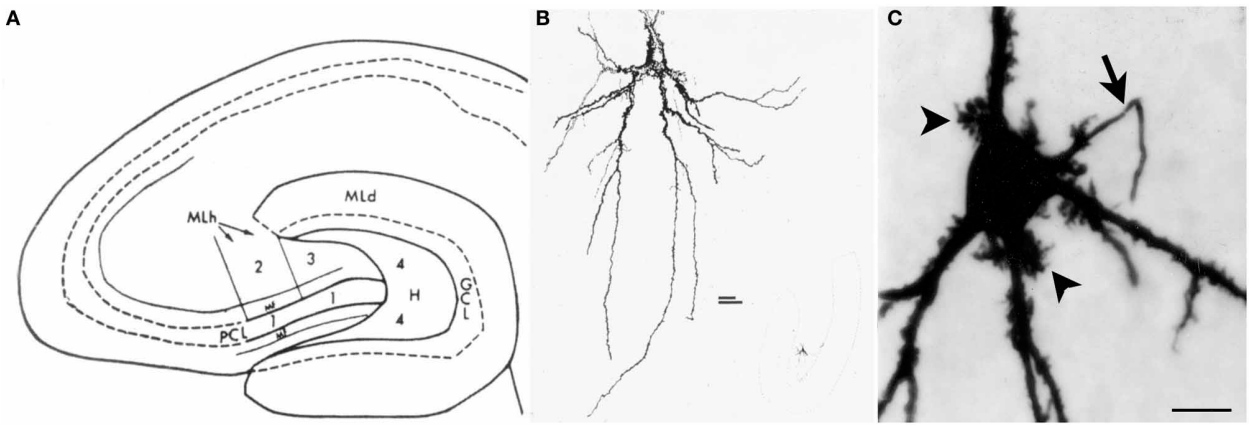

FIGURE 1 | Introduction to the hilus and mossy cells. (A) A schematic of the rat hippocampus from Amaral (1978) in horizontal section shows the location of the hilus (zone 4). GCL, granule cell layer; H, hilus; ML, molecular layer; MF, mossy fiber; PCL, pyramidal cell layer. **(B)** A drawing of a mossy cell from the same study (Amaral, 1978). **(C)** A mossy cell that was physiologically-identified in hippocampal slices from an adult male rat and filled with Neurobiotin from Scharfman et al. (2001). An arrow points to the axon; arrowheads point to thorny excrescences. Calibration = 20 μm.

discussed as dorsal, since it contains both septal areas and more caudal areas.

Since the landmark paper by Amaral (1978), that described hilar neurons from Golgi-stained tissue of the rat, much more has become known about the basic structural and functional characteristics of mossy cells, and their potential contribution to the DG and CA3 network. Below we discuss the fundamental characteristics of mossy cells, and then discuss the hypotheses about their function, vulnerability, and implications for disease.

DIVERSE CHARACTERISTICS OF MOSSY CELLS AND THE QUESTION THEY RAISE: WHAT IS A MOSSY CELL?

EARLY STUDIES OF THE AXON PROJECTION OF MOSSY CELLS AND THE QUESTIONS THEY RAISED

Before much was known about hilar mossy cells, a great deal of work was already being conducted to understand the commissural projection of large hilar neurons—which later became identified as the axon projection of mossy cells, as well as some other types of DG neurons. The axon projection was called the commissural/associational (C/A) pathway and projected to distal "lamellae" of the DG ipsilaterally and the contralateral DG. It formed the major source of afferents to the inner molecular layer (**Figures 2**, **3**; Ribak et al., 1985). Most of these studies were conducted in rats and were based on tract-tracing techniques. Some of the data showed remarkably specificity: the contralateral projection to the inner molecular layer targeted a similar location along the septotemporal axis as the cell bodies of origin ("homotopic"; **Figure 3**).

Most of these studies suggested that the cells of origin of the C/A pathway were large neurons in the hilus (large referring to the size of the cell body). However, it was never entirely clear that these large neurons were exclusively mossy cells or that large hilar neurons were only mossy cells. One reason to be cautious was that some rather small-sized hilar neurons appeared to contribute to the C/A projection (Ribak et al., 1985). These relatively small hilar neurons seemed unlikely to be mossy cells based on the idea that mossy cells have a large soma.

Might other neurons besides mossy cells contribute to the C/A pathway? Did some mossy cells in fact have small cell bodies? Additional studies supported both ideas. Regarding the heterogeneity of neurons contributing to the C/A pathway, it became clear that other hilar neurons than mossy cells have a commissural projection. One study was physiological: in the anesthetized rat, electrical stimulation of the commissure could inhibit the granule cell population spike evoked by a prior stimulus to the perforant path (Douglas et al., 1983). These data suggested that there was a GABAergic contribution to the commissural pathway, which would be unlikely to be mossy cells because they are glutamatergic (although at the time this was debated). Anatomical analyses of commissurally projecting neurons of the DG showed that GABAergic neurons which co-localize somatostatin or neuropeptide Y project contralaterally—although they do not innervate the inner molecular layer in the contralateral hemisphere, like mossy cells (Bakst et al., 1986; Goodman and Sloviter, 1992; Deller et al., 1994, 1995). In addition, parvalbumin-expressing GABAergic neurons at the granule cell layer/hilar border project contralaterally (Goodman and Sloviter, 1992).

Together these studies led to some question about the location of the mossy cell axon projection—and suggested that mossy cells cannot be defined by a contralateral projection alone. Moreover, it is not possible to define them as a neuron with an inner molecular layer projection. The reason is that CA3 pyramidal cells, mostly in area CA3c and in temporal hippocampus, project to the inner molecular layer (Li et al., 1994).

A greater understanding of the mossy cell axon was made possible by analysis of the axons of intracellularly-labeled hilar cells which had thorny excrescences in the rat (Buckmaster et al., 1996). The labeled cells gave rise to both an ipsilateral and contralateral terminal plexus in the inner molecular layer. Within the ipsilateral projection, the intracellularly-labeled cells had their most extensive projection to the inner molecular layer in distant lamellae relative to the cell body (**Figure 3**). Interestingly, the projections of intracellularly-labeled mossy cells were not the same. Mossy cells located in the temporal part of the hippocampus

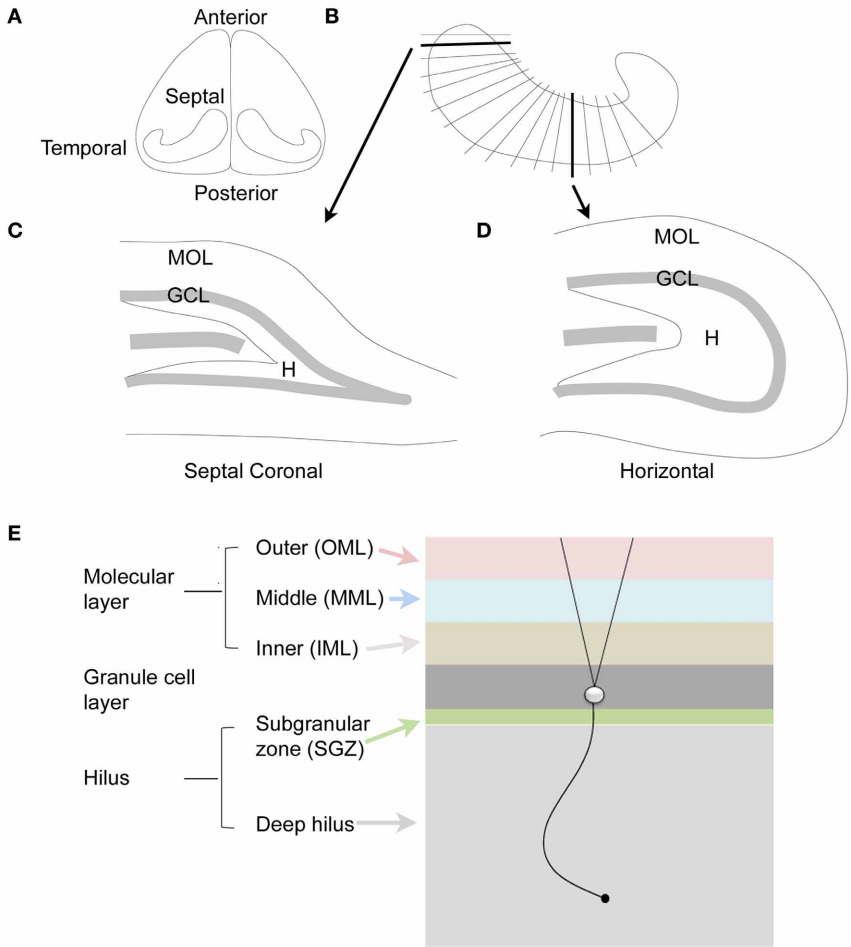

FIGURE 2 | The dentate gyrus of the rodent. (A) Dorsal view of the rodent hippocampus. **(B)** A schematic of the lamellar organization of the hippocampus. Two sections are shown in the coronal plane and horizontal plane as indicated by the arrows. **(C)** A coronal section from septal hippocampus is illustrated. MOL, molecular layer; GCL, granule cell layer; H, hilus. **(D)** A horizontal section from temporal hippocampus is illustrated. **(E)** The laminar organization of the DG is illustrated, with a single granule cell to show the orientation of dendrites and the granule cell axon, which is called a mossy fiber. The molecular layer is divided into three zones that are approximately the same width: outer molecular layer (light red); middle molecular layer (light blue); and inner molecular layer (light brown). The granule cell layer (dark gray) has several layers of densely-packed granule cells. Below the granule cell layer is a small subgranular zone (light green) containing hilar neurons and precursors of granule cells. The hilus includes the subgranular zone and a larger area that ends with area CA3c. The zone near CA3c is sometimes called the deep hilus (light gray).

projected very far, to distant septal locations. However, mossy cells located in the septal region did not project as far into the temporal hippocampus (**Figure 3**; Buckmaster et al., 1996). These data were consistent with earlier studies using different methods, which suggested that there was a more extensive spread of the C/A pathway from temporal to septal hippocampus in the mouse (West et al., 1979). Similar results have also been found in the mouse, where calretinin can be used to stain the mossy cells of temporal hippocampus (Blasco-Ibanez and Freund, 1997; Fujise et al., 1998), but in septal hippocampus of the mouse and in rat, calretinin does not stain mossy cells (although calretinin does stain mossy cells in the human; Seress et al., 2008). In mouse, an antibody to calretinin stained the inner molecular layer throughout the septotemporal extent of the DG, even though cell bodies of mossy cells were stained by the antibody in temporal hippocampus only. These data suggested that temporal mossy cells have axons which are highly divergent (Blasco-Ibanez and Freund, 1997).

EARLY PHYSIOLOGICAL STUDIES OF MOSSY CELLS AND THE QUESTIONS THEY RAISED

The first intracellular recordings from mossy cells were made in hippocampal slices of the guinea pig. These initial studies provided data that led to a reconsideration of the definition of a mossy cell because some cells with dense proximal spines—but not clear thorny excrescences—could not be distinguished from cells with robust thorns. This raised the question: are mossy cells defined by robust thorny excrescences, or is there some variability?

In the recordings, hilar cells were sampled at random with sharp electrodes (i.e., without visualization of the cell before impalement), after physiological properties were characterized,

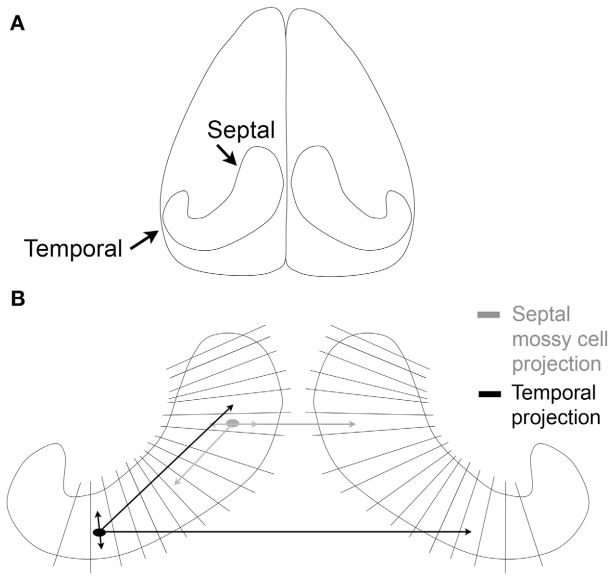

FIGURE 3 | The commissural/associational (C/A) pathway. (A) An illustration of the brain viewed from above shows the orientation of the hippocampus of the rodent. **(B)** The lamellae of the hippocampus are illustrated schematically. Mossy cells located near the temporal pole of the hippocampus (black) project to septal areas and to the temporal hippocampus contralaterally. The projections that are local terminate primarily in the hilus; the projections to distant lamellae terminate primarily on granule cell dendrites in the inner molecular layer. Mossy cells located in septal hippocampus (gray) have similar local and distant projections but the distant projection does not extend as far from the cell body as it does for temporal mossy cells.

the cell was filled with dye to correlate physiological properties with gross morphological characteristics such as the size of the cell body, and presence of thorny excrescences. The results showed that there was a substantial fraction of neurons in the hilus with physiological properties similar to regular-spiking glutamatergic neurons in other parts of the CNS; the other group of hilar neurons was similar to fast-spiking or slow-spiking GABAergic neurons (below these are all discussed as fast-spiking for simplicity) (Scharfman and Schwartzkroin, 1988; Scharfman, 1992a). The cell bodies of the regular-spiking neurons were usually large and the proximal dendrites were typically large in diameter (relative to granule cells) and covered with thorny excrescences but this was not the case for the fast-spiking cells (Scharfman and Schwartzkroin, 1988). The fast-spiking neurons were generally aspinous, or had spines but they were primarily on dendrites that were not proximal to the soma (**Figure 4**).

Therefore, there was an apparent division based on physiology and morphology and the regular-spiking neurons appeared to be mossy cells whereas the fast-spiking neurons corresponded to GABAergic neurons. However, the regular-spiking neurons did not always have numerous thorny excrescences (**Figure 4**). Some of the dendrites merely appeared to be large in diameter and rather "bumpy" which had been shown before (Frotscher et al., 1991). In addition, the somata of the regular-spiking cells were not necessarily larger than the fast-spiking neurons (**Figure 4**), suggesting that numerous thorny excrescences and a large cell body did not necessarily define mossy cells. The distal dendrites of the regular-spiking neurons were sometimes beaded and lacked spines. These characteristics—beaded, aspiny dendrites—are considered to be common characteristics of interneurons. Therefore, the characteristics of distal dendrites of mossy cells did not seem to be useful in defining them either. Moreover, some fast-spiking neurons had very large (thick) dendrites and spines (**Figure 4**), suggesting that mossy cells could not be defined by dendrites with a large diameter.

Variations in thorny excrescences in mossy cells also are evident when species are compared. For example, thorny excrescences of hilar cells in the hamster and in humans seem far more "exuberant" than the guinea pig or rat (Murakawa and Kosaka, 2001; Seress et al., 2004; Abraham et al., 2005). Below we argue that exuberant thorny excrescences are not a defining feature of mossy cells, because the cells with robust thorny excrescences (**Figure 1C**) can not be discriminated from cells with dense proximal spines (**Figure 4**) using physiological criteria. When the axon is visible, the main branch exits the hilus and enters stratum oriens of CA3, as one would expect for a mossy cells. Therefore, there appears to be some variability in the "moss" and size of mossy cells.

A PROPOSAL FOR CRITERIA TO DEFINE MOSSY CELLS

Below we suggest the criteria to define a mossy cell based on the data about hilar neurons obtained to date, and based on practical considerations. Each criterion in itself is insufficient to define a mossy cell; together they make a compelling case for a mossy cell.

1. A cell body in the hilus, defined as zone 4 of Amaral (1978).
2. Glutamate as the primary transmitter (other markers are less valuable, as discussed below).
3. An axon that innervates the inner molecular layer.
4. Proximal dendrites with numerous large spines (distal dendrites may be misleading and thorny excrescences are not an absolute requirement).
5. A series of physiological characteristics that distinguish the cell from GABAergic interneurons and CA3 pyramidal cells.

Cell body in the hilus

It is hard to argue against the idea that a hilar cell must have a cell body in the hilus. However, the definition of the hilus is not trivial, because the border with CA3c can easily be misconstrued. As shown in **Figure 1**, Amaral defined the hilus as a specific area between the two blades of the granule cell layer (Amaral, 1978). However, the hilus is not simply the area of the DG that is located between the two blades. Area CA3c (nomenclature of Lorente De Nó, 1934) inserts into the DG, and is not part of the DG (Amaral, 1978). The hilus surrounds the area CA3c cell layer as well as the dendrites of CA3c pyramidal cells; it does not only avoid the cell layer (Amaral, 1978). In the coronal plane of septal hippocampus in rodents, it is difficult to sample neurons from the hilus because area CA3c encompasses the majority of the space between the supra and infrapyramidal blades; there is only a very small area

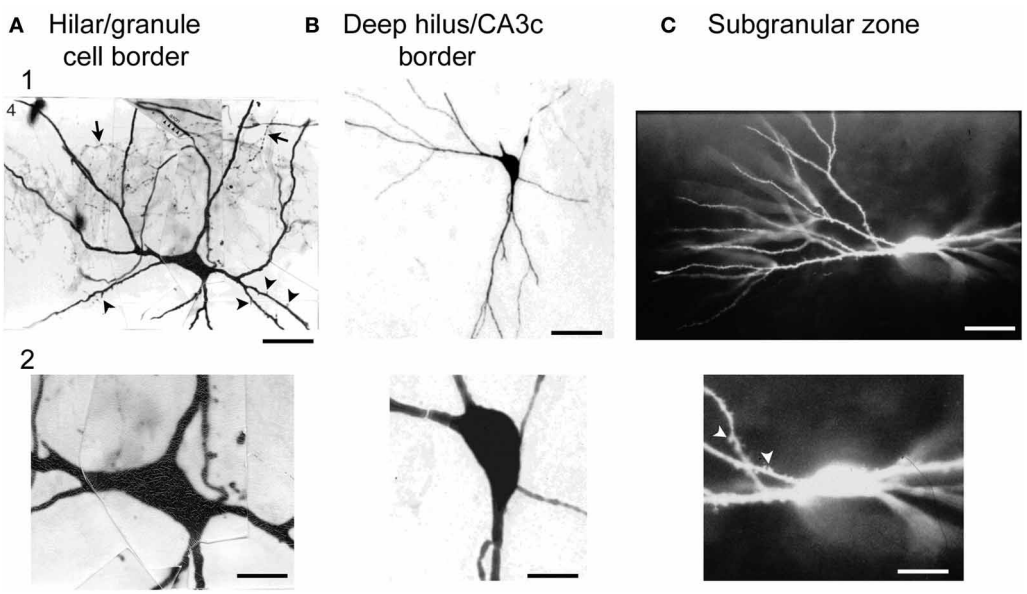

FIGURE 4 | Large cells of the hilus are not always mossy cells. (A) A physiologically-identified fast-spiking cell with a basket cell axon, located at the border of the granule cell layer and the hilus. Arrows point to the axon. Arrowheads point to spines. Note the large size of the cell body. Calibration = 30 μm **(A1)**; 15 μm **(A2)**. From Scharfman (1995a). **(B)** A physiologically-identified GABAergic neuron located in the deep hilus near area CA3c with a large cell body. Same calibration as **(A)**. **(C)** A neuron with dense spines all over its dendrites, with physiological characteristics that were not possible to discriminate from mossy cells with large thorny excrescences. This neuron was filled with Lucifer yellow and located on the border of the subgranular zone and the deep hilus. Same calibration as **(A)**. From Scharfman (1993a).

where the hilus is located (**Figures 1**, **2**). In the horizontal plane, the hilus is a larger area (**Figures 1**, **2**).

How does one define the border of the hilus with area CA3c? This is relatively straightforward with some staining techniques such as cresyl-violet. Alternatively, almost any stain of the mossy fiber pathway will stain the hilus, but in area CA3c it will only stain stratum lucidum. When there is no staining of the tissue to visualize the CA3c/hilar border, one can identify a cell of interest and then stain the area *posthoc*. Without staining, however, cells near CA3c are difficult to define because cells at the tip of CA3c sometimes appear to be "mossy" but their physiology suggests they are pyramidal cells (**Figure 5**; Scharfman, 1993b). One criterion that sets these area CA3c cells apart from mossy cells of the hilus is the ability of intracellular current injection to trigger a burst of decrementing action potentials on a triangular depolarization, a typical type of intrinsic firing behavior of CA3 pyramidal cells (**Figure 5**; Scharfman, 1993b). This is not a characteristic of mossy cells that are close (within 100 μm) to the granule cell layer. When the molecular or granule cell layer is stimulated, an evoked IPSP is a second criterion: in CA3c neurons these IPSPs are robust (**Figure 5**; Scharfman, 1993a) but this is not the case for mossy cells located close to the granule cell layer. Other characteristics have also been used to distinguish area CA3c pyramidal cells from mossy cells (Buckmaster et al., 1993).

Some of these distinguishing characteristics require close attention to recording conditions. For example, burst firing has been reported in mossy cells of the mouse if the recordings are made in the temporal DG. They occur when ionotropic glutamate receptors and $GABA_A$ receptors are blocked (Jinno et al., 2003).

It is important to note that the definition of the hilus, and therefore the hilar/CA3c border, varies with species. In the primate, CA3c is very large and extends very far into the DG. The distance from the granule cell layer/hilar border to CA3c—i.e., the hilus—can be very small.

Glutamate as the primary neurotransmitter

Currently mossy cells can be easily distinguished from GABAergic neurons in the hilus because mossy cells are glutamatergic. However, this criterion was not always so clear. One reason to consider that mossy cells might be GABAergic was based on early studies of the inner molecular layer where commissural afferents included type I and type II synapses (Laatsch and Cowan, 1966). Without specific antibodies to glutamate, or direct assessment of monosynaptically-connected neurons, it remained arguable whether mossy cells were a type of GABAergic neuron or were glutamatergic until the early 1990's. Two studies provided evidence that mossy cells were glutamatergic, one anatomical and the second physiological. The first anatomical demonstration of glutamate immunoreactivity was made in Golgi-impregnated mossy cells (Soriano and Frotscher, 1994). The physiological study used hippocampal slices to impale mossy cells—which were confirmed to be regular-spiking, hilar, and had thorny excrescences—and simultaneously recorded from neurons in the granule cell layer until a monosynaptic connection was identified. That study showed for the first time that mossy cells produced unitary EPSPs in granule cells, supporting the hypothesis that mossy cells were glutamatergic (Scharfman, 1995b). Interestingly, the monosynaptic connections between mossy cells and granule cells were

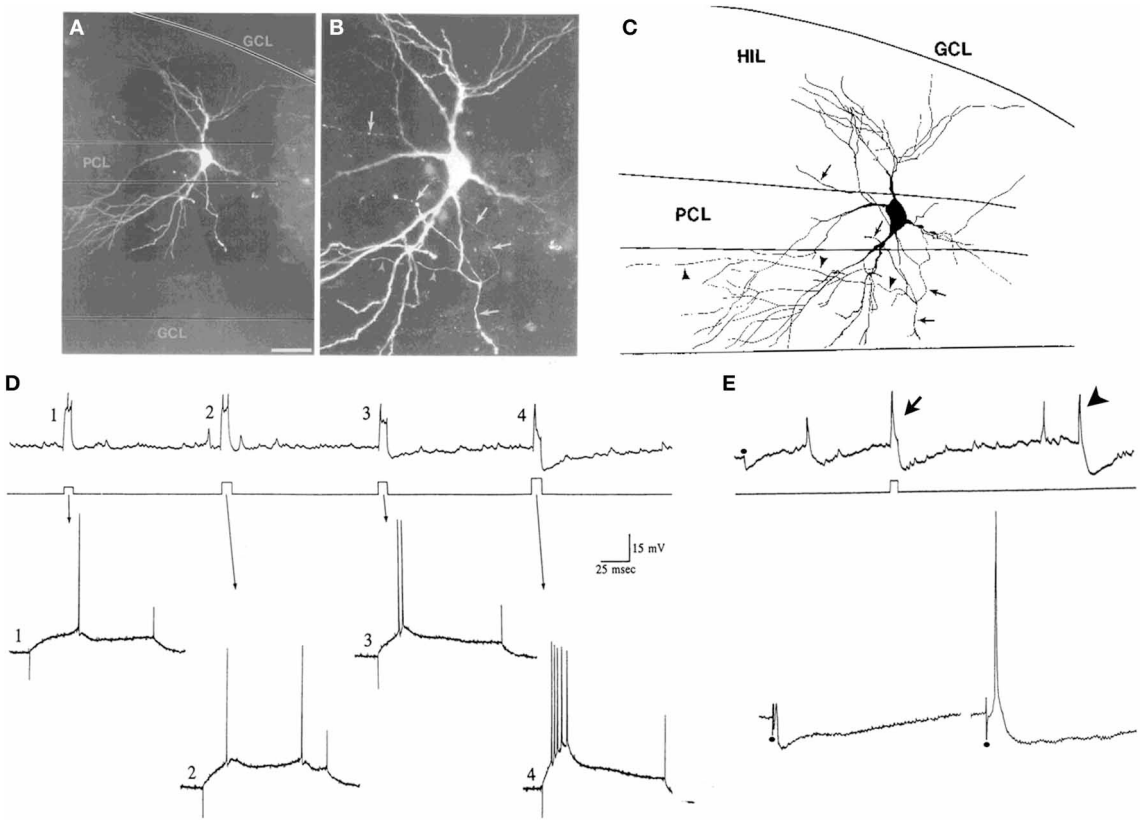

FIGURE 5 | Characteristics of CA3c "pyramidal cells" and mossy cells. **(A,B)** Pyramidal cells of CA3c often have morphology that is not pyramidal-like in that the cell body and proximal dendrites are not pyramidal. They are not interneurons because of their dense spines and physiology. The example shown is from a neuron that was physiologically-identified as a pyramidal cell because of its intrinsic burst firing **(D)**. The merged images through multiple focal planes are shown. Calibration [located in **(A)**] = 100 μm for **(A)** and 20 μm for **(B)**. **(C)** A drawing of the cell in **(A,B)** is shown. Arrowheads indicate the part of the axon that terminated in area CA3. The arrows point to the part of the axon that gave rise to collaterals in the hilus. GCL, granule cell layer; HIL, hilus; PCL, pyramidal cell layer of CA3c. **(D,E)** Physiological discrimination of CA3c neurons from hilar mossy cells. **(D)** A continuous recording from a neuron in CA3c (top) that exhibited firing behavior of a pyramidal cell rather than a mossy cell. During the record, a series of increasing currents are triggered (middle) to elicit firing and the firing behavior is expanded below (arrows). Weak currents (#1–3) did not elicit burst firing but the strongest current command did (#4). The burst in #4 has a characteristic decrement in action potential amplitude, and rides on a triangular depolarization, followed by a large afterhyperpolarization. In contrast, these types of bursts are not found in mossy cells under these recording conditions, and the afterhyperpolarizations are not either. **(E)** CA3c pyramidal cells can also be discriminated from mossy cells by a large IPSP triggered by perforant path or molecular layer stimulation. Top: A continuous record from a CA3c cell showing an IPSP evoked in response to molecular layer stimulation (at the dot) and an afterhyperpolarization following directly-evoked action potentials (arrow). An arrowhead marks a spontaneous burst of action potentials followed by an afterhyperpolarization. Bottom: A response of the same cell to stronger stimuli (at the dots). On the right, the response to the strongest stimulus is shown, which elicited an action potential followed by hyperpolarization, characteristic of pyramidal cells under these recording conditions, but not mossy cells. **(A–E)** are from Scharfman (1993b).

weak; they were only detected when a $GABA_A$ receptor antagonist was present. In more recent studies using patch recordings and younger tissue, much more robust excitatory connections were evident from mossy cells to GABAergic neurons of the hilus (Larimer and Strowbridge, 2008). One interpretation of these data is that mossy cells may innervate hilar GABAergic neurons close to the mossy cell soma, but preferentially innervate granule cells in distal areas of the hippocampus. Another implication is related to the study of Larimer and Strowbridge, which used young animals (less than 30 days old). Their study suggests that early in life, mossy cells may form a primarily excitatory connection to local GABAergic neurons and this is later refined as their long axon forms synaptic connections to distal granule cells.

Using immunocytochemistry, it is now common to identify mossy cells in the hilus by their immunoreactivity to GluR2/3, a marker of glutamatergic neurons (Leranth et al., 1996). One potential problem, however, is that some granule cells [ectopic granule cells; (Scharfman et al., 2007)] exist in the hilus too. However, they are rare under most conditions, compared to mossy cells (McCloskey et al., 2006; Jiao and Nadler, 2007). Ectopic granule cells arise in greater numbers after pathology. For example, after status epilepticus (SE) in adult rats, GluR2/3- immunoreactive granule cells are common in the hilus (McCloskey et al., 2006; Jiao and Nadler, 2007).

Other markers besides GluR2/3 can be used to identify mossy cells but few are selective. In the mouse, mossy cells in

temporal hippocampus express calretinin, as mentioned above. However, there are some hilar GABAergic neurons that express calretinin in rat and mouse (Liu et al., 1996; Martinez et al., 1999) and young granule cells at the granule cell layer/hilar border express calretinin in rats and mice (Brandt et al., 2003; Scharfman et al., 2007). In humans, cocaine- and amphetamine-transcript peptide (CART) stains mossy cells (Seress et al., 2004), but not in rodents. In the rat, one of the glucocorticoid receptors (type II) is present on mossy cells (Patel and Bulloch, 2003). The α8 integrin subunit also stains mossy cells in rats, but not selectively—somatostatin/neuropeptide Y immunoreactive cells stain also (Einheber et al., 2001). Calcitonin-gene-regulated peptide (CGRP)-immunoreactivity is another way to distinguish mossy cells in rat (Bulloch et al., 1996; Freund et al., 1997).

An axon that innervates the inner molecular layer

Exceptions to the statement that mossy cells project to the inner molecular layer have not been reported. All neurons with dense proximal spines or thorny excrescences, where an axon has been possible to trace, exhibit an inner molecular layer projection. Therefore, we suggest that one criterion that defines mossy cells is an axon that projects to the inner molecular layer.

However, in some experimental conditions, it is not always possible to determine that an axon is present in the molecular layer. For example, it is hard to find a mossy cell axon in the inner molecular layer in most hippocampal slices. In these slices, however, it is often possible to trace the major branch of the axon to its point of exit from the DG in stratum oriens of area CA3b/c. It can be distinguished from axon collaterals by its large diameter, and the fact that most axon collaterals are restricted to the hilus. In contrast to mossy cells, other hilar cell types do not have this axon projection, and neurons in area CA3c do not either, making it a practical method to differentiate mossy cells in hippocampal slices from other cell types.

It is not widely appreciated that the mossy cell also has a dense local axon collateral plexus in the hilus, which was emphasized in early studies of mossy cells (Frotscher et al., 1991). In recordings of mossy cells in hippocampal slices, there is a dense network of hilar collaterals (Scharfman and Schwartzkroin, 1988; Buckmaster et al., 1992; Larimer and Strowbridge, 2008), which have implications for the potential functional role of mossy cells. The local axon collaterals are depicted schematically in **Figure 3** and discussed further below.

Although it is often hard to find the branches of the local axon that extend into the inner molecular layer in slices, empirical evidence suggests they are present. Thus, the mossy cell axon that ends in the inner molecular layer was found after injecting dye into mossy cells in hippocampal slices which were only 400 μm thick (Buckmaster et al., 1992). Furthermore, effects of mossy cells on granule cells have been reported in 400 μm-thick hippocampal slices (Scharfman, 1995b; Jackson and Scharfman, 1996). Changes in physiology of the DG in hippocampal slices have also been detected before and after selective ablation of mossy cells (Ratzliff et al., 2004).

Regarding other inputs to the inner molecular layer besides mossy cells, there is a long list of inputs that are notable. CA3c pyramidal cells that are located in the temporal pole of the hippocampus project to the inner molecular layer (Li et al., 1994). The supramammillary nucleus sends projections to the border of the inner molecular layer and the granule cell layer (Leranth and Hajszan, 2007). Hilar GABAergic neurons provide GABAergic input [HICAP cells; (Han et al., 1993)]. Diverse brainstem nuclei (dorsal raphe, locus coeruleus) project to the molecular layer, including the inner molecular layer (Amaral and Campbell, 1986; Swanson et al., 1987).

Proximal dendrites with numerous spines

Based on the inability to discriminate physiological differences between cells with obvious thorny excrescences (**Figure 1C**) and cells with dense proximal spines but thorny excrescences that are not as clear (**Figure 4C**), it seems reasonable to suggest that mossy cells are characterized by large proximal spines, whether or not they can be called thorny excrescences. This is practically useful because the discrimination between dense spines and small thorny excrescences is somewhat subjective, in our view. The proximal dendrites are the most important area to consider in this assessment because distal dendrites of mossy cells may have spines that are far less robust, and some interneurons have distal dendrites where spines are robust.

Physiological characteristics that distinguish mossy cells from other cell types

Intrinsic properties. Mossy cells that were initially characterized in guinea pig slices, and subsequently in slices of rat and other species, have "regular-spiking" physiology. Classically the term "regular-spiking" refers to the width (duration) of the action potential. The longer duration of the action potential of mossy cells compared to GABAergic neurons is very easy to discriminate, whether the action potential is triggered by direct current, it occurs spontaneously, or it occurs in response to synaptic stimulation.

However, there are a few potential problems with the implementation of this criterion. One is the fact that almost any cell, if unhealthy, develops a broader action potential. And, in slices, the vulnerability of mossy cells to trauma appears to make them unhealthy unless great care is taken to prepare the slices. Therefore, other criteria are useful. For example, an additional characteristic that is useful to discriminate mossy cells is the ratio of the rate of rise to the rate of decay of the action potential. The ratio is much greater than the one for mossy cells and pyramidal cells but approximates one for GABAergic neurons (Scharfman, 1993b, 1995a).

Additional physiological characteristics of mossy cells in slices distinguished them from other cell types. For example, mossy cells have very long time constants (>20 ms in the guinea pig or rat) which are similar to CA3c pyramidal cells. In contrast, granule cells and interneurons have relatively short time constants (<15 ms). The absolute numbers may vary depending on the recording method (sharp or patch) but the relative differences remain, making this criterion very useful. Mossy cells also have a very small afterhyperpolarization (AHP) following an action potential compared to GABAergic neurons. Interneurons have large AHPs and typically have much less variability in the AHP from one command pulse to the next, and have much less adaptation, than mossy cells [**Figure 6** (Scharfman, 1992a, 1995a; Buhl et al., 1994; Lübke et al., 1998)].

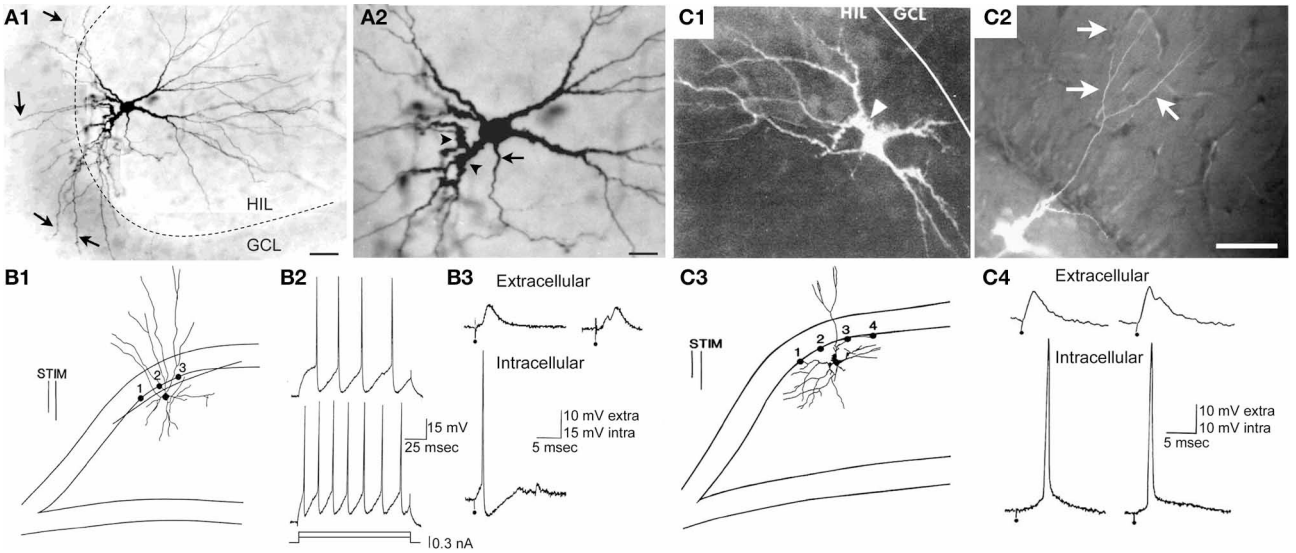

FIGURE 6 | A subset of hilar cells have low thresholds in response to electrical stimulation of the perforant path in rat hippocampal slices. **(A1)** Mossy cells often have dendrites in the molecular layer if their cell body is located near the granule cell layer. A Neurobiotin-filled physiologically-identified mossy cell is shown as an example. There are numerous dendrites entering the granule cell layer (GCL) and molecular layer (arrows). The dotted line marks the border of the HIL and GCL. Calibration = 80 μm. **(A2)** The same cell is shown at higher magnification. The arrow indicates the axon; arrowheads mark thorny excrescences. More examples are shown in Scharfman (1991). Calibration = 40 μm. **(A)** is from Scharfman et al. (2001). **(B1)** A drawing of a hilar interneuron with a low threshold is shown. **(B1–B3)** Are sites where the response to electrical stimulation of the molecular layer was recorded to evaluate granule cell responses to the same stimulus. The bipolar stimulating electrode is indicated by two parallel lines (STIM). **(B2)** Intracellular current (0.15, 0.3 nA) was used to evaluate firing behavior, and the responses demonstrated typical firing of GABAergic neurons: weak spike frequency adaptation. **(B3)** Top (extracellular): the response recorded extracellularly at site #1 at weak (left) and strong (right) intensities of stimulation. Bottom (intracellular): simultaneously recording of the response to the weak stimulus in the interneuron shown in **(B1)** The interneuron reached threshold but there was no indication of suprathreshold activation of granule cells at the same stimulus strength. At the higher intensity of stimulation, a population spike occurred, signaling firing in granule cells. Calibration: 10 mV, extracellular; 15 mV, intracellular. **(C1,C2)** A mossy cell with a molecular layer dendrite is shown after filling the cell with Lucifer yellow in a rat hippocampal slice. This dendrite bifurcated after exiting the granule cell layer and reached the outer molecular layer. In the outer two-thirds of the molecular layer there were additional branches (arrows in **C2**). The arrowhead **(C1)** marks a thorny excrescence. Calibration = 100 μm. **(C3)** A drawing of the cell shown in **(C1,C2)**. **(C4)** Simultaneous extracellular recording from the granule cell layer at the site closest to the stimulating electrode in **(C3)** and intracellular recording from the mossy cell shows a lower threshold for action potential generation in the mossy cell compared to the field potential. It is important to note that it might only take 1 granule cell action potential to activate the mossy cell because of the large quantal size of a granule cell unitary EPSP in a mossy cell (Scharfman et al., 1990) and this might not be reflected in the field potential, which is an average of many cells located only near the recording electrode. Therefore, many locations were sampled, especially those near the stimulating electrode where a granule cell might be directly activated, before concluding that the mossy cell had a relatively low threshold compared to adjacent granule cells. **(B–C)** are from Scharfman (1991).

The firing behavior of a mossy cell seems easier to distinguish from other hilar neurons using a sharp electrode than a patch electrode (Lübke et al., 1998), probably because a patch electrode has constituents that affect firing substantially and if the same internal solution for the patch electrode is used across cells, the more the firing of different cells is similar.

Synaptic responses. One characteristic of mossy cells is a large, frequent barrage of spontaneous synaptic input (Scharfman and Schwartzkroin, 1988; Strowbridge et al., 1992; Scharfman, 1993a; Soltesz and Mody, 1994). At resting potential, this is evident as depolarizations which can trigger action potentials, which are blocked by excitatory amino acid receptor antagonists, so they are EPSPs. Presumably the majority of the input is due to spontaneous release from mossy fiber boutons, but mossy cells also receive local input from CA3 pyramidal cells, and cut axons of extrinsic inputs to the hilus may release transmitter also. Mossy cells are innervated by GABAergic cells, and when glutamate receptors are blocked, inhibitory potentials or IPSCs are readily detected (Scharfman, 1992b; Soltesz and Mody, 1994). In contrast, hilar interneurons have spontaneous input that is much smaller and has faster kinetics (Scharfman et al., 1990; Livsey and Vicini, 1992).

When stimulating electrodes are used to evaluate synaptic inputs to hilar neurons, EPSPs and IPSPs can be evoked by perforant path stimulation in almost all cells. There is extensive variation within a given hilar cell type (Scharfman, 1995a), and as a result, this information—while very important—does not clarify the hilar cell type easily.

ARE THERE SUBTYPES OF MOSSY CELLS?

In light of the variability in many of the characteristics of mossy cells, one might suggest that there could be subtypes of mossy cells. For example, one subtype has dense spines on their proximal dendrites, but no thorny excrescences, and another subtype might have thorny excrescences. This division would certainly be

possible to make, but does not seem useful, because physiological or functional distinctions are not evident when comparing cells with dense proximal spines and cells with thorny excrescences.

However, there is one division that seems useful, because it is detectable anatomically and also physiologically: some of the mossy cells recorded in rat hippocampal slices have a low threshold for action potential generation when the perforant path is stimulated electrically in slices, compared to granule cells located nearby (Scharfman, 1991). Thus, perforant path stimulation can evoke action potentials in these "low threshold" mossy cells before the stimulus is increased sufficiently to elicit a detectable population spike in the granule cells next to it, or action potentials in a granule cell selected at random from that population. The mossy cells with low thresholds are usually located close to the granule cell layer, and have a relatively thin dendrite that passes into the molecular layer and can either stop in the inner or middle molecular layer or extend to the hippocampal fissure (Scharfman, 1991; **Figure 6**). In contrast, mossy cells without these dendrites appear to have a threshold similar to or higher than granule cells in the same slice and are activated at a latency consistent with a perforant path-to-granule cell-to-mossy cell pathway (i.e., disynaptic). Therefore, it seems reasonable to suggest that mossy cells with low thresholds are a subtype of mossy cell (**Figure 7**). There also are hilar GABAergic interneurons with dendrites in the molecular layer and low thresholds to perforant path stimulation in hippocampal slices [**Figure 6** (Scharfman, 1991)], which could be innervated by perforant path fibers that innervate hilar GABAergic dendrites (Deller et al., 1996) or perforant path innervation of molecular layer dendrites [**Figure 6** (Scharfman, 1991)]. These GABAergic hilar neurons with low thresholds and both molecular layer and hilar dendrites may correspond to HIPP cells which co-express somatostatin and neuropeptide Y (see **Figure 7**).

The pathway that causes the short latency, low threshold activation of hilar cells with molecular layer dendrites could be the perforant path, based on the demonstration that perforant path fibers in the molecular layer innervate GABAergic neurons. There is no anatomical evidence that the perforant path innervates mossy cell dendrites in the molecular layer, however. One study that could be relevant showed that deep layer entorhinal neurons have axons that enter the inner molecular layer, granule cell layer, and hilus (Deller et al., 1996). That study suggested that the axons innervated GABAergic neurons, not mossy cells. However, some axons terminated on spines, so it is possible mossy cell dendrites were contacted. In summary, both mossy cells and hilar GABAergic neurons with dendrites in the molecular layer are neurons that appear to have low thresholds. The reason for their low thresholds could be direct innervation by the perforant path, but this explanation is not as well developed for mossy cells as it is for GABAergic neurons.

Notably, the neurons with low thresholds are a subset of mossy cells in the normal rat, but appear to be rare in some species, such as the mouse (Kowalski et al., 2009). In the primate, mossy cells with molecular layer dendrites and even CA3c pyramidal cells with molecular layer dendrites have been shown [the "dentate-CA3 cell"; (Buckmaster and Amaral, 2001)]. The numbers of these cells relative to the entire population of mossy cells and CA3c pyramidal cells is not clear, but it seems likely that they

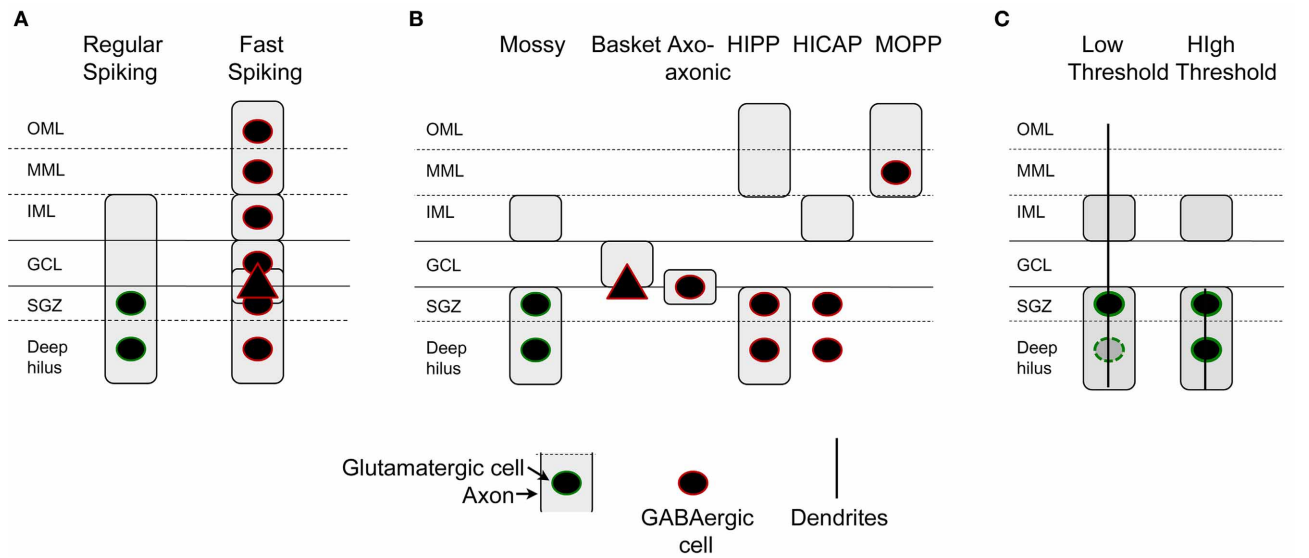

FIGURE 7 | Characterization of dentate gyrus non-granule cells. (A) Intrinsic electrophysiology of DG non-granule cells include two classes primarily, those cells that are regular-spiking and those that are not. Regular-spiking cells are mossy cells with hilar cell bodies and an axon in all layers but the outer and middle molecular layers. Fast-spiking cells are found in all layers and have axons that are in all layers. **(B)** Axon location indicates at least six types of non-granule cells. GABAergic neurons include basket cells, typically with a pyramidal cell-shaped soma, axo-axonic cells, HIPP cells, HICAP cells, and MOPP cells (Han et al., 1993; Freund and Buzsáki, 1996). Recent studies suggest that neurogliaform cells and ivy cells exist (Armstrong et al., 2011, 2012). **(C)** Mossy cells can be divided into two categories based on the location of their dendrites, cell body, and threshold to stimulation of the perforant path. Cells with dendrites in the molecular layer and primarily located near the cell layer have low thresholds for activation by the perforant path.

are a minority. In contrast, the reeler mouse is vastly different (Kowalski et al., 2009), where disorganization of the cell layers of the DG is accompanied by many mossy cell dendrites in the molecular layer, which are innervated by the perforant path (Kowalski et al., 2009).

VULNERABILITY OF MOSSY CELLS

The vulnerability of the hilar region or "endfolium" in humans has been known for some time. One of the first studies to suggest that hilar neurons might be vulnerable relative to other hippocampal cell types was a study of postmortem brain samples from patients with temporal lobe epilepsy (TLE). It was noted that endfolium sclerosis, where only hilar neuron loss occurs, was often evident. In addition, there was often damage in other hippocampal subfields such as CA1 and CA3 (Margerison and Corsellis, 1966). The results suggested that hilar neuron loss might be a "common denominator" in TLE, and led to the hypothesis that hilar neuron loss might cause TLE.

In 1987 a study was published that attempted to simulate endfolium sclerosis in rats by prolonged activation of DG granule cells by intermittent perforant path stimulation for 24 h (Sloviter, 1987). It was shown that hilar neurons which lacked GABA immunoreactivity (presumably mossy cells) were vulnerable. This was notable because a leading hypothesis for epilepsy at the time was a loss of GABAergic neurons—not loss of glutamatergic neurons (Ribak et al., 1979).

Sloviter and colleagues showed using silver stain that terminals in the inner molecular layer were degenerated after prolonged stimulation, which also suggested that mossy cells were damaged. Together with earlier studies (Olney et al., 1983; Sloviter, 1983) and consistent with other ideas at the time (Mattson et al., 1989), it was hypothesized that release of glutamate from the large boutons of granule cells was excitotoxic to hilar cells such as mossy cells (Olney et al., 1986).

As animal models of TLE were developed, investigators began to study neuronal loss in the hilus after insults and injury that are risk factors for TLE, including a brief period of severe continuous seizures (SE). Hilar neuron loss was documented in these animals, and included both mossy cells and HIPP cells (Maglóczky and Freund, 1993, 1995; Mitchell et al., 1995, 1997), which was later studied in more detail by others (Buckmaster and Jongen-Relo, 1999; Sun et al., 2007). After hypoxia/ischemia, mossy cells and HIPP cells were also reduced in number (Johansen et al., 1987; Crain et al., 1988; Represa et al., 1991; Hsu and Buzsáki, 1993; Matsuyama et al., 1993). After fluid-percussive injury, a model of traumatic brain injury, a large reduction in mossy cells and HIPP cells occurred (Lowenstein et al., 1992; Santhakumar et al., 2000). In all of these conditions, granule cells were spared, suggesting a selective vulnerability of hilar mossy cells and HIPP cells.

Many questions were raised by the results. What was the normal role of mossy cells and HIPP cells? Did mossy cell and HIPP cell loss cause TLE? To date there is no method to selectively remove mossy cells or HIPP cells or to silence them, so investigators have used the animal models where they are reduced in number to try to gain insight into these questions.

UNDERSTANDING MOSSY CELLS BY EXAMINING THEIR VULNERABILITY

One hypothesis for the vulnerability of hilar mossy cells and HIPP neurons was based on the fact that markers of calcium binding proteins did not stain mossy cells and HIPP cells. Two calcium binding proteins were investigated primarily: parvalbumin, a marker of relatively resistant perisomatic targeting GABAergic cells, and calbindin D28K (CaBP), which primarily stains granule cells within the DG. The correlation between staining for these two calcium binding proteins and relative resistance to injury, taken together with the idea that excitotoxicity was caused by calcium accumulation, led to the hypothesis that calcium binding capacity was strong in resistant neurons and weak in vulnerable neurons (Sloviter, 1989). Therefore, it was suggested that mossy cells and HIPP cells were vulnerable because they lacked calcium binding capacity. When granule cell input was strong, excitotoxicity occurred more readily than in other cell types, because intracellular calcium buffering was limited. In support of that hypothesis, intracellular calcium chelation by a synthetic calcium chelator, BAPTA, led to resistance of hilar mossy cells and hilar interneurons to prolonged perforant path stimulation in rat hippocampal slices (Scharfman and Schwartzkroin, 1989). This hypothesis was also supported by anatomical studies showing that the relatively resistant CA2 region expresses CaBP (Leranth and Ribak, 1991). Moreover, we found that CaBP expression occurred in surviving hilar neurons after SE, suggesting that those hilar cells which survive might express CaBP *de novo* as an endogenous mechanism for protection (Scharfman et al., 2002b; Scharfman, 2012a). However, it has not been proved, to our knowledge, that calcium binding proteins are the reason for vulnerability or resistance. In fact, exceptions to the correlation between CaBP and parvalbumin expression have been described, which argued against the hypothesis (Freund et al., 1990, 1992; Bouilleret et al., 2000).

Another hypothesis for the vulnerability of hilar mossy cells is the nature of their mossy fiber input (Schwartzkroin et al., 1996). It appears that mossy cells receive more of the "massive" mossy fiber boutons—relative to the smaller boutons of mossy fibers—than the GABAergic hilar cells and CA3 pyramidal cells, although quantitative comparisons are unavailable. Also, the large mossy fiber boutons are proximal to the soma of mossy cells where they are likely to have the most impact. It is clear when recording from mossy cells that they receive a great deal of excitatory drive, because there is usually a continuous barrage of depolarizing input in the form of EPSPs. This barrage may indeed place the cells at risk of excitotoxicity during injury, because when slices are made without a great deal of care, the mossy cells with the greatest frequency of these spontaneous EPSPs are harder to detect compared to slices with more attention to preservation of the hippocampus. This observation—albeit an anecdotal one—suggests that the mossy cells with the greatest spontaneous activity did not survive the trauma of slice preparation but mossy cells with less spontaneous input did.

Another regulator of vulnerability, which has been examined mostly in HIPP cells, is expression of striatal enriched protein tyrosine phosphatase; STEP) (Choi et al., 2007). HIPP cells have low expression, and other hilar cells (possibly mossy cells) appear

to also exhibit low expression based on the micrographs that are published, whereas some large cells near the HIPP cells in the hilus also have low expression of STEP (Choi et al., 2007). When challenged with an insult, STEP can rescue HIPP cells (Choi et al., 2007). HIPP cells are also vulnerable in response to degeneration of the septohippocampal projection (Zhang et al., 1998), and are reduced in number in postmortem specimens of individuals with Alzheimer's disease (Chan-Palay, 1987); vulnerability in Alzheimer's disease may also be the case for mossy cells but less evidence is published for mossy cells compared to HIPP cells (Scharfman, 2012a).

UNDERSTANDING THE FUNCTIONAL ROLE OF MOSSY CELLS

INFERENCES BASED ON THE CONSEQUENCES OF MOSSY CELL LOSS

The dormant basket cell hypothesis

Based on the apparent loss of hilar mossy cells, and preservation of GABAergic basket cells after prolonged perforant path stimulation in the rat, it was proposed that hyperexcitability following mossy cell loss was caused by inadequate activation of basket cells by mossy cells (Sloviter, 1991). Basket cells are a major subtype of interneuron in the DG, which play a major role in perisomatic inhibition of granule cells. Without mossy cell input, the basket cells were suggested to be "dormant"—fully functional, but lacking a major source of afferent input (**Figure 8**). Evidence for this hypothesis was provided by several studies, each consistent with the idea that basket cells were present and functional, but lacked their normal excitatory input (Sloviter, 1991, 1994). The idea of dormant basket cells was also applied to other circuits (Bekenstein and Lothman, 1993).

Since that time, the dormant basket cell hypothesis has been questioned. One reason is that loss of HIPP cells might also cause hyperexcitability. Another reason is that granule cells provide strong afferent input to basket cells and are resistant to insult and injury. Also, additional data have suggested that postsynaptic changes in GABAergic synapses on granule cells occur under conditions of mossy cell loss (Brooks-Kayal et al., 1998; Mtchedlishvili et al., 2001; Zhang and Buckmaster, 2009) so presynaptic mechanisms are not necessary to invoke. The idea that the basket cell is the major cell type that controls granule cell excitability has also been modified; it is now clear that other subtypes of GABAergic interneurons are very important (Freund and Buzsáki, 1996). Therefore, the "dormant" basket cell hypothesis has several potential limitations (Bernard et al., 1998). An alternative to the dormant basket cell hypothesis, for example, is a relatively recent idea that NaV1.1 sodium channels of DG basket cells are altered in epilepsy or Alzheimer's disease, but afferent input is unchanged. For example, in mouse models of familial Alzheimer's disease, it has been suggested that Nav1.1 sodium channels are reduced at the cell surface of GABAergic basket cells of the DG, leading to disinhibition of granule cells; in some genetic forms of epilepsy (Generalized epilepsy with febrile seizures-plus; Severe myoclonic epilepsy in infancy), mutations in Nav1.1 cause the disease (Catterall et al., 2010; Scharfman, 2012b; Verret et al., 2012).

Irritable mossy cell hypothesis

Vulnerability of mossy cells was also addressed by detailed studies of the fluid-percussive injury model of traumatic brain injury in rats. In this animal model, it was shown that mossy cell loss occurred 1 week following injury, and mossy cell loss was not necessarily greater than the loss of GABAergic neurons (Santhakumar et al., 2000). The relative loss of mossy cells vs. GABAergic neurons was hard to address because—as the authors noted—injury changes expression levels of proteins used to identify GABAergic neurons. The authors conducted mRNA expression studies to support their findings from immunocytochemistry, although even mRNA measurements have caveats, as the authors pointed out. Nevertheless, it was clear that there were surviving mossy cells after brain injury, and granule cell hyperexcitability developed. Interestingly, the hyperexcitability of granule cells resembled the findings of the prolonged perforant path stimulation model, i.e., a stimulus to the perforant path evoked a short train of 2–4 population spikes of granule cells in the injured animals. The results were also similar to other studies of fluid percussion injury where destruction of hilar cells and a short train of 2–4 population spikes were recorded in response to stimulation of the perforant path (Lowenstein et al., 1992). Importantly, surviving mossy cells were more active in slices from the injured animals, and it was suggested that this mossy cell hyperexcitability could directly cause the granule cell hyperexcitability in distal hippocampus (**Figure 8**). It was proposed that surviving mossy cells became "irritable" (more excitable) after injury, and contributed to hyperexcitability of distal granule cells as a result (Santhakumar et al., 2000, 2005; Ratzliff et al., 2002).

The irritable mossy cell hypothesis is important in light of recent approaches to animal models of epilepsy where the use of SE to induce hippocampal injury has been modified. Instead of producing complete hilar loss by prolonged SE, a less severe SE is induced which produces less damage and less hilar loss (Scharfman et al., 2001, 2002a, 2009). SE severity is reduced by administration of an anticonvulsant (e.g., diazepam) $\leq$1 h after seizures begin. The result is less damage to hilar mossy cells, hilar GABAergic neurons, and the rest of the brain (Scharfman et al., 2001, 2002a).

Animals that were examined that experienced SE with reduced severity showed effects that supported the irritable mossy cell hypothesis. Surviving mossy cells exhibited spontaneous burst discharges called paroxysmal depolarization shifts (Scharfman et al., 2001), the hallmark behavior of epileptic cortical principal cells (Prince, 1968; Ayala, 1983). A subset of additional hilar cells which were fast-spiking, and therefore GABAergic neurons, also exhibited these discharges (Scharfman et al., 2001). The generator of the epileptiform activity was area CA3, and activity reached the hilus by the backprojecting CA3 axon collaterals (Scharfman, 2007). Thus, severing the junction between the DG and CA3 silenced the DG mossy cells (Scharfman, 1994b). The results suggested that, in both an animal model of traumatic injury and an animal model of epilepsy, mossy cells did not necessarily die, and the surviving mossy cells became hyperexcitable.

Based on these two hypotheses, the dormant basket cell hypothesis and the irritable mossy cell hypothesis (**Figure 8**), there are two major concepts that have developed to explain the functional role of mossy cells in the DG. First, mossy cells are critical for inhibition of granule cells because of their excitatory effect on GABAergic neurons, which in turn inhibit granule cells. Second, mossy cells have a potentially powerful direct excitatory

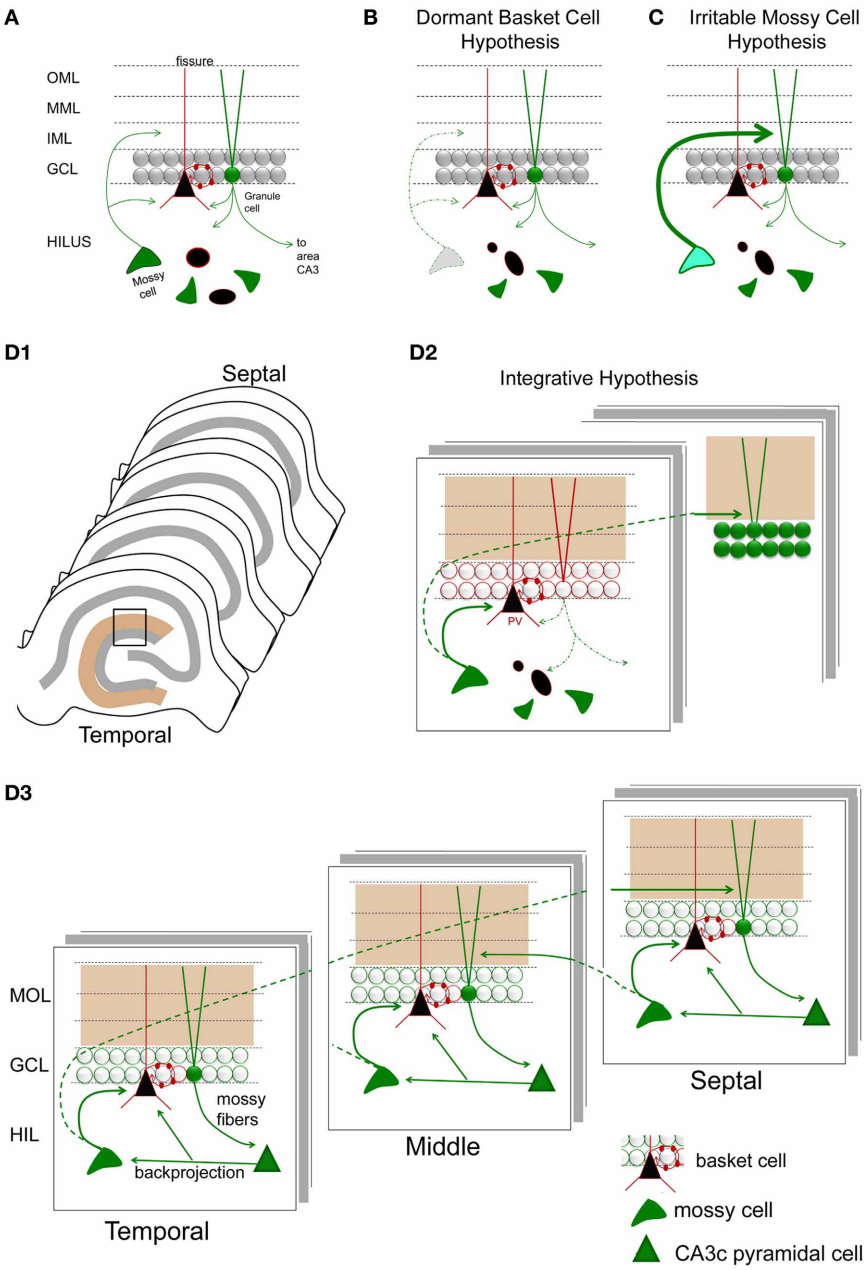

FIGURE 8 | Hypotheses for mossy cell vulnerability and function. (A) An illustration of the circuit components used in parts **(B–D)**. Only some cell types in the DG are shown. Green cells and fibers represent glutamatergic cells and their axons; black cells and their red processes represent GABAergic neurons and their dendrites/axons. The triangular black cell represents the prototype of the GABAergic neuron, the basket cell. **(B)** The dormant basket cell hypothesis is illustrated schematically. Without mossy cell afferent input, basket cells do not have sufficient afferent input to inhibit granule cells. The result is disinhibition of granule cells. **(C)** The irritable mossy cell hypothesis is illustrated schematically. When mossy cells are activated, they directly excite granule cells. After traumatic brain injury, they discharge more. The net effect is more granule cell excitation. **(D1)** A representation of the lamellae of the hippocampus is shown. Brown = molecular layer. Gray = cell layers. **(D2)** A hypothesis that incorporates aspects of the dormant basket cell and irritable mossy cell hypotheses. (a) Mossy cell axons near their cell body, i.e., within the lamella of the mossy cell soma, innervate GABAergic neurons primarily, leading to inhibition of adjacent granule cells; (b) in distant lamella, the same mossy cells primarily excite granule cells. **(D3)** A schematic that illustrates a modification of the hypothesis of Lisman et al. (2005) to account for differences in circuitry across the septohippocampal axis, and GABAergic inhibition by the backprojecting axon collaterals of CA3 pyramidal cells. Following granule cell activation by the perforant path, CA3 activation by the mossy fibers will be followed by excitation of GABAergic neurons in the DG by CA3 backprojections [including the hilar dendrites of basket cells as shown; (Kneisler and Dingledine, 1995)]. The backprojection also innervates mossy cells which excite local GABAergic neurons. The result is silencing of recently active granule cells. In distal hippocampus, granule cells will be stimulated by the same mossy cells. CA3 backprojections in that location will then activate mossy cells which will project back to a lamella close to where activity began. This lamella is unlikely to be precisely the same as the original one because the extent that temporal mossy cells project to septal hippocampus is greater than the extent that septal mossy cells project to temporal levels. Note that the circuitry is simplified in the schematic for the purposes of illustration.

role on distal granule cells. How does one reconcile these two ideas?

AN INTEGRATIVE HYPOTHESIS FOR MOSSY CELL FUNCTION

Both hypotheses may be correct. Local to the cell body of the MC, there is a local plexus of mossy cell axon collaterals that could be primarily inhibitory; this idea is supported by the results showing that mossy cells have monosynaptic excitatory connections with local inhibitory neurons in hippocampal slices using paired recordings (Scharfman, 1995b; Larimer and Strowbridge, 2008). If $GABA_A$ receptors are blocked, monosynaptic excitatory connections of mossy cells to granule cells can be detected (Scharfman, 1995b), suggesting that normally GABAergic inhibition masked excitatory effects of mossy cells on granule cells. However, other studies have shown that excitatory actions of MCs can be detected in hippocampal slices even when $GABA_A$ receptors are not blocked (Jackson and Scharfman, 1996).

Distal to the area where the mossy cell body is located, the mossy cell axon appears to primarily innervate granule cells. This idea is supported by quantitative studies of the mossy cell projection distal to the location of the cell body. At these distal locations the mossy cell axon preferentially innervates granule cells compared to GABAergic neurons (Buckmaster et al., 1996).

Based on these data, the following circuitry is suggested (**Figure 8D**): upon activation of a granule cell by entorhinal cortex, local inhibition of granule cells by mossy cells limits the activation of the recently-activated granule cell. Reducing the activation of these granule cells may be important for functions related to pattern separation, where it is not ideal for granule cells to discharge persistently. When pattern separation is simulated by a computational model of the DG network, removal of mossy cells indeed degrades the ability of the network to distinguish a set of overlapping input patterns (Myers and Scharfman, 2009, 2011). In addition to local inhibition of granule cells that were recently active, mossy cells could be important to activate distal granule cells which were not activated by the initial entorhinal input. Therefore, local inhibition and distal excitation of granule cells by mossy cells could be an effective modulation of the DG network to promote pattern separation by granule cells.

This hypothesis is complementary to one that was proposed before that suggests the DG and mossy cells are important to associative memory (Buckmaster and Schwartzkroin, 1994). It is also complementary to the idea that mossy cells are critical to the ability of the hippocampus to learn sequences of information (Lisman et al., 2005). In the model proposed by Lisman et al. (2005), area CA3 is an autoassociative network and the DG is heteroassociative; the granule cells and CA3 interact to perform the task of sequence learning and sequence prediction. In this DG-CA3 network, input from the DG is provided to the CA3 autoassociator, which performs pattern completion along recurrent collaterals among pyramidal cells; the resulting pattern is provided back to DG via the CA3 backprojection; and the DG then performs heteroassociation to predict the next inputs which will arrive from entorhinal cortex. Together, DG and CA3 can learn and reproduce sequences of patterns via this reciprocal loop. Mossy cells play a critical role in this network in two ways. First, mossy cells mediate excitatory input from CA3 to granule cells (the pathway is CA3 pyramidal cell-to-mossy cell-to-granule cell). Second, mossy cells themselves can mediate an additional heteroassociative pathway (as proposed by Lisman et al., 2005) because mossy cells form a second reciprocal loop with granule cells.

Although the models of Myers and Scharfman (2011), which stress granule cell inhibition, and of Lisman et al. (2005), which stress granule cell excitation, appear opposing, the three dimensional structure of the hippocampus may provide a way to reconcile these ideas, diagrammed in **Figure 8D**. Specifically, it has been shown that the CA3 backprojection innervates both GABAergic interneurons and mossy cells. In hippocampal slices, normally the inhibition dominates, probably because most of the axon projection of mossy cells that excite granule cells is transected (Scharfman, 1994a,b). However, this may not be the case *in vivo*. Rather, in a given lamella, area CA3 excites mossy cells which in turn activate distal granule cells, and at the same time CA3 excites GABAergic neurons which inhibit granule cells within the lamella. Inhibition of granule cells within the lamella could potentially promote pattern separation as proposed by Myers and Scharfman (2011), while activation of distal granule cells by mossy cells could provide the heteroassociative component of the Lisman et al. (2005) model. These distal granule cells would update area CA3 neurons in the same distal part of hippocampus because mossy fiber axons of granule cells are a lamellar pathway. Thus, a focus on the three-dimensional structure of DG-CA3 circuitry may promote understanding of multiple functions within the same substrate.

AN EXPLANATION FOR MOSSY CELL VULNERABILITY BASED ON THEIR NORMAL ROLE IN THE DENTATE GYRUS

A corollary to this hypothesis is that mossy cells are relays to granule cells, and their high sensitivity is important to the activation of otherwise silent granule cells. This function may be critical and therefore worth the "price" of a high risk of excitotoxicity to mossy cells.

One reason to suggest that mossy cells are relays is based on their afferent inputs relative to granule cells. Mossy cells receive numerous intrinsic and extrinsic inputs which do not innervate granule cells. For example, CA3 pyramidal cells innervate mossy cells throughout a large part of the septohippocampal axis, but only in temporal hippocampus does CA3 innervate granule cells (Li et al., 1994). The fact that mossy cells are the only dentate neuron with the glucocorticoid receptor subtype 2 receptor (Patel and Bulloch, 2003) suggests a potential role in stress that is absent in granule cells. There also is a great deal of extrinsic subcortical input to the hilus, and in some cases, the input to the hilus appears to be greater than the molecular layer, suggesting that the input has a greater effect on hilar neurons than granule cells (Amaral and Campbell, 1986; Swanson et al., 1987). For example, serotoninergic fibers are dense in the subgranular zone compared to the molecular layer (Swanson et al., 1987). Dopaminergic fibers and norardrenergic fibers also appear to innervate the hilus more than the molecular layer (Swanson et al., 1987). However, there is some disagreement about the relative patterns of inputs from these ascending brainstem systems, possibly due to species differences and differences among the antibodies that have been

employed (compare Amaral and Campbell, 1986 with Swanson et al., 1987). It is also important to be cautious in the interpretation of function based on immunocytochemistry, because the pharmacological effects of the transmitters in these fiber pathways are likely to be complex given the large numbers of receptor subtypes.

Mossy cells are well designed to serve as a relay cell for other reasons. For example, mossy cells have a resting potential close to threshold and receive a constant barrage of mossy fiber input that keeps them even closer to threshold (Scharfman and Schwartzkroin, 1988; Scharfman, 1993a). Mossy cells also have a characteristic that may be important if they are a relay cell to granule cell, because the characteristic predisposes them not to activate granule cells too much: if mossy cells are induced to fire repetitively in response to a strong glutamatergic or direct stimulus, their ability to discharge decays. Their action potential broadens, shortens, and ultimately they stop firing (Scharfman and Schwartzkroin, 1989, 1990). On the other hand, it has been reported that the reverse is true under some conditions (Strowbridge et al., 1992), which suggests a potential for plasticity of relay function.

There is one "problem" with the idea that mossy cells are important as a relay of information to granule cells: the unitary EPSP of mossy cells to granule cells seems quite weak and often fails (Scharfman, 1995b). However, when granule cells are depolarized, and potentially there is also a decrease in GABAergic inhibition of the granule cells, mossy cell input strengthens (Scharfman, 1995b). Therefore, if a septal GABAergic input (for example) disinhibits the granule cells, which appears to be its primary function in the DG (Freund and Antal, 1988), it may also disinhibit a mossy cell, making distal granule cells more likely to be activated by input from mossy cells. Another combination that would be potent is noradrenergic depolarization of granule cells (Lacaille and Harley, 1985; Lacaille and Schwartzkroin, 1988; Dahl and Sarvey, 1989) at the same time as a mossy cell input activates the granule cell. Taken together, the data from paired intracellular recording and studies of neuromodulators suggests that granule cells will be activated best when there is septohippocampal tone or brainstem activation. That would mean times of spatial exploration and/or flight/fright such as when a predator nears. Indeed, mossy cells do discharge during theta rhythm (Soltesz et al., 1993) and it was predicted that they would have an important role based on these data and others *in vivo* data (Buckmaster and Schwartzkroin, 1994; Bragin et al., 1995; Penttonen et al., 1997). These studies are consistent with the idea that the mossy cell is important to relay to granule cells information about the environment or context.

CONCLUSION

Mossy cells of the DG are glutamatergic neurons that have intrinsic and circuit properties that make them ideal to activate granule cells, which is likely to be necessary because the granule cells are quiescent, hyperpolarized neurons. That quiescence seems necessary for cognitive functions such as pattern separation but leaves granule cells at risk of suboptimal activation. Mossy cells could serve to inhibit local granule cells so they are not activated too much by an input, supporting pattern separation, but activate granule cells in distal DG lamellae to relay or "broadcast" information that might otherwise be undetected, which may support heterassociative function. For this potentially important role, mossy cells may pay a "price"—vulnerability to insults or injuries that are associated with release of high concentrations of glutamate from the mossy fibers.

ACKNOWLEDGMENTS

Supported by MH-090606, the Alzheimer's Association and the New York State Office of Mental Health.

REFERENCES

Abraham, H., Czeh, B., Fuchs, E., and Seress, L. (2005). Mossy cells and different subpopulations of pyramidal neurons are immunoreactive for cocaine- and amphetamine-regulated transcript peptide in the hippocampal formation of non-human primates and tree shrew (*Tupaia belangeri*). *Neuroscience* 136, 231–240.

Amaral, D. (1978). A Golgi study of cell types in the hilar region of the hippocampus in the rat. *J. Comp. Neurol.* 15, 851–914.

Amaral, D. G., and Campbell, M. J. (1986). Transmitter systems in the primate dentate gyrus. *Hum. Neurobiol.* 5, 169–180.

Amaral, D. G., Scharfman, H. E., and Lavenex, P. (2007). The dentate gyrus: fundamental neuroanatomical organization (dentate gyrus for dummies). *Prog. Brain Res.* 163, 3–22.

Armstrong, C., Krook-Magnuson, E., and Soltesz, I. (2012). Neurogliaform and ivy cells: a major family of nNOS expressing GABAergic Neurons. *Front. Neural Circuits* 6:23. doi: 10.3389/fncir.2012.00023

Armstrong, C., Szabadics, J., Tamas, G., and Soltesz, I. (2011). Neurogliaform cells in the molecular layer of the dentate gyrus as feed-forward gamma-aminobutyric acidergic modulators of entorhinal-hippocampal interplay. *J. Comp. Neurol.* 519, 1476–1491.

Ayala, G. F. (1983). The paroxysmal depolarizing shift. *Prog. Clin. Biol. Res.* 124, 15–21.

Bakst, I., Avendano, C., Morrison, J. H., and Amaral, D. G. (1986). An experimental analysis of the origins of somatostatin-like immunoreactivity in the dentate gyrus of the rat. *J. Neurosci.* 6, 1452–1462.

Bekenstein, J. W., and Lothman, E. W. (1993). Dormancy of inhibitory interneurons in a model of temporal lobe epilepsy. *Science* 259, 97–100.

Bernard, C., Esclapez, M., Hirsch, J. C., and Ben-Ari, Y. (1998). Interneurones are not so dormant in temporal lobe epilepsy: a critical reappraisal of the dormant basket cell hypothesis. *Epilepsy Res.* 32, 93–103.

Blackstad, T. W., and Kjaerheim, A. (1961). Special axo-dendritic synapses in the hippocampal cortex: electron and light microscopic studies on the layer of mossy fibers. *J. Comp. Neurol.* 117, 133–159.

Blasco-Ibanez, J. M., and Freund, T. F. (1997). Distribution, ultrastructure, and connectivity of calretinin-immunoreactive mossy cells of the mouse dentate gyrus. *Hippocampus* 7, 307–320.

Bouilleret, V., Schwaller, B., Schurmans, S., Celio, M. R., and Fritschy, J. M. (2000). Neurodegenerative and morphogenic changes in a mouse model of temporal lobe epilepsy do not depend on the expression of the calcium-binding proteins parvalbumin, calbindin, or calretinin. *Neuroscience* 97, 47–58.

Bragin, A., Jando, G., Nadasdy, Z., van Landeghem, M., and Buzsáki, G. (1995). Dentate EEG spikes and associated interneuronal population bursts in the hippocampal hilar region of the rat. *J. Neurophysiol.* 73, 1691–1705.

Brandt, M. D., Jessberger, S., Steiner, B., Kronenberg, G., Reuter, K., Bick-Sander, A., et al. (2003). Transient calretinin expression defines early postmitotic step of neuronal differentiation in adult hippocampal neurogenesis of mice. *Mol. Cell. Neurosci.* 24, 603–613.

Brooks-Kayal, A. R., Shumate, M. D., Jin, H., Rikhter, T. Y., and Coulter, D. A. (1998). Selective changes in

single cell GABA(A) receptor subunit expression and function in temporal lobe epilepsy. *Nat. Med.* 4, 1166–1172.

Buckmaster, P., Wenzel, H., Kunkel, D., and Schwartzkroin, P. (1996). Axon arbors and synaptic connections of hippocampal mossy cells in the rat *in vivo*. *J. Comp. Neurol.* 366, 271–292.

Buckmaster, P. S., and Amaral, D. G. (2001). Intracellular recording and labeling of mossy cells and proximal CA3 pyramidal cells in macaque monkeys. *J. Comp. Neurol.* 430, 264–281.

Buckmaster, P. S., and Jongen-Relo, A. L. (1999). Highly specific neuron loss preserves lateral inhibitory circuits in the dentate gyrus of kainate-induced epileptic rats. *J. Neurosci.* 19, 9519–9529.

Buckmaster, P. S., and Schwartzkroin, P. A. (1994). Hippocampal mossy cell function: a speculative view. *Hippocampus* 4, 393–402.

Buckmaster, P. S., Strowbridge, B. W., Kunkel, D. D., Schmiege, D. L., and Schwartzkroin, P. A. (1992). Mossy cell axonal projections to the dentate gyrus molecular layer in the rat hippocampal slice. *Hippocampus* 2, 349–362.

Buckmaster, P. S., Strowbridge, B. W., and Schwartzkroin, P. A. (1993). A comparison of rat hippocampal mossy cells and CA3c pyramidal cells. *J. Neurophysiol.* 70, 1281–1299.

Buhl, E. H., Han, Z. S., Lorinczi, Z., Stezhka, V. V., Karnup, S. V., and Somogyi, P. (1994). Physiological properties of anatomically identified axo-axonic cells in the rat hippocampus. *J. Neurophysiol.* 71, 1289–1307.

Bulloch, K., Prasad, A., Conrad, C. D., McEwen, B. S., and Milner, T. A. (1996). Calcitonin gene-related peptide level in the rat dentate gyrus increases after damage. *Neuroreport* 7, 1036–1040.

Catterall, W. A., Kalume, F., and Oakley, J. C. (2010). NaV1.1 channels and epilepsy. *J. Physiol.* 588, 1849–1859.

Chan-Palay, V. (1987). Somatostatin immunoreactive neurons in the human hippocampus and cortex shown by immunogold/silver intensification on vibratome sections: coexistence with neuropeptide Y neurons, and effects in Alzheimer-type dementia. *J. Comp. Neurol.* 260, 201–223.

Choi, Y. S., Lin, S. L., Lee, B., Kurup, P., Cho, H. Y., Naegele, J. R., et al. (2007). Status epilepticus-induced somatostatinergic hilar interneuron degeneration is regulated by striatal enriched protein tyrosine phosphatase. *J. Neurosci.* 27, 2999–3009.

Crain, B. J., Westerkam, W. D., Harrison, A. H., and Nadler, J. V. (1988). Selective neuronal death after transient forebrain ischemia in the *Mongolian gerbil*: a silver impregnation study. *Neuroscience* 27, 387–402.

Dahl, D., and Sarvey, J. M. (1989). Norepinephrine induces pathway-specific long-lasting potentiation and depression in the hippocampal dentate gyrus. *Proc. Natl. Acad. Sci. U.S.A.* 86, 4776–4780.

Deller, T., Martinez, A., Nitsch, R., and Frotscher, M. (1996). A novel entorhinal projection to the rat dentate gyrus: direct innervation of proximal dendrites and cell bodies of granule cells and GABAergic neurons. *J. Neurosci.* 16, 3322–3233.

Deller, T., Nitsch, R., and Frotscher, M. (1994). Associational and commissural afferents of parvalbumin-immunoreactive neurons in the rat hippocampus: a combined immunocytochemical and PHA-L study. *J. Comp. Neurol.* 350, 612–622.

Deller, T., Nitsch, R., and Frotscher, M. (1995). Phaseolus vulgaris-leucoagglutinin tracing of commissural fibers to the rat dentate gyrus: evidence for a previously unknown commissural projection to the outer molecular layer. *J. Comp. Neurol.* 352, 55–68.

Douglas, R. M., McNaughton, B. L., and Goddard, G. V. (1983). Commissural inhibition and facilitation of granule cell discharge in fascia dentata. *J. Comp. Neurol.* 219, 285–294.

Einheber, S., Pierce, J. P., Chow, D., Znamensky, V., Schnapp, L. M., and Milner, T. A. (2001). Dentate hilar mossy cells and somatostatin-containing neurons are immunoreactive for the alpha8 integrin subunit: characterization in normal and kainic acid-treated rats. *Neuroscience* 105, 619–638.

Freund, T. F., and Antal, M. (1988). GABA-containing neurons in the septum control inhibitory interneurons in the hippocampus. *Nature* 336, 170–173.

Freund, T. F., and Buzsáki, G. (1996). Interneurons of the hippocampus. *Hippocampus* 6, 347–470.

Freund, T. F., Buzsáki, G., Leon, A., Baimbridge, K. G., and Somogyi, P. (1990). Relationship of neuronal vulnerability and calcium binding protein immunoreactivity in ischemia. *Exp. Brain Res.* 83, 55–66.

Freund, T. F., Hajos, N., Acsady, L., Gorcs, T. J., and Katona, I. (1997). Mossy cells of the rat dentate gyrus are immunoreactive for calcitonin gene-related peptide (CGRP). *Eur. J. Neurosci.* 9, 1815–1830.

Freund, T. F., Ylinen, A., Miettinen, R., Pitkanen, A., Lahtinen, H., Baimbridge, K. G., et al. (1992). Pattern of neuronal death in the rat hippocampus after status epilepticus. Relationship to calcium binding protein content and ischemic vulnerability. *Brain Res. Bull.* 28, 27–38.

Frotscher, M., Seress, L., Schwerdtfeger, W. K., and Buhl, E. (1991). The mossy cells of the fascia dentata: a comparative study of their fine structure and synaptic connections in rodents and primates. *J. Comp. Neurol.* 312, 145–163.

Fujise, N., Liu, Y., Hori, N., and Kosaka, T. (1998). Distribution of calretinin immunoreactivity in the mouse dentate gyrus: II. Mossy cells, with special reference to their dorsoventral difference in calretinin immunoreactivity. *Neuroscience* 82, 181–200.

Goodman, J. H., and Sloviter, R. S. (1992). Evidence for commissurally projecting parvalbumin-immunoreactive basket cells in the dentate gyrus of the rat. *Hippocampus* 2, 13–21.

Han, Z. S., Buhl, E. H., Lorinczi, Z., and Somogyi, P. (1993). A high degree of spatial selectivity in the axonal and dendritic domains of physiologically identified local-circuit neurons in the dentate gyrus of the rat hippocampus. *Eur. J. Neurosci.* 5, 395–410.

Hsu, M., and Buzsáki, G. (1993). Vulnerability of mossy fiber targets in the rat hippocampus to forebrain ischemia. *J. Neurosci.* 13, 3964–3979.

Jackson, M. B., and Scharfman, H. E. (1996). Positive feedback from hilar mossy cells to granule cells in the dentate gyrus revealed by voltage-sensitive dye and microelectrode recording. *J. Neurophysiol.* 76, 601–616.

Jiao, Y., and Nadler, J. V. (2007). Stereological analysis of GluR2-immunoreactive hilar neurons in the pilocarpine model of temporal lobe epilepsy: correlation of cell loss with mossy fiber sprouting. *Exp. Neurol.* 205, 569–582.

Jinno, S., Ishizuka, S., and Kosaka, T. (2003). Ionic currents underlying rhythmic bursting of ventral mossy cells in the developing mouse dentate gyrus. *Eur. J. Neurosci.* 17, 1338–1354.

Johansen, F., Zimmer, J., and Diemer, N. (1987). Early loss somatostatin neurons in the dentate hilus after cerebral ischemia in the rat precedes CA-1 pyramidal cell loss. *Acta Neurophysiol.* 58, 110–114.

Kneisler, T. B., and Dingledine, R. (1995). Synaptic input from CA3 pyramidal cells to dentate basket cells in rat hippocampus. *J. Physiol.* 487(Pt 1), 125–146.

Kotti, T., Tapiola, T., Riekkinen, P. J., and Miettinen, R. Sr. (1996). The calretinin-containing mossy cells survive excitotoxic insult in the gerbil dentate gyrus. Comparison of excitotoxicity-induced neuropathological changes in the gerbil and rat. *Eur. J. Neurosci.* 8, 2371–2378.

Kowalski, J., Geuting, M., Paul, S., Dieni, S., Laurens, J., Zhao, S., et al. (2009). Proper layering is important for precisely timed activation of hippocampal mossy cells. *Cereb. Cortex* 20, 2043–2054.

Laatsch, R. H., and Cowan, W. M. (1966). Electron microscopic studies of the dentate gyrus of the rat. I. Normal structure with special reference to synaptic organization. *J. Comp. Neurol.* 128, 359–395.

Lacaille, J. C., and Harley, C. W. (1985). The action of norepinephrine in the dentate gyrus: beta-mediated facilitation of evoked potentials *in vitro*. *Brain Res.* 358, 210–220.

Lacaille, J. C., and Schwartzkroin, P. A. (1988). Intracellular responses of rat hippocampal granule cells *in vitro* to discrete applications of norepinephrine. *Neurosci. Lett.* 89, 176–181.

Larimer, P., and Strowbridge, B. W. (2008). Nonrandom local circuits in the dentate gyrus. *J. Neurosci.* 28, 12212–12223.

Leranth, C., and Hajszan, T. (2007). Extrinsic afferent systems to the dentate gyrus. *Prog. Brain Res.* 163, 63–84.

Leranth, C., and Ribak, C. E. (1991). Calcium-binding proteins are concentrated in the CA2 field of the monkey hippocampus: a possible key to this region's resistance to epileptic damage. *Exp. Brain Res.* 85, 129–136.

Leranth, C., Szeidemann, Z., Hsu, M., and Buzsáki, G. (1996). AMPA receptors in the rat and primate hippocampus: a possible absence of GluR2/3 subunits in most interneurons. *Neuroscience* 70, 631–652.

Li, X., Somogyi, P., Ylinen, A., and Buzsáki, G. (1994). The hippocampal CA3 network: an *in vivo* intracellular labeling study. *J. Comp. Neurol.* 339, 181–208.

Lisman, J. E., Talamini, L. M., and Raffone, A. (2005). Recall of memory sequences by interaction of the dentate and CA3: a revised model of the phase precession. *Neural Netw.* 18, 1191–1201.

Liu, Y., Fujise, N., and Kosaka, T. (1996). Distribution of calretinin immunoreactivity in the mouse dentate gyrus. I. General description. *Exp. Brain Res.* 108, 389–403.

Livsey, C. T., and Vicini, S. (1992). Slower spontaneous excitatory postsynaptic currents in spiny versus aspiny hilar neurons. *Neuron* 8, 745–755.

Lorente De Nó, R. (1934). Studies on the structure of the cerebral cortex. Continuation of the study of the ammonic system. *J. Psychol. Neurol.* 46, 113–177.

Lowenstein, D. H., Thomas, M. J., Smith, D. H., and McIntosh, T. K. (1992). Selective vulnerability of dentate hilar neurons following traumatic brain injury: a potential mechanistic link between head trauma and disorders of the hippocampus. *J. Neurosci.* 12, 4846–4853.

Lübke, J., Frotscher, M., and Spruston, N. (1998). Specialized electrophysiological properties of anatomically identified neurons in the hilar region of the rat fascia dentata. *J. Neurophysiol.* 79, 1518–1534.

Maglóczky, Z., and Freund, T. F. (1993). Selective neuronal death in the contralateral hippocampus following unilateral kainate injections into the CA3 subfield. *Neuroscience* 56, 317–335.

Maglóczky, Z., and Freund, T. F. (1995). Delayed cell death in the contralateral hippocampus following kainate injection into the CA3 subfield. *Neuroscience* 66, 847–860.

Margerison, J. H., and Corsellis, J. A. (1966). Epilepsy and the temporal lobes. A clinical, electroencephalographic and neuropathological study of the brain in epilepsy, with particular reference to the temporal lobes. *Brain* 89, 499–530.

Martinez, A., Ruiz, M., and Soriano, E. (1999). Spiny calretinin-immunoreactive neurons in the hilus and CA3 region of the rat hippocampus: local axon circuits, synaptic connections, and glutamic acid decarboxylase 65/67 mRNA expression. *J. Comp. Neurol.* 404, 438–448.

Matsuyama, T., Tsuchiyama, M., Nakamura, H., Matsumoto, M., and Sugita, M. (1993). Hilar somatostatin neurons are more vulnerable to an ischemic insult than CA1 pyramidal neurons. *J. Cereb. Blood Flow Metab.* 13, 229–234.

Mattson, M. P., Guthrie, P. B., and Kater, S. B. (1989). Intrinsic factors in the selective vulnerability of hippocampal pyramidal neurons. *Prog. Clin. Biol. Res.* 317, 333–351.

McCloskey, D. P., Hintz, T. M., Pierce, J. P., and Scharfman, H. E. (2006). Stereological methods reveal the robust size and stability of ectopic hilar granule cells after pilocarpine-induced status epilepticus in the adult rat. *Eur. J. Neurosci.* 24, 2203–2210.

Mitchell, J., Cook, I., and Hervey, V. (1997). Effect of seizures on hippocampal peptidergic neurons. *Neuropathol. Appl. Neurobiol.* 23, 299–306.

Mitchell, J., Gatherer, M., and Sundstrom, L. E. (1995). Loss of hilar somatostatin neurons following tetanus toxin-induced seizures. *Acta Neuropathol.* 89, 425–430.

Mtchedlishvili, Z., Bertram, E. H., and Kapur, J. (2001). Diminished allopregnanolone enhancement of GABA(A) receptor currents in a rat model of chronic temporal lobe epilepsy. *J. Physiol.* 537, 453–465.

Murakawa, R., and Kosaka, T. (2001). Structural features of mossy cells in the hamster dentate gyrus, with special reference to somatic thorny excrescences. *J. Comp. Neurol.* 329, 113–126.

Myers, C. E., and Scharfman, H. E. (2009). A role for hilar cells in pattern separation in the dentate gyrus: a computational approach. *Hippocampus* 19, 321–337.

Myers, C. E., and Scharfman, H. E. (2011). Pattern separation in the dentate gyrus: a role for the CA3 backprojection. *Hippocampus* 21, 1190–1215.

Olney, J., de Gubareff, T., and Sloviter, R. (1983). "Epileptic" brain damage in rats induced by sustained electrical stimulation of the perforant path. II. Ultrastructural analysis of acute hippocampal pathology. *Brain Res. Bull.* 10, 699–712.

Olney, J. W., Collins, R. C., and Sloviter, R. S. (1986). Excitotoxic mechanisms of epileptic brain damage. *Adv. Neurol.* 44, 857–877.

Patel, A., and Bulloch, K. (2003). Type II glucocorticoid receptor immunoreactivity in the mossy cells of the rat and the mouse hippocampus. *Hippocampus* 13, 59–66.

Penttonen, M., Kamondi, A., Sik, A., Acsady, L., and Buzsáki, G. (1997). Feed-forward and feed-back activation of the dentate gyrus *in vivo* during dentate spikes and sharp wave bursts. *Hippocampus* 7, 437–450.

Prince, D. A. (1968). The depolarization shift in "epileptic" neurons. *Exp. Neurol.* 21, 467–485.

Ramon y Cajal, S. (1911). *Histologie du Systeme Nerveux de l'Homme et des Vertebretes*. Paris: Malione.

Ratzliff, A. H., Howard, A. L., Santhakumar, V., Osapay, I., and Soltesz, I. (2004). Rapid deletion of mossy cells does not result in a hyperexcitable dentate gyrus: implications for epileptogenesis. *J. Neurosci.* 24, 2259–2269.

Ratzliff, A. H., Santhakumar, V., Howard, A., and Soltesz, I. (2002). Mossy cells in epilepsy: rigor mortis or vigor mortis? *Trends Neurosci.* 25, 140–144.

Represa, A., Crepel, V., and Ben-Ari, Y. (1991). Transient cerebral ischemia induces changes in SRIF mRNA in the fascia dentata. *Brain Res. Mol. Brain Res.* 10, 337–342.

Ribak, C. E., Harris, A. B., Vaughn, J. E., and Roberts, E. (1979). Inhibitory, GABAergic nerve terminals decrease at sites of focal epilepsy. *Science* 205, 211–214.

Ribak, C. E., Seress, L., and Amaral, D. G. (1985). The development, ultrastructure and synaptic connections of the mossy cells of the dentate gyrus. *J. Neurocytol.* 14, 835–857.

Rose, M. (1926). Der allocortex bei tier und mensch. *J. Psychol. Neurol.* 34, 1–99.

Santhakumar, V., Aradi, I., and Soltesz, I. (2005). Role of mossy fiber sprouting and mossy cell loss in hyperexcitability: a network model of the dentate gyrus incorporating cell types and axonal topography. *J. Neurophysiol.* 93, 437–453.

Santhakumar, V., Bender, R., Frotscher, M., Ross, S. T., Hollrigel, G. S., Toth, Z., et al. (2000). Granule cell hyperexcitability in the early post-traumatic rat dentate gyrus: the 'irritable mossy cell' hypothesis. *J. Physiol.* 524(Pt 1), 117–134.

Scharfman, H. (1992a). Differentiation of rat dentate neurons by morphology and electrophysiology in hippocampal slices: granule cells, spiny hilar cells and aspiny 'fast-spiking' cells. *Epilepsy Res. Suppl.* 7, 93–109.

Scharfman, H. E. (1992b). Blockade of excitation reveals inhibition of dentate spiny hilar neurons recorded in rat hippocampal slices. *J. Neurophysiol.* 68, 978–984.

Scharfman, H., Goodman, J., and McCloskey, D. (2007). Ectopic granule cells of the rat dentate gyrus. *Dev. Neurosci.* 29, 14–27.

Scharfman, H., and Schwartzkroin, P. (1988). Electrophysiology of morphologically identified mossy cells of the dentate hilus recorded in guinea pig hippocampal slices. *J. Neurosci.* 8, 3819–3821.

Scharfman, H., Sollas, A., Smith, K., Jackson, M., and Goodman, J. (2002a). Structural and functional asymmetry in the normal and epileptic rat dentate gyrus. *J. Comp. Neurol.* 454, 424–439.

Scharfman, H. E., Sollas, A. L., and Goodman, J. H. (2002b). Spontaneous recurrent seizures after pilocarpine-induced status epilepticus activate calbindin-immunoreactive hilar cells of the rat dentate gyrus. *Neuroscience* 111, 71–81.

Scharfman, H. E. (1991). Dentate hilar cells with dendrites in the molecular layer have lower thresholds for synaptic activation by perforant path than granule cells. *J. Neurosci.* 11, 1660–1673.

Scharfman, H. E. (1993a). Characteristics of spontaneous and evoked EPSPs recorded from dentate spiny hilar cells in rat hippocampal slices. *J. Neurophysiol.* 70, 742–757.

Scharfman, H. E. (1993b). Spiny neurons of area CA3c in rat hippocampal slices have similar electrophysiological characteristics and synaptic responses despite morphological variation. *Hippocampus* 3, 9–28.

Scharfman, H. E. (1994a). EPSPs of dentate gyrus granule cells during epileptiform bursts of dentate hilar "mossy" cells and area CA3 pyramidal cells in disinhibited rat hippocampal slices. *J. Neurosci.* 14, 6041–6057.

Scharfman, H. E. (1994b). Synchronization of area CA3 hippocampal pyramidal cells and non-granule cells of the dentate gyrus in bicuculline-treated rat hippocampal slices. *Neuroscience* 59, 245–257.

Scharfman, H. E. (1995a). Electrophysiological diversity of pyramidal-shaped neurons at the granule cell layer/hilus border of the rat dentate gyrus recorded *in vitro*. *Hippocampus* 5, 287–305.

Scharfman, H. E. (1995b). Electrophysiological evidence that dentate hilar mossy cells are excitatory and innervate both granule cells and interneurons. *J. Neurophysiol.* 74, 179–194.

Scharfman, H. E. (2007). The CA3 "backprojection" to the dentate gyrus. *Prog. Brain Res.* 163, 627–637.

Scharfman, H. E. (2012a). Alzheimer's disease and epilepsy: insight from animal models. *Future Neurol.* 7, 177–192.

Scharfman, H. E. (2012b). Untangling Alzheimer's disease and epilepsy. *Epilepsy Curr.* 12, 178–183.

Scharfman, H. E., Kunkel, D. D., and Schwartzkroin, P. A. (1990). Synaptic connections of dentate granule cells and hilar neurons: results of paired intracellular recordings and intracellular horseradish peroxidase injections. *Neuroscience* 37, 693–707.

Scharfman, H. E., Malthankar-Phatak, G. H., Friedman, D., Pearce, P., McCloskey, D. P., Harden, C. L., et al. (2009). A rat model of epilepsy in women: a tool to study physiological interactions between endocrine systems and seizures. *Endocrinology* 150, 4437–4442.

Scharfman, H. E., and Schwartzkroin, P. A. (1989). Protection of dentate hilar cells from prolonged stimulation by intracellular calcium chelation. *Science* 246, 257–260.

Scharfman, H. E., and Schwartzkroin, P. A. (1990). Responses of cells of the rat fascia dentata to prolonged stimulation of the perforant path: sensitivity of hilar cells and changes in granule cell excitability. *Neuroscience* 35, 491–504.

Scharfman, H. E., Smith, K. L., Goodman, J. H., and Sollas, A. L. (2001). Survival of dentate hilar mossy cells after pilocarpine-induced seizures and their synchronized burst discharges with area CA3 pyramidal cells. *Neuroscience* 104, 741–759.

Scharfman, H. E., and Witter, M. P. (2007). *Preface. The Dentate Gyrus: A Comprehensive Guide to Structure, Function and Clinical Implications*. New York, NY: Elsevier.

Schwartzkroin, P. A., Buckmaster, P. S., Strowbridge, B. W., Kunkel, D. D., Owens, J., and Pokorny, J. Jr. (1996). Possible mechanisms of seizure-related cell damage in the dentate hilus. *Epilepsy Res. Suppl.* 12, 317–324.

Seress, L., Abrahám, H., Czéh, B., Fuchs, E., and Léránth, C. (2008). Calretinin expression in hilar mossy cells of the hippocampal dentate gyrus of nonhuman primates and humans. *Hippocampus* 18, 425–434.

Seress, L., Abraham, H., Doczi, T., Lazar, G., and Kozicz, T. (2004). Cocaine- and amphetamine-regulated transcript peptide (CART) is a selective marker of rat granule cells and of human mossy cells in the hippocampal dentate gyrus. *Neuroscience* 125, 13–24.

Seress, L., and Mrzljak, L. (1992). Postnatal development of mossy cells in the human dentate gyrus: a light microscopic Golgi study. *Hippocampus* 2, 127–141.

Seress, L., and Ribak, C. E. (1995). Postnatal development and synaptic connections of hilar mossy cells in the hippocampal dentate gyrus of rhesus monkeys. *J. Comp. Neurol.* 355, 93–110.

Sloviter, R. (1983). "Epileptic" brain damage in rats induced by sustained electrical stimulation of the perforant path. I. Acute electrophysiological and light microscopical studies. *Brain Res. Bull.* 10, 675–697.

Sloviter, R. (1987). Decreased hippocampal inhibition and a selective loss of intemeurons in experimental epilepsy. *Science* 235, 73–76.

Sloviter, R. S. (1989). Calcium-binding protein (calbindin-D28k) and parvalbumin immunocytochemistry: localization in the rat hippocampus with specific reference to the selective vulnerability of hippocampal neurons to seizure activity. *J. Comp. Neurol.* 280, 183–196.

Sloviter, R. S. (1991). Permanently altered hippocampal structure, excitability, and inhibition after experimental status epilepticus in the rat: the "dormant basket cell" hypothesis and its possible relevance to temporal lobe epilepsy. *Hippocampus* 1, 41–66.

Sloviter, R. S. (1994). The functional organization of the hippocampal dentate gyrus and its relevance to the pathogenesis of temporal lobe epilepsy. *Ann. Neurol.* 35, 640–654.

Soltesz, I., Bourassa, J., and Deschanes, M. (1993). The behavior of mossy cells of the rat dentate gyrus during theta oscillations *in vivo*. *Neuroscience* 57, 555–564.

Soltesz, I., and Mody, I. (1994). Patch-clamp recordings reveal powerful GABAergic inhibition in dentate hilar neurons. *J. Neurosci.* 14, 2365–2376.

Soriano, E., and Frotscher, M. (1994). Mossy cells of the rat fascia dentata are glutamate-immunoreactive. *Hippocampus* 4, 65–69.

Strowbridge, B. W., Buckmaster, P. S., and Schwartzkroin, P. A. (1992). Potentiation of spontaneous synaptic activity in rat mossy cells. *Neurosci. Lett.* 142, 205–210.

Sun, C., Mtchedlishvili, Z., Bertram, E. H., Erisir, A., and Kapur, J. (2007). Selective loss of dentate hilar interneurons contributes to reduced synaptic inhibition of granule cells in an electrical stimulation-based animal model of temporal lobe epilepsy. *J. Comp. Neurol.* 500, 876–993.

Swanson, L. W., Kohler, C., and Bjorklund, A. (1987). "The limbic region. I: the septohippocampal system," in: *Handbook of Chemical Neuroanatomy, Vol. 5, Integrated Systems of the CNS, Part, I,* eds T. Hokfelt, A. Bjorklund, and L. W. Swanson (Amsterdam: Elsevier), 125–277.

Verret, L., Mann, E. O., Hang, G. B., Barth, A. M., Cobos, I., Ho, K., et al. (2012). Inhibitory interneuron deficit links altered network activity and cognitive dysfunction in Alzheimer model. *Cell* 149, 708–721.

West, J. R., Nornes, H. O., Barnes, C. L., and Bronfenbrenner, M. (1979). The cells of origin of the commissural afferents to the area dentata in the mouse. *Brain Res.* 160, 203–215.

Zhang, W., and Buckmaster, P. S. (2009). Dysfunction of the dentate basket cell circuit in a rat model of temporal lobe epilepsy. *J. Neurosci.* 29, 7846–7856.

Zhang, Z. J., Lappi, D. A., Wrenn, C. C., Milner, T. A., and Wiley, R. G. (1998). Selective lesion of the cholinergic basal forebrain causes a loss of cortical neuropeptide Y and somatostatin neurons. *Brain Res.* 800, 198–206.

Conflict of Interest Statement: The authors declare that the research was conducted in the absence of any commercial or financial relationships that could be construed as a potential conflict of interest.

Received: 17 September 2012; accepted: 02 December 2012; published online: 09 January 2013.

Citation: Scharfman HE and Myers CE (2013) Hilar mossy cells of the dentate gyrus: a historical perspective. Front. Neural Circuits ***6****:106. doi: 10.3389/fncir.2012.00106*

frontiers in
NEURAL CIRCUITS

REVIEW ARTICLE
published: 18 December 2012
doi: 10.3389/fncir.2012.00103

Structural plasticity of spines at giant mossy fiber synapses

Shanting Zhao[1], Daniel Studer[2], Xuejun Chai[1], Werner Graber[2], Nils Brose[3], Sigrun Nestel[4], Christina Young[4], E. Patricia Rodriguez[5], Kurt Saetzler[5] and Michael Frotscher[1]*

[1] Center for Molecular Neurobiology Hamburg, Institute for Structural Neurobiology, Hamburg, Germany
[2] Institute of Anatomy, University of Bern, Bern, Switzerland
[3] Department of Molecular Neurobiology, Max Planck Institute for Experimental Medicine, Göttingen, Germany
[4] Department of Neuroanatomy, Institute of Anatomy and Cell Biology, Albert Ludwigs University Freiburg, Freiburg, Germany
[5] School of Biomedical Science, University of Ulster, Coleraine, UK

Edited by:
Peter Jonas, Institute of Science and Technology Austria, Austria

Reviewed by:
Laszlo Acsady, Institute of Experimental Medicine, Hungary
Martin Korte, TU Braunschweig, Germany

***Correspondence:**
Michael Frotscher, Center for Molecular Neurobiology Hamburg, Institute for Structural Neurobiology, Martinistrasse 52, D-20246 Hamburg, Germany.
e-mail: michael.frotscher@zmnh.uni-hamburg.de

The granule cells of the dentate gyrus give rise to thin unmyelinated axons, the mossy fibers. They form giant presynaptic boutons impinging on large complex spines on the proximal dendritic portions of hilar mossy cells and CA3 pyramidal neurons. While these anatomical characteristics have been known for some time, it remained unclear whether functional changes at mossy fiber synapses such as long-term potentiation (LTP) are associated with structural changes. Since subtle structural changes may escape a fine-structural analysis when the tissue is fixed by using aldehydes and is dehydrated in ethanol, rapid high-pressure freezing (HPF) of the tissue was applied. Slice cultures of hippocampus were prepared and incubated *in vitro* for 2 weeks. Then, chemical LTP (cLTP) was induced by the application of 25 mM tetraethylammonium (TEA) for 10 min. Whole-cell patch-clamp recordings from CA3 pyramidal neurons revealed a highly significant potentiation of mossy fiber synapses when compared to control conditions before the application of TEA. Next, the slice cultures were subjected to HPF, cryosubstitution, and embedding in Epon for a fine-structural analysis. When compared to control tissue, we noticed a significant decrease of synaptic vesicles in mossy fiber boutons and a concomitant increase in the length of the presynaptic membrane. On the postsynaptic side, we observed the formation of small, finger-like protrusions, emanating from the large complex spines. These short protrusions gave rise to active zones that were shorter than those normally found on the thorny excrescences. However, the total number of active zones was significantly increased. Of note, none of these cLTP-induced structural changes was observed in slice cultures from Munc13-1 deficient mouse mutants showing severely impaired vesicle priming and docking. In conclusion, application of HPF allowed us to monitor cLTP-induced structural reorganization of mossy fiber synapses.

Keywords: synaptic ultrastructure, high-pressure freezing, mossy fiber LTP, dendritic spine, actin cytoskeleton, dentate gyrus, granule cells

INTRODUCTION

The giant synapses formed by hippocampal mossy fibers, the axons of dentate gyrus granule cells, have attracted researchers soon after the introduction of electron microscopy (EM) to the study of the nervous system (Blackstad and Kjaerheim, 1961; Hamlyn, 1962). Via the mossy fiber synapses, the granule cells transmit afferent, multisensory input from the entorhinal cortex to the hippocampus proper. Intuitively, one expects that the granule cells are bipolar neurons in order to serve this function. Indeed, they send their dendrites into the dentate molecular layer where the afferents from the entorhinal cortex are known to terminate in a laminated fashion. This input side of the granule cells is clearly segregated from their output side, represented by the mossy fibers projecting to the hilus and farther to hippocampal region CA3. The layer of granule cell somata is forming a "border" between the two sides. In fact, in the normal dentate gyrus, granule cells rarely show basal dendrites extending into the hilus so that they could become a target of other granule cell axons. It has been shown that hilar ectopic granule cells receive many more excitatory synapses and show epileptiform burst activity unlike normal granule cells in the dentate granule cell layer (Dashtipour et al., 2001; Scharfman et al., 2007). Hence, granule cell ectopia resulting from an aberrant migration of the granule cells during development has been assumed to increase the susceptibility to developing limbic seizures and epilepsy in adulthood (Koyama et al., 2012). While this may be the case, granule cell ectopia may also be a secondary effect that can be provoked in normal mature animals by unilateral injection of the glutamate receptor agonist kainate into the hippocampus (Bouilleret et al., 1999; Heinrich et al., 2006). Application of kainate renders the animals epileptic, and they then develop a prominent, secondary granule cell ectopia, called granule cell dispersion. For the purpose of the present study it may be sufficient to point out that the information flow is mainly unidirectional in the normal dentate gyrus conveying the multisensory entorhinal input to the hippocampus via essentially two synapses, the synapses formed

by the entorhinal fibers on the granule cell dendrites and the synapses that the mossy fibers establish with hilar neurons and CA3 pyramidal cells, respectively.

The input from the entorhinal cortex is not the only input to the granule cell dendrites. The commissural/associational fibers terminating on proximal granule cell dendrites are derived from distant hilar mossy cells that transmit input from other segments (lamellae) of the longitudinal axis of the hippocampus. The mossy fibers, in turn, play an important role in the activation of local (intralamellar) mossy cells. Other target cells of granule cell axons are the various types of GABAergic interneuron (Frotscher, 1985, 1989; Acsády et al., 1998) that by recurrent and feed-forward inhibition, respectively, keep the balance between excitation and inhibition in the dentate-hippocampal network.

In this review, we will first summarize what is known about the mossy fibers and their characteristic synaptic specializations on hippocampal CA3 pyramidal neurons. We will make an attempt to understand the functional significance of the unique structural components of mossy fiber synapses, and we will study the structural plasticity of mossy fiber synapses using high-pressure freezing (HPF), an approach that allowed us to overcome some of the disadvantages of conventional aldehyde fixation for EM.

THE SPECIALIZED MOSSY FIBER SYNAPSE

What is so special about the giant mossy fiber synapse? The thin unmyelinated granule cell axon originates at the basal pole of the granule cell soma and travels through the hilus toward hippocampal region CA3. In its course, it gives rise to regularly spaced boutons *en passage* for the contact with various types of hilar neuron. Toward CA3, the mossy fibers form a dense fiber bundle that occupies stratum lucidum. Depending on the genetic background, some mossy fibers also run through the layer of pyramidal cells (intrapyramidal mossy fibers) and underneath the pyramidal layer (infrapyramidal bundle, Schwegler et al., 1981). The mossy fiber projection ends abruptly at the border to CA2/CA1. Thus, the CA1 pyramidal cells do not get direct granule cell input, suggesting that the information flow from the entorhinal cortex via the granule cells requires just another processing before it is allowed to enter the CA1 region (there is, however, a direct entorhinal input to the CA1 pyramidal cells). One is tempted to speculate that at the level of the CA3 pyramidal cells there is a comparative evaluation of the individual granule cell projections, likely by abundant connections among CA3 pyramidal cells, aimed at providing the CA1 neurons with a more complete pattern of the lamellar granule cell input from the dentate gyrus, whereby contextual information is provided by direct projections from the entorhinal cortex to the hippocampus proper (Lisman, 1999).

WHAT DOES THE PARTICULAR FINE STRUCTURE OF THE MOSSY FIBER SYNAPSE TELL US ABOUT ITS FUNCTIONAL ROLE IN THE DENTATE—HIPPOCAMPAL CIRCUIT?

The location of mossy fiber boutons on proximal dendritic portions, i.e., close to the site of action potential generation, the enormous bouton size (2–5 μm in diameter), the abundance of clear synaptic vesicles (approximately 25,000) intermingled by dense–core vesicles, and the large number of release sites (up to 45 release sites, see Chicurel and Harris, 1992; Rollenhagen et al., 2007) strongly suggests that this synapse plays an important role in the information flow within the "trisynaptic pathway" (Andersen et al., 1971) connecting the entorhinal cortex with the hippocampus proper via the granule cells. It is likely that depolarization of the presynaptic mossy fiber axon leading to Ca^{2+} influx into the mossy fiber bouton will result in the simultaneous activation of several of the 45 contact zones, thereby increasing the reliability of transmission at the mossy fiber synapse. The particular fine structure of a mossy fiber synapse is illustrated in **Figure 1**. Here, the tissue was not fixed by using aldehydes and dehydrated in ascending series of ethanol. The tissue (slice culture of mouse hippocampus) was shock-frozen under high-pressure in less than a second (Zhao et al., 2012), thereby preserving the characteristic ultrastructural details of this synapse and avoiding ethanol-induced shrinkage of tissue components. While the fine-structural characteristics of mossy fiber synapses have been known for more than 50 years (Blackstad and Kjaerheim, 1961; Hamlyn, 1962) and were all described by studying tissue fixed in aldehyde solution and dehydrated in ethanol, the study of rapid, subtle changes at mossy fiber synapses, in particular at the giant postsynaptic spines, likely requires a rapid "fixation" procedure such as HPF. We will show in fact, that the mossy fiber synapse is a highly dynamic structure and that functional synaptic plasticity is associated with structural changes in the presynaptic bouton as well as the postsynaptic spine compartment.

STRUCTURAL CHANGES ASSOCIATED WITH FUNCTIONAL PLASTICITY AT MOSSY FIBER SYNAPSES

A variety of recent studies have shown that synaptic plasticity such as long-term potentiation (LTP) is associated with structural changes at synapses, particularly in the number and size of dendritic spines (Engert and Bonhoeffer, 1999; Matsuzaki et al., 2001; Yuste and Bonhoeffer, 2001; Yang et al., 2008). Are functional changes at mossy fiber synapses associated with structural changes? With the concept that induction of chemical LTP (cLTP) results in the stimulation of virtually all potentiatable mossy fiber synapses in contrast to electrical stimulation that activates an indeterminate number of synapses (Hosokawa et al., 1995), we induced cLTP by the application of tetraethylammonium (TEA; 25 mM) to hippocampal slice cultures for 10 min. Following washout, we recorded from CA3 pyramidal cells using the patch-clamp technique in the whole-cell mode. As shown previously (Suzuki and Okada, 2009; Zhao et al., 2012), there was a strong potentiation of excitatory postsynaptic potentials (EPSPs) 10–15 min after washout. Next, slice cultures exposed to TEA for 10 min were subjected to HPF and embedded for EM (Zhao et al., 2012). Control slice cultures were treated exactly the same way except that they were not exposed to TEA. In addition, we used slice cultures from Munc13-1 mouse mutants in which synaptic vesicle priming and docking is compromised (Augustin et al., 1999).

We measured the following parameters of mossy fiber synapses in random sections of control cultures and cultures treated with TEA: Number of clear synaptic vesicles (we also made an attempt

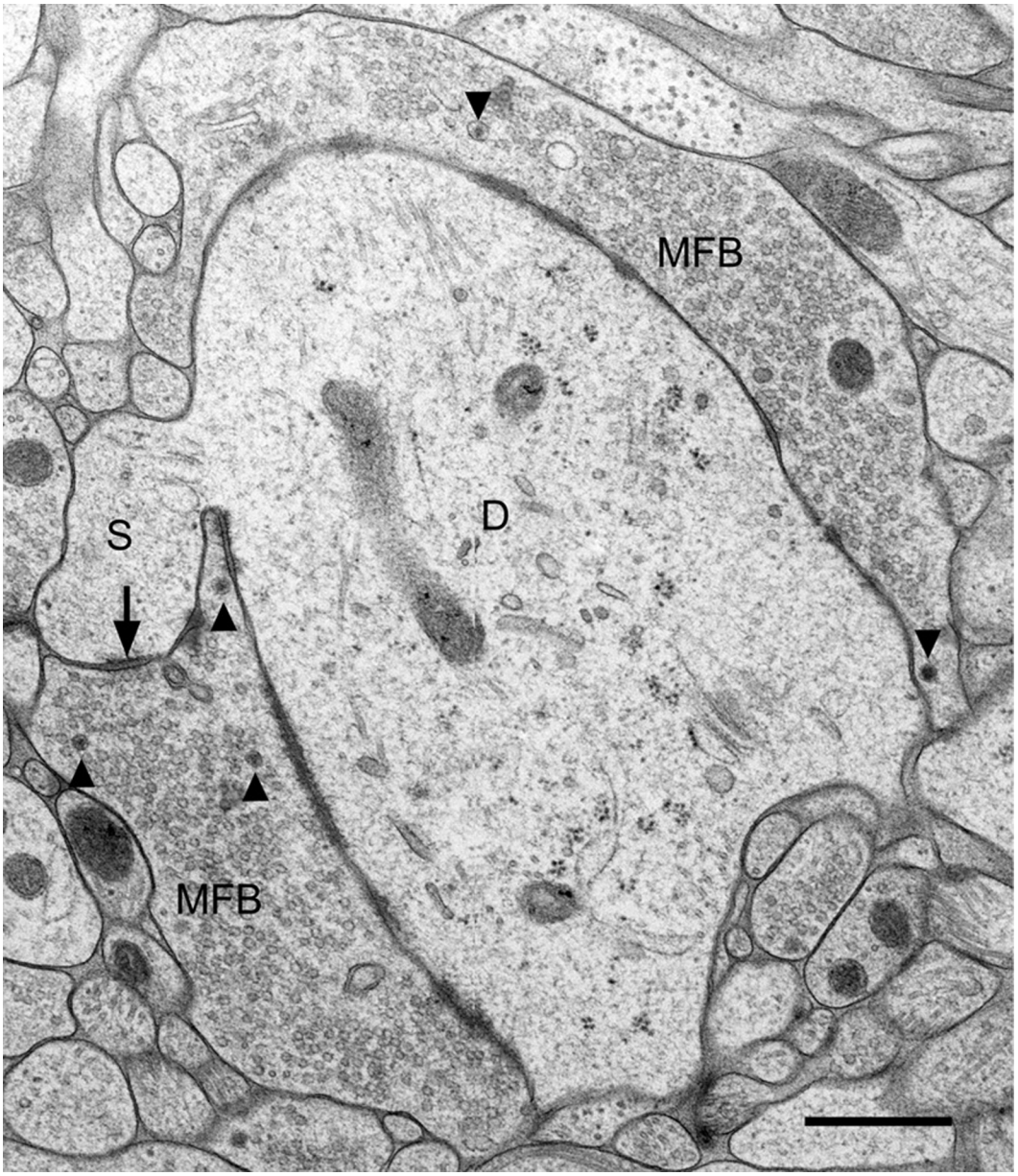

FIGURE 1 | Fine structure of a large mossy fiber bouton (MFB) and its postsynaptic element, a proximal dendrite (D) of a CA3 pyramidal cell. The large complex spine (S) establishes synaptic contact (arrow) with the mossy fiber bouton. Arrowheads point to dense-core vesicles. Slice culture of hippocampus following high-pressure freezing, cryosubstitution, and embedding in Epon. Scale bar: 0.5 μm.

to quantify dense-core vesicles but their number was too low for a statistical analysis), area and perimeter of mossy fiber boutons, number and area of postsynaptic spines, number and length of synaptic contacts (active zones or release sites).

Electron microscopic analysis of high-pressure frozen slice cultures—controls and TEA-exposed cultures—revealed an exceptional preservation of fine-structural detail (**Figure 1**).

Not only were the membranes of mossy fiber boutons and of postsynaptic spines and dendrites very smooth and crisp, also intracellular organelles such as microtubules, mitochondria, endoplasmic reticulum, synaptic vesicles, and in particular active zones were clearly identifiable. Postsynaptic densities extended fine fibrillar structures, likely protein accumulations, from the subsynaptic web into the spine cytoplasm. Occasionally, vesicles showed small extensions tethering them to other vesicles or to the presynaptic membrane specialization.

The excellent tissue preservation allowed for a thorough quantitative analysis of the various tissue components and for a comparison with tissue fixed conventionally by transcardial perfusion with aldehyde solutions (see Zhao et al., 2012). When comparing control slice cultures with slice cultures exposed to TEA for 10 min, we noticed a highly significant reduction in the

number of clear synaptic vesicles/μm^2 mossy fiber bouton area (control: 183 ± 76 SD; TEA: 104 ± 43 SD; $p = 0.000015$, Zhao et al., 2012). This decrease in vesicle number was associated with an increase in the ratio of bouton perimeter/bouton area in the TEA-treated cultures (control: 3.85 ± 1.15 SD; TEA: 6.05 ± 1.52 SD; $p = 0.00000018$, Zhao et al., 2012). Since no significant differences between controls and stimulated cultures were found in a comparison of mossy fiber bouton area, we interpret these findings as resulting from an increased length and a more convoluted course of the presynaptic bouton membrane following the fusion of many synaptic vesicles.

On the postsynaptic side, we observed in the TEA-exposed cultures numerous finger-like protrusions extending from the large complex spines or *excrescences* into the presynaptic bouton (**Figure 2**). Accordingly, quantitative analysis revealed a highly significant increase in the number of spine profiles/μm^2 bouton area in the TEA-treated cultures when compared to controls (control: 0.42 ± 0.54 SD; TEA: 4.32 ± 2.19 SD; $p = 1.569 \times 10^{-10}$, Zhao et al., 2012). Similarly, spine area/mossy fiber bouton area was increased in the potentiated cultures (control: 0.134 ± 0.043 SD; TEA: 0.227 ± 0.078 SD; $p = 0.0173$, Zhao et al., 2012). Next, we wanted to know whether this *de novo* formation of spines was accompanied by an increase in the number of active zones. Indeed, we observed a significant increase in the number of synaptic contacts/μm^2 bouton area in the potentiated cultures (control: 2.64 ± 1.21 SD; TEA: 3.63 ± 1.42 SD; $p = 0.00882$). However, the mean length of active zones was decreased when compared to control cultures (control: 221.8 nm ± 75.04 nm SD; TEA: 168.69 nm ± 28.63 nm SD; $p = 0.04031$, Zhao et al., 2012), suggesting that in the potentiated cultures many synapses were still immature.

We regarded it as an important result and additional control for the present experiments that none of the changes in synaptic structure found in the potentiated cultures was observed in potentiated slice cultures from mutant mice deficient in Munc13-1 (Zhao et al., 2012). Munc13-1 is known to be important for the fusion competence of synaptic vesicles (Augustin et al., 1999), and mutant mice deficient in Munc13-1 show severely compromised vesicle docking and fusion. Together, the present findings suggest that cLTP-induced by a 10-min exposure to TEA resulted in the fusion of many vesicles that, in turn, increased the length of the presynaptic mossy fiber bouton membrane. These changes were accompanied on the postsynaptic side by the formation of new spines and synaptic contacts. In Munc13-1 mutants, in which vesicle priming, docking and fusion are compromised, these changes were not observed. We hypothesize that under *in vivo* conditions, when only a limited number of granule cells are activated by specific input from the entorhinal cortex, their respective individual mossy fiber synapses are strengthened by closely related pre- and postsynaptic mechanisms eventually leading to additional spines and synaptic contacts.

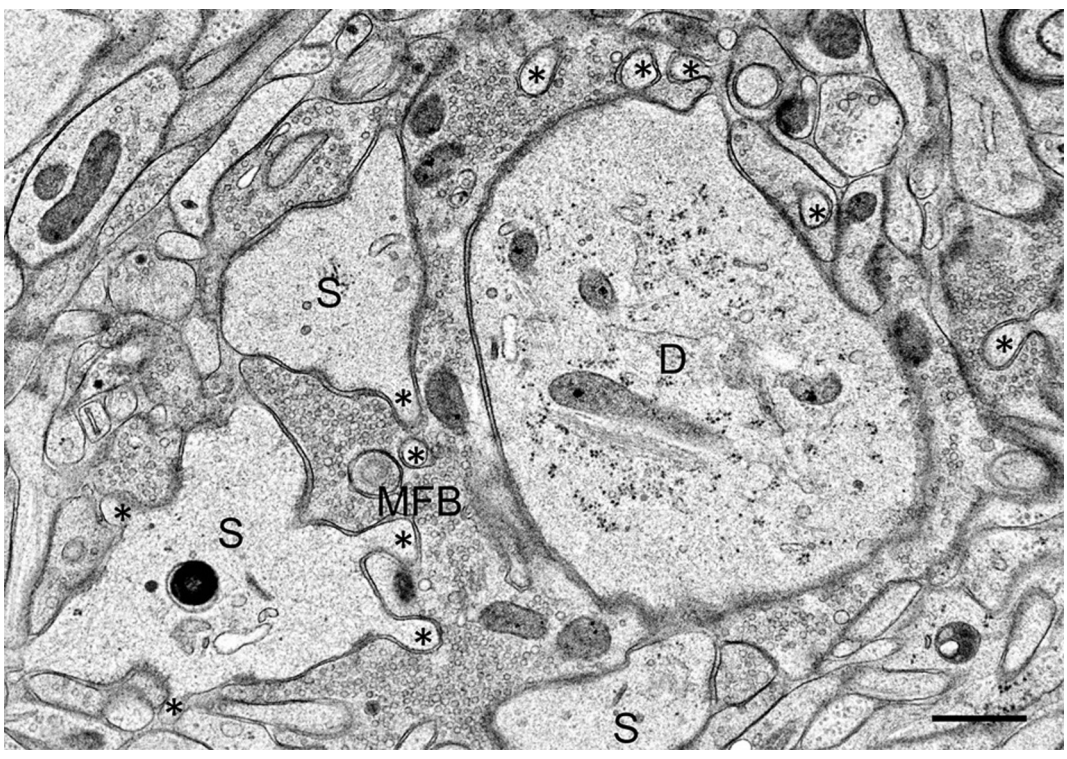

FIGURE 2 | Mossy fiber bouton (MFB) and its postsynaptic spines (S) in a hippocampal slice culture exposed to TEA for 10 min prior to high-pressure freezing. Note finger-shaped small extensions (asterisks) emerging from the large complex spines. D, proximal CA3 pyramidal cell dendrite. Scale bar: 0.5 μm.

WHAT MECHANISMS MIGHT UNDERLIE THE cLTP-INDUCED REMODELING OF MOSSY FIBER SYNAPSES?

In the potentiated cultures we observed an increase in the number of spines and active zones. One way to explain the extension of the finger-shaped protrusions from the postsynaptic complex spines is by assuming that this enlargement of the postsynaptic surface occurred in response to presynaptic membrane growth resulting from the fusion of numerous vesicles (Zhao et al., 2012). Pre- and postsynaptic membranes of mossy fiber synapses are attached to each other by abundant synaptic contacts that do not only represent release sites but sites of strong mechanical contact (Gray and Whittaker, 1962), likely by virtue of numerous cell adhesion molecules at synaptic sites (Washbourne et al., 2004; Hortsch and Umemori, 2009). Alternatively, there might be active growth of postsynaptic spines and synaptic contacts. Indeed, our studies have shown that both spines and active zones were smaller than in controls, suggesting that these synaptic structures were still growing after the 10-min stimulation period. It has been shown that LTP induction in CA1 is associated with *de novo* formation and growth of dendritic spines, respectively (Engert and Bonhoeffer, 1999; Yuste and Bonhoeffer, 2001; Matsuzaki et al., 2004; Yang et al., 2008). Growth of spines is accompanied by an increase in the number of functional glutamate receptors (Matsuzaki et al., 2001; Noguchi et al., 2005; Béïque et al., 2006; Zito et al., 2009; Kasai et al., 2010) that are likely to contribute to LTP and memory consolidation.

Growth of spines is associated with remodeling of the actin cytoskeleton, which is particularly enriched in dendritic spines (Matus, 2000). Indeed, a variety of studies have provided evidence for changes in actin filaments to be linked to changes in spine shape under various experimental conditions (Fischer et al., 1998, 2000; Matus, 2000; Star et al., 2002; Fukazawa et al., 2003; Okamoto et al., 2004; Hotulainen et al., 2009; Hotulainen and Hoogenraad, 2010). Remodeling of spine structure in synaptic plasticity was found to involve changes in the equilibrium between F-actin and G-actin by actin polymerizing/depolymerizing molecules. Thus, opposing shifts in the relative amounts of F-actin and G-actin have been observed in bidirectional synaptic plasticity: LTP shifted the equilibrium toward F-actin, associated with an increase in the size of spines on CA1 pyramidal neurons; long-term depression (LTD) shifted the equilibrium toward G-actin and resulted in smaller spines (Okamoto et al., 2004). Consistent with increased actin polymerization and an increase in spine size, phosphorylated cofilin (p-cofilin) was found increased in LTP in hippocampal region CA1 (Chen et al., 2007; Rex et al., 2009). Cofilin is an actin-depolymerizing protein and involved in cytoskeletal remodeling associated with changes in cell shape (Bamburg, 1999). Phosphorylation of cofilin at serine3 renders it unable to depolymerize F-actin (Arber et al., 1998; Yang et al., 1998), thereby stabilizing the actin cytoskeleton. In preliminary studies using high-pressure frozen material and immunogold staining for p-cofilin following embedding in Lowicryl HM20, we observed labeling specifically at synaptic sites (Zhao et al., unpublished observations). Similar synaptic location of cofilin has been reported previously using an antibody against the N-terminal region of human cofilin (Racz and Weinberg, 2006). Future studies need to determine to what extent changes in the actin cytoskeleton and in the phosphorylation of cofilin are involved in the cLTP-induced structural plasticity of spines postsynaptic to giant mossy fiber boutons.

DISCUSSION AND OUTLOOK

The results presented here provide evidence for functional changes such as synaptic potentiation at mossy fiber synapses to be associated with structural changes, in particular a *de novo* formation of spines and synaptic contacts. Thus, our results confirm and extend previous studies on LTP-induced structural changes in spines of CA1 pyramidal neurons. Our findings in mossy fiber synapses imply that a selective activation of single granule cells, for instance by strong input from the entorhinal cortex, strengthens their respective synapses on hilar mossy cells and CA3 pyramidal neurons by the formation of additional synaptic contacts and spines postsynaptic to these particular mossy fiber boutons. As a result, the respective mossy fiber synapses will become more convoluted and complex. Indeed, previous studies have shown that long-term experience resulted in rearrangements of presynaptic mossy fiber boutons (Galimberti et al., 2006, 2010; Rekart et al., 2007; Routtenberg, 2010). At a systemic level, these more complex mossy fiber synapses may reinforce transmission in the trisynaptic pathway in the particular lamella of the activated granule cell(s). Thus, by virtue of the preferentially transverse course of the mossy fibers (transverse to the longitudinal axis of the hippocampus, Blackstad et al., 1970) individual lamellae will be activated; however, by the simultaneous activation of the mossy cells that project along the longitudinal axis of the hippocampus, the impulse will not remain restricted to the lamella but will be propagated to distant septo-temporal segments of the hippocampus.

What signaling pathways and molecular mechanisms might underlie the *de novo* formation of spines and synaptic contacts? Previous studies in CA1 have not only shown that LTP induces spine formation (Engert and Bonhoeffer, 1999; Yuste and Bonhoeffer, 2001; Matsuzaki et al., 2004; Yang et al., 2008), but have also provided evidence for an involvement of brain-derived neurotrophic factor (BDNF) in LTP (Korte et al., 1995; Lu et al., 2008). BDNF is particularly enriched in hippocampal mossy fibers (Danzer and McNamara, 2004), and we have recently shown that it is localized to dense-core vesicles of mossy fiber boutons (Dieni et al., 2012). One is tempted to speculate that the structural plasticity of mossy fiber synapses described here is regulated by BDNF released from dense-core vesicles in an activity-dependent manner. It has been shown recently that phosphorylation of TrkB, the cognate receptor for BDNF, by the proline-directed serine/threonine kinase Cdk5 is required for activity-dependent plasticity of dendritic spines and spatial memory (Lai et al., 2012). Future studies in slice cultures from BDNF-deficient mutant mice will show to what extent the structural plasticity of mossy fiber synapses described here is affected by a BDNF deficiency.

Electron microscopy does not allow one to study the time course of structural changes at mossy fiber synapses. How rapid are these changes in response to mossy fiber stimulation?

In order to address this issue, we have recently begun to patch-clamp CA3 pyramidal cells and hilar mossy cells, respectively, and have filled them with the fluorescent marker Alexa 594-dextran (red). Presynaptic mossy fiber axons were stained by the extracellular application of Alexa 588-dextran (green). This experimental design will allow us to monitor pre- and postsynaptic changes at identified mossy fiber synapses using real-time microscopy (Frotscher et al., 2007). Together with the use of slice cultures from BDNF-deficient mice and from other mutants with modifications of candidate molecules, this approach will allow us to obtain further insight into the mechanisms underlying the structural plasticity of mossy fiber synapses.

ACKNOWLEDGMENTS

The present studies were supported by grants from the Deutsche Forschungsgemeinschaft (SFB 780: project A4) and the Swiss National Foundation (grant number: 3100AO_118394). Michael Frotscher is Senior Research Professor of the Hertie Foundation.

REFERENCES

Acsády, L., Kamondi, A., Sík, A., Freund, T., and Buzsáki, G. (1998). GABAergic cells are the major postsynaptic targets of mossy fibers in the rat hippocampus. *J. Neurosci.* 18, 3386–3403.

Andersen, P., Bliss, T. V. P., and Skrede, K. K. (1971). Lamellar organization of hippocampal excitatory pathways. *Exp. Brain Res.* 13, 222–238.

Arber, S., Barbayannis, F. A., Hanser, H., Schneider, C., Stanyon, C. A., Bernard, O., et al. (1998). Regulation of actin dynamics through phosphorylation of cofilin by LIM-kinase. *Nature* 393, 805–809.

Augustin, I., Rosenmund, C., Südhof, T. C., and Brose, N. (1999). Munc13-1 is essential for fusion competence of glutamatergic synaptic vesicles. *Nature* 400, 457–461.

Bamburg, J. R. (1999). Proteins of the ADF/cofilin family: essential regulators of actin dynamics. *Annu. Rev. Cell Biol.* 15, 185–230.

Béïque, J.-C., Lin, D.-T., Kang, M.-G., Aizawa, H., Takamiya, K., and Huganir, R. L. (2006). Synapse-specific regulation of AMPA receptor function by PSD-95. *Proc. Natl. Acad. Sci. U.S.A.* 103, 19535–19540.

Blackstad, T. W., Brink, K., Hem, J., and Jeune, B. (1970). Distribution of hippocampal mossy fibers in the rat. An experimental study with silver impregnation methods. *J. Comp. Neurol.* 138, 433–449.

Blackstad, T. W., and Kjaerheim, A. (1961). Special axo-dendritic synapses in the hippocampal cortex: electron and light microscopic studies on the layer of mossy fibers. *J. Comp. Neurol.* 117, 133–159.

Bouilleret, V., Ridoux, V., Depaulis, A., Marescaux, C., Nehlig, A., and Le Gal La Salle, G. (1999). Recurrent seizures and hippocampal sclerosis following intrahippocampal kainate injection in adult mice: electroencephalography, histopathology and synaptic reorganization similar to mesial temporal lobe epilepsy. *Neuroscience* 89, 717–729.

Chen, L. Y., Rex, C. S., Casale, M. S., Gall, C. M., and Lynch, G. (2007). Changes in synaptic morphology accompany actin signaling during LTP. *J. Neurosci.* 27, 5363–5372.

Chicurel, M. E., and Harris, K. M. (1992). Three-dimensional analysis of the structure and composition of CA3 branched dendritic spines and their synaptic relationships with mossy fiber boutons in the rat hippocampus. *J. Comp. Neurol.* 325, 169–182.

Danzer, S. C., and McNamara, J. O. (2004). Localization of brain-derived neurotrophic factor to distinct terminals of mossy fiber axons implies regulation of both excitation and feedforward inhibition of CA3 pyramidal cells. *J. Neurosci.* 24, 11346–11355.

Dashtipour, K., Tran, P. H., Okazaki, M. M., Nadler, J. V., and Ribak, C. E. (2001). Ultrastructural features and synaptic connections of hilar ectopic granule cells in the rat dentate gyrus are different from those of granule cells in the granule cell layer. *Brain Res.* 890, 261–271.

Dieni, S., Matsumoto, T., Dekkers, M., Rauskolb, S., Ionescu, M. S., Deogracias, R., et al. (2012). BDNF and its pro-peptide are stored in presynaptic dense core vesicles in brain neurons. *J. Cell Biol.* 196, 775–788.

Engert, F., and Bonhoeffer, T. (1999). Dendritic spine changes associated with hippocampal long-term synaptic plasticity. *Nature* 399, 66–70.

Fischer, M., Kaech, S., Knutti, D., and Matus, A. (1998). Rapid actin-based plasticity in dendritic spines. *Neuron* 20, 847–854.

Fischer, M., Kaech, S., Wagner, U., Brinkhaus, H., and Matus, A. (2000). Glutamate receptors regulate actin-based plasticity in dendritic spines. *Nat. Neurosci.* 3, 887–894.

Frotscher, M. (1985). Mossy fibres form synapses with identified pyramidal basket cells in the CA3 region of the guinea-pig hippocampus: a combined Golgi-electron microscope study. *J. Neurocytol.* 14, 245–259.

Frotscher, M. (1989). Mossy fiber synapses on glutamate decarboxylase-immunoreactive neurons: evidence for feed-forward inhibition in the CA3 region of the hippocampus. *Exp. Brain Res.* 75, 441–445.

Frotscher, M., Zhao, S., Graber, W., Drakew, A., and Studer, D. (2007). New ways of looking at synapses. *Histochem. Cell Biol.* 128, 91–96.

Fukazawa, Y., Saitoh, Y., Ozawa, F., Ohta, Y., Mizuno, K., and Inokuchi, K. (2003). Hippocampal LTP is accompanied by enhanced F-actin content within the dendritic spine that is essential for late LTP maintenance *in vivo*. *Neuron* 38, 447–460.

Galimberti, I., Bednarek, E., Donato, F., and Caroni, P. (2010). EphA4 signaling in juveniles establishes topographic specificity of structural plasticity in the hippocampus. *Neuron* 65, 627–642.

Galimberti, I., Gogolla, N., Alberi, S., Santos, A. F., Muller, D., and Caroni, P. (2006). Long-term rearrangements of hippocampal mossy fiber terminal connectivity in the adult regulated by experience. *Neuron* 50, 749–763.

Gray, E. G., and Whittaker, V. P. (1962). The isolation of nerve endings from brain: an electron-microscopic study of cell fragments derived by homogenization and centrifugation. *J. Anat.* 96, 79–88.

Hamlyn, L. H. (1962). The fine structure of the mossy fibre endings in the hippocampus of the rabbit. *J. Anat.* 96, 112–120.

Heinrich, C., Nitta, N., Flubacher, A., Müller, M., Fahrner, A., Kirsch, M., et al. (2006). Reelin deficiency and displacement of mature neurons, but not neurogenesis, underlie the formation of granule cell dispersion in the epileptic hippocampus. *J. Neurosci.* 26, 4701–4713.

Hortsch, M., and Umemori, H. (eds.). (2009). *The Sticky Synapse*. Berlin: Springer.

Hosokawa, T., Rusakov, D. A., Bliss, T. V., and Fine, A. (1995). Repeated confocal imaging of individual dendritic spines in the living hippocampal slice: evidence for changes in length and orientation associated with chemically induced LTP. *J. Neurosci.* 15, 5560–5573.

Hotulainen, P., and Hoogenraad, C. C. (2010). Actin in dendritic spines: connecting dynamics to function. *J. Cell Biol.* 189, 619–629.

Hotulainen, P., Llano, O., Smirnov, S., Tanhuanpää, K., Faix, J., Rivera, C., et al. (2009). Defining mechanisms of actin polymerization and depolymerization during dendritic spine morphogenesis. *J. Cell Biol.* 185, 323–339.

Kasai, H., Fukuda, M., Watanabe, S., Hayashi-Takagi, A., and Noguchi, J. (2010). Structural dynamics of dendritic spines in memory and cognition. *Trends Neurosci.* 33, 121–129.

Korte, M., Carroll, P., Wolf, E., Brem, G., Thoenen, H., and Bonhoeffer, T. (1995). Hippocampal long-term potentiation is impaired in mice lacking brain-derived neurotrophic factor. *Proc. Natl. Acad. Sci. U.S.A.* 92, 8856–8860.

Koyama, R., Tao, K., Sasaki, T., Ichikawa, J., Miyamoto, D., Muramatsu, R., et al. (2012). GABAergic excitation after febrile seizures induces ectopic granule cells and adult epilepsy. *Nat. Med.* 18, 1271–1278.

Lai, K.-O., Wong, A. S. L., Cheung, M.-C., Xu, P., Liang, Z., Lok, K.-C., et al. (2012). TrkB phosphorylation by Cdk5 is required for activity-dependent structural plasticity and spatial memory. *Nat. Neurosci.*15, 1506–1515.

Lisman, J. E. (1999). Relating hippocampal circuitry to function: recall of memory sequences by reciprocal dentate-CA3 interactions. *Neuron* 22, 233–242.

Lu, Y., Christian, K., and Lu, B. (2008). BDNF: a key regulator for protein synthesis-dependent LTP and long-term memory? *Neurobiol. Learn. Mem.* 89, 312–323.

Matsuzaki, M., Ellis-Davies, G. C. R., Nemoto, T., Miyashita, Y., Iino, M.,

and Kasai, H. (2001). Dendritic spine geometry is critical for AMPA receptor expression in hippocampal CA1 pyramidal neurons. *Nat. Neurosci.* 4, 1086–1092.

Matsuzaki, M., Honkura, N., Ellis-Davies, G. C. R., and Kasai, H. (2004). Structural basis of long-term potentiation in single dendritic spines. *Nature* 429, 761–766.

Matus, A. (2000). Actin-based plasticity in dendritic spines. *Science* 290, 754–758.

Noguchi, J., Matsuzaki, M., Ellis-Davies, G. C. R., and Kasai, H. (2005). Spine-neck geometry determines NMDA receptor-dependent Ca2+ signaling in dendrites. *Neuron* 46, 609–622.

Okamoto, K.-I., Nagai, T., Miyawaki, A., and Hayashi, Y. (2004). Rapid and persistent modulation of actin dynamics regulates postsynaptic reorganization underlying bidirectional plasticity. *Nat. Neurosci.* 7, 1104–1112.

Racz, B., and Weinberg, R. J. (2006). Spatial organization of cofilin in dendritic spines. *Neuroscience* 138, 447–456.

Rekart, J. L., Sandoval, C. J., Bermudez-Rattoni, F., and Routtenberg, A. (2007). Remodeling of hippocampal mossy fibers is selectively induced seven days after the acquisition of a spatial but not a cued reference memory task. *Learn. Mem.* 14, 416–421.

Rex, C. S., Chen, L. Y., Sharma, A., Liu, J., Babayan, A. H., Gall, C. M., et al. (2009). Different Rho GTPase-dependent signaling pathways initiate sequential steps in the consolidation of long-term potentiation. *J. Cell Biol.* 186, 85–97.

Rollenhagen, A., Sätzler, K., Rodriguez, E. P., Jonas, P., Frotscher, M., and Lübke, J. H. R. (2007). Structural determinants of transmission at large hippocampal mossy fiber synapses. *J. Neurosci.* 27, 10434–10444.

Routtenberg, A. (2010). Adult learning and remodeling of hippocampal mossy fibers: unheralded participant in circuitry for long-lasting spatial memory. *Hippocampus* 20, 44–45.

Scharfman, H., Goodman, J., and McCloskey, D. (2007). Ectopic granule cells of the rat dentate gyrus. *Dev. Neurosci.* 29, 14–27.

Schwegler, H., Lipp, H. P., Van der Loos, H., and Buselmaier, W. (1981). Individual hippocampal mossy fiber distribution in mice correlates with two-way avoidance performance. *Science* 214, 817–819.

Star, E. N., Kwiatkowski, D. J., and Murthy, V. N. (2002). Rapid turnover of actin in dendritic spines and its regulation by activity. *Nat. Neurosci.* 5, 239–246.

Suzuki, E., and Okada, T. (2009). TEA-induced long-term potentiation at hippocampal mossy fiber-CA3 synapses: characteristics of its induction and expression. *Brain Res.* 1247, 21–27.

Washbourne, P., Dityatev, A., Scheiffele, P., Biederer, T., Weiner, J. A., Christopherson, K. S., et al. (2004). Cell adhesion molecules in synapse formation. *J. Neurosci.* 24, 9244–9249.

Yang, N., Higuchi, O., Ohashi, K., Nagata, K., Wada, A., Kangawa, K., et al. (1998). Cofilin phosphorylation by LIM-kinase 1 and its role in Rac-mediated actin reorganization. *Nature* 393, 809–812.

Yang, Y., Wang, X., Frerking, M., and Zhou, Q. (2008). Spine expansion and stabilization associated with long-term potentiation. *J. Neurosci.* 28, 5740–5751.

Yuste, R., and Bonhoeffer, T. (2001). Morphological changes in dendritic spines associated with long-term synaptic plasticity. *Annu. Rev. Neurosci.* 24, 1071–1089.

Zhao, S., Studer, D., Chai, X., Graber, W., Brose, N., Nestel, S., et al. (2012). Structural plasticity of hippocampal mossy fiber synapses as revealed by high-pressure freezing. *J. Comp. Neurol.* 520, 2340–2351.

Zito, K., Scheuss, V., Knott, G., Hill, T., and Svoboda, K. (2009). Rapid functional maturation of nascent dendritic spines. *Neuron* 61, 247–258.

Conflict of Interest Statement: The authors declare that the research was conducted in the absence of any commercial or financial relationships that could be construed as a potential conflict of interest.

Received: 03 September 2012; paper pending published: 10 October 2012; accepted: 22 November 2012; published online: 18 December 2012.

Citation: Zhao S, Studer D, Chai X, Graber W, Brose N, Nestel S, Young C, Rodriguez EP, Saetzler K and Frotscher M (2012) Structural plasticity of spines at giant mossy fiber synapses. Front. Neural Circuits ***6****:103. doi: 10.3389/fncir. 2012.00103*

frontiers in
NEURAL CIRCUITS

REVIEW ARTICLE
published: 09 January 2013
doi: 10.3389/fncir.2012.00112

Ionotropic receptors at hippocampal mossy fibers: roles in axonal excitability, synaptic transmission, and plasticity

Arnaud J. Ruiz[1]* and Dimitri M. Kullmann[2]*

[1] *Department of Pharmacology, UCL School of Pharmacy, London, UK*
[2] *Department of Clinical and Experimental Epilepsy, UCL Institute of Neurology, London, UK*

Edited by:
Peter Jonas, Institute of Science and Technology Austria, Austria

Reviewed by:
Nicholas P. Vyleta, Institute of Science and Technology Austria, Austria
Josef Bischofberger, University of Basel, Switzerland

****Correspondence:***
Arnaud J. Ruiz, Department of Pharmacology, UCL School of Pharmacy, Brunswick Square, London WC1N 1AX, UK.
e-mail: a.ruiz@ucl.ac.uk
Dimitri M. Kullmann, Department of Clinical and Experimental Epilepsy, UCL Institute of Neurology, Queen Square, London WC1N 3BG, UK.
e-mail: d.kullmann@ucl.ac.uk

Dentate granule cells process information from the enthorinal cortex en route to the hippocampus proper. These neurons have a very negative resting membrane potential and are relatively silent in the slice preparation. They are also subject to strong feed-forward inhibition. Their unmyelinated axon or mossy fiber ramifies extensively in the hilus and projects to stratum lucidum where it makes giant en-passant boutons with CA3 pyramidal neurons. There is compelling evidence that mossy fiber boutons express presynaptic $GABA_A$ receptors, which are commonly found in granule cell dendrites. There is also suggestive evidence for the presence of other ionotropic receptors, including glycine, NMDA, and kainate receptors, in mossy fiber boutons. These presynaptic receptors have been proposed to lead to mossy fiber membrane depolarization. How this phenomenon alters the excitability of synaptic boutons, the shape of presynaptic action potentials, Ca^{2+} influx and neurotransmitter release has remained elusive, but high-resolution live imaging of individual varicosities and direct patch-clamp recordings have begun to shed light on these phenomena. Presynaptic $GABA_A$ and kainate receptors have also been reported to facilitate the induction of long-term potentiation at mossy fiber—CA3 synapses. Although mossy fibers are highly specialized, some of the principles emerging at this connection may apply elsewhere in the CNS.

Keywords: 2-photon microscopy, $GABA_A$ receptor, granule cell, immunogold, kainate receptor, mossy fiber bouton, NMDA receptor, single channel

INTRODUCTION

There are approximately one million granule cells within the rat dentate gyrus, all projecting a thin unmyelinated axon that forms a single parent fiber in stratum lucidum, where it makes synaptic contacts onto CA3 pyramidal cells and various types of interneurones (Amaral et al., 1990; Acsady et al., 1998). These unusual axons (or mossy fibers) provide one of the most powerful glutamatergic input in the brain amid the low basal firing rate observed in granule cells *in vivo* (<0.5 Hz) and the inability of granule cells to fire action potentials for extended periods of time (Jung and McNaughton, 1993). Mossy fiber—CA3 synapses express a unique form of frequency-dependent facilitation of transmitter release that has a pronounced effect with only modest increases in presynaptic firing frequency (Salin et al., 1996), hence driving CA3 network activity very efficiently (Wiebe and Staubli, 1999; Henze et al., 2002). In addition, mossy fiber—CA3 synapses express presynaptic forms of long-term plasticity (LTP and LTD) that are expressed by persistent changes in the probability of glutamate release (Nicoll and Schmitz, 2005).

It is now emerging that many of these physiological processes are regulated by ionotropic receptors localized in presynaptic and perisynaptic membranes in mossy fibers themselves. In this paper, we discuss recent advances in our understanding of presynaptic receptor function at hippocampal mossy fiber synapses and expand on the view that they act as important modulators of synaptic transmission and plasticity in CA3 targets. We first introduce some of the techniques that have been employed to investigate presynaptic ionotropic receptors at mossy fibers. We then review the evidence showing the types of ionotropic receptors and the potential sources of neurotransmitters that can activate them, the downstream signaling mechanisms that ensue, and the differing forms of synaptic plasticity mediated by these receptors at synapses formed onto CA3 pyramidal neurons.

Several criteria must be met to unambiguously identify presynaptic ionotropic receptors in axon terminals. These include (1) ultrastructural localization of a particular receptor subunit to the presynaptic membrane, (2) detection of single channel activity in an excised patch from the presynaptic membrane; (3) evidence that exogenous activation of the receptor affects the presynaptic membrane potential or resistance. Moreover, (4) to argue that the receptor has a physiological role, it is necessary to show that it can be activated by the endogenous neurotransmitter upon activation of appropriate axons, and that this can be blocked or modulated by selective ligands.

METHODS AVAILABLE TO INVESTIGATE PRESYNAPTIC RECEPTOR FUNCTION

Among the plethora of experimental approaches available for measuring changes in axonal excitability and release probability consecutive to receptor activation, only high-resolution imaging

and presynaptic recordings allow direct access to the presynaptic compartment (**Figure 1**). All other methods that rely on electrophysiology and statistical analysis (miniature synaptic current frequency analysis, CV analysis and paired-pulse ratio of amplitude of electrically-evoked responses) can only yield indirect estimates and suffer serious drawbacks since the recordings are being made either from postsynaptic targets, the somatic compartment, or the extracellular space.

Briefly, when recording from postsynaptic cells, activation of the presynaptic receptor should affect the frequency of miniature synaptic currents in preference to their amplitudes, and the paired-pulse ratio of two consecutively evoked synaptic currents should be increased or decreased by presynaptic receptor activation (Zucker et al., 1998). However, using the paired-pulse ratio as a sole indicator of presynaptic receptor activation should be made with caution since postsynaptic mechanisms can also contribute (Kirischuk et al., 2002), and an autoreceptor function can also occlude the change in paired-pulse ratio expected of a presynaptic modulation. A complementary analysis is to compare the CV with the mean amplitude of evoked synaptic currents to deduce whether variation in synaptic efficacy has a presynaptic or postsynaptic locus. Generally, proportionate changes in CV^{-2} and mean amplitude imply presynaptic modulation of transmitter release, whereas changes to the mean amplitude without change in CV^{-2} imply modulation of postsynaptic receptors (Edwards et al., 1989; Manabe et al., 1993). However, further complications arise from this kind of analysis when considering other parameters that can influence baseline receptor occupancy and diffusion and uptake of neurotransmitters, such as the recording temperature (Rusakov and Kullmann, 1998; Perrais and Ropert, 1999).

Several other electrophysiological techniques can be deployed to investigate the effect of receptor activation on axonal excitability (Wall, 1958), the vast majority of which makes use of extracellular electrical stimulation combined with single axon unit recordings or recordings of the compound presynaptic action potential (the afferent volley). These methods often lack spatial resolution and can be sensitive to drift, hampering the analysis of the effect of receptor activation on single fiber threshold. They are also extremely sensitive to ionic shifts in the extracellular space, in particular to K^+ that tends to accumulate during repetitive activity and can alter fiber threshold.

An alternative method to measure changes in fiber excitability is to record antidromic action potentials evoked via a stimulus electrode positioned in the axonal projection zone. In the voltage-clamp configuration, these are detected as action currents. Two approaches have been taken to examine changes in the probability for evoking antidromic action currents consecutive to receptor modulation. In its most simple implementation, a threshold-straddling stimulus is applied so that the success rate for evoking antidromic action currents is set to ∼50%. Local application of drugs acting on axonal receptors should increase or decrease the success rate. A variant of the method is to cycle the stimulus

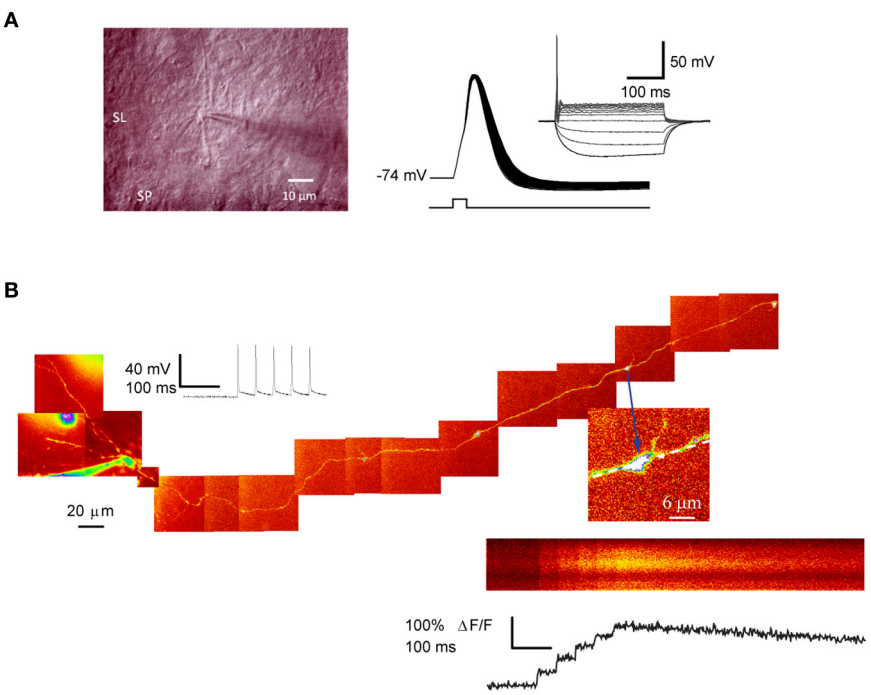

FIGURE 1 | Patch-clamp recording and 2-photon excitation fluorescence imaging from single giant mossy fiber boutons. (A) Left, IR–DIC photomicrograph of a putative mossy fiber bouton in juxtaposition with a dendrite located in stratum-lucidum. Right: action potentials evoked by a single depolarizing current step (1 nA, 0.5 ms) repeated at 50 Hz. Note the spike broadening. Inset shows the I–V relation (−30 to 60 pA, 300 ms; 10 pA increment). **(B)** Ca^{2+} imaging in a dentate granule cell filled with Alexa 594. The montage was obtained from Kalman-filtered averages of 10–15-µm stacks. Arrow indicates a giant mossy fiber bouton in stratum lucidum selected for imaging. Line-scan and fluorescence transients recorded from the same bouton, in response to five somatic action potentials. Panel **(A)** image and AP traces courtesy of Dr. D. Engel and panel **(B)** from Scott and Rusakov (2006).

through a saw-tooth intensity pattern ranging from 100% failures to 100% success for evoking an action current. Here, the effect of the drug on axonal receptors is examined over the entire stimulus—response relation. However, a recurrent problem with these approaches is that they rely on the integrity of axonal projections connected to their parent somata, a situation that occurs in about 12–15% of our slices.

An important breakthrough that allowed direct assessment was the development of direct patch-clamp recordings from large mossy fiber terminals (Geiger and Jonas, 2000; Bischofberger et al., 2006), thus enabling a detailed characterization of the pharmacological and biophysical properties of presynaptic receptors at single channel level. Although these recordings have provided important insights into the relation between receptor activation and presynaptic membrane potential, they inevitably perturb intraterminal ionic gradients because the size of the bouton is very small in relation to the patch pipette. This is particularly problematic when measuring the membrane potential from whole-terminal recordings because this method clamps $[K^+]_i$ and because the input resistance of the clamped structure is comparable to the seal resistance (Verheugen et al., 1999; Tyzio et al., 2003). It also affects the $[Cl^-]_i$ which has been estimated ∼20 mM in the Calyx of Held (Price and Trussell, 2006), therefore potentially compromising the driving force for $GABA_A$ receptor and glycine receptor mediated ion fluxes.

The membrane potential of mossy fiber boutons can in principle be estimated non-invasively (Fricker et al., 1999; Verheugen et al., 1999). When recording in bouton-attached mode with a high $[K^+]$ pipette solution and applying a voltage ramp (from a holding potential of −100 to +200 mV), a K^+ conductance is activated such that the K^+ current reverses when the pipette potential is equal to the transmembrane potential. There are several shortcomings of this bouton-attached configuration mainly related to the small size of the patched structure: first, the $[K^+]_i$ in the terminal is unknown and is assumed to be as high as in the somatic compartment, but this potential source of error has only a minor influence (Fricker et al., 1999). Second, a major bias occurs when the seal resistance is equivalent or lower than the resistance of the patch, in which case, most of the K^+ current will be shunt (It should not however influence the potential at which the current changes polarity). That said, gramicidin perforated-patch recordings, which normally do not perturb $[Cl^-]_i$ have not been successfully applied to mossy fiber boutons.

Large mossy fiber varicosities can be visualized in living slices with two-photon excitation fluorescence imaging integrated with patch-clamp electrophysiology (Scott and Rusakov, 2006, 2008; Nistico et al., 2012). Granule cell loading with a morphological tracer such as Alexa Fluor 594 (20–40 μM), together with a high-affinity Ca^{2+} indicator, Fluo-4 (200 μM), or Oregon Green BAPTA-1 (200 μM), then potentially allows Ca^{2+} signaling in unambiguously identified mossy fiber boutons. This depends on tracing the axon from the soma through the hilus and into stratum lucidum. The success rate for imaging a giant mossy fiber bouton in CA3 supplied by a given granule cell is however low, because it depends on the integrity of a lengthy mossy fiber connected to its parent soma.

Presynaptic ionotropic receptors can also been investigated in acutely dissociated CA3 pyramidal neurons, which can be isolated with adherent functional synaptic terminals. This technique (Akaike and Moorhouse, 2003) offers the advantage that single presynaptic terminals and boutons can be visualized using fluorescent markers and can be focally stimulated with a glass micropipette. Adherent contacts are functional and generate spontaneous postsynaptic currents over a reasonable period of time, thus enabling pharmacological manipulation of presynaptic receptors. The method has been successfully applied to CA3 pyramidal neurons (Jang et al., 2006). However, it is mainly restricted to proximal contacts since the dissociation procedure eliminates most of dendritic processes in postsynaptic neurons.

PRESYNAPTIC $GABA_A$ RECEPTORS

Modulation of transmitter release at a synapse was first demonstrated in the pioneering studies of Dudel and Kuffler (1961) and Eccles (1964) who showed that presynaptic GABA receptors inhibited transmitter release from crustacean motor neuron terminals and vertebrate sensory neuron terminals in the spinal cord, respectively. Since then, presynaptic $GABA_A$ receptors have been described in the retina (Tachibana and Kaneko, 1984; Lukasiewicz and Werblin, 1994), the cerebellum (Trigo et al., 2007), the posterior pituitary (Zhang and Jackson, 1993), thalamic nuclei (Jang et al., 2001), and higher cortical structures where they have been shown to modulate axonal excitability and the release of neurotransmitters (Kullmann et al., 2005).

$GABA_A$ receptors depolarize presynaptic axons because $[Cl^-]_i$ is relatively high, reflecting absence of the main extrusion system KCC2 (Gulyas et al., 2001; Hubner et al., 2001). Opening of $GABA_A$ receptors may interfere with the propagation of action potentials by decreasing membrane resistivity (Segev, 1990; Cattaert and El Manira, 1999; Wachowiak and Cohen, 1999; Verdier et al., 2003; Alle and Geiger, 2007). Others have argued that $GABA_A$ receptor-mediated depolarization could decrease the driving force for Ca^{2+} and/or inactivate Na^+ channels (Graham and Redman, 1994). However, presynaptic depolarization consecutive to $GABA_A$ receptor activation enhances neurotransmitter release at the MNTB synapse in the auditory brainstem (Turecek and Trussell, 2001, 2002). This effect appears to be mediated by an increase in basal Ca^{2+} (Awatramani et al., 2005), and recent evidence suggests that P/Q-type Ca^{2+} channels can be enhanced in a $[Ca^{2+}]_i$-dependent manner (Ishikawa et al., 2005; Hori and Takahashi, 2009).

Nearly a decade ago, we provided the first demonstration that presynaptic $GABA_A$ receptors occur in axon terminals in the hippocampus (Ruiz et al., 2003). We obtained both ultrastructural and pharmacological evidence consistent with the presence of presynaptic $GABA_A$ receptors containing α_2 (**Figure 2A**) subunits (see also Jang et al., 2006; Alle and Geiger, 2007). By altering $[Cl^-]_i$ within individual granule cells we showed that the $GABA_A$ receptor agonist muscimol produced opposite changes in the probability for evoking antidromic action potentials (**Figure 2B**). Opposite effects on axonal excitability were also obtained by applying the $GABA_A$ receptor blocker SR95531 (gabazine) depending on $[Cl^-]_i$, suggesting that these receptors are tonically active. These results could only be explained by the

presence of $GABA_A$ receptors on mossy fibers. Measurements of single channel openings of presynaptic $GABA_A$ receptors in outside-out patches from mossy fiber boutons yielded an estimate 36 pS (Alle and Geiger, 2007), similar to the main conductance state of $GABA_A$ receptors found in other preparations (Jones and Westbrook, 1995; Turecek and Trussell, 2002), but slightly larger than our own measurements (24 pS; Ruiz et al., 2010). Their expression is also developmentally regulated. Nakamura et al. (2007) showed that mossy fiber $GABA_A$ receptors are involved in the activity-dependent facilitation of the fiber volley via depolarizing GABA actions, a phenomenon that gradually decreased with development and eventually vanished at around postnatal day 30. In contrast, Alle and Geiger (2007) found that functional presynaptic $GABA_A$ receptors are conserved during development as witnessed by the presence of $GABA_A$ receptor-mediated currents in mossy fiber boutons from 3 month old rats.

What is the normal mode of activation of these receptors? We demonstrated that mossy fiber excitability was modulated by trains of stimuli designed to release GABA from neighboring inhibitory synapses, implying that presynaptic $GABA_A$ receptors could be activated by GABA spillover (Ruiz et al., 2003). This finding was later confirmed by Alle and Geiger (2007) who characterized a slow and small amplitude current in mossy fiber boutons, in response to stimulus trains (**Figure 2C**). These spillover currents were abolished by application of the $GABA_A$ receptor antagonist gabazine, whereas blocking the main GABA

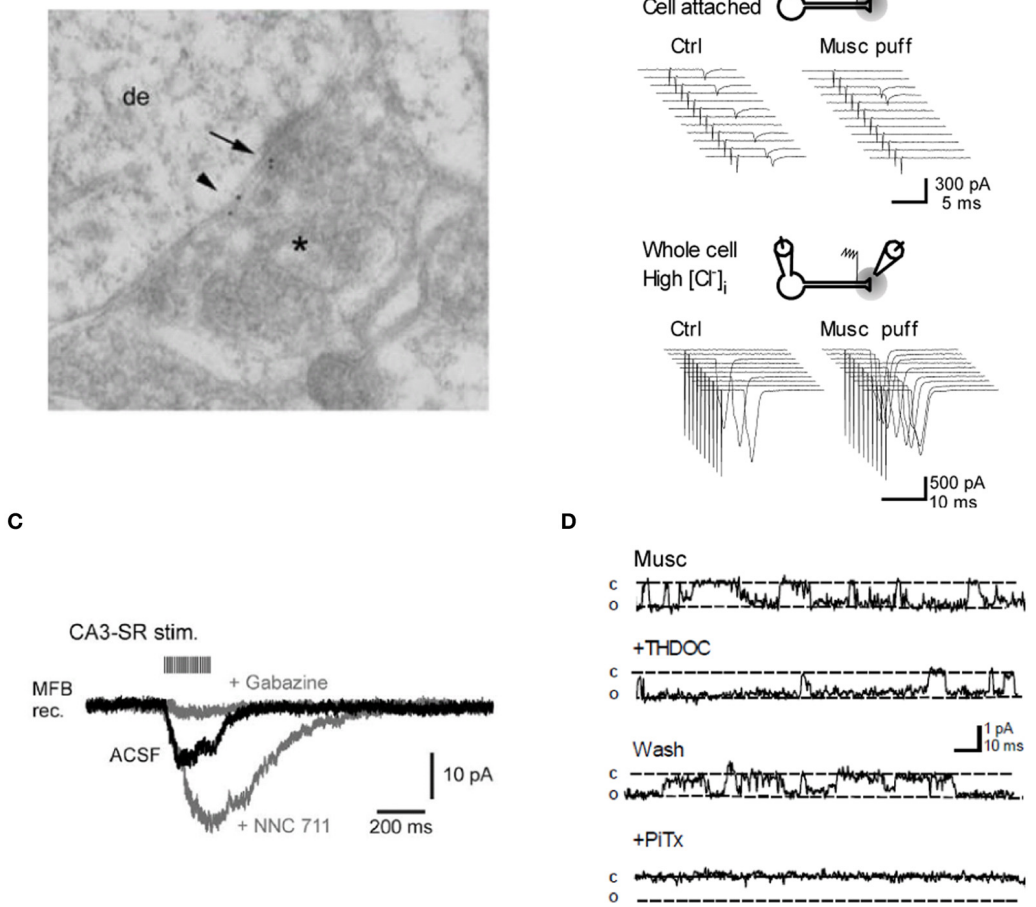

FIGURE 2 | Evidence for $GABA_A$ receptors modulating mossy fiber excitability. (A) Post-embedding immunolocalization of the $GABA_A$ receptor subunit α_2 in a presumptive large mossy fiber terminal. (Asterisk indicates the presynaptic profile). Labeling is present at the synaptic cleft (arrow) and at extrasynaptic axonal membranes (small arrowhead). **(B)** Top, intermittent antidromic action currents. Local pressure application of the $GABA_A$ agonist muscimol close to the stimulation site decreased the axon excitability. Bottom, following "break-in" with a pipette containing a high $[Cl^-]$, the same application of muscimol caused an increase in axon excitability. Sweeps on the right are from one example cell. **(C)** Spill-over $GABA_A$ receptor-mediated currents in a mossy fiber bouton held in voltage-clamp. Twenty pulses at 100 Hz applied to stratum radiatum in area CA3. Gray traces, successive bath application of the GAT 1 blocker NNC 711 (1 μM) and the $GABA_A$ receptor antagonist gabazine (10 μM). **(D)** Muscimol-activated single channel currents in an outside-out patch from a mossy fiber bouton recorded with symmetrical $[Cl^-]$. Superfusion of the neurosteroid THDOC (10 nM) reversibly prolongs the apparent open probability of the channel whereas the $GABA_A$ receptor antagonist picrotoxine blocks the current. Panels **(A, B,** and **D)** were reproduced from Ruiz et al. (2003, 2010) and panel **(C)** from Alle and Geiger (2007).

uptake system GAT-1 with NNC-711 enhanced them. The results argued that presynaptic $GABA_A$ receptors can detect activity-dependent fluctuations in the extracellular GABA concentration (see also Nakamura et al., 2007) as shown for a form of $GABA_B$ receptor-mediated signaling at these terminals (Vogt and Nicoll, 1999; Chandler et al., 2003; Safiulina and Cherubini, 2009).

Dentate granule cells express tonically active $GABA_A$ receptors, which are sensitive to physiological concentrations of tetrahydrodeoxycorticosterone (THDOC), an endogenous neurosteroid that is relatively selective for δ-subunit containing receptors (Stell et al., 2003). We found that 10 nM THDOC reversibly reduces the excitability of mossy fibers, mimicking the effect of $GABA_A$ receptor agonists and suggesting that high-affinity δ-subunit containing receptors (in addition to α_2) are present in the axon. Similar results were obtained with the hypnotic compound THIP (gaboxadol, 100 nM), which is a relatively selective agonist at $GABA_A$ receptors that lack γ subunits. Finally, we confirmed that THDOC increased the apparent open probability of $GABA_A$ receptors in outside-out patches from mossy fiber boutons but had no effect on the single-channel conductance (**Figure 2D**).

We further showed that tonically-active presynaptic $GABA_A$ receptors depolarize mossy fibers and modulate the input resistance of mossy fiber boutons, as well as the shape of presynaptic action potentials (**Figure 3A**). Blocking $GABA_A$ receptors with gabazine hyperpolarized mossy fiber boutons and reduced spike half-width, whereas THDOC had the opposite depolarizing effect and broadened action potentials. These results diverged from those of Alle and Geiger (2007) who did not detect a change in mossy fiber bouton input resistance or membrane potential as a consequence of $GABA_A$ receptor blockade. The reason for this discrepancy is unclear but it could involve differences in rat strains (Wistar vs. Sprague-Dawley), recording temperature and state of neuromodulation, for example by zinc or dynorphin. Notwithstanding these differences, the presence of both high- and low-affinity presynaptic $GABA_A$ receptors suggests a richness of phasic and tonic modulation of synaptic transmission at mossy fiber—CA3 synapses.

We also detected a strong influence of $GABA_A$ receptors on action-potential dependent Ca^{2+} transients in single axonal varicosities imaged with 2-photon excitation fluorescence microscopy (**Figure 3B**). We showed that the $GABA_A$ receptor antagonist gabazine decreased the amplitude of action-potential evoked Ca^{2+} transients whereas THDOC had the opposite effect. These results demonstrated that tonically-active $GABA_A$ receptors contribute to presynaptic depolarization and Ca^{2+} influx when a single action potential invades a mossy fiber varicosity. To assess the

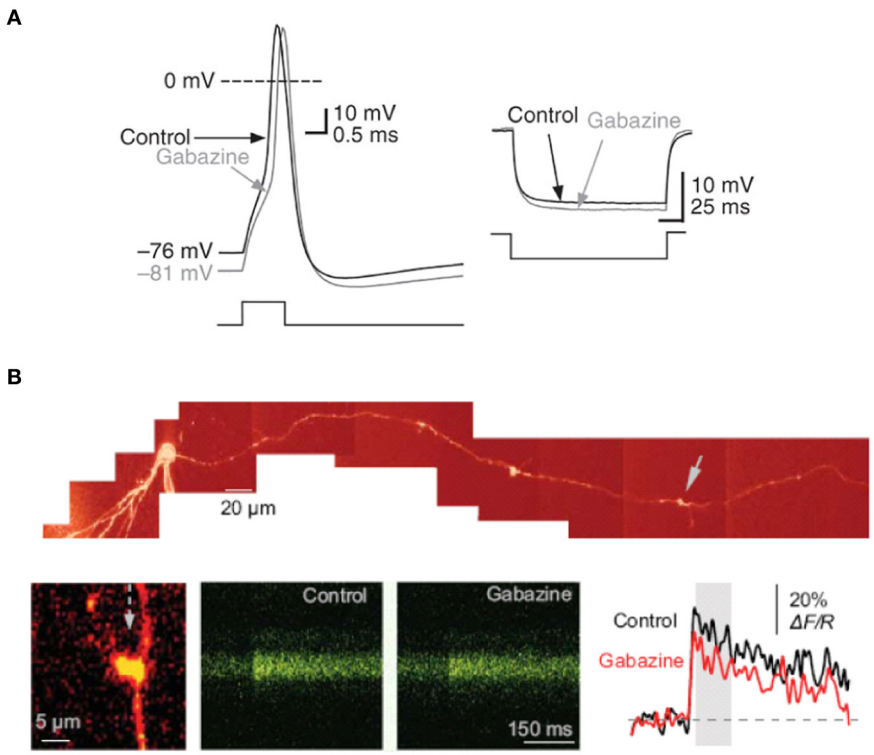

FIGURE 3 | Tonically-active $GABA_A$ receptor–mediated currents modulate the electrical properties of mossy fiber boutons. (A) Current-clamp recording from a mossy fiber bouton with 20 mM $[Cl^-]_i$. Left, sample traces showing the action potential before (black) and after (gray) superfusion of gabazine (5 µM). Right, response to hyperpolarizing current injection showing an increase in mossy fiber input resistance in gabazine. **(B)** Tonically-active $GABA_A$ receptors enhance presynaptic action potential-dependent Ca^{2+} transients in giant mossy fiber boutons. Top, reconstruction of a dentate granule cell (Alexa Fluor 594 channel, $\lambda x = 800$ nm). Arrows indicate giant boutons with characteristic thin filopodia. Bottom, blocking $GABA_A$ receptors with gabazine reduced spike-dependent presynaptic Ca^{2+} entry. Line scans and traces are Ca^{2+} responses in the mossy fiber bouton shown on the left following a single action potential induced at the soma, in control conditions and in 1 µM gabazine. Reproduced from Ruiz et al. (2010).

contribution of presynaptic $GABA_A$ receptors to glutamatergic transmission we recorded from CA3 pyramidal neurons with a pipette solution containing CsF and 4,4′-diisothiocyanostilbene-2,2′-disulfonic acid (DIDS) to block postsynaptic $GABA_A$ receptors intracellularly, while leaving presynaptic receptors unaffected (**Figure 4A**). Local pressure application of THDOC reversibly increased the amplitude of evoked excitatory postsynaptic currents (EPSCs) whereas gabazine decreased it, implying that presynaptic $GABA_A$ receptor normally exert a bidirectional control over dentate gyrus—CA3 neurotransmission. Finally, we demonstrated that blocking presynaptic $GABA_A$ receptors impaired the induction of mossy fiber LTP (**Figure 4B**). A straightforward explanation for this finding was that tonic $GABA_A$ receptor mediated presynaptic depolarization has a permissive role in mossy fiber LTP because its induction is steeply dependent on the presynaptic membrane potential and Ca^{2+} influx (Castillo et al., 1994; Schmitz et al., 2003; Nicoll and Schmitz, 2005). Although the evidence for presynaptic $GABA_A$ receptors is compelling some puzzles remain. For instance, muscimol decreases mossy fiber excitability even though $GABA_A$ receptor activation depolarizes boutons (Alle and Geiger, 2007; Ruiz et al., 2010). Reduced excitability can potentially be explained by partial inactivation of Na^+ channels. Furthermore, although differences in apparent affinity of $GABA_A$ receptors suggest that multiple biophysically distinct receptors coexist in the same boutons they have not been resolved at single channel resolution.

PRESYNAPTIC GLYCINE RECEPTORS

Glycine is a common neurotransmitter in the spinal cord and the brainstem whose action on glycine receptors activates a Cl^- conductance. Glycine and glycine receptors are, however, not

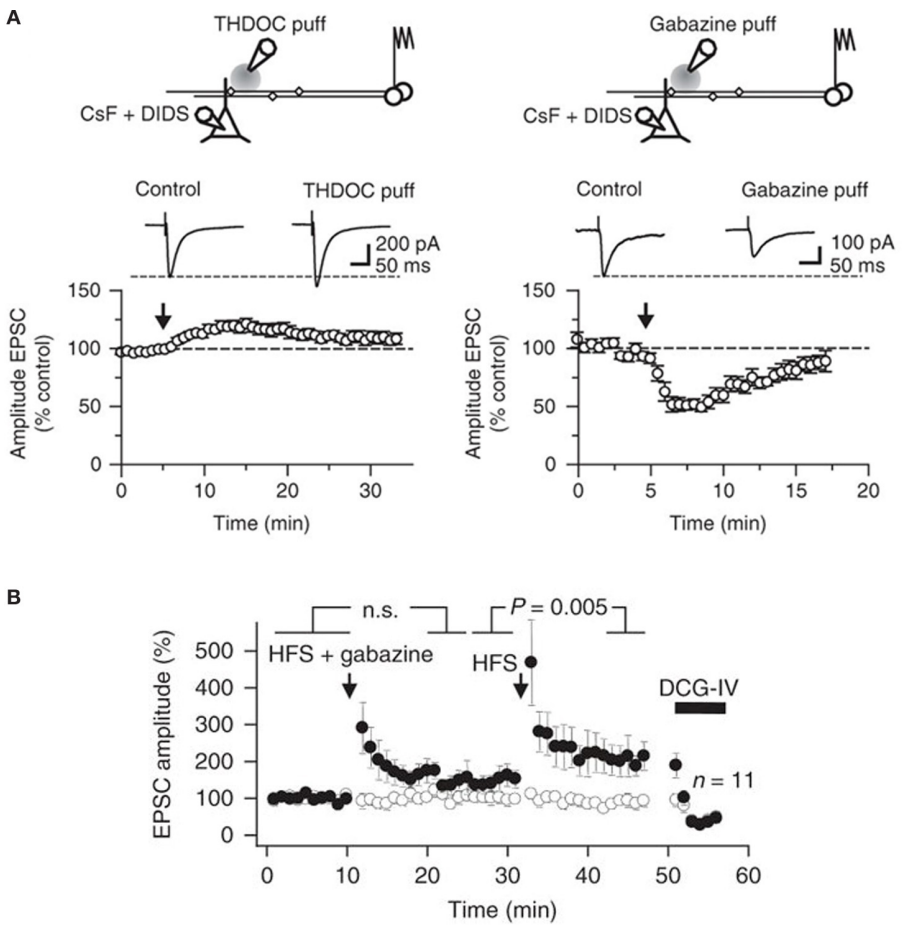

FIGURE 4 | Bidirectional modulation of synaptic transmission via tonically active $GABA_A$ receptors at mossy fibers. (A) Top, schematic illustrating the experimental design used to study presynaptic $GABA_A$ receptors at mossy fiber—CA3 synapses. Postsynaptic $GABA_A$ receptors in CA3 pyramidal cells were blocked using an intracellular pipette solution containing CsF and DIDS. A pressure-application pipette containing THDOC (50 nM, left) was positioned ∼50–200 μm from the apical dendrite of the recorded neurons. Bottom, time course of the effects of pressure application of THDOC (left; $n = 8$). Traces are averages of 10 consecutive EPSCs before and after drug application. The effect of gabazine (10 μM) applied as in **(A)** is also shown (right; $n = 6$). **(B)** EPSC amplitudes recorded in a CA3 pyramidal neuron in response to stimulation of two pathways. High frequency stimulation (HFS) was delivered to one pathway (filled symbols) at the times indicated, either together with local pressure application of gabazine in stratum lucidum (HFS + gabazine) or alone (HFS). DCG-IV was applied at the end of the experiment to confirm that the responses were profoundly depressed, typical of mossy fibers. Average time course of 11 experiments (error bars indicate s.e.m). Reproduced from Ruiz et al. (2010).

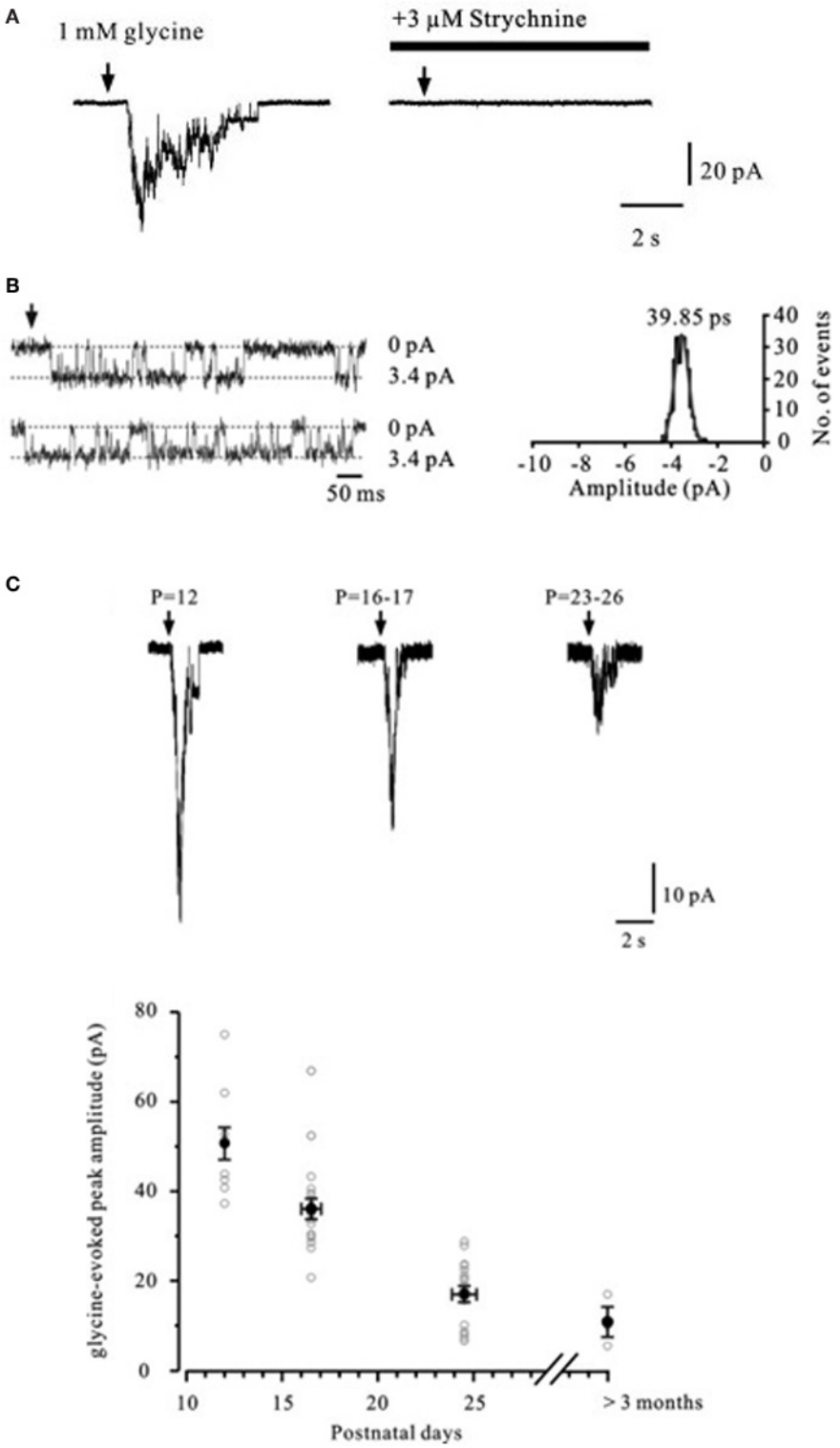

FIGURE 5 | Glycine-evoked currents in mossy fiber boutons. (A) Currents in a mossy fiber bouton evoked by focal application of 1 mM glycine. Superfusion of the glycine receptor antagonist strychnine (3 μM) completely blocks the current. Arrows indicate glycine puff-application. **(B)** Left, representative traces of single-channel currents in an isolated outside-out patch from a mossy fiber bouton (P12) evoked by continuous application of 1 mM glycine (symmetrical [Cl^-]). Dashed lines indicate either baseline current or glycine induced inward current during channel opening. Right, Gaussian fit to the single-channel current amplitude histogram indicates a single-channel conductance of 40 pS. **(C)** Currents evoked by 1 mM glycine recorded from mossy fiber boutons in different age groups. Reproduced from Kubota et al. (2010).

restricted to these regions, nor do they always promote inhibition. Glycine receptors have been reported in the cerebellum and the hippocampus (Araki et al., 1988). Glycine receptors in the forebrain are mainly found at extrasynaptic sites in postsynaptic membranes or even presynaptically (Harvey and Rigo, 2010). In the retina, presynaptic glycine receptors localize in rod cells terminals where they inhibit transmission by hyperpolarization and a shunting mechanism (Morkve and Hartveit, 2009). Presynaptic glycine receptors enhance glutamate release at the MNTB synapse by promoting small depolarization's of the nerve terminal (Turecek and Trussell, 2001). Interestingly, presynaptic glycine receptor activation in the ventral tegmental area enhances GABA release in young neurons but has an inhibitory effect in older neurons (Ye et al., 2004). Thus, the direction in which transmitter release is regulated by presynaptic glycine receptors varies within the CNS and during development, and this can affect both excitatory and inhibitory neurotransmitters.

In the hippocampus, the evidence for functional presynaptic glycine receptors is sparse. Exogenously applied glycine significantly increased the frequency of spontaneous EPSCs recorded from mechanically dissociated rat dentate hilar neurons attached with native presynaptic nerve terminals (Lee et al., 2009). The enhancing effect of glycine on synaptic transmission was blocked by the specific glycine receptor antagonist strychnine, but was unaffected by picrotoxin. The evidence that these receptors are expressed at mossy fibers again comes from direct patch-clamp recordings and single channel analysis (Kubota et al., 2010). As shown in **Figure 5A**, immature mossy fiber boutons challenged with glycine displayed inward currents that were blocked by strychnine. Glycine-gated channels showed a main conductance of 40 pS (**Figure 5B**) but multiple conductance states were observed, consistent with expression of both homo- and hetero-oligomeric glycine receptors (Takahashi and Momiyama, 1991; Singer and Berger, 1999). The expression profile of presynaptic glycine receptors at mossy fibers declined dramatically with age (**Figure 5C**) in sharp contrast with those found at the Calyx of Held (Turecek and Trussell, 2001, 2002).

PRESYNAPTIC NMDA RECEPTORS

One of the first demonstration that presynaptic NMDA receptors occur on axon terminals in the CNS came from the immunolocalization of the NMDA receptor subunit NR1 in both the dorsal and ventral horns of the rat spinal cord, particularly near the active zones, suggesting a modulatory role in transmitter release (Liu et al., 1994). These receptors were later found to modulate the release of glutamate and substance P from nociceptive fibers (Liu et al., 1997) and glutamate release from primary sensory neurons (Bardoni et al., 2004). In the cerebellum, presynaptic NMDA receptors facilitate GABA release at basket cell—Purkinje cell synapses via retrograde signaling and release of Ca^{2+} from internal stores (Duguid and Smart, 2004). In cortical regions, Berretta and Jones (1996) introduced a trick to specifically block NMDA receptors in postsynaptic cells, leaving presynaptic NMDA receptors available for pharmacological manipulation. They recorded in whole-cell mode from layer II enthorinal cortex neurons with a pipette solution containing 1 mM MK-801 to block NMDA receptors intracellularly. They showed that superfusion of the NMDA receptor antagonist D-AP5 resulted in a decrease of the frequency of miniature EPSCs with little effect on the amplitude, suggesting that tonically-activated NMDA receptors facilitate glutamate release also at cortical synapses. Finally, in the juvenile rat barrel cortex, presynaptic NR2B-containing NMDA receptors enhance AMPA receptor-mediated synaptic transmission at layer 4 to layers 2/3 synapses (Brasier and Feldman, 2008).

Recently, presynaptic NMDA receptors have been implicated in spike-timing dependent long-term depression at neocortical synapses (Sjostrom et al., 2003; Buchanan et al., 2012). This process requires the co-activation of CB1 receptors and is developmentally regulated such that in the juvenile, the NR3A subunit enhances spontaneous and evoked glutamate release and is required for spike timing-dependent long-term depression, whereas in the adult, NR2B-containing presynaptic NMDA receptors enhance neurotransmission in the absence of Mg^{2+}, implying that they function under depolarizing conditions. Recently, a new caged compound has demonstrated axonal NMDA receptors required for induction and the presynaptic locus of expression of LTD at layer 4-layer 2/3 synapses (Rodriguez-Moreno et al., 2012). The evidence for presynaptic NMDA receptors in cortical neurons is however incomplete, and one study failed to detect them using axonal Ca^{2+} imaging (Pugh and Jahr, 2012).

Evidence for presynaptic NMDA receptors at mossy fiber synapses is also incomplete. In the monkey hippocampus, monoclonal antibodies raised against the NMDA receptor subunits NR1 and NR2 stained stratum lucidum but not postsynaptic targets (Siegel et al., 1994). The detection of NMDA receptors subunits in the mossy fiber projection zone does not, however, prove the presence of functionally active presynaptic receptors. A study reporting NMDA receptors using patch-clamp recordings from mossy fiber boutons has only been reported in abstract form (Alle and Geiger, 2005). Thus, evidence that NMDA receptors are expressed in mossy fiber terminals is far from conclusive.

PRESYNAPTIC KAINATE RECEPTORS

In contrast with AMPA and NMDA receptors, kainate receptors play a relatively small role in fast glutamatergic transmission at most synapses. Some exceptions are mossy fiber synapses, and thalamo-cortical synapses early in development, where they mediate slow and small amplitude EPSCs (Castillo et al., 1997; Vignes and Collingridge, 1997; Kidd et al., 2002). There is however, abundant evidence for kainate receptor expression in presynaptic terminals where they modulate the plastic properties of both excitatory and inhibitory connections (reviewed by Kullmann, 2001; Pinheiro and Mulle, 2008; Contractor et al., 2012). In the hippocampus, early binding studies using (3)H-radiolabelled kainate as ligand (Foster et al., 1981; Monaghan and Cotman, 1982; Bahn et al., 1994) have shown the presence of high-affinity binding sites restricted to stratum lucidum, where mossy fibers terminate. This staining pattern was dramatically reduced by selective destruction of dentate granule cells with the antimitotic agent colchicine (Represa et al., 1987), suggesting that kainate receptors are expressed in the axon or in presynaptic terminals. Immunohistochemical experiments with monoclonal antibodies directed against GluK1 and GluK2 also stained stratum lucidum (Petralia et al., 1994), in line with previous results.

The effects of kainate on dentate gyrus—CA3 neurotransmission are concentration-dependent and bimodal: superfusion of a low dose of kainate (50–200 nM) has been reported to facilitate evoked EPSC recorded in CA3 pyramidal neurons whereas higher doses (1–5 μM) have a depressant effect. The facilitation of mossy fiber EPSCs consecutive to the application of a low concentration of kainate is accompanied by an enhancement of the presynaptic fiber volley (**Figure 6A**; Kamiya and Ozawa, 2000; Schmitz et al., 2001) and by a decrease in the threshold for evoking antidromic action potentials recorded in granule cells (Kamiya and Ozawa, 2000), consistent with a presynaptic expression of kainate receptors. One explanation for these effects is that mild depolarization could inactivate K^+ channels whereas inactivation of presynaptic Ca^{2+} channels may occur with large doses of kainate. Presynaptic kainate eceptors could be activated by synaptic release of glutamate from neighboring mossy fibers or associational-commisural fibers, thus mimicking the effect of exogenous agonist application on the fiber volley and threshold (Schmitz et al., 2000).

Although kainate receptors contribute to the large frequency-dependent short-term plasticity of mossy fiber synapses, the identity of the subunits that mediate these effects is unclear. Studies performed in knock-out mice indicate that presynaptic kainate receptors containing the GluK2 (Contractor et al., 2001; Breustedt and Schmitz, 2004; Rodriguez-Moreno and Sihra, 2007) and GluK3 subunits (Pinheiro et al., 2007; Perrais et al., 2009) facilitate the induction of this form of synaptic plasticity whereas other studies have identified GluK1 as a principal player (Bortolotto et al., 1999; Lauri et al., 2001; More et al., 2004). The reasons for these discrepancies are unknown, but some of the GluK1 antagonists used in these studies could also block receptors containing the GluK3 subunit (Perrais et al., 2009). GluK3 is thought to underlie the effects mediated by presynaptic kainate receptors. Receptors containing this subunit have a low sensitivity for glutamate, are highly Ca^{2+}-permeable, desensitize rapidly and are subject to a voltage-dependent block by intracellular spermine. However, the view that kainate receptors participate in short-term plasticity at mossy fiber—CA3 synapses was recently challenged by Kwon and Castillo (2008). The authors found no evidence that presynaptic kainate receptors facilitate transmitter release on CA3 pyramidal neurons over a wide range of stimulus frequencies delivered to mossy fibers, and argued that actions generally attributed to presynaptic

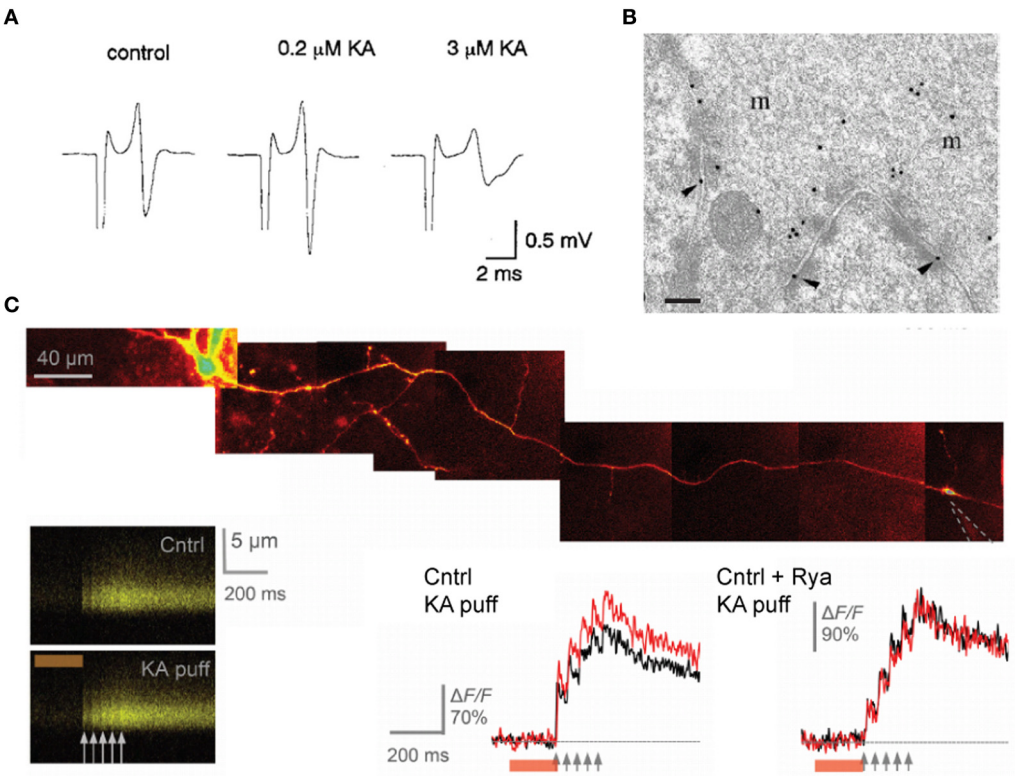

FIGURE 6 | presynaptic kainate receptors modulate mossy fiber excitability and Ca^{2+} influx in single varicosities. (A) Representative traces of the afferent volley before and during superfusion of low and high doses of kainate, as indicated. **(B)** High-magnification micrograph of stratum lucidum showing a mossy fiber terminal labeled with antibody fragments directed against GluK4. Immunogold particles are found along the presynaptic membrane. Scale bar, 20 nm. **(C)** Local kainate application mobilizes Ca^{2+}-store and boosts action-potential-evoked Ca^{2+}entry in giant mossy fiber boutons. Top, a granule cell axon is traced from the soma and a patch pipette (dotted lines) is approached near a giant mossy fiber bouton. Kainate is pressure ejected together with Alexa Fluor 594 from the pipette using a 200 ms pressure pulse (line-scans). Local pressure application of kainate has no effect on the baseline resting Ca^{2+} but increases action-potential-evoked Ca^{2+} entry in the imaged bouton. Ca^{2+} store depletion with ryanodine abolishes the presynaptic effects of kainate application. Panel **(A)** is reproduced from Kamiya and Ozawa (2000), panel **(B)** from Darstein et al. (2003) and panel **(C)** from Scott et al. (2008).

kainate receptors are likely due to activation of the recurrent CA3 network.

Two studies have provided solid and direct evidence that these receptors actually occur in presynaptic and perisynaptic membranes in mossy fibers. The first study is the immunolocalization of kainate receptor subunits at ultrastructural level performed by Darstein et al. (2003). The authors showed that both GluK4 and GluK5 subunits localize presynaptically, with a preferential expression for GluK4, whereas GluK5 is mainly found in postsynaptic membranes (**Figure 6B**). Interestingly, antibodies against these two subunits also pulled-down GluK2 in hippocampal membrane extracts but failed to detect GluK3 subunits, whose localization is thought to be presynaptic (Pinheiro et al., 2007). The second report by Scott et al. (2008) used high resolution multi-photon imaging and pharmacology. Here the authors showed that individual action potentials evoke an increase in intracellular Ca^{2+} in presynaptic varicosities which is enhanced by kainate receptor activation, and contribute to activity-dependent facilitation of synaptic transmission in CA3 pyramidal neurons (**Figure 6C**). Whether glutamate released from a single varicosity acts on kainate receptors located on that same varicosity remains, however, to be demonstrated.

Kainate receptors are also thought to facilitate the induction of long-term potentiation in CA3 pyramidal neurons (Bortolotto et al., 1999; Lauri et al., 2001; Schmitz et al., 2003; Pinheiro et al., 2007). Again, conflictive reports have emerged in the literature about their role in the phenomenon (Kullmann, 2001). Recently, it has been argued that differences in kainate receptor involvement in mossy fiber long-term potentiation depend on slice orientation (Sherwood et al., 2012). In transverse slices, LTP was found resistant to GluK1 antagonists whereas in parasagittal slices LTP was consistently blocked by these agents. Whatever the explanations, we believe that many answers will come from direct recordings from mossy fiber boutons and a detailed characterization of the effects of kainate on the presynaptic membrane potential.

FUNCTIONAL IMPLICATIONS

Presynaptic modulation via ionotropic receptors may have broader implications for information processing and hippocampal physiology than previously thought. Endogenous levels of glutamate, GABA or glycine in brain tissue seem sufficient to promote baseline activity of high-affinity receptors, whereas receptors with lower affinities might be activated only after sustained activity and during a short time window consecutive to neurotransmitter release. For example, presynaptic kainate receptors at thalamo-cortical synapses depress glutamate release during repetitive activation at frequencies >50 Hz (Kidd et al., 2002), but presynaptic $GABA_A$ receptors at mossy fibers regulate glutamate release when presynaptic activity spans a wider range of frequencies (Nakamura et al., 2007). Presynaptic ionotropic receptors are also subject to neuromodulation from a large variety of hormones, cations, and other neurotransmitters, including monoamines and neurosteroids, whose levels fluctuate extensively in physiological states and behavioral tasks as well as in pathological conditions. Finally, the permissive and synergistic effect of presynaptic $GABA_A$ and kainate receptors on mossy fiber LTP highlight a powerful mechanism for information storage in CA3 networks. It also serves the basis for homeostatic regulation of feed-forward and frequency-tuned inhibition at a major input to the hippocampus proper.

CONCLUSIONS

An increasing diversity of receptors normally found in dendrites are also localized in axon terminals where they mediate fast and local regulation of presynaptic excitability, Ca^{2+} influx and neurotransmitter release. A common feature of these receptors is that their activation leads to membrane depolarization and shunting, which in turn alter spike shape and the relation between Ca^{2+} influx and release probability. Direct recordings from mossy fiber boutons have provided some of the most compelling insights into the identity, localization, and physiological roles of these receptors.

REFERENCES

Acsady, L., Kamondi, A., Sik, A., Freund, T., and Buzsaki, G. (1998). GABAergic cells are the major postsynaptic targets of mossy fibers in the rat hippocampus. *J. Neurosci.* 18, 3386–3403.

Akaike, N., and Moorhouse, A. J. (2003). Techniques: applications of the nerve-bouton preparation in neuropharmacology. *Trends Pharmacol. Sci.* 24, 44–47.

Alle, H., and Geiger, J. R. (2005). NMDA receptors in hippocampal mossy fibers. *Acta Physiol.* 186(Suppl.), 650.

Alle, H., and Geiger, J. R. (2007). GABAergic spill-over transmission onto hippocampal mossy fiber boutons. *J. Neurosci.* 27, 942–950.

Amaral, D. G., Ishizuka, N., and Claiborne, B. (1990). Neurons, numbers and the hippocampal network. *Prog. Brain Res.* 83, 1–11.

Araki, T., Yamano, M., Murakami, T., Wanaka, A., Betz, H., and Tohyama, M. (1988). Localization of glycine receptors in the rat central nervous system: an immunocytochemical analysis using monoclonal antibody. *Neuroscience* 25, 613–624.

Awatramani, G. B., Price, G. D., and Trussell, L. O. (2005). Modulation of transmitter release by presynaptic resting potential and background calcium levels. *Neuron* 48, 109–121.

Bahn, S., Volk, B., and Wisden, W. (1994). Kainate receptor gene expression in the developing rat brain. *J. Neurosci.* 14, 5525–5547.

Bardoni, R., Torsney, C., Tong, C. K., Prandini, M., and Macdermott, A. B. (2004). Presynaptic NMDA receptors modulate glutamate release from primary sensory neurons in rat spinal cord dorsal horn. *J. Neurosci.* 24, 2774–2781.

Berretta, N., and Jones, R. S. (1996). Tonic facilitation of glutamate release by presynaptic N-methyl-D-aspartate autoreceptors in the entorhinal cortex. *Neuroscience* 75, 339–344.

Bischofberger, J., Engel, D., Li, L., Geiger, J. R., and Jonas, P. (2006). Patch-clamp recording from mossy fiber terminals in hippocampal slices. *Nat. Protoc.* 1, 2075–2081.

Bortolotto, Z. A., Clarke, V. R., Delany, C. M., Parry, M. C., Smolders, I., Vignes, M., et al. (1999). Kainate receptors are involved in synaptic plasticity. *Nature* 402, 297–301.

Brasier, D. J., and Feldman, D. E. (2008). Synapse-specific expression of functional presynaptic NMDA receptors in rat somatosensory cortex. *J. Neurosci.* 28, 2199–2211.

Breustedt, J., and Schmitz, D. (2004). Assessing the role of GLUK5 and GLUK6 at hippocampal mossy fiber synapses. *J. Neurosci.* 24, 10093–10098.

Buchanan, K. A., Blackman, A. V., Moreau, A. W., Elgar, D., Costa, R. P., Lalanne, T., et al. (2012). Target-specific expression of presynaptic NMDA receptors in neocortical microcircuits. *Neuron* 75, 451–466.

Castillo, P. E., Malenka, R. C., and Nicoll, R. A. (1997). Kainate receptors mediate a slow postsynaptic current in hippocampal CA3 neurons. *Nature* 388, 182–186.

Castillo, P. E., Weisskopf, M. G., and Nicoll, R. A. (1994). The role of Ca2+ channels in hippocampal mossy fiber synaptic transmission

and long-term potentiation. *Neuron* 12, 261–269.

Cattaert, D., and El Manira, A. (1999). Shunting versus inactivation: analysis of presynaptic inhibitory mechanisms in primary afferents of the crayfish. *J. Neurosci.* 19, 6079–6089.

Chandler, K. E., Princivalle, A. P., Fabian-Fine, R., Bowery, N. G., Kullmann, D. M., and Walker, M. C. (2003). Plasticity of GABA(B) receptor-mediated heterosynaptic interactions at mossy fibers after status epilepticus. *J. Neurosci.* 23, 11382–11391.

Contractor, A., Mulle, C., and Swanson, G. T. (2012). Kainate receptors coming of age: milestones of two decades of research. *Trends Neurosci.* 34, 154–163.

Contractor, A., Swanson, G., and Heinemann, S. F. (2001). Kainate receptors are involved in short- and long-term plasticity at mossy fiber synapses in the hippocampus. *Neuron* 29, 209–216.

Darstein, M., Petralia, R. S., Swanson, G. T., Wenthold, R. J., and Heinemann, S. F. (2003). Distribution of kainate receptor subunits at hippocampal mossy fiber synapses. *J. Neurosci.* 23, 8013–8019.

Dudel, J., and Kuffler, S. W. (1961). Presynaptic inhibition at the crayfish neuromuscular junction. *J. Physiol.* 155, 543–562.

Duguid, I. C., and Smart, T. G. (2004). Retrograde activation of presynaptic NMDA receptors enhances GABA release at cerebellar interneuron-Purkinje cell synapses. *Nat. Neurosci.* 7, 525–533.

Eccles, J. C. (1964). Presynaptic inhibition in the spinal cord. *Prog. Brain Res.* 12, 65–91.

Edwards, F. R., Harrison, P. J., Jack, J. J., and Kullmann, D. M. (1989). Reduction by baclofen of monosynaptic EPSPs in lumbosacral motoneurones of the anaesthetized cat. *J. Physiol. (Lond.)* 416, 539–556.

Foster, A. C., Mena, E. E., Monaghan, D. T., and Cotman, C. W. (1981). Synaptic localization of kainic acid binding sites. *Nature* 289, 73–75.

Fricker, D., Verheugen, J. A., and Miles, R. (1999). Cell-attached measurements of the firing threshold of rat hippocampal neurones. *J. Physiol.* 517(Pt 3), 791–804.

Geiger, J. R., and Jonas, P. (2000). Dynamic control of presynaptic Ca(2+) inflow by fast-inactivating K(+) channels in hippocampal mossy fiber boutons. *Neuron* 28, 927–939.

Graham, B., and Redman, S. (1994). A simulation of action potentials in synaptic boutons during presynaptic inhibition. *J. Neurophysiol.* 71, 538–549.

Gulyas, A. I., Sik, A., Payne, J. A., Kaila, K., and Freund, T. F. (2001). The KCl cotransporter, KCC2, is highly expressed in the vicinity of excitatory synapses in the rat hippocampus. *Eur. J. Neurosci.* 13, 2205–2217.

Harvey, R. J., and Rigo, J. M. (2010). Glycinergic transmission: physiological, developmental and pathological implications. *Front. Mol. Neurosci.* 3:115. doi: 10.3389/fnmol.2010.00115

Henze, D. A., Wittner, L., and Buzsaki, G. (2002). Single granule cells reliably discharge targets in the hippocampal CA3 network *in vivo*. *Nat. Neurosci.* 5, 790–795.

Hori, T., and Takahashi, T. (2009). Mechanisms underlying short-term modulation of transmitter release by presynaptic depolarization. *J. Physiol.* 587, 2987–3000.

Hubner, C. A., Stein, V., Hermans-Borgmeyer, I., Meyer, T., Ballanyi, K., and Jentsch, T. J. (2001). Disruption of KCC2 reveals an essential role of K-Cl cotransport already in early synaptic inhibition. *Neuron* 30, 515–524.

Ishikawa, T., Kaneko, M., Shin, H. S., and Takahashi, T. (2005). Presynaptic N-type and P/Q-type Ca2+ channels mediating synaptic transmission at the calyx of Held of mice. *J. Physiol.* 568, 199–209.

Jang, I. S., Jeong, H. J., and Akaike, N. (2001). Contribution of the Na-K-Cl cotransporter on GABA(A) receptor-mediated presynaptic depolarization in excitatory nerve terminals. *J. Neurosci.* 21, 5962–5972.

Jang, I. S., Nakamura, M., Ito, Y., and Akaike, N. (2006). Presynaptic GABAA receptors facilitate spontaneous glutamate release from presynaptic terminals on mechanically dissociated rat CA3 pyramidal neurons. *Neuroscience* 138, 25–35.

Jones, M. V., and Westbrook, G. L. (1995). Desensitized states prolong GABAA channel responses to brief agonist pulses. *Neuron* 15, 181–191.

Jung, M. W., and McNaughton, B. L. (1993). Spatial selectivity of unit activity in the hippocampal granular layer. *Hippocampus* 3, 165–182.

Kamiya, H., and Ozawa, S. (2000). Kainate receptor-mediated presynaptic inhibition at the mouse hippocampal mossy fibre synapse. *J. Physiol.* 523(Pt 3), 653–665.

Kidd, F. L., Coumis, U., Collingridge, G. L., Crabtree, J. W., and Isaac, J. T. (2002). A presynaptic kainate receptor is involved in regulating the dynamic properties of thalamocortical synapses during development. *Neuron* 34, 635–646.

Kirischuk, S., Clements, J. D., and Grantyn, R. (2002). Presynaptic and postsynaptic mechanisms underlie paired pulse depression at single GABAergic boutons in rat collicular cultures. *J. Physiol.* 543, 99–116.

Kubota, H., Alle, H., Betz, H., and Geiger, J. R. (2010). Presynaptic glycine receptors on hippocampal mossy fibers. *Biochem. Biophys. Res. Commun.* 393, 587–591.

Kullmann, D. M. (2001). Presynaptic kainate receptors in the hippocampus: slowly emerging from obscurity. *Neuron* 32, 561–564.

Kullmann, D. M., Ruiz, A., Rusakov, D. M., Scott, R., Semyanov, A., and Walker, M. C. (2005). Presynaptic, extrasynaptic and axonal GABAA receptors in the CNS: where and why? *Prog. Biophys. Mol. Biol.* 87, 33–46.

Kwon, H. B., and Castillo, P. E. (2008). Role of glutamate autoreceptors at hippocampal mossy fiber synapses. *Neuron* 60, 1082–1094.

Lauri, S. E., Bortolotto, Z. A., Bleakman, D., Ornstein, P. L., Lodge, D., Isaac, J. T., et al. (2001). A critical role of a facilitatory presynaptic kainate receptor in mossy fiber LTP. *Neuron* 32, 697–709.

Lee, E. A., Cho, J. H., Choi, I. S., Nakamura, M., Park, H. M., Lee, J. J., et al. (2009). Presynaptic glycine receptors facilitate spontaneous glutamate release onto hilar neurons in the rat hippocampus. *J. Neurochem.* 109, 275–286.

Liu, H., Mantyh, P. W., and Basbaum, A. I. (1997). NMDA-receptor regulation of substance P release from primary afferent nociceptors. *Nature* 386, 721–724.

Liu, H., Wang, H., Sheng, M., Jan, L. Y., Jan, Y. N., and Basbaum, A. I. (1994). Evidence for presynaptic N-methyl-D-aspartate autoreceptors in the spinal cord dorsal horn. *Proc. Natl. Acad. Sci. U.S.A.* 91, 8383–8387.

Lukasiewicz, P. D., and Werblin, F. S. (1994). A novel GABA receptor modulates synaptic transmission from bipolar to ganglion and amacrine cells in the tiger salamander retina. *J. Neurosci.* 14, 1213–1223.

Manabe, T., Wyllie, D. J., Perkel, D. J., and Nicoll, R. A. (1993). Modulation of synaptic transmission and long-term potentiation: effects on paired pulse facilitation and EPSC variance in the CA1 region of the hippocampus. *J. Neurophysiol.* 70, 1451–1459.

Monaghan, D. T., and Cotman, C. W. (1982). The distribution of [3H]kainic acid binding sites in rat CNS as determined by autoradiography. *Brain Res.* 252, 91–100.

More, J. C., Nistico, R., Dolman, N. P., Clarke, V. R., Alt, A. J., Ogden, A. M., et al. (2004). Characterisation of UBP296: a novel, potent and selective kainate receptor antagonist. *Neuropharmacology* 47, 46–64.

Morkve, S. H., and Hartveit, E. (2009). Properties of glycine receptors underlying synaptic currents in presynaptic axon terminals of rod bipolar cells in the rat retina. *J. Physiol.* 587, 3813–3830.

Nakamura, M., Sekino, Y., and Manabe, T. (2007). GABAergic interneurons facilitate mossy fiber excitability in the developing hippocampus. *J. Neurosci.* 27, 1365–1373.

Nicoll, R. A., and Schmitz, D. (2005). Synaptic plasticity at hippocampal mossy fibre synapses. *Nat. Rev. Neurosci.* 6, 863–876.

Nistico, R., Dargan, S. L., Amici, M., Collingridge, G. L., and Bortolotto, Z. A. (2012). Synergistic interactions between kainate and mGlu receptors regulate bouton Ca signalling and mossy fibre LTP. *Sci. Rep.* 1, 103.

Perrais, D., Coussen, F., and Mulle, C. (2009). Atypical functional properties of GluK3-containing kainate receptors. *J. Neurosci.* 29, 15499–15510.

Perrais, D., Pinheiro, P. S., Jane, D. E., and Mulle, C. (2009). Antagonism of recombinant and native GluK3-containing kainate receptors. *Neuropharmacology* 56, 131–140.

Perrais, D., and Ropert, N. (1999). Effect of zolpidem on miniature IPSCs and occupancy of postsynaptic GABAA receptors in central synapses. *J. Neurosci.* 19, 578–588.

Petralia, R. S., Wang, Y. X., and Wenthold, R. J. (1994). Histological and ultrastructural localization of the kainate receptor subunits, KA2 and GluR6/7, in the rat nervous system using selective antipeptide antibodies. *J. Comp. Neurol.* 349, 85–110.

Pinheiro, P. S., and Mulle, C. (2008). Presynaptic glutamate receptors: physiological functions and mechanisms of action. *Nat. Rev. Neurosci.* 9, 423–436.

Pinheiro, P. S., Perrais, D., Coussen, F., Barhanin, J., Bettler, B., Mann, J. R., et al. (2007). GluR7 is an essential subunit of presynaptic

kainate autoreceptors at hippocampal mossy fiber synapses. *Proc. Natl. Acad. Sci. U.S.A.* 104, 12181–12186.

Price, G. D., and Trussell, L. O. (2006). Estimate of the chloride concentration in a central glutamatergic terminal: a gramicidin perforated-patch study on the calyx of Held. *J. Neurosci.* 26, 11432–11436.

Pugh, J. R., and Jahr, C. E. (2012). NMDA receptor agonists fail to alter release from cerebellar basket cells. *J. Neurosci.* 31, 16550–16555.

Represa, A., Tremblay, E., and Ben-Ari, Y. (1987). Kainate binding sites in the hippocampal mossy fibers: localization and plasticity. *Neuroscience* 20, 739–748.

Rodriguez-Moreno, A., Kohl, M. M., Reeve, J. E., Eaton, T. R., Collins, H. A., Anderson, H. L., et al. (2012). Presynaptic induction and expression of timing-dependent long-term depression demonstrated by compartment-specific photorelease of a use-dependent NMDA receptor antagonist. *J. Neurosci.* 31, 8564–8569.

Rodriguez-Moreno, A., and Sihra, T. S. (2007). Metabotropic actions of kainate receptors in the CNS. *J. Neurochem.* 103, 2121–2135.

Ruiz, A., Campanac, E., Scott, R. S., Rusakov, D. A., and Kullmann, D. M. (2010). Presynaptic GABAA receptors enhance transmission and LTP induction at hippocampal mossy fiber synapses. *Nat. Neurosci.* 13, 431–438.

Ruiz, A., Fabian-Fine, R., Scott, R., Walker, M. C., Rusakov, D. A., and Kullmann, D. M. (2003). GABAA receptors at hippocampal mossy fibers. *Neuron* 39, 961–973.

Rusakov, D. A., and Kullmann, D. M. (1998). Extrasynaptic glutamate diffusion in the hippocampus: ultrastructural constraints, uptake, and receptor activation. *J. Neurosci.* 18, 3158–3170.

Safiulina, V. F., and Cherubini, E. (2009). At immature mossy fibers-CA3 connections, activation of presynaptic GABA(B) receptors by endogenously released GABA contributes to synapses silencing. *Front. Cell. Neurosci.* 3:1. doi: 10.3389/neuro.03.001.2009

Salin, P. A., Scanziani, M., Malenka, R. C., and Nicoll, R. A. (1996). Distinct short-term plasticity at two excitatory synapses in the hippocampus. *Proc. Natl. Acad. Sci. U.S.A.* 93, 13304–13309.

Schmitz, D., Frerking, M., and Nicoll, R. A. (2000). Synaptic activation of presynaptic kainate receptors on hippocampal mossy fiber synapses. *Neuron* 27, 327–338.

Schmitz, D., Mellor, J., Breustedt, J., and Nicoll, R. A. (2003). Presynaptic kainate receptors impart an associative property to hippocampal mossy fiber long-term potentiation. *Nat. Neurosci.* 6, 1058–1063.

Schmitz, D., Mellor, J., and Nicoll, R. A. (2001). Presynaptic kainate receptor mediation of frequency facilitation at hippocampal mossy fiber synapses. *Science* 291, 1972–1976.

Scott, R., Lalic, T., Kullmann, D. M., Capogna, M., and Rusakov, D. A. (2008). Target-cell specificity of kainate autoreceptor and Ca2+-store-dependent short-term plasticity at hippocampal mossy fiber synapses. *J. Neurosci.* 28, 13139–13149.

Scott, R., and Rusakov, D. A. (2006). Main determinants of presynaptic Ca2+ dynamics at individual mossy fiber-CA3 pyramidal cell synapses. *J. Neurosci.* 26, 7071–7081.

Scott, R., and Rusakov, D. A. (2008). Ca2+ stores and use-dependent facilitation of presynaptic Ca2+ signaling. *Proc. Natl. Acad. Sci. U.S.A.* 105, E80. author reply E81.

Segev, I. (1990). Computer study of presynaptic inhibition controlling the spread of action potentials into axonal terminals. *J. Neurophysiol.* 63, 987–998.

Sherwood, J. L., Amici, M., Dargan, S. L., Culley, G. R., Fitzjohn, S. M., Jane, D. E., et al. (2012). Differences in kainate receptor involvement in hippocampal mossy fibre long-term potentiation depending on slice orientation. *Neurochem. Int.* 61, 482–489.

Siegel, S. J., Brose, N., Janssen, W. G., Gasic, G. P., Jahn, R., Heinemann, S. F., et al. (1994). Regional, cellular, and ultrastructural distribution of N-methyl-D-aspartate receptor subunit 1 in monkey hippocampus. *Proc. Natl. Acad. Sci. U.S.A.* 91, 564–568.

Singer, J. H., and Berger, A. J. (1999). Contribution of single-channel properties to the time course and amplitude variance of quantal glycine currents recorded in rat motoneurons. *J. Neurophysiol.* 81, 1608–1616.

Sjostrom, P. J., Turrigiano, G. G., and Nelson, S. B. (2003). Neocortical LTD via coincident activation of presynaptic NMDA and cannabinoid receptors. *Neuron* 39, 641–654.

Stell, B. M., Brickley, S. G., Tang, C. Y., Farrant, M., and Mody, I. (2003). Neuroactive steroids reduce neuronal excitability by selectively enhancing tonic inhibition mediated by delta subunit-containing GABAA receptors. *Proc. Natl. Acad. Sci. U.S.A.* 100, 14439–14444.

Tachibana, M., and Kaneko, A. (1984). gamma-Aminobutyric acid acts at axon terminals of turtle photoreceptors: difference in sensitivity among cell types. *Proc. Natl. Acad. Sci. U.S.A.* 81, 7961–7964.

Takahashi, T., and Momiyama, A. (1991). Single-channel currents underlying glycinergic inhibitory postsynaptic responses in spinal neurons. *Neuron* 7, 965–969.

Trigo, F. F., Chat, M., and Marty, A. (2007). Enhancement of GABA release through endogenous activation of axonal GABA(A) receptors in juvenile cerebellum. *J. Neurosci.* 27, 12452–12463.

Turecek, R., and Trussell, L. O. (2001). Presynaptic glycine receptors enhance transmitter release at a mammalian central synapse. *Nature* 411, 587–590.

Turecek, R., and Trussell, L. O. (2002). Reciprocal developmental regulation of presynaptic ionotropic receptors. *Proc. Natl. Acad. Sci. U.S.A.* 99, 13884–13889.

Tyzio, R., Ivanov, A., Bernard, C., Holmes, G. L., Ben-Ari, Y., and Khazipov, R. (2003). Membrane potential of CA3 hippocampal pyramidal cells during postnatal development. *J. Neurophysiol.* 90, 2964–2972.

Verdier, D., Lund, J. P., and Kolta, A. (2003). GABAergic control of action potential propagation along axonal branches of mammalian sensory neurons. *J. Neurosci.* 23, 2002–2007.

Verheugen, J. A., Fricker, D., and Miles, R. (1999). Noninvasive measurements of the membrane potential and GABAergic action in hippocampal interneurons. *J. Neurosci.* 19, 2546–2555.

Vignes, M., and Collingridge, G. L. (1997). The synaptic activation of kainate receptors. *Nature* 388, 179–182.

Vogt, K. E., and Nicoll, R. A. (1999). Glutamate and gamma-aminobutyric acid mediate a heterosynaptic depression at mossy fiber synapses in the hippocampus. *Proc. Natl. Acad. Sci. U.S.A.* 96, 1118–1122.

Wachowiak, M., and Cohen, L. B. (1999). Presynaptic inhibition of primary olfactory afferents mediated by different mechanisms in lobster and turtle. *J. Neurosci.* 19, 8808–8817.

Wall, P. D. (1958). Excitability changes in afferent fibre terminations and their relation to slow potentials. *J. Physiol.* 142, 1–21.

Wiebe, S. P., and Staubli, U. V. (1999). Dynamic filtering of recognition memory codes in the hippocampus. *J. Neurosci.* 19, 10562–10574.

Ye, J. H., Wang, F., Krnjevic, K., Wang, W., Xiong, Z. G., and Zhang, J. (2004). Presynaptic glycine receptors on GABAergic terminals facilitate discharge of dopaminergic neurons in ventral tegmental area. *J. Neurosci.* 24, 8961–8974.

Zhang, S. J., and Jackson, M. B. (1993). GABA-activated chloride channels in secretory nerve endings. *Science* 259, 531–534.

Zucker, R. S., Kullmann, D. M., and Bennett, M. (1998). "Release of neurotransmitters," in *Fundamental Neuroscience,* eds M. J. Zigmond, F. E. Bloom, S. C. Landis, J. L. Roberts, and L. R. Squire (London: Academic Press), 155–192.

Conflict of Interest Statement: The authors declare that the research was conducted in the absence of any commercial or financial relationships that could be construed as a potential conflict of interest.

Received: 15 October 2012; accepted: 10 December 2012; published online: 09 January 2013.

Citation: Ruiz AJ and Kullmann DM (2013) Ionotropic receptors at hippocampal mossy fibers: roles in axonal excitability, synaptic transmission, and plasticity. Front. Neural Circuits ***6****:112. doi: 10.3389/fncir.2012.00112*

frontiers in
NEURAL CIRCUITS

ORIGINAL RESEARCH ARTICLE
published: 16 November 2012
doi: 10.3389/fncir.2012.00085

Competition from newborn granule cells does not drive axonal retraction of silenced old granule cells in the adult hippocampus

Carla M. Lopez[1], Kenneth A. Pelkey[1]*, Ramesh Chittajallu[1], Toshiaki Nakashiba[2], Katalin Tóth[3], Susumu Tonegawa[2] and Chris J. McBain[1]

[1] Program in Developmental Neurobiology, Eunice Kennedy-Shriver National Institute of Child Health and Human Development, National Institutes of Health, Bethesda, MD, USA
[2] RIKEN-MIT Center for Neural Circuit Genetics and The Picower Institute for Learning and Memory, Massachusetts Institute of Technology, Cambridge, MA, USA
[3] Department of Psychiatry and Neuroscience, Quebec Mental Health Institute, Université Laval, Quebec City, QC, Canada

Edited by:
Peter Jonas, Institute of Science and Technology, Austria

Reviewed by:
Peer Wulff, University of Aberdeen, UK
Ayumu Tashiro, Nanyang Technological University, Singapore

***Correspondence:**
Kenneth A. Pelkey, Porter Neuroscience Research Center, 35 Lincoln Drive, MSC 3715, Bethesda, MD 20892-3715, USA.
e-mail: pelkeyk2@mail.nih.gov

In the developing nervous system synaptic refinement, typified by the neuromuscular junction where supernumerary connections are eliminated by axon retraction leaving the postsynaptic target innervated by a single dominant input, critically regulates neuronal circuit formation. Whether such competition-based pruning continues in established circuits of mature animals remains unknown. This question is particularly relevant in the context of adult neurogenesis where newborn cells must integrate into preexisting circuits, and thus, potentially compete with functionally mature synapses to gain access to their postsynaptic targets. The hippocampus plays an important role in memory formation/retrieval and the dentate gyrus (DG) subfield exhibits continued neurogenesis into adulthood. Therefore, this region contains both mature granule cells (old GCs) and immature recently born GCs that are generated throughout adult life (young GCs), providing a neurogenic niche model to examine the role of competition in synaptic refinement. Recent work from an independent group in developing animals indicated that embryonically/early postnatal generated GCs placed at a competitive disadvantage by selective expression of tetanus toxin (TeTX) to prevent synaptic release rapidly retracted their axons, and that this retraction was driven by competition from newborn GCs lacking TeTX. In contrast, following 3–6 months of selective TeTX expression in old GCs of adult mice we did not observe any evidence of axon retraction. Indeed ultrastructural analyses indicated that the terminals of silenced GCs even maintained synaptic contact with their postsynaptic targets. Furthermore, we did not detect any significant differences in the electrophysiological properties between old GCs in control and TeTX conditions. Thus, our data demonstrate a remarkable stability in the face of a relatively prolonged period of altered synaptic competition between two populations of neurons within the adult brain.

Keywords: neurogenesis, mossy fibers, hippocampal, activity-dependent circuit refinement, tetanus toxin, Moloney virus

INTRODUCTION

The subgranular zone of the hippocampal dentate gyrus (DG) represents one of only two privileged sites within the mammalian central nervous system where adult neurogenesis occurs, providing a continuous source of newborn granule cells (GCs) throughout postnatal life (Deng et al., 2010; Ming and Song, 2011). Newborn GCs initially exhibit molecular, anatomical, and physiological properties distinct from their mature counterparts; however, within approximately 4–8 weeks of maturation newborn GCs appear phenotypically indistinguishable from the preexisting mature GC cohort (Laplagne et al., 2006; Ge et al., 2008). Thus, in adult mice the mature GC population comprises both embryonically/early postnatal generated GCs as well as postnatally derived GCs beyond roughly 2 months of age (hereafter referred to as old GCs). Whereas active adult neurogenesis was once widely regarded as a simple neuronal replacement mechanism, recent studies indicate that newborn GCs make unique contributions to hippocampal-dependent learning and episodic memory. Specifically, newborn GCs critically participate in the formation of distinct memories of similar events by encoding unique representations of the spatial relationships of a given experience. This "pattern separation" function of the hippocampus is essential for discriminating between similar episodic memories with overlapping features and is compromised or enhanced in animals with disrupted or augmented postnatal neurogenesis respectively (Clelland et al., 2009; Creer et al., 2010; Sahay et al., 2011; Nakashiba et al., 2012; Tronel et al., 2012).

To mediate pattern separation newborn GCs must become synaptically integrated into a preexisting hippocampal network. In the developing nervous system synapse formation and refinement are activity-dependent processes and competition between afferents for common postsynaptic targets ultimately dictates mature circuit innervation patterns (Katz and Shatz, 1996; Sanes and Lichtman, 1999; Yu et al., 2004; Hashimoto and Kano, 2005). This raises the possibility that newborn GCs must compete with old GCs to receive afferent input from the entorhinal cortex (EC) and to innervate postsynaptic targets such as CA3 pyramidal cells when integrating into the DG-CA3 circuit (Toni et al., 2007, 2008; Bergami and Berninger, 2012). Consistent with this possibility a study in developing animals (2–4 weeks of age) found that synaptic silencing of old GCs by selective expression of tetanus toxin (TeTX) light chain promoted retraction of their mossy fiber (MF) axons in a manner driven by competition from newborn GCs that continued to transmit to their postsynaptic targets (Yasuda et al., 2011). Moreover, following MF retraction the population of TeTX expressing inactive GCs began to die off beyond postnatal day 25 indicating that competition from newborn GCs may ultimately dictate overall survival of old GCs during the first postnatal month (Yasuda et al., 2011). Whether such competition-based axon refinement and cell survival occurs in the adult DG was not determined. However, in a recent investigation examining the functional roles of old GCs and adult generated newborn GCs in learning and memory we generated a transgenic line of mice that conditionally/inducibly express TeTX selectively in old GCs beyond 4–6 weeks of age (DG-TeTX mice) and did not observe any evidence of cell death or axon retraction in the silenced GCs (Nakashiba et al., 2012). Indeed electrophysiological experiments in tissue from control and activated DG-TeTX adult mice indicated comparable MF axon densities, inconsistent with significant axon retraction and cell death in silenced GCs [(Nakashiba et al., 2012) and see **Figure 1**]. Moreover, the full recovery of MF transmission in activated DG-TeTX mice after turning-off TeTX expression (i.e., the transgenic strategy employed allows for inducible and fully reversible synaptic silencing) further argues against significant axon retraction and cell death within the synaptically silenced GC cohort (Nakashiba et al., 2012).

Here we specifically examined the impact of prolonged synaptic silencing on the properties of old GCs in adult mice using a combination of electrophysiology, immunocytochemistry, and electron microscopy to compare activated DG-TeTX mice and their control littermates. Our data reveal a remarkable stability in the morphological and electrophysiological properties of old GCs following 3–6 months of synaptic silencing. Thus, in contrast to developing systems, neither the survival of old GCs nor

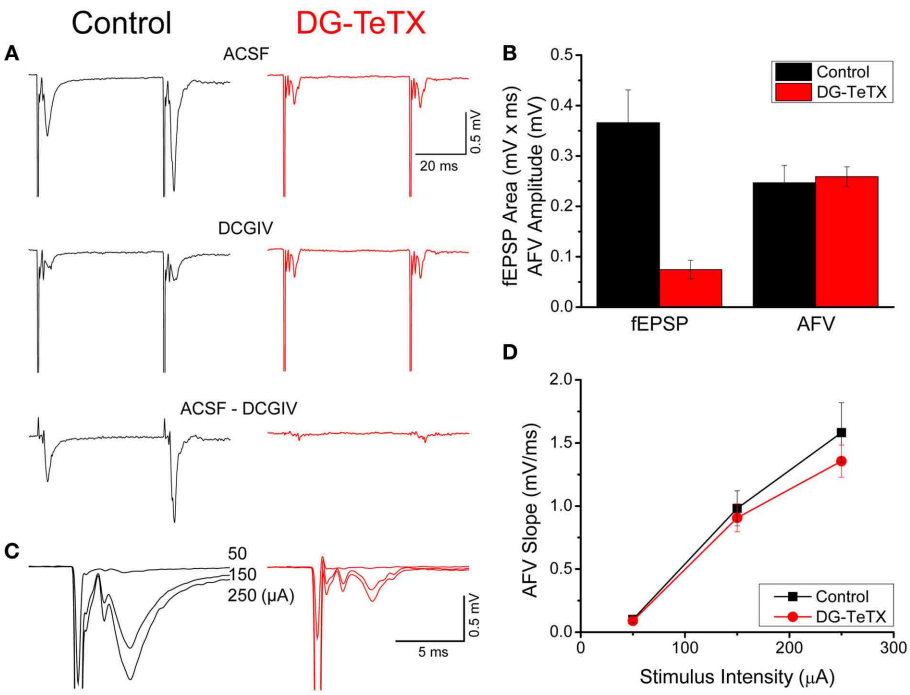

FIGURE 1 | Impaired MF-CA3 transmission but normal MF excitability in activated DG-TeTX mice. (A) Representative fEPSP waveforms recorded in CA3 stratum lucidum evoked by stimulation in the DG GC layer obtained in control and activated DG-TeTX (DG-TeTX) mice in control (ACSF, upper traces) and DCGIV (1 μM) containing ACSF (DCGIV, middle traces). Traces are the average of 6 consecutive individual sweeps obtained in each condition (scale bars 20 ms/0.5 mV). The pure MF-CA3-mediated fEPSP is obtained by digital subtraction of the DCGIV condition waveform from the control condition waveform (bottom traces). **(B)** Group data bar chart summary of the MF-CA3 fEPSP areas and AFV amplitudes observed in control ($n = 10$ slices from 7 animals) and DG-TeTX ($n = 7$ slices from 5 animals) mice. **(C)** Representative fEPSP waveforms from control and DG-TeTX mice obtained at the three different stimulus intensities indicated (traces are the average of 6 events obtained at each stimulus intensity, scale bars 5 ms/0.5 mV). **(D)** AFV input-output functions for control ($n = 8$ slices from 5 mice) and activated DG-TeTX mice ($n = 10$ slices, from 5 mice).

maintenance of their MF projections are dictated by output-based competition with newborn GCs in the adult brain.

MATERIALS AND METHODS

All procedures relating to animal care and treatment conformed to Institutional and NIH guidelines.

GENERATION OF MICE

DG-TeTX mice maintained in a C57BL/6 genetic background harbor three transgenes; POMC-Cre (TG1), αCamKII-loxP-STOP-loxP-tTA (Tg2), and TetO-TeTX (Tg3-TeTX) as previously described in Nakashiba et al. (2012). To obtain DG-TeTX mice, heterozygous Tg1 × Tg3 – TeTX (*POMC-Cre/+, TetO-TeTX/+*) mice were crossed to generate homozygous double transgenic mice (*POMC-Cre/POMC-Cre, TetO-TeTX/TetO-TeTX*). Male homozygous mice were then bred with the female Tg2 (*αCamKII-loxP-STOP-loxP-tTA/+*). Half of the resultant progeny was thus heterozygous triple-transgenic mice (*POMC-Cre/+, TetO-TeTX/+, αCamKII-loxP-STOP-loxP-tTA/+*), herein referred to as DG-TeTX mice. The other half of the progeny was thus heterozygous double transgenic mice (*POMC-Cre/+, TetO-TeTX/+, +/+*), which did not express TeTX and therefore served as control mice. Breeding pairs and their progeny for experiments were maintained on a Dox diet, and then all experiments were performed on tissue from adult mice (3–8 months old) maintained on a Dox free diet for at least 2 months to induce TeTX expression in DG-TeTX mice.

VIRUS GENERATION AND INJECTION

We used a Moloney viral vector to express GFP obtained from Dr. Carlos Lois (M.I.T.). Moloney viral particles were produced as previously described in Nakashiba et al. (2012). Viral titers were $\sim 10^9$ infectious units/ml. DG-TeTX mice and their control littermates (12–16 weeks old) were anesthetized with avertin and stereotaxically injected at two sites targeting the right DG (0.9 μl of viral aliquot per site). The stereotaxic coordinate for the first site was 2.06 mm posterior from bregma, 1.25 mm lateral from the midline, and 1.75 mm ventral from the brain surface. The second site was 2.70 mm posterior from bregma, 2.00 mm lateral from the midline, and 1.75 mm ventral from the brain surface. The scalp incision was sutured, and postinjection analgesics were given to aid recovery (1.5 mg/kg, Metacam).

IMMUNOHISTOCHEMISTRY

For immunohistochemical visualization of the stratum lucidum and adult-born GFP + GCs, mice were perfused transcardially using a 0.1 M PBS solution containing 4% paraformaldehyde followed by overnight postfixation at 4°C. Brains were then cryoprotected in 30% sucrose/PBS at 4°C, sliced to 50 μm thickness using a microtome. After washing in PBS, free-floating sections were blocked for 2 h at room temperature in a PBS/0.5% Triton X-100/1% BSA/10% normal goat serum (NGS) solution before being incubated overnight at 4°C with anti-calbindin (mouse, 1:1000; Sigma), and anti-GFP (chicken, 1:1000, Aves) antibodies. Primary antibodies were diluted in a PBS/0.5% Triton X-100/1% BSA/10% NGS (BGT-PBS). Slices were washed with BGT-PBS before being incubated for 2 h at room temperature with secondary antibodies diluted in BGT-PBS. After washing in PBS, slices were mounted on Superfrost Plus microscope slides (Fisherbrand, Hampton, NH). Secondary antibodies were used in the following concentrations: goat anti-chicken Alexa Fluor 488 and goat anti-mouse Alexa Fluor 555 (1:1000; Invitrogen). Although the transgene construct for the Tg3-TeTX was initially generated as a fusion protein with GFP, we failed to detect any GFP-TeTX fusion protein in the DG-TeTX mice with this immunostaining procedure (data not shown). Thus, signals detected by anti-GFP here are mostly derived from GFP introduced by the Moloney virus. Fluorescent images were captured using a Zeiss LSM 780 inverted confocal microscope (Zeiss, Germany). To quantify the extent of old GC MF projections into CA3 in individual sections we measured the length of a curved line tracing the GFP signal through stratum lucidum toward CA2 from a straight line drawn connecting the ends of the upper and lower blades of the DG (Zhao et al., 2006). A total of 3–12 sections per animal from similar levels of the hippocampus were examined.

ELECTRON MICROSCOPY

Animals used for the electron microscopy were deeply anesthetized and transcardially perfused first with a buffered sodium sulphide solution (12 g $Na_2S.9H_2O$ and 12 g $NaH_2PO_4.H_2O$ in 1000 ml of distilled water, pH 7.4; 0.05 M) for 1 min, then with a buffered 3% glutaraldehyde solution in 0.12 M PBS (pH 7.4) for 20 min, and finally with the sodium sulphide solution again for 15 min. Brains were removed from the skull, post-fixed in the 3% buffered glutaraldehyde solution for 2 h and sectioned with a Vibratome at 50 μm. Free-floating sections were washed with Tris buffer (pH 7.4) for 5 min periods in order to eliminate adsorbed phosphate ions, which would react with silver ions, causing an unwanted precipitation. Thereafter, sections were placed in the physical developer containing sodium tungstate as protective colloid, hydroquinone as reducing agent, sodium acetate and acetic acid to adjust the pH and silver nitrate for further details see Seress and Gallyas (2000). The process of development was stopped by placing the sections into 1% sodium thiosulfate for 1 min. Next, the sections were washed with Tris buffer for 5 min, then osmificated with 1% OsO_4 for 1 h, dehydrated, and flat-embedded in Durcupan according to routine electron-microscopic procedure. After microscopic examination, the area of interest was cut, re-embedded, and thin sectioned. The resulting thin sections were then stained with uranyl acetate and lead citrate and imaged using a Tecnai electron microscope.

Quantification

Black particles indicating zinc were used to identify MF terminals. Quantification of area measurements was done by an observer who was blinded to the genotype of the samples. Surface area measurements were done manually using Fiji software.

In Vitro SLICE PHYSIOLOGY

Hippocampal slices (300 μm thick) were prepared from 3- to 8-month-old DG-TeTX mice and their control littermates. Mice were anesthetized with isoflurane, and brains were dissected in

partial sucrose artificial cerebrospinal fluid (ACSF) containing (in mM): 80 NaCl, 3.5 KCl, 1.25 H_2PO_4, 25 $NaHCO_3$, 4.5 $MgSO_4$, 0.5 $CaCl_2$, 10 glucose and 90 sucrose, equilibrated with 95% O_2 and 5% CO_2. The brains were hemisected, and transverse slices were cut using a VT-1000S vibratome (Leica Microsystems). The slices were then incubated in the above solution at 35°C for 30 min and then kept at room temperature in the same solution until use.

For extracellular field recordings, slices were transferred to a recording chamber and perfused (3–5 ml/min, 32–35°C) with ACSF composed of (in mM): 130 NaCl, 24 $NaHCO_3$, 3.5 KCl, 1.25 NaH_2PO4, 2.5 $CaCl_2$, 1.5 $MgCl_2$, 10 glucose, 0.05 ± dl-AP5, and 0.01 bicuculline methobromide, saturated with 95% O_2 and 5% CO_2, pH 7.4. Field excitatory postsynaptic potentials (fEPSPs) were recorded using electrodes (2–3 MΩ) pulled from borosilicate glass (World Precision Instruments) filled with oxygenated ACSF and connected to a Multiclamp 700A amplifier (Axon Instruments, Foster City, CA). Mossy fiber to CA3 pyramid (MF→CA3) fEPSPs were recorded by placing the recording electrode in stratum lucidum and evoking synaptic responses at 0.1 Hz by stimulation (150-μs duration, 0.05- to 0.25-mA intensity) via a constant-current isolation unit (A360, World Precision Instruments, Sarasota, FL) connected to glass electrode filled with oxygenated ACSF placed in the DG cell layer. Data acquisition (filtered at 3 kHz and digitized at 20 kHz) and analysis were performed using a PC equipped with pClamp 9.2 software (Axon Instruments).

MF afferent fiber volley (AFV) input-output (I/O) relations were obtained by stepping the stimulus intensity from 0.05 mA to 0.25 mA. Then fEPSPs monitored at a single stimulus intensity that gave AFVs of between 0.2 and 0.3 mVs were obtained in control ACSF and again in the presence of DCGIV (2 μM, Tocris). Averaged waveforms (10 consecutive sweeps) obtained in DCGIV were digitally subtracted from the corresponding averaged waveform obtained in control ACSF to obtain pure MF→CA3 fEPSPs (Kamiya et al., 1996). For analysis, the area of the pure MF→CA3 fEPSPs was determined in the first 2.5 ms after the end of the AFV determined prior to the digital subtraction. Area was used rather than peak or slope because MF→CA3 fEPSPs have complicated waveforms that may confound peak or slope measurements, particularly in the activated DG-TeTX mice (Henze et al., 2000; Nakashiba et al., 2012). AFV amplitudes and slopes were measured directly from non-DCGIV-subtracted traces.

To characterize the electrophysiological properties of individual mature GCs we performed whole-cell patch clamp recordings in slices prepared from 4 to 6 month old mice 3–4 weeks after Moloney virus injection targeting GFP negative GCs near the inner molecular layer. Slices were perfused (3–5 ml/min) with extracellular solution composed of (in mM) 130 NaCl, 24 $NaHCO_3$, 3.5 KCl, 1.25 NaH_2PO_4, 2.5 $CaCl_2$, 1.5 $MgCl_2$, and 10 glucose, saturated with 95% O_2 and 5% CO_2 (pH 7.4). Recordings were performed at 32–34°C with electrodes (3–5 MΩ) pulled from borosilicate glass (World precision instruments) filled with either (in mM) 150 K-gluconate, 3 $MgCl_2$, 0.5 EGTA, 2 MgATP, 0.3 Na2GTP, and 10 HEPES plus 2 mg/ml biocytin for characterization of membrane properties and LTP experiments or 130 CsCl, 8.5 NaCl, 0.5 EGTA, 4 MgATP, 0.5 Na2GTP, 5 QX-314Cl, and 10 HEPES for basic postsynaptic current (excitatory and inhibitory) characterization. Whole-cell patch clamp recordings were made using a Multiclamp 700A or 700B amplifier (Molecular Devices, Sunnyvale, CA) in current- or voltage clamp-mode. The signals were filtered at 3 kHz (Bessel filter; Frequency Devices, Haverhill, MA) and digitized at 20 kHz (Digidata 1322A or 1440A and pClamp 9.2 or 10.2 Software; Molecular Devices). Recordings were not corrected for a liquid junction potential.

The resting membrane potential was noted immediately upon achieving a whole-cell configuration. The membrane potential was then biased to −60 mV by constant current injection. The input resistance (R_m) was measured using a linear regression of voltage deflections (±15 mV from the resting potential, ∼60 mV) in response to 2-s current steps of 6–10 different amplitudes in 5-pA steps. The membrane time constant (Tau_m) was calculated from the mean responses to 20 successive hyperpolarizing current pulses (−20 pA; 400 ms) and was determined by fitting voltage responses with a single exponential function. Action potential (AP) threshold was defined as the voltage at which the slope trajectory reached 10 mV/ms and AP amplitude was defined as the difference in membrane potential between the threshold and the peak. Spike half-width was defined as the duration of the AP at half of the determined amplitude. These properties were measured for the first two APs elicited by a depolarizing 800 ms current pulse of amplitude that was just sufficient to bring the cell to threshold for AP generation. Firing frequency was calculated from the number of spikes observed during the 800 ms window during a current injection twice this amount. All intrinsic electrophysiological parameters were measured in pClamp or using procedures written in Igor 6 (Wavemetrics, Portland, OR).

Spontaneous inhibitory postsynaptic currents (sIPSCs) were pharmacologically isolated by the addition of DNQX (10 μM) and dl-AP5 (50 μM) to the perfusing medium and recorded as inward currents at a holding potential of −70 mV with the chloride reversal potential set to 0 mV (CsCl-based internal). Events were detected using a template matching algorithm and analyzed in pClamp. At the end of the recordings, bicuculline (10 μM) was added to the perfusing medium to determine the tonic GABAergic current. Spontaneous and evoked excitatory postsynaptic currents (s/eEPSCs) were pharmacologically isolated by the addition of bicuculline (10 μM) to the perfusing medium. sEPSCs were recorded at a holding potential of −70 mV and detected by a template matching strategy and analyzed in pClamp. eEPSCs were elicited at 0.1 Hz as paired pulses (20 Hz) by low-intensity microstimulation (100 μs duration; 10–30 μA intensity) via a constant-current isolation unit (A360, World Precision Instruments, Sarasota, FL) connected to a patch electrode filled with oxygenated extracellular solution placed in the middle molecular layer. The AMPA receptor-mediated component was determined from the peak of the eEPSC (the first event of paired pulses) observed at a holding potential of −70 mV, and the NMDA receptor-mediated component was measured 25 ms after the peak at a holding potential of +40 mV. Paired pulse ratios (PPRs) were calculated as the mean P2/mean P1, where P1 was the amplitude of the first evoked current and P2 was the amplitude of the second synaptic current obtained for consecutive individual traces.

For LTP experiments, bicuculline was added to the perfusing medium, and AMPAR-mediated EPSCs were monitored in voltage clamp mode ($V_h = -70$ mV) before (2–3 min) and after (15–20 min) LTP induction with a theta burst stimulation (TBS) protocol (Schmidt-Hieber et al., 2004). TBS was performed in current clamp mode with the membrane potential biased to −60 mV via constant current injection. TBS consisted of 10 trains of stimuli at 5 Hz, with each train consisting of 10 stimuli at 100 Hz. The duration of each train was paired with a postsynaptic depolarizing current injection of 300–400 pA that was sufficient to evoke a burst of postsynaptic APs. This was repeated four times at a frequency of 0.1 Hz, after which the recording configuration was switched back to voltage clamp mode, and AMPAR-mediated EPSCs were monitored as described above for a minimum of 20 min post-TBS.

For all electrophysiological parameters tested each cell was treated as an independent observation. Data are presented as means ± SEMs unless otherwise indicated. Data sets were subjected to a Normality Test and statistical significance was assessed using parametric (Student's *t*-test for normally distributed data sets) or nonparametric (Mann–Whitney test for data sets not normally distributed) analyses as appropriate.

For anatomical reconstruction of recorded cells after biocytin filling during whole-cell recordings, slices were fixed with 4% paraformaldehyde and stored at 4°C then permeabilized with 0.3% Triton X-100 and incubated with Alexa Fluor 555-conjugated streptavidin (Molecular Probes). Resectioned slices were mounted on gelatin-coated slides using Mowiol mounting medium. Cells were visualized using epifluorescence microscopy (Olympus AX70) and images for representative examples were obtained with a Leica TCS SP2 RS Confocal Microcope. Frames of maximum projection images were created from stacks (2 μm steps) and stitched together in Adobe Photoshop.

RESULTS

To examine the role of activity and competition in regulating hippocampal GC anatomy and function we compared several features of old GCs from adult activated triple transgenic DG-TeTX mice (Nakashiba et al., 2012) with those from control littermate adult mice (Control). In the DG-TeTX mice, TeTX expression is induced selectively and comprehensively in old GCs (beyond 4–6 weeks of age) when the mice are kept on a doxycycline (Dox) free diet, thus, effectively silencing the synaptic output of the vast majority of GCs by preventing presynaptic vesicle fusion (Nakashiba et al., 2012). In contrast, due to the delayed onset of αCamKII promoter activity (see methods) newborn GCs in DG-TeTX mice cannot be induced to express TeTX within the first 4–6 weeks after their genesis (Nakashiba et al., 2012) leaving them release competent and potentially placing them at a competitive advantage within the hippocampal circuit. Consistent with our prior observations, activated DG-TeTX mice exhibited severely impaired MF transmission as revealed by an almost complete loss of MF-CA3 fEPSPs in DG-TeTX mice kept on a Dox free diet for 2–3 months (**Figures 1A,B**). It is important to note that although young GCs remain release competent their potential contribution to the MF-CA3 fEPSP is minimal due to their low numbers [<5% of the entire GC population, (Imayoshi et al., 2008)] and the sparse nature of GC release sites (Amaral and Dent, 1981; Claiborne et al., 1993; Henze et al., 2000). Despite deficiencies in the fEPSPs of activated DG-TeTX mice, MF excitability was comparable to control animals as indicated by examination of the MF AFVs (**Figure 1B**). Indeed I/O functions of AFVs in activated DG-TeTX mice revealed no significant differences with those obtained from control mice (**Figures 1C,D**). Because the AFV reflects the simultaneous activation of multiple tightly packed axons near the recording electrode its magnitude serves as a proxy measure for the density of MF axons within stratum lucidum where the recordings are made. While our experiments do not allow us to determine an absolute value of fiber density the comparable I/O curves obtained in control and DG-TeTX mice indicate similar MF densities providing initial evidence that old GCs silenced in activated DG-TeTX mice remain healthy and do not retract their MF axons from stratum lucidum.

Next we probed for evidence of competition-based MF retraction by examining individually labeled axons of silenced GCs. To label individual GCs we injected a genetically modified Moloney viral vector encoding GFP into the DG of control and activated DG-TeTX mice to specifically infect a small cohort of newborn GCs generated at or shortly after the time of viral infection (Van Praag et al., 2002; Tashiro et al., 2006; Zhao et al., 2006). Immediately following viral injection the animals were placed on a Dox free diet and allowed to survive for an additional 3–6 months providing sufficient time for the labeled cohort of cells to enter the old GC population and become silenced in the mutant mice by induction of TeTX as the cells aged beyond 4–6 weeks. Individual GFP labeled MFs were found to project into CA3 stratum lucidum in both control and activated DG-TeTX mice with no obvious signs of axon retraction in the silenced fibers (**Figure 2**). Indeed in both lines of mice GFP labeled fibers with regularly spaced MF boutons (MFBs) coursed through the entire CA3 stratum lucidum region, revealed by co-staining for calbindin (**Figure 2A**), terminating at the distal junction with CA2 revealed by co-staining for the CA2 pyramidal cell marker RGS14 [**Figure 2B**; (Lee et al., 2010)]. Quantification of the extent of old GC MF projections into CA3 by measuring the distance from the hilar border to the farthest projections of GFP labeled fibers (Zhao et al., 2006) revealed no significant differences between control (1220 ± 31 μm, $n = 4$ mice) and activated DG-TeTX mice (1271 ± 51 μm, $n = 5$ mice; $p = 0.4$, *t*-test). Upon closer inspection at higher magnification typical MFBs with associated filopodial extensions were evident (**Figure 2C**) in control and mutant animals, but we found no evidence of axon degeneration such as retraction bulbs or axosomes that were previously reported for silenced MFs in young developing mice (Yasuda et al., 2011).

The persistence of MFBs along the axons of old GCs in activated DG-TeTX mice suggests that the silenced terminals maintain structural contact with postsynaptic targets despite their lack of vesicle-mediated transmission consistent with the ability to recover MF-CA3 transmission when DG-TeTX mice are re-treated with Dox (Nakashiba et al., 2012). To examine the effects of synaptic silencing on the ultrastructural features of MFBs and associated postsynaptic elements we compared terminals in

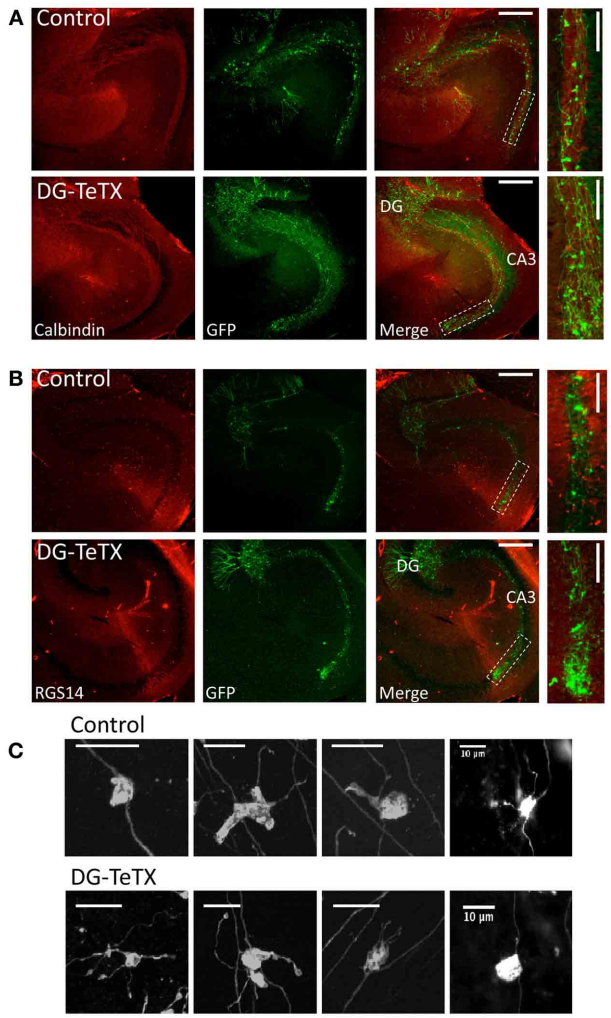

FIGURE 2 | Normal MF projection throughout CA3 stratum lucidum in activated DG-TeTX mice. (A) Representative images of hippocampal sections obtained from control (upper panels) and activated DG-TeTX mice (lower panels) stained for calbindin (red) to label stratum lucidum and GFP (green) to label silenced old GCs (at least 3 months of age) that were infected with GFP encoding Moloney Virus at their time of genesis (scale bars 300 μm). Boxed region in the merged images indicate regions that were digitally magnified in images at the far right (scale bars 100 μm). **(B)** Similar to **(A)** except that the sections were stained for GFP (green) and RGS14 (red) to label CA2 pyramidal cells demarcating the distal boundary of CA3. **(C)** Images of representative GFP labeled MFBs from old GCs in sections from control (upper panels) and activated DG-TeTX mice (lower panels). Similar observations were obtained in a total of 5 mutant and 4 control mice examined 3–6 months after viral infection and maintained under Dox free conditions for this entire period (mutant mice were examined at 100, 127, 182, 182, and 178 days postinfection and control mice were examined in parallel at 100, 127, 189, and 162 days postinfection).

control and activated DG-TeTX mice using electron microscopy. To easily identify MFBs, sections were neoTimm stained to reveal the zinc rich MF projections (Haug, 1967; Ibata and Otsuka, 1969; Amaral and Dent, 1981). Importantly, at the light microscopy level a strong zinc signal was clearly evident throughout the entire stratum lucidum in hippocampal sections from both control and activated DG-TeTX mice consistent with maintained MF projections to distal CA3 in silenced GCs (**Figures 3A,B**). At the EM level typical zinc labeled MF terminals with multiple release sites and associated postsynaptic densities were readily encountered in tissue from both control and activated DG-TeTX mice with no evidence of axon retraction or degeneration (**Figures 3C–F**). As expected from our analyses of AFVs (**Figures 1B–D**), MF density in randomly selected areas of the stratum lucidum was similar in control and activated DG-TeTX mice with ∼10% of the total surface identified as MF terminals in both samples (**Figure 3G**; $8.4 \pm 1.2\%$ in control; $8 \pm 0.87\%$ in DG-TeTX samples). Moreover, the density of MF synaptic contacts, calculated from the total length of synaptic specializations formed by a single terminal and the surface area of the bouton, was comparable between control and DG-TeTX mice suggesting that silenced terminals maintain a physical interaction with target postsynaptic elements (**Figure 3H**; $0.22 \pm 0.03\,\mu m$ synapse/μm^2 terminal and $0.2 \pm 0.03\,\mu m$ synapse/μm^2 terminal in control and DG-TeTX samples, respectively). Surprisingly, despite the deficiency in VAMP2-mediated release, vesicle density in terminals of DG-TeTX mice was similar to that in control terminals (**Figure 3I**; 189 ± 8 vesicles/μm^2 in control and 193 ± 12 vesicles/μm^2 in DG-TeTX samples). Closer examination of synaptic vesicles revealed that while vesicle density was similar between the two genotypes, vesicle size distributions were not (**Figures 3J,K**). In control tissue vesicle size showed little variability, and the average vesicle area was $1.47 \times 10^{-3} \pm 2.02 \times 10^{-5}\ \mu m^2$ (corresponding to 42 nm vesicle diameter). In DG-TeTX samples the distribution of vesicle size was larger with a noticeable skew toward larger vesicles ($2.24 \times 10^{-3} \pm 7.22 \times 10^{-5}\ \mu m^2$). Although the limited number of mice examined at the ultrastuctural level precludes statistical comparisons between the genotypes our observations generally confirm that MF axons of old silenced GCs remain stable projecting throughout CA3 stratum lucidum. Moreover, the maintenance of an anatomically defined synaptic contact by silenced terminals in activated DG-TeTX mice suggests that the recovery of transmission upon reversal of TeTX expression by treatment with Dox does not reflect a massive rewiring of the circuit but rather a simple resumption of communication at preexisting connections.

Our data to this point indicate that TeTX expressing GCs maintain stable electrically active MF projections throughout the DG-CA3 circuit. However, it remains possible that the silenced old GCs undergo other homeostatically induced changes due to altered participation within the circuit (Desai, 2003; Davis, 2006; Turrigiano, 2012). In our previous study we did not detect any differences in the electrophysiological properties of young (3–4 week old) adult generated GCs in control and activated DG-TeTX mice (Nakashiba et al., 2012). In both lines of mice the newborn cells exhibited immature intrinsic membrane properties and excitatory/inhibitory postsynaptic response profiles typical for cells of their age indicating that being placed at a competitive advantage in activated DG-TeTX mice did not promote enhanced maturation of these physiological properties of adult generated GCs (Nakashiba et al., 2012). However, whether any electrophysiological changes occurred in the synaptically silenced old GCs was not previously tested. Thus, in a final series of experiments

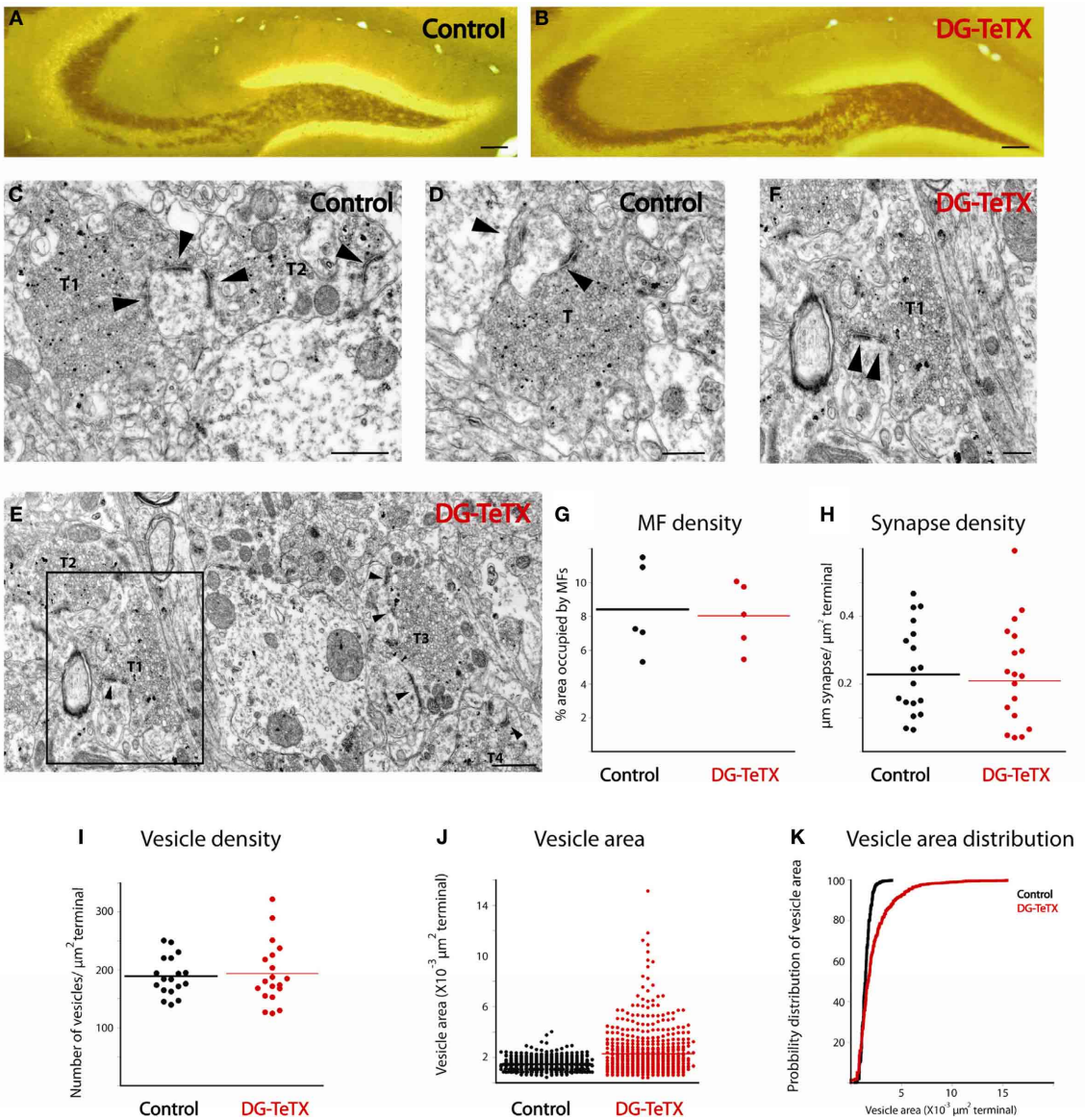

FIGURE 3 | Ultrastructural comparison of active and silenced MF terminals. (A,B) Mossy fiber tracks in representative sections from control **(A)** and DG-TeTX **(B)** mice are labeled with neoTimm staining. **(C–F)** Representative electron micrographs demonstrate that mossy fiber terminals (T) form multiple synaptic contacts (arrowheads) with their postsynaptic targets in control **(C,D)** and in DG-TeTX **(E,F)** mice. Zinc-labeled terminals (T1–T3) are abundant in the stratum lucidum of DG-TeTX samples **(E)**, T1 is shown in panel F at higher magnification where the high degree of variability in vesicle size is clearly evident. **(G)** The density of mossy fibers measured as a ratio of the percentage of surface area covered by zinc-positive large presynaptic specializations was similar in the stratum lucidum of control and DG-TeTX animals ($n = 5$ sections per animal, 1 mouse per genotype). **(H,I)** Synapse density (**H**, $n = 20$ terminals examined across the 5 sections for each genotype) and vesicle density (**I**, $n = 20$ terminals examined across the 5 sections for each genotype) was also comparable between the two groups. **(J)** Plots of vesicle area reveal a typical uniform vesicle size in control samples but a higher degree of variability in DG-TeTX mice. **(K)** Cumulative probability distribution of vesicle size measurements plotted in **(J)** revealing the skew toward larger vesicles in DG-TeTX mice ($n = 620$ vesicles in 20 terminals across 5 sections from 1 mouse per genotype). Scale bars: (**A,B**: 200 µm, **C–E**: 400 nm, **F**: 800 nm).

we performed whole-cell patch clamp recordings targeting old GCs in acute hippocampal slices from 4–6 month old control and activated DG-TeTX mice to determine if long-term silencing of synaptic output precipitates any changes in basic membrane or postsynaptic properties of GCs. No significant differences were observed between old GCs from the two genotypes for any of the basic membrane and spiking properties assayed including resting membrane potential, input resistance, membrane time constant, and spike frequency/duration (**Figures 4A–D** and **Table 1**, p-values ranged from 0.1 to 1.0). In addition silenced and control GCs received similar levels of excitatory and inhibitory drive as assessed by monitoring spontaneous glutamatergic and

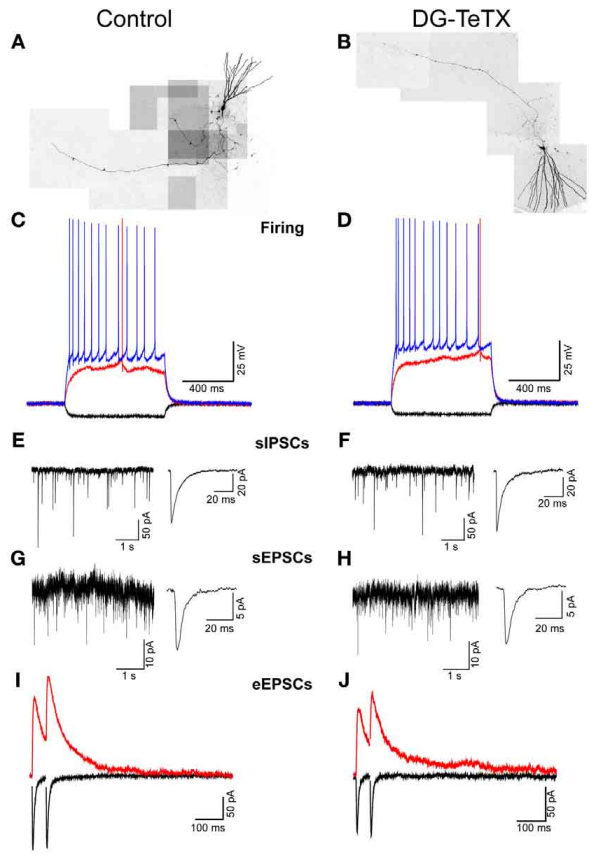

FIGURE 4 | Prolonged blockade of the synaptic output from old GCs does not alter their electrophysiological characteristics. **(A,B)** Composite images of representative old GCs recorded in slices from control **(A)** and activated DG-TeTX **(B)** mice. **(C,D)** Traces from representative recordings obtained in old GCs of control **(C)** and activated DG-TeTX mice **(D)** showing membrane responses to hyperpolarizing (−50 pA; black traces), just threshold level depolarizing (red traces) and twice threshold level depolarizing (blue traces) current pulses. **(E–H)** Representative gap-free traces of pharmacologically isolated spontaneous $GABA_A$ receptor- and AMPA receptor-mediated IPSCs **(E,F)** and EPSCs **(G,H)** with ensemble averages (right traces) obtained in old GCs of control **(E,G)** and DG-TeTX **(F,H)** mice. **(I,J)** Paired pulse (50 ms inter-stimulus interval) perforant path-evoked EPSCs at a holding potential of −70 mV (black traces, to monitor the AMPAR-mediated component) and at a holding potential of +40 mV (red traces, to reveal the NMDAR-mediated component) in representative recordings from old GCs in control **(I)** and DG-TeTX **(J)** mice.

Table 1 | Summary of electrophysiological properties of mature granule cells.

	Control mice	DG-TeTX mice
Intrinsic membrane properties	**($n = 14$ cells from 5 mice)**	**($n = 15$ cells from 4 mice)**
Resting potential (mV)	−71 ± 1	−68 ± 2
Input resistance (MΩ)	199 ± 14	225 ± 27
Time constant (ms)	23 ± 2	19 ± 2
Membrane capacitance (pF)	117 ± 9	94 ± 8
Frequency at 2× threshold (Hz)	23 ± 2	19 ± 2
Spike threshold (mV)	−35 ± 2	−35 ± 2
Spike amplitude (mV)	77 ± 3	74 ± 3
Spike half-width (ms)	0.84 ± 0.04	0.87 ± 0.06
Spike maximal decay (mV/ms)	−93 ± 5	−90 ± 6
IPSC properties	**($n = 8$ cells from 3 mice)**	**($n = 3$ cells from 2 mice)**
sIPSC amplitude (pA)	−60 ± 5	−64 ± 14
sIPSC frequency (Hz)	5 ± 0.4	4.3 ± 1.1
sIPSC τ_{decay} (ms)	7.6 ± 0.4	8.2 ± 0.5
$GABA_{tonic}$(pA)	−30 ± 8	−45 ± 19
EPSC properties	**($n = 6$ cells s/eEPSCs, 5 cells LTP from 3 mice)**	**($n = 6$ cells s/eEPSCs, 6 cells LTP from 4 mice)**
sEPSC amplitude (pA)	−11 ± 1	−10 ± 0.6
sEPSC frequency (Hz)	1.6 ± 0.3	1.3 ± 0.2
sEPSC τ_{decay} (ms)	5.6 ± 0.5	5.8 ± 0.3
eEPSC AMPA/NMDA ratio	1.3 ± 0.2	1.5 ± 0.2
eEPSC PPR	1.0 ± 0.04	1.2 ± 0.09
$eEPSC_{NMDA}$ τ_{decay} (ms)	73 ± 3	83 ± 7
eEPSC TBS LTP (% control)	212 ± 47	191 ± 50

GABAergic synaptic events as well as tonic GABAergic inhibition (**Figures 4E–H** and **Table 1**). Comparison of control and activated DG-TeTX old GCs revealed no differences in any of the synaptic properties assayed including inhibitory/excitatory postsynaptic current kinetics, AMPA/NMDA ratios, and short-term synaptic plasticity at perforant path inputs (**Figures 4I,J** and **Table 1**, p-values ranged 0.2–0.9). Moreover, silenced GCs in activated DG-TeTX mice exhibited theta-burst stimulation-induced long-term potentiation (LTP) of excitatory synaptic transmission that was comparable to active GCs in control mice (**Figures 5A,B** and **Table 1**, $p = 0.8$). In both genotypes LTP was associated with a reduction in PPR consistent with an increase in presynaptic function during the expression of this plasticity (**Figures 5A,B**). Together, these findings indicate that prolonged blockade of synaptic output from old GCs does not precipitate overt changes in their basic electrophysiological and synaptic input properties arguing against any significant homeostatically induced plasticity in the cells due to altered network participation.

DISCUSSION

Neuronal cell replacement strategies offer incredible therapeutic potential for circuit repair in neurodegenerative disorders or following traumatic brain injury (Lopez-Bendito and Arlotta, 2012). However, the realization of this potential requires a thorough understanding of the cellular mechanisms underlying the integration of new neurons into mature existing neural networks. A wealth of data supports a role for active competition between presynaptic terminals of individual neurons in establishing and sculpting network connectivity in the developing nervous system (Katz and Shatz, 1996; Sanes and Lichtman, 1999; Yu et al., 2004;

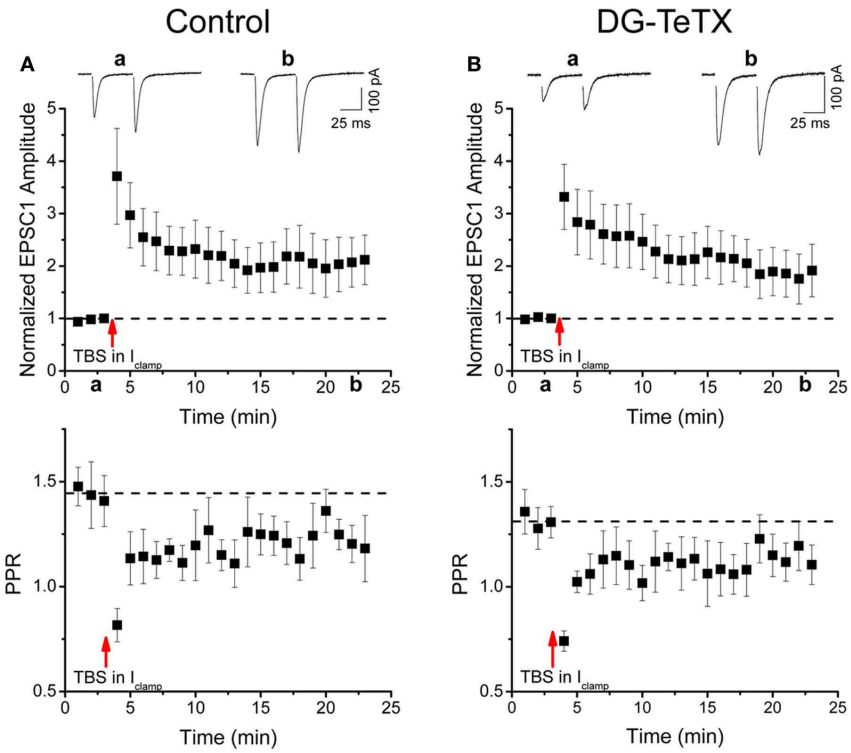

FIGURE 5 | Normal LTP of perforant path inputs to old GCs in activated DG-TeTX mice. (A,B) The upper panels are pooled data time course plots showing LTP of perforant path-evoked AMPA receptor-mediated EPSCs in response to a theta burst induction protocol in old GCs of control (**A**, $n = 5$ cells from 3 animals) and activated DG-TeTX (**B**, $n = 6$ cells from 4 animals) mice. Inset traces show EPSCs taken at the times indicated on the *x*-axis. Lower panels show the corresponding pooled data time course plots of the paired pulse ratios for AMPA receptor-mediated EPSC peak amplitudes (PPRS) in control and activated DG-TeTX mice.

Hashimoto and Kano, 2005), but whether the circuit integration of new neurons into preexisting adult circuits relies upon similar competition-based axonal refinement is unclear. In a previous study examining the role of young and old GCs in DG function we did not obtain any evidence for altered maturation or circuit integration of newborn GCs in activated DG-TeTX adult mice (Nakashiba et al., 2012). In this model the newborn GCs should be at a competitive advantage in terms of communicating with downstream DG and CA3 postsynaptic targets compared to old GCs that are prevented from releasing transmitter due to the selective expression of TeTX. In the present study we utilized the same neuronal competition model focusing on the silenced old GC population to determine if being placed at a competitive disadvantage within the circuit precipitated any changes in their MF projections or electrophysiological properties. In developing sensory circuits, cerebellum, and neuromuscular junctions neurons placed at such a competitive disadvantage retract their axons following destabilization of their presynaptic terminals triggered by competitive interactions with more active axons innervating the same postsynaptic targets (Fladby and Jansen, 1990; Antonini and Stryker, 1993; Buffelli et al., 2003; Ruthazer et al., 2003; Yu et al., 2004; Hashimoto and Kano, 2005; Hua et al., 2005). In contrast we found no evidence of axon retraction in silenced old GCs of adult DG-TeTX mice. Indeed our electrophysiological, immunocytochemical, and EM data all indicated that the MF axons of presynaptically silenced GCs continue to project throughout the entire extent of CA3 despite potential competitive influences from continuously generated newborn GCs. The silenced axons even retained typical presynaptic specializations, the giant MFBs, in association with postsynaptic targets in stratum lucidum suggesting that VAMP2-dependent release is dispensable in the maintenance of the structural integrity of established MF synapses in adult mice. One caveat to this interpretation of our EM data is that we could not distinguish between terminals of old silenced GCs versus those belonging to newborn GCs leaving open the possibility that our failure to observe terminal changes at the EM level in DG-TeTX mice simply reflects preferential examination of unsilenced terminals from newborn GCs. However, since DG-TeTX mice do not exhibit enhanced neurogenesis (Nakashiba et al., 2012) and newborn GCs comprise only a small proportion of the overall GC population, the similar densities of MFBs in control and DG-TeTX mice argues that our data sets are overwhelmingly comprised of terminals from old silenced GCs in mice of both genotypes. Finally, we found no differences in the basic electrical and synaptic input properties of active and silenced GCs indicating that altered circuit participation of old GCs in activated DG-TeTX mice did not promote homeostatic plasticity of cell membrane properties or excitatory/inhibitory synaptic input to these cells. Together these findings reveal a remarkable stability in the morphological and electrical

properties of old GCs following prolonged periods of synaptic silencing.

Our findings contrast starkly with observations in the developing hippocampus of juvenile mice. Using a similar TeTX-based strategy, but with mutants that express TeTX from early postnatal stages, Yasuda et al. (2011) found that silenced GCs undergo axon retraction and elimination in mice 3–4 weeks of age. The TeTX expressing GCs initially projected normally into CA3 within the first two weeks postnatally but then retracted their axons during the 3rd and 4th postnatal weeks and ultimately died after axon elimination. Importantly, this process was prevented by pharmacological global inhibition of circuit activity or suppression of neurogenesis beyond the second postnatal week indicating that axon elimination and cell death of the silenced GCs was driven by activity-dependent competition from newborn GCs that did not express TeTX (Yasuda et al., 2011). Interestingly, in the same study the authors reported a similar competition-based axon elimination in juvenile mice for afferents from the EC and for CA1 pyramidal cell axons (Yasuda et al., 2011). In both cases when TeTX expression was limited to approximately half of the EC and CA1 fibers the authors found an activity-dependent elimination of TeTX expressing axons, presumably driven by the remaining release competent EC and CA1 fibers. Our failure to observe such competition driven axon refinement in the adult hippocampus suggests that this process is limited to a critical period during the first month of hippocampal development or potentially the first 4 weeks postgenesis of an adult born GC. In our model GCs cannot be induced to express TeTX until approximately 6 weeks of age, suggesting that sometime between 3 and 6 weeks of age the synaptic connections made by a GC become immune to any destabilizing influence from more active neighboring fibers that would disrupt the integrity of less active axons and associated terminals. Alternatively, it is possible that by 6 weeks of age the relative contribution of newborn GCs to the entire MF pathway is too small to drive competition-based retraction of large numbers of old GC axons. Such limited competition may only promote axon retraction of a small percentage of silenced old GCs below the detection limits of our experimental approaches. While future experiments designed to increase the degree of competition by enhancing neurogenesis or reducing the percentage of TeTX expressing cells would be informative, our current findings clearly indicate that under basal conditions the competition driven by newborn GCs does not promote gross axon retraction of the entire silenced old GC population in adult mice. Despite the structural immunity to competition observed in silenced GCs, it remains possible that young and old GCs still compete for synaptic control over downstream postsynaptic targets in adult mice. For instance a recent investigation in slice culture indicates that differences in the activity levels among neighboring synapses regulates MFB motility, suggesting that synaptic remodeling events may be influenced by activity-dependent competition (Chierzi et al., 2012). Alternatively, competing inputs to common postsynaptic targets may influence the efficacy of existing synapses without promoting axon retraction by triggering changes in presynaptic release or postsynaptic responsiveness. Future investigations will be necessary to probe for such heterosynaptic plasticity interactions between young and old GCs and may provide insight into the cellular mechanisms underlying the distinct circuit functions of these cohorts in mediating pattern separation and completion.

ACKNOWLEDGMENTS

We thank Daniel Abebe, Xiaoqing Yuan, Modesto R. Peralta III, and Philippe Lemieux for providing expert technical assistance as well as Jennie Z. Young for critical reading. RGS14 antibody was generously provided by Dr. John Helper. This work was supported by the Howard Hughes Medical Institute, Otsuka Maryland Research Institute, the Picower Foundation, and NIH grants R01-MH078821 and P50-MH58880 to Susumu Tonegawa; NICHD intramural funding to Chris J. McBain; and CIHR grant MOP 81142 to Katalin Tóth.

REFERENCES

Amaral, D. G., and Dent, J. A. (1981). Development of the mossy fibers of the dentate gyrus: I. A light and electron microscopic study of the mossy fibers and their expansions. *J. Comp. Neurol.* 195, 51–86.

Antonini, A., and Stryker, M. P. (1993). Rapid remodeling of axonal arbors in the visual cortex. *Science* 260, 1819–1821.

Bergami, M., and Berninger, B. (2012). A fight for survival: the challenges faced by a newborn neuron integrating in the adult hippocampus. *Dev. Neurobiol.* 72, 1016–1031.

Buffelli, M., Burgess, R. W., Feng, G., Lobe, C. G., Lichtman, J. W., and Sanes, J. R. (2003). Genetic evidence that relative synaptic efficacy biases the outcome of synaptic competition. *Nature* 424, 430–434.

Chierzi, S., Stachniak, T. J., Trudel, E., Bourque, C. W., and Murai, K. K. (2012). Activity maintains structural plasticity of mossy fiber terminals in the hippocampus. *Mol. Cell. Neurosci.* 50, 260–271.

Claiborne, B. J., Xiang, Z., and Brown, T. H. (1993). Hippocampal circuitry complicates analysis of long-term potentiation in mossy fiber synapses. *Hippocampus* 3, 115–121.

Clelland, C. D., Choi, M., Romberg, C., Clemenson, G. D. Jr., Fragniere, A., Tyers, P., et al. (2009). A functional role for adult hippocampal neurogenesis in spatial pattern separation. *Science* 325, 210–213.

Creer, D. J., Romberg, C., Saksida, L. M., Van Praag, H., and Bussey, T. J. (2010). Running enhances spatial pattern separation in mice. *Proc. Natl. Acad. Sci. U.S.A.* 107, 2367–2372.

Davis, G. W. (2006). Homeostatic control of neural activity: from phenomenology to molecular design. *Annu. Rev. Neurosci.* 29, 307–323.

Deng, W., Aimone, J. B., and Gage, F. H. (2010). New neurons and new memories: how does adult hippocampal neurogenesis affect learning and memory? *Nat. Rev. Neurosci.* 11, 339–350.

Desai, N. S. (2003). Homeostatic plasticity in the CNS: synaptic and intrinsic forms. *J. Physiol. Paris* 97, 391–402.

Fladby, T., and Jansen, J. K. (1990). Development of homogeneous fast and slow motor units in the neonatal mouse soleus muscle. *Development* 109, 723–732.

Ge, S., Sailor, K. A., Ming, G. L., and Song, H. (2008). Synaptic integration and plasticity of new neurons in the adult hippocampus. *J. Physiol.* 586, 3759–3765.

Hashimoto, K., and Kano, M. (2005). Postnatal development and synapse elimination of climbing fiber to Purkinje cell projection in the cerebellum. *Neurosci. Res.* 53, 221–228.

Haug, F. M. (1967). Electron microscopical localization of the zinc in hippocampal mossy fibre synapses by a modified sulfide silver procedure. *Histochemie* 8, 355–368.

Henze, D. A., Urban, N. N., and Barrionuevo, G. (2000). The multifarious hippocampal mossy fiber pathway: a review. *Neuroscience* 98, 407–427.

Hua, J. Y., Smear, M. C., Baier, H., and Smith, S. J. (2005). Regulation of axon growth *in vivo* by activity-based competition. *Nature* 434, 1022–1026.

Ibata, Y., and Otsuka, N. (1969). Electron microscopic demonstration of zinc in the hippocampal formation using Timm's sulfide silver technique. *J. Histochem. Cytochem.* 17, 171–175.

Imayoshi, I., Sakamoto, M., Ohtsuka, T., Takao, K., Miyakawa, T., Yamaguchi, M., et al. (2008). Roles of continuous neurogenesis in the structural and functional integrity of the adult forebrain. *Nat. Neurosci.* 11, 1153–1161.

Kamiya, H., Shinozaki, H., and Yamamoto, C. (1996). Activation of metabotropic glutamate receptor type 2/3 suppresses transmission at rat hippocampal mossy fibre synapses. *J. Physiol.* 493(Pt 2), 447–455.

Katz, L. C., and Shatz, C. J. (1996). Synaptic activity and the construction of cortical circuits. *Science* 274, 1133–1138.

Laplagne, D. A., Esposito, M. S., Piatti, V. C., Morgenstern, N. A., Zhao, C., Van Praag, H., et al. (2006). Functional convergence of neurons generated in the developing and adult hippocampus. *PLoS Biol.* 4:e409. doi: 10.1371/journal.pbio.0040409

Lee, S. E., Simons, S. B., Heldt, S. A., Zhao, M., Schroeder, J. P., Vellano, C. P., et al. (2010). RGS14 is a natural suppressor of both synaptic plasticity in CA2 neurons and hippocampal-based learning and memory. *Proc. Natl. Acad. Sci. U.S.A.* 107, 16994–16998.

Lopez-Bendito, G., and Arlotta, P. (2012). Cell replacement therapies for nervous system regeneration. *Dev. Neurobiol.* 72, 145–152.

Ming, G. L., and Song, H. (2011). Adult neurogenesis in the mammalian brain: significant answers and significant questions. *Neuron* 70, 687–702.

Nakashiba, T., Cushman, J. D., Pelkey, K. A., Renaudineau, S., Buhl, D. L., McHugh, T. J., et al. (2012). Young dentate granule cells mediate pattern separation, whereas old granule cells facilitate pattern completion. *Cell* 149, 188–201.

Ruthazer, E. S., Akerman, C. J., and Cline, H. T. (2003). Control of axon branch dynamics by correlated activity *in vivo*. *Science* 301, 66–70.

Sahay, A., Scobie, K. N., Hill, A. S., O'Carroll, C. M., Kheirbek, M. A., Burghardt, N. S., et al. (2011). Increasing adult hippocampal neurogenesis is sufficient to improve pattern separation. *Nature* 472, 466–470.

Sanes, J. R., and Lichtman, J. W. (1999). Development of the vertebrate neuromuscular junction. *Annu. Rev. Neurosci.* 22, 389–442.

Schmidt-Hieber, C., Jonas, P., and Bischofberger, J. (2004). Enhanced synaptic plasticity in newly generated granule cells of the adult hippocampus. *Nature* 429, 184–187.

Seress, L., and Gallyas, F. (2000). The use of a sodium tungstate developer markedly improves the electron microscopic localization of zinc by the Timm method. *J. Neurosci. Methods* 100, 33–39.

Tashiro, A., Zhao, C., and Gage, F. H. (2006). Retrovirus-mediated single-cell gene knockout technique in adult newborn neurons *in vivo*. *Nat. Protoc.* 1, 3049–3055.

Toni, N., Laplagne, D. A., Zhao, C., Lombardi, G., Ribak, C. E., Gage, F. H., et al. (2008). Neurons born in the adult dentate gyrus form functional synapses with target cells. *Nat. Neurosci.* 11, 901–907.

Toni, N., Teng, E. M., Bushong, E. A., Aimone, J. B., Zhao, C., Consiglio, A., et al. (2007). Synapse formation on neurons born in the adult hippocampus. *Nat. Neurosci.* 10, 727–734.

Tronel, S., Belnoue, L., Grosjean, N., Revest, J. M., Piazza, P. V., Koehl, M., et al. (2012). Adult-born neurons are necessary for extended contextual discrimination. *Hippocampus* 22, 292–298.

Turrigiano, G. (2012). Homeostatic synaptic plasticity: local and global mechanisms for stabilizing neuronal function. *Cold Spring Harb. Perspect. Biol.* 4, a005736.

Van Praag, H., Schinder, A. F., Christie, B. R., Toni, N., Palmer, T. D., and Gage, F. H. (2002). Functional neurogenesis in the adult hippocampus. *Nature* 415, 1030–1034.

Yasuda, M., Johnson-Venkatesh, E. M., Zhang, H., Parent, J. M., Sutton, M. A., and Umemori, H. (2011). Multiple forms of activity-dependent competition refine hippocampal circuits *in vivo*. *Neuron* 70, 1128–1142.

Yu, C. R., Power, J., Barnea, G., O'Donnell, S., Brown, H. E., Osborne, J., et al. (2004). Spontaneous neural activity is required for the establishment and maintenance of the olfactory sensory map. *Neuron* 42, 553–566.

Zhao, C., Teng, E. M., Summers, R. G. Jr., Ming, G. L., and Gage, F. H. (2006). Distinct morphological stages of dentate granule neuron maturation in the adult mouse hippocampus. *J. Neurosci.* 26, 3–11.

Conflict of Interest Statement: The authors declare that the research was conducted in the absence of any commercial or financial relationships that could be construed as a potential conflict of interest.

Received: 31 August 2012; paper pending published: 24 September 2012; accepted: 29 October 2012; published online: 16 November 2012.

Citation: Lopez CM, Pelkey KA, Chittajallu R, Nakashiba T, Tóth K, Tonegawa S and McBain CJ (2012) Competition from newborn granule cells does not drive axonal retraction of silenced old granule cells in the adult hippocampus. Front. Neural Circuits ***6****:85. doi: 10.3389/fncir.2012.00085*

frontiers in
NEURAL CIRCUITS

REVIEW ARTICLE
published: 08 January 2013
doi: 10.3389/fncir.2012.00113

Dynamic functions of GABA signaling during granule cell maturation

***Cristina V. Dieni*[†]*, Jessica H. Chancey*[†] *and Linda S. Overstreet-Wadiche**

Department of Neurobiology, University of Alabama at Birmingham, Birmingham, AL, USA

Edited by:
Peter Jonas, Institute of Science and Technology Austria, Austria

Reviewed by:
Zoltan Nusser, Institute of Experimental Medicine, Hungary
Christoph Schmidt-Hieber, University College London, UK
Marco Capogna, Medical Research Council, UK

***Correspondence:**
Linda S. Overstreet-Wadiche, Department of Neurobiology, University of Alabama at Birmingham, 1825 University Blvd, Birmingham, AL 35294, USA.
e-mail: lwadiche@uab.edu

[†] *These authors equally contributed to this work.*

The dentate gyrus is one of the few areas of the brain where new neurons are generated throughout life. Neural activity influences multiple stages of neurogenesis, thereby allowing experience to regulate the production of new neurons. It is now well established that $GABA_A$ receptor-mediated signaling plays a pivotal role in mediating activity-dependent regulation of adult neurogenesis. GABA first acts as a trophic signal that depolarizes progenitors and early post mitotic granule cells, enabling network activity to control molecular cascades essential for proliferation, survival and growth. Following the development of glutamatergic synaptic inputs, GABA signaling switches from excitatory to inhibitory. Thereafter robust synaptic inhibition enforces low spiking probability of granule cells in response to cortical excitatory inputs and maintains the sparse activity patterns characteristic of this brain region. Here we review these dynamic functions of GABA across granule cell maturation, focusing on the potential role of specific interneuron circuits at progressive developmental stages. We further highlight questions that remain unanswered about GABA signaling in granule cell development and excitability.

Keywords: dentate gyrus, adult neurogenesis, interneuron, parvalbumin, neurogliaform, neural stem cell, neuroprogenitor, activity-dependent

INTRODUCTION

The dentate gyrus (DG) contains a pool of neuronal stem cells that generates new dentate granule cells (GCs) throughout the life of mammals, including humans (Eriksson et al., 1998). These adult-generated neurons become synaptically integrated into the existing circuitry and participate in normal hippocampal function. While the role of adult neurogenesis in behavior is not fully understood, treatments that enhance neurogenesis, such as environmental enrichment, exercise and electrical stimulation, are well known to enhance cognitive performance whereas treatments that reduce neurogenesis typically impair performance [reviewed by Deng et al. (2010)]. The DG has long been associated with the computational task of pattern separation, i.e., the ability to transform a set of similar inputs into a more distinct pattern of outputs (Marr, 1971). Interestingly, selective manipulations of neurogenesis reliably affect performance in tasks that involve spatial pattern separation (Clelland et al., 2009; Sahay et al., 2011; Nakashiba et al., 2012), suggesting that ongoing neurogenesis is required for this normal dentate function. Other roles of adult neurogenesis in time encoding and memory resolution have also been proposed (Becker and Wojtowicz, 2007; Deng et al., 2010; Aimone et al., 2011).

Adult neurogenesis encompasses the proliferation, differentiation, and maturation of new GCs that are continually added to the dentate. The continuum of neuronal development can be simplified into the stepwise progression of neural stem cells (Type I cells) into progenitors (Type II cells), differentiation of post mitotic newborn neurons, and the synaptic integration of immature GCs, with each stage exhibiting different physiological properties [**Figure 1**; reviewed by Mongiat and Schinder (2011)]. The absolute number of cells generated each day depends on rodent age and species, with estimates ranging between 2000 and 9000 under basal conditions (Kempermann et al., 1997b; Cameron and McKay, 2001). Adult generated neurons that survive the first few weeks following cell birth are likely to persist long term (Dayer et al., 2003), allowing adult generated neurons to accumulate over time, potentially achieving up to 10% of the total granule cell population (Lagace et al., 2007; Imayoshi et al., 2008). Yet the majority of newly generated cells undergo apoptosis within the week after division (Hayes and Nowakowski, 2002; Sierra et al., 2010), resulting in a population of immature neurons that is a small percentage of the total population of GCs. In young adult mice, it has been estimated that ~10–12 day-old GCs comprise about 3% of the population (Pugh et al., 2011) and 4-week old immature GCs comprise <1% of the population (Kempermann et al., 1997b), whereas in rats there is about twice as many surviving immature GCs (Snyder et al., 2009).

Recent interest has focused on how the population of immature adult generated neurons between 1 and 2 months post-mitosis can make contributions to various hippocampal-dependent behaviors (Kim et al., 2012). During this developmental period immature neurons are fully integrated in hippocampal network, receiving cortical afferents and forming functional output synapses with hilar and CA3 neurons (Esposito et al., 2005; Toni et al., 2007), yet they also retain distinctive immature properties that make them more responsive to synaptic activation. Stimulation of cortical afferents *in vitro* triggers spiking and

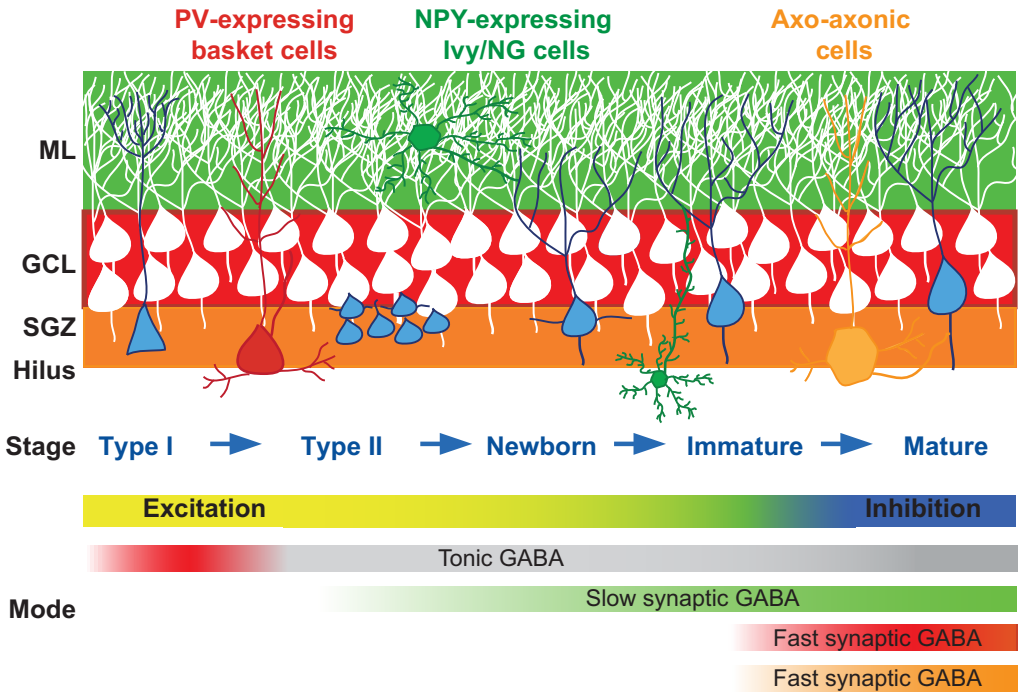

FIGURE 1 | GABAergic innervation in adult neurogenesis. Cartoon depiction of the stages of GC maturation highlighting the sequence of interneuron innervation. Progressive stages of GC maturation are indicated by the blue cells. Select interneurons and their axonal targeting regions are indicated by the corresponding shaded areas (red, PV^+ basket cells; green, Ivy/NG cells; orange, axo-axonal cells). The shift in function of GABA signaling from excitation to inhibition, and the sequence and modes of signaling from interneuron subtypes are indicated in the gradient bars below. The sequence of innervation by numerous other dentate interneuron subtypes [reviewed in Houser (2007)] is not yet known so not included. SGZ, subgranule zone; GCL, granule cell layer; ML, molecular layer.

synaptic plasticity in a greater fraction of immature GCs compared to mature GCs (Schmidt-Hieber et al., 2004; Ge et al., 2007b; Marin-Burgin et al., 2012). This proclivity for excitation is in sharp contrast with the overall sparse population coding evident in the DG *in vivo*, where only a fraction of GCs are activated by sensory stimulation in behaving rodents (Jung and McNaughton, 1993; Chawla et al., 2005; Neunuebel and Knierim, 2012). Thus it has been proposed that the small population of excitable immature GCs can make a significant contribution to overall network function due to preferential recruitment over mature GCs (Kee et al., 2007; Snyder et al., 2009; Alme et al., 2010; Marin-Burgin et al., 2012), but see also (Stone et al., 2011).

The realization that adult neurogenesis is highly regulated by stimuli like exercise and environmental enrichment contributed to its widespread acceptance as a physiologically relevant phenomenon (Kempermann et al., 1997a; van Praag et al., 1999). Each process underlying neurogenesis from stem cell quiescence through synaptic integration is regulated by a surprisingly large number of physiological and pathological stimuli (Ming and Song, 2011). The profound extrinsic regulation of adult neurogenesis identified in animal models represents a dramatic form of plasticity in the adult brain and a potential therapeutic target for human conditions. Considerable effort is underway to uncover the mechanisms that mediate adaptability. One well established mechanism for activity-dependent regulation of neurogenesis is the translation of network activity to newborn neurons using the neurotransmitter GABA (Ben-Ari et al., 2007; Ge et al., 2007a). Although GABA is the principal inhibitory neurotransmitter for mature neurons, GABA acts as a trophic factor for immature neurons and progenitor cells via Cl^--mediated depolarization. Here we review the dynamic role of GABA across GC development, highlighting the interneuron circuits that potentially serve distinct trophic and inhibitory functions. Although the focus is $GABA_A$ receptor (GABAR)-mediated signaling, it is also relevant to note that dentate interneurons express a variety of other signaling molecules that influence adult neurogenesis that have been reviewed elsewhere (Masiulis et al., 2011).

DIVERSITY IN $GABA_A$ RECEPTOR-MEDIATED SIGNALING

There is substantial potential for diversity and specialization in signaling mediated by GABARs. Sources of diversity include the large number of distinct interneuron subtypes with differing contributions to network activity, flexibility in the polarity of GABAR- mediated postsynaptic potentials achieved via regulation of intracellular Cl^- concentration, the multiple modes of transmission mediated by tonic and phasic activation of GABARs, and numerous combinations of receptor subunits that can comprise receptors with differing GABA affinities and activation/inactivation kinetics. How newly generated GCs take advantage of the diversity in GABA signaling mechanisms at

different developmental stages is just beginning to be understood. First we briefly describe these fundamental mechanisms.

DIVERSITY OF GABAergic INTERNEURONS

GABAergic interneurons in the hippocampus comprise a heterogeneous population that can be classified by a variety of morphological, neurochemical, and physiological criteria (Maccaferri and Lacaille, 2003). An important criterion is based on the idea that interneuron functions are dictated by the specificity of their postsynaptic target-domain (Freund and Buzsaki, 1996). For example, axo–axonic and basket cells form synapses exclusively on the axon initial segments and proximal somatodendritic regions of principal cells, respectively, whereas numerous other interneuron subtypes target dendritic regions. It is well established that inhibition mediated by dendritic vs. perisomatic projecting interneurons differentially contribute to neural integration (Miles et al., 1996). Distinctive domain innervation allows single principal cells to take advantage of the overall diversity and specialization of interneuron functions by performing a variety of different computational tasks simultaneously in a spatially segregated manner (Klausberger and Somogyi, 2008). In the context of adult neurogenesis, the variety of interneuron subtypes raises questions about how these precise patterns of innervation are achieved, how the sequence of innervation contributes to the activity-dependent maturation of newborn cells, and how the innervation pattern contributes to the switch in the role of GABA signaling from an early trophic factor into complex regulator of neural timing and synchronization. In the simplest case, the laminar organization of interneuron axonal arborization is expected to determine the temporal sequence of synaptogenesis by interneuron subtypes, as dentate GCs born in the subgranular zone encounter increasing varieties of interneurons as newly formed neurites expand throughout the layers of the DG (**Figure 1**). Elucidating the precise sequence of GC innervation by interneuron subtypes will provide insight into how specific interneuron circuits subserve distinct functions during the course of GC maturation.

THE POLARITY OF $GABA_A$ RECEPTOR MEDIATED RESPONSES

GABA released from interneurons acts at postsynaptic ionotropic GABARs that are permeable to Cl^-, allowing shifts intracellular $[Cl^-]$ to alter the polarity of the postsynaptic response. Neuroprogenitors and immature neurons express high levels of the sodium-potassium-chloride exchanger NKCC1 that maintains high intracellular $[Cl^-]$ using sodium and potassium gradients. High intracellular $[Cl^-]$ results in GABAR-mediated depolarization since the Cl^- reversal potential $E_{[Cl^-]}$ is typically significantly more positive than the resting membrane potential (Ben-Ari, 2007). As maturation proceeds, up regulation of the potassium chloride coupled co-transporter KCC2 reduces intracellular $[Cl^-]$ to low mature levels, typically switching GABA responses from depolarizing to hyperpolarizing (Rivera et al., 1999). Sequential expression of NKCC1 and KCC2 is likewise thought to be responsible for the developmental shift in $E_{[Cl^-]}$ from approximately −40 mV in newborn GCs to more negative than −65 mV in mature GCs (Overstreet-Wadiche et al., 2005; Ge et al., 2006; Chiang et al., 2012; Sauer et al., 2012). The shift in the polarity of GABAergic responses in adult generated neurons occurs before the 4th week of maturation (Ge et al., 2006), and presumably is involved in the transition away from trophic functions that primarily rely on depolarization-mediated Ca^{2+} influx (Tozuka et al., 2005; Overstreet-Wadiche et al., 2006). However, the very negative resting membrane potential of GCs (below −75 mV) means that GABAR-mediated responses continue to depolarize even mature GCs (Chiang et al., 2012; Sauer et al., 2012). Depolarizing GABAR responses are typically inhibitory since the $E_{[Cl^-]}$ is hyperpolarized from the threshold for action potential generation and GABAR-mediated conductances shunt excitatory signals (Staley and Mody, 1992; Smith and Jahr, 2002), although modeling predicts that depolarizing GABAR responses in mature GCs could have excitatory actions depending on the exact timing and location of GABAergic postsynaptic currents (GPSCs) (Chiang et al., 2012).

MULTIPLE MODES OF GABAergic TRANSMISSION

Whether depolarizing or hyperpolarizing, GABAR-mediated signaling occurs in two modes termed phasic and tonic (Farrant and Nusser, 2005). Phasic signaling refers to conventional synaptic transmission, in which GABA is released from presynaptic vesicles and activates postsynaptic GABARs on a rapid timescale. Tonic signaling refers to the activation of GABARs by ambient levels of GABA in the extracellular space. The different concentration profiles of GABA underlying synaptic and tonic signaling have significant consequences for GABAR function. The high (>1 mM) and brief (<1 ms) concentration profile in the synaptic cleft triggers rapid activation and deactivation of synaptic receptors (Mozrzymas, 2004), whereas persistent low concentrations of GABA favor receptor desensitization over activation (Overstreet et al., 2000). Despite accumulation of receptors in desensitized states, a large population of receptors exposed to low ambient [GABA] will equilibrate between desensitized, open and unbound states to generate steady-state conductances that can be large enough to affect excitability of dentate GCs (Overstreet and Westbrook, 2001; Nusser and Mody, 2002).

The source of GABA mediating phasic signaling is action potential-driven or spontaneous fusion of synaptic vesicles from presynaptic terminals, whereas the source of GABA mediating tonic signaling is less clear. Unlike extracellular levels of glutamate that are maintained in the low nM range by the 3:1 Na^+: glutamate stoichiometry of glutamate transporters (Herman and Jahr, 2007; Tzingounis and Wadiche, 2007), the 2:1 Na^+: GABA stoichiometry of GABA transporters predicts that a higher extracellular level of GABA (hundreds of nM) could persist in the absence of other sources of GABA release (Richerson and Wu, 2003; Farrant and Nusser, 2005). Ongoing synaptic release of GABA also contributes to the ambient concentration, potentially allowing regional and temporal regulation of extracellular tonic signaling to reflect ongoing network activity (Farrant and Nusser, 2005).

Synaptic vesicles containing GABA are released at morphologically identifiable presynaptic terminals with GABA acting at GABARs clustered at postsynaptic sites across the synaptic cleft. Thus phasic signaling is precisely localized to synapses although in some cases GABA diffusion outside the synapse can activate

nearby extrasynaptic (perisynaptic) receptors (Kullmann, 2000). In contrast, it is not known whether there is regional specificity in the distribution of tonic GABAR currents across subcellular locations, although there is general agreement that tonic GABAR currents are primarily generated by extrasynaptic GABARs (see below).

Interestingly, a 3rd form of synaptic signaling that is intermediate between phasic and tonic signaling is used by specific subtypes of GABAergic interneurons (Szabadics et al., 2007). This form of transmission is mediated by the Ivy/Neurogliaform family of interneurons (Ivy/NG cells), and has recently been established to mediate slow inhibitory postsynaptic currents (IPSCs) sometimes termed $GABA_{Aslow}$ (Capogna and Pearce, 2011). In contrast to the large and fast GABA transients produced at typical synapses made by perisomatic-projecting interneurons such as basket cells, GABA released from Ivy/NG cells presynaptic terminals generates a prolonged GABA transient with a low peak concentration that results in IPSCs with slow kinetics (Karayannis et al., 2010). The unusual GABA concentration transient could result from GABA released into the extracellular space from densely spaced neurogliaform presynaptic terminals, in a form of volume transmission (Olah et al., 2009; Capogna and Pearce, 2011).

HETEROGENEITY OF $GABA_A$ RECEPTOR SUBUNITS

GABARs are heteropentameric channels typically composed of 2α and 2β subunits and either a γ or a δ subunit. Tonic and synaptic GABA signaling are associated with various GABAR subunits that have different biophysical properties and subcellular localizations [reviewed in Farrant and Nusser (2005)]. In dentate GCs, tonic signaling is mediated by extra- or peri-synaptically located α4, α5, and δ subunit containing GABARs (Stell et al., 2003; Chandra et al., 2006; Duveau et al., 2011). Conversely, α1, α2, and γ2 receptors are often clustered at synapses (Nusser et al., 1995; Sun et al., 2004) but consistent with the idea that subunits are not completely segregated these receptors are also found extrasynaptically. γ2 subunits are required for initial synaptic clustering and maintenance of GABARs within the synapse, and predominately found at synaptic sites (Essrich et al., 1998; Schweizer et al., 2003). Compensation and injury alters the expression levels and localization of subunits, suggesting flexibility in localization and function. For example, in epilepsy models there is altered expression and localization of δ and α2 subunits in dentate GCs that impair both tonic and phasic inhibition (Peng et al., 2002; Zhang et al., 2007; Rajasekaran et al., 2010). Furthermore, the subunit organizations of synaptic and non-synaptic GABAR clusters are dynamically regulated across development (Hutcheon et al., 2000, 2004).

TROPHIC ROLE OF GABA IN EARLY DEVELOPMENT OF DENTATE GRANULE CELLS

The trophic function of GABA in neuronal development has been studied extensively in the neonatal brain. Pioneering work in the developing cortex showed that GABARs located on proliferating neuroprogenitor cells provide a depolarizing signal that increases intracellular calcium $[(Ca^{2+})_i]$ through the action of voltage-gated calcium channels (VGCCs), resulting in a reduction in DNA synthesis (LoTurco et al., 1995). Subsequent studies have established a common theme involving Ca^{2+} influx provided by GABAR-depolarization as a key component for many aspects of neuronal development, including proliferation, differentiation, and morphological maturation. The large literature establishing the role of GABA in neurodevelopment in both the developing and adult brain has been reviewed elsewhere (Ben-Ari et al., 2007; Ge et al., 2007a; Sernagor et al., 2010). Here we focus on reviewing recent studies delineating the contribution of specific GABARs and circuits to the development of adult generated dentate GCs.

Similar to principal cells in many developing brain regions, innervation by local GABAergic interneurons is established prior to glutamatergic synaptogenesis (Ambrogini et al., 2004; Esposito et al., 2005; Ge et al., 2006; Overstreet-Wadiche and Westbrook, 2006; Piatti et al., 2006), and the sequence of GABAergic innervation of newly generated cells follows the sequence established in the developing dentate where GPSCs with slow rise and decay kinetics are present prior to GPSCs with fast kinetics (Hollrigel and Soltesz, 1997; Liu et al., 1998; Esposito et al., 2005; Overstreet-Wadiche et al., 2005). Analogous to the synaptically "silent" immature neurons identified in the neonatal brain (Owens et al., 1999; Tyzio et al., 1999), neural stem cells and progenitors in the adult dentate also have tonic GABAR signaling prior to the formation of functional synapses.

GABAR SIGNALING IN TYPE I STEM CELL PROLIFERATION

Radial glial cells (Type I cells) that express nestin are the putative neural stem cells of the adult DG (Seri et al., 2001; Bonaguidi et al., 2012). Located in the subgranular zone (**Figures 1** and **2**), Type I cells express the glial marker GFAP and have astrocytic properties including low input resistance and a resting potential near the K^+ equilibrium potential (Filippov et al., 2003; Fukuda et al., 2003). Two reports indicate that Type I cells have functional GABARs that respond to high concentrations of exogenously applied GABA (Wang et al., 2005; Song et al., 2012), although GABA-evoked currents were not detected in another study (Tozuka et al., 2005). Type I cells do not have GABA synaptic innervation since both electrical stimulation and light-driven activation of parvalbumin (PV)-expressing interneurons fail to evoke synaptic currents (**Figure 2A**; Song et al., 2012). However, Song et al. (2012) proposed that tonic currents mediated by γ_2-GABARs promote quiescence since knockout of the γ_2 GABAR enhanced proliferation of Type I cells. Repression of stem cell proliferation by tonic GABAR signaling is likewise supported by the increased proliferation of progenitors seen in germline α_4 GABAR knockout mice that have impaired tonic GABAR signaling in adult-generated progeny (Duveau et al., 2011). Tonic GABAR signaling in mature GCs is typically mediated by $\alpha_4\beta_2\delta$ GABARs (Farrant and Nusser, 2005), but δ-GABAR subunit knockout mice did not have any of the deficits seen in the α_4 knockout (Duveau et al., 2011). Thus, GABARs involved in tonic signaling in progenitors may be different than those of mature GCs. Indeed, γ_2-GABAR subunits are typically associated with phasic GABAergic signaling since the γ_2 subunit is essential for clustering receptors at synaptic sites (Essrich et al., 1998). It will be important to establish the mechanism by which tonic GABAR

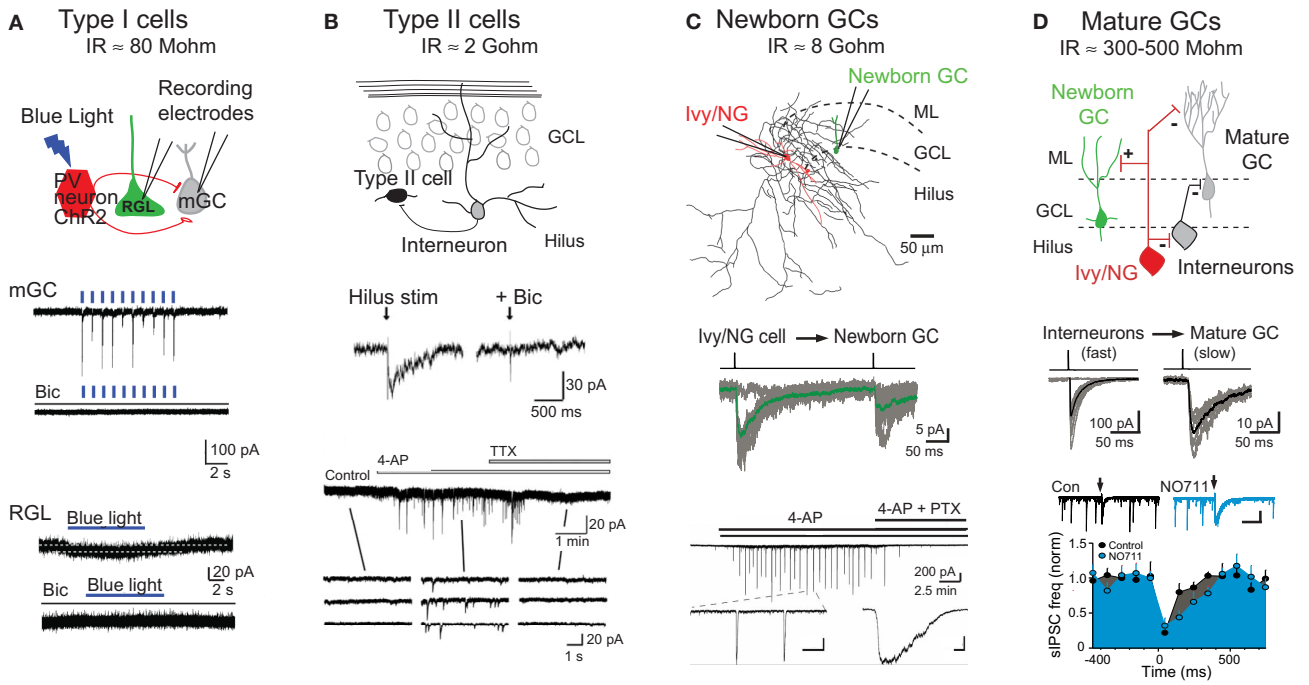

FIGURE 2 | Modes of GABAR signaling during GC development. **(A)** Tonic signaling to Type I radial glial-like stem cells: Top, schematic depiction of whole cell patch clamp recording from mature granule cells (mGCs) or Type I GFP$^+$ radial glial-like stem cells (RGLs) during photoactivation of PV$^+$ interneurons expressing channelrhodopsin (ChR2). Middle, photoactivation of ChR2$^+$PV$^+$ interneurons (indicated by blue lines, 1 Hz) generates large synaptic currents in mature GCs that are blocked by the GABAR antagonist bicuculline (Bic). Bottom, photoactivation of ChR2$^+$PV$^+$ interneurons (blue bar, 8 Hz) generates small tonic currents in Type I RGLs that are blocked by bicuculline. Adapted from Song et al. (2012) with permission from Macmillan Publishers Ltd. Estimates for input resistance (IR) of Type I and Type II cells are from Fukuda et al. (2003). **(B)** Synaptic signaling to Type II neuroprogenitors: Top, schematic depiction of innervation of Type II cells by dentate interneurons. Middle, hilar stimulation evokes inward currents in Type II cells that are blocked by bicuculline. Bottom, the frequency of spontaneous activity in Type II cells is increased by bath application of 4-aminopyridine (4-AP; 100 µM), a potassium channel blocker that causes synchronous firing of dentate interneurons (Michelson and Wong, 1994; Markwardt et al., 2011). 4-AP-induced currents are blocked by tetrodotoxin (TTX). Insets show currents on an expanded time scale. Adapted from Tozuka et al. (2005) with permission from Elsevier. **(C)** Synaptic signaling to newborn GCs by Ivy/NG interneurons: Top, reconstructed Ivy/NG interneuron (red cell body and dendrites, black axon) from a paired recording with a POMC-GFP$^+$ newborn GC (green). ML, molecular layer. Middle, current injection into presynaptic Ivy/NG cells evokes slow GPSCs in newborn GCs. The averaged unitary IPSC (green) is overlaid on individual currents (gray). From Markwardt et al. (2011). Bottom, bath application of 4-AP (100 µM) induces synaptic currents in newborn GCs that are blocked by picrotoxin (PTX). Insets show currents on expanded time scales [scale bars are 200 pA and 10 s (left) or 500 ms (right)]. From Markwardt et al. (2009). The estimate for IR of newborn GCs is from Overstreet et al. (2004). **(D)** Heterogeneous synaptic signaling to mature GCs: Top, schematic depiction showing that mature GCs are innervated by a variety of interneuron subtypes including Ivy/NG cells and perisomatic projecting interneurons. Ivy/NG cells also provide slow GABAergic inhibition to perisomatic-projecting interneurons. Middle, current injection in individual interneurons evokes either fast (left) or slow (right) uIPSCs in mature GCs, reflecting the heterogeneity of innervation. Bottom, spontaneous GPSCs in mature GCs arise from perisomatic-projecting interneurons (Soltesz et al., 1995). The frequency of sGPSCs is reduced by stimulation of the ML (arrows) that evokes slow NO711-sensitive IPSCs in mature GCs (insets) and perisomatic projecting interneurons (not shown). Together these results support the circuit diagram shown above. Scale in inset, 300 pA, 500 ms. Adapted from Markwardt et al. (2011). The estimate of IR for mature GCs is from Schmidt-Hieber et al. (2004) and Overstreet et al. (2004).

signaling through γ_2 or α_4 subunits contributes to stem cell proliferation, since the characteristics of Ca^{2+} influx generated by tonic depolarization of low-input resistance Type I cells will likely be distinct from Ca^{2+} transients generated by phasic GABAR signaling to later stage progenitors and newborn GCs that have high input resistance.

Interestingly, PV$^+$ interneurons have a preferential role in promoting tonic GABAR signaling to Type I neural stem cells. PV$^+$ interneurons form perisomatic basket-like synapses with mature GCs and have several functional specializations for rapid and precise phasic transmission (Bartos et al., 2001; Bucurenciu et al., 2008; Hu et al., 2010). Using the selective expression of light-activated channelrhodopsin (ChR2) in specific subtypes of interneurons, Song et al. (2012) showed that repetitive activation of PV$^+$ expressing interneurons, but not somatostatin- or vasoactive intestinal peptide (VIP)-expressing interneurons, increased tonic GABAR currents in Type I cells in acute slices (**Figure 2A**). Furthermore, ChR2 activation of PV$^+$ interneurons over a period of days *in vivo* reduced proliferation of Type I cells, whereas inactivation of PV$^+$ cells with Halorhodopsin increased proliferation. Together these results suggest that despite the specializations the promote fast phasic GABA release from PV$^+$ interneurons to mature GCs, PV$^+$ interneuron activity regulates Type I stem cell quiescence via tonic GABAR signaling. The involvement of PV$^+$

interneurons in proliferation is also supported by enhanced proliferation but reduced differentiation of progenitor cells when the BDNF receptor TrkB is selectively deleted from PV^+ interneurons (Waterhouse et al., 2012). Thus PV^+ interneurons have diverse roles GC function including modulation of proliferation via tonic signaling as well as control of mature GCs excitability by phasic signaling.

GABAR SIGNALING IN TYPE II PROGENITOR DIFFERENTIATION

Type II cells comprise a heterogeneous population of progenitors that arise from Type 1 neural stem cells with variable mitotic capabilities and marker expression (Encinas and Enikolopov, 2008; Bonaguidi et al., 2012). Notably, the immature neuronal marker doublecortin is expressed in the "oldest" Type II progenitors. No longer displaying astrocytic properties, Type II cells are smaller than Type I cells with only minor processes, and they have high input resistance and heterogeneous voltage gated currents (Wang et al., 2005). Most Type II cells express functional GABARs (Tozuka et al., 2005; Wang et al., 2005), but robust tonic GABAR currents were not detected in nestin-GFP expressing Type II cells (Tozuka et al., 2005). Tonic GABAR currents are prominent, however, in adult generated cells at 3 days following retroviral infection (Ge et al., 2006), a time point when Type II progenitors are expected to comprise a large percentage of retroviral-labeled cells. Although tonic and phasic GABAergic signaling in distinct subtypes of Type II cells is not yet precisely defined, it is clear that during this period synaptic input are first detected in response to focal stimulation of the molecular layer and hilus (**Figure 2B**; Tozuka et al., 2005; Wang et al., 2005).

GABAergic signaling to Type II cells caused depolarization that increased $[Ca^{2+}]_i$ via voltage gated calcium channels (Tozuka et al., 2005). Treating cultured slices with GABA caused proliferating cells to differentiate, measured as in increase in *neuroD*, a gene required for granule cell differentiation. These results suggests that GABA-mediated depolarization drives Type II cells to leave the cell cycle and differentiate via the down regulation of anti-neuronal genes and up regulation of *neuroD,* establishing one mechanism underlying the so-called "excitation-neurogenesis" coupling previously identified by NMDAR activation of progenitors in culture (Deisseroth et al., 2004; Deisseroth and Malenka, 2005). GABAR mediated depolarization can also promote CREB signaling needed for cell survival. A large proportion of Type II progenitors undergo apoptosis, followed by a smaller proportion of cells undergoing apoptosis over the next 2–3 weeks after the transition to post mitotic newborn neuron (Sierra et al., 2010). Jagasia et al. (2009) demonstrated that cell autonomous loss of GABA depolarization leads to cell death of 1–2 week-old cells, an effect that is rescued by CREB signaling. Since selectively blocking tonic signaling in developing GCs by deletion of the α4 GABAR subunit did not alter newborn neuron survival (Duveau et al., 2011), phasic rather than tonic GABAR signaling may be involved in promoting survival during the differentiation of Type II progenitors into newborn post mitotic GCs (see below).

The trophic role of GABA in GC maturation was elegantly established by knocking down NKCC1 expression in proliferating progenitors in order to block the depolarizing action of GABA throughout GC maturation (Ge et al., 2006). Two-week old newborn GCs that lack NKCC1 had shorter and less complex dendritic trees, and a delay in the development of glutamatergic synaptic inputs compared to 2-week-old control GCs. Although the mode of GABAR signaling and the developmental stage that were involved in these maturational delays were not specifically identified, subsequent work showed that deletion of α_4-GABARs selectively blocks tonic signaling and impairs dendritic development in 2-week-old newborn GCs (Duveau et al., 2011). Thus early tonic GABAR signaling plays a role in dictating the rate of morphological maturation. On the other hand, deletion of the α_2-GABAR subunit that is typically found in synapses disrupted dendritic structure in 1-month-old cells (Duveau et al., 2011). Together these results suggest that tonic and phasic signals have distinct and stage-specific trophic functions in Type II progenitors and newly post mitotic GCs.

GABAR SIGNALING TO NEWLY POST MITOTIC GCs

Although little is known about the source and modes of GABAergic signaling to Type II progenitors, GABAergic signaling to newly post mitotic GCs has been extensively studied. Esposito et al. (2005) demonstrated that retroviral labeled newborn GCs between 1–3 weeks post-infection had evoked GPSCs with slow rise and decay kinetics similar to slow dendritic IPSCs observed in mature GCs and neurons in other brain regions. Evoked GPSCs with fast kinetics were only detected in retroviral labeled GCs that were ∼4 week-old, suggesting that synapses mediating slow GPSCs develop prior to GABAergic synapses that mediate fast GPSCs generated at perisomatic locations. A GABAR antagonist applied to the dendritic region blocked slow evoked currents, supporting the dendritic origin for the earliest inputs (Esposito et al., 2005). Similarly, newborn GCs identified in proopiomelanocortin-GFP (POMC-GFP) reporter mice also received exclusively slow spontaneous and evoked GPSCs (Overstreet-Wadiche et al., 2005, 2006). These results suggest that early developing slow GABAR-mediated synaptic signaling could promote depolarization and Ca^{2+} influx needed for trophic functions, whereas later developing perisomatic synapses that mediate fast inhibitory currents may not be required to control neural output until after the development of excitatory glutamatergic synapses.

The mechanisms responsible for the early slow GABAR signaling in newborn GCs was studied in POMC-GFP reporter mice that allow identification of post mitotic newborn GCs with relatively uniform intrinsic excitable properties and morphology (Overstreet et al., 2004). This developmental stage is typically achieved at 10–12 days post-mitosis, when slow GABAR signaling is depolarizing and AMPA receptor-mediated transmission is not yet established (Overstreet-Wadiche et al., 2005, 2006). Markwardt et al. (2009) conducted a series of experiments to determine if slow synaptic currents resulted from non-specific spillover from nearby perisomatic terminals on mature GCs or dedicated inputs to newborn cells. GPSCs at perisomatic synapses have fast rise and decay times due to fast release mechanisms and the close proximity of postsynaptic receptors to the brief and high concentration of GABA within the cleft (Bartos and Elgueta,

2012), and are minimally affected by blockade of GABA transporters (Overstreet and Westbrook, 2003). However, the GABA transport antagonist NO711 robustly increased the amplitude, rise and decay times of GPSCs in newborn GCs, suggesting that the receptors underlying GPSCs were located far from the site of GABA release (Markwardt et al., 2009). Furthermore, impeding diffusion in the extracellular space enhanced GPSCs in newborn GCs but not fast GPSCs in mature GCs, suggesting that receptors on newborn GCs are far from saturation. Directly comparing the sensitivity of GPSCs to the low affinity antagonist TPMPA (Jones et al., 2001) confirmed that a lower concentration of GABA generated GPSCs in newborn GCs. These results are consistent with the possibility that slow GPSCs in newborn GCs result from spillover from perisomatic synapses on mature GCs, yet subsequent results ruled out this idea. First, a manipulation expected to reduce spillover transmission by reducing the density of active release sites did not preferentially decrease GPSCs in newborn GCs, and second, GPSCs in newborn GCs were enhanced by blockade of presynaptic $GABA_B$ receptors whereas GPSCs in mature GCs were not, suggesting that the source of slow GPSCs in newborn GCs are unlikely the perisomatic terminals on mature GCs (Markwardt et al., 2009).

An alternative possibility to reconcile the results for and against spillover signaling was that slow GPSCs in newborn GC are generated by specific interneuron subtypes that mediate $GABA_{Aslow}$ in the cortex, since $GABA_{Aslow}$ also has characteristics of spillover even when it is generated by activation of a single interneuron (Szabadics et al., 2007). In support of this possibility, Markwardt et al. (2009) found coincident spontaneous slow GPSCs in simultaneous recordings from mature and newborn GCs, suggesting the existence of an interneuron subtype that mediates slow GPSCs in both newborn and mature GCs. This possibility was confirmed by the subsequent demonstration that single interneurons of the Ivy/NG family generate slow GPSCs in mature GCs (Armstrong et al., 2011) and newborn GCs (**Figure 2C**; Markwardt et al., 2011). Although almost all POMC-GFP labeled newborn GCs have slow evoked GPSCs, Markwardt et al. (2011) found that the probability of achieving a paired recording between a presynaptic interneuron and a newborn GC was very low compared to finding interneurons connected to mature GCs, likely reflecting the sparse innervation of newborn GCs. Furthermore, mature GCs received synapses from a wide variety of interneuron subtypes, whereas most (75%) of the presynaptic interneurons to newborn GCs had characteristics of Ivy/NG cells (the remaining presynaptic interneurons were not identifiable). Interestingly, bath application of the K^+ channel blocker 4-AP generated low-frequency rhythmic firing in Ivy/NG interneurons resulting in phasic and tonic GABAR currents in newborn GCs (**Figure 2C**) that was correlated with inhibition in other interneuron subtypes (Markwardt et al., 2011). Further recordings from interneurons and mature GCs suggested that slow GABAR inhibition of other interneurons reduces spontaneous IPSCs in mature GCs (**Figure 2D**), demonstrating potential interactions between interneuron subtypes that mediate fast and slow inhibition. This idea is consistent with prior studies of $GABA_{Aslow}$ in the CA1 (Capogna and Pearce, 2011), as well as the connectivity of Ivy/NG interneurons in the dentate molecular layer (Armstrong et al., 2011). A greater understanding of the interactions between specific interneuron subtypes will provide important insight into the complex roles of GABAergic circuits in controlling neurogenesis.

As mentioned above, synaptic GABAR signaling to newly post mitotic GCs could have a role in survival, since blockade of GABA depolarization at or prior to this stage reduces survival dependent on CREB activation (Jagasia et al., 2009), and there is an increase in GABA synaptic activity in newborn GCs associated with manipulations that enhance survival (Ambrogini et al., 2010; Chancey and Overstreet-Wadiche, unpublished). Recent results from our lab also suggest a novel role for slow GABAR signaling in providing the depolarization necessary for the activity-dependent incorporation of AMPA-type glutamate receptors at the first silent NMDAR-only synapses on newborn GCs (Chancey et al., 2012). These findings may provide experimental evidence supporting the longstanding idea that synaptic GABA depolarization allows synapse unsilencing at the first NMDAR-only glutamatergic synapses on developing neurons (Ben-Ari et al., 1997) and establish one specific mechanism whereby GABAR-mediated depolarization contributes to the functional integration of adult generated GCs (Ge et al., 2006).

INHIBITORY CIRCUITS CONTROL GRANULE CELL OUTPUT

Together the studies described above demonstrate that GABA-mediated depolarization has trophic functions for all stages of granule cell development, from proliferation to synaptic integration. Early GABAergic signaling is associated with relatively slow and/or persistent activation of GABARs via ambient GABA in the extracellular space and a spillover-like mode of signaling from interneurons of the Ivy/NG family. Future work may determine how these forms of signaling are particularly suited to specific trophic functions. However, upon the development of glutamatergic synapses (represented by the transition from newborn GC to immature GC in **Figure 1**), inhibitory functions of GABA are likely required to control the output of immature GCs that retain high intrinsic excitability (Schmidt-Hieber et al., 2004; Esposito et al., 2005). Although many questions remain unanswered about the mechanisms and timing of the switch in trophic GABAergic signaling to the conventional inhibitory function, key events are the hyperpolarizing shift in the $E_{[Cl^-]}$ and the development of perisomatic synapses that mediate fast IPSCs. These two changes occur between 2–4 weeks post-mitosis, overlapping with the period when cortical afferents are establishing functional glutamatergic synapses (Esposito et al., 2005; Ge et al., 2006; Mongiat et al., 2009). Despite the significant differences between the intrinsic properties and synaptic connectivity of developing and mature GCs, both neonatal and postnatal derived GCs appear to ultimately converge into a functionally homogeneous population once full maturation is complete (Laplagne et al., 2006, 2007).

REDUCED INHIBITION OF IMMATURE GCs PROMOTES SYNAPTIC ACTIVATION

Mounting evidence suggests that the physiological significance of adult neurogenesis derives from the distinctive, yet transient,

properties of immature GCs that could endow them with a unique function in network activity. This idea has lead to intense interest in delineating the properties of immature GCs that are different from mature GCs, with an emphasis on intrinsic excitability and synaptic plasticity. The high input resistance of immature GCs results in large voltage responses produced from small membrane conductances, allowing action potential threshold to be achieved in response to small excitatory inputs (Schmidt-Hieber et al., 2004; Esposito et al., 2005; Mongiat et al., 2009). Immature GCs also display increased propensity for glutamatergic synaptic plasticity compared to mature GCs (Wang et al., 2000; Schmidt-Hieber et al., 2004; Ge et al., 2007b; Li et al., 2012). Since only a small fraction of dentate GCs fire action potentials in response to sensory stimulation in behaving rodents, the high excitability and plasticity of immature GCs could result in the preferential activation of immature GCs (Kee et al., 2007; Snyder et al., 2009; Alme et al., 2010), thereby allowing even a small population of adult generated GCs to contribute to network activity.

Recent findings directly demonstrate that immature GCs are more likely to fire action potentials in response to synaptic stimulation than mature GCs (Marin-Burgin et al., 2012). These authors used Ca^{2+} imaging and single cell recordings to show that stimulation of the perforant path triggers spiking in a greater fraction of immature GCs than mature GCs, and that immature GCs require a lower input strength (i.e., number of activated inputs) to elicit spiking. Enhanced activation of immature (4-week-old) GCs resulted from reduced inhibition relative to excitation, evidenced by the strong effect of GABAR blockade on activation of mature GCs but not immature GCs. The $E_{[Cl^-]}$ of immature GCs was nearly as hyperpolarized as $E_{[Cl^-]}$ of mature GCs, indicating the polarity of GABAR responses was not responsible for reduced inhibition, and the peak ratio of excitation to inhibition was also similar. However, the rise time of perisomatic-evoked IPSCs in immature GCs was slower than the rise time of perisomatic IPSCs in mature GCs, resulting in a higher ratio of excitation to inhibition at the time of spike initiation (Marin-Burgin et al., 2012). These results demonstrate that the slow kinetics of IPSCs contributes to greater synaptic activation of immature GCs. Whether slow kinetics resulted from differences in relative innervation by perisomatic projecting PV^+ and CCK^+ basket cells that differ in their speed of signaling (Bartos and Elgueta, 2012) or developmental differences in postsynaptic GABAR subunits (Hollrigel and Soltesz, 1997) will be interesting to test. Notably, these results reveal that the precise properties of interneuron signaling to immature GCs have important consequences for determining their role in network activity.

POWERFUL INHIBITORY CIRCUITS MAINTAIN SPARSE ACTIVATION OF MATURE GCs

The important role of GABAR signaling across all stages of GCs development is perhaps not surprising, given the well-established role of synaptic inhibition in the "gating function" of the DG. Historically the dentate has been viewed as a filter or gate that restricts the flow of neural activity through the hippocampus, particularly in the context of pathologies that promote epileptogenesis (Dudek and Sutula, 2007). The DG has also received considerable attention for its physiological function in the computational task of pattern separation, or the ability to differentiate similar but different patterns of spatial or sensory inputs (Stella et al., unpublished; Vivar et al., unpublished). Both dentate gating and pattern separation require sparse activation of the numerous GCs and accordingly, physiological stimuli in behaving rodents activates only small subsets of dentate GCs (Jung and McNaughton, 1993; Chawla et al., 2005; Alme et al., 2010; Neunuebel and Knierim, 2012). Sparse activation is also apparent *in vitro* by minimal activation of GCs in response to afferent input from the perforant path; however widespread activation results even with incomplete blockade of GABARs (Coulter and Carlson, 2007). The central role of inhibitory circuits in the formation of granule cell place fields has been modeled as a competitive network phenomenon that engages strong feedback inhibition to silence the majority of GCs (de Almeida et al., 2009; Renno-Costa et al., 2010), consistent with strong activity-induced inhibition identified *in vivo* (Sloviter, 1991). *In vitro* work also demonstrates that perforant path stimulation preferentially recruits fast spiking interneurons that control the output of GCs in a frequency-dependent manner (Ewell and Jones, 2010). Numerous types of interneurons innervate mature GCs, including those defined by the location of their somato-dendritic and axonal domains such as molecular layer perforant path-associated (MOPP) cells and hilar commissural-association (HICAP) cells [reviewed by Houser (2007)], as well as interneurons defined by their physiological properties and neurochemical content such as PV^+ and CCK^+ basket cells (Hefft and Jonas, 2005), somatostatin-expressing cells (Zhang et al., 2009) and nitric-oxide expressing neurogliaform cells (Armstrong et al., 2011). It would be interesting to determine how specific interneuron subtypes contribute to sparse activation of GCs and behavioral performance of tasks that require information processing by the DG.

CONCLUSIONS

GABA-mediated signaling is involved in all stages of dentate GC maturation and function. Early in GC development, slow forms of GABA-mediated depolarization provide trophic signals necessary for regulating proliferation, differentiation, survival, and synaptic integration. Then during a transient time period between GABAergic excitation and the full development of fast synaptic inhibition, reduced inhibition contributes to the high responsiveness of young GCs to cortical inputs. Once GCs become fully mature, fast and powerful synaptic inhibition shapes GC output, allowing for the sparse population coding necessary for DG functions including pattern separation. Specific subtypes of interneurons, modes of GABAR activation, and GABAR subunits serve distinct roles in each stage of GC development, illustrating the diversity of GABAR signaling mechanisms and also raising many additional unanswered questions. For example, it is not clear what controls the sequence and timing of innervation by all the various DG interneuron subtypes, nor the timing of the switch in GABA signaling from trophic depolarization to predominantly inhibition. There is also very little known about postsynaptic $GABA_B$ receptor signaling, despite evidence that neurogenesis can be altered by blockade

of $GABA_B$ receptors (Felice et al., 2012). Immature GCs, however, do express functional presynaptic $GABA_B$ receptors that modulate presynaptic excitability (Cabezas et al., 2012). Finally, the extent to which GABAergic mechanisms contribute to regulation of neurogenesis in specific pathological or physiological conditions is just beginning to be explored (Li et al., 2009; Sun et al., 2009; Song et al., 2012). Future studies will provide new insights into how the diversity of GABAR mediated signaling in the DG contributes to dynamic regulation of GC development and excitability.

REFERENCES

Aimone, J. B., Deng, W., and Gage, F. H. (2011). Resolving new memories: a critical look at the dentate gyrus, adult neurogenesis, and pattern separation. *Neuron* 70, 589–596.

Alme, C. B., Buzzetti, R. A., Marrone, D. F., Leutgeb, J. K., Chawla, M. K., Schaner, M. J., et al. (2010). Hippocampal granule cells opt for early retirement. *Hippocampus* 20, 1109–1123.

Ambrogini, P., Cuppini, R., Lattanzi, D., Ciuffoli, S., Frontini, A., and Fanelli, M. (2010). Synaptogenesis in adult-generated hippocampal granule cells is affected by behavioral experiences. *Hippocampus* 20, 799–810.

Ambrogini, P., Lattanzi, D., Ciuffoli, S., Agostini, D., Bertini, L., Stocchi, V., et al. (2004). Morpho-functional characterization of neuronal cells at different stages of maturation in granule cell layer of adult rat dentate gyrus. *Brain Res.* 1017, 21–31.

Armstrong, C., Szabadics, J., Tamas, G., and Soltesz, I. (2011). Neurogliaform cells in the molecular layer of the dentate gyrus as feed-forward gamma-aminobutyric acidergic modulators of entorhinal-hippocampal interplay. *J. Comp. Neurol.* 519, 1476–1491.

Bartos, M., and Elgueta, C. (2012). Functional characteristics of parvalbumin- and cholecystokinin-expressing basket cells. *J. Physiol.* 590, 669–681.

Bartos, M., Vida, I., Frotscher, M., Geiger, J. R., and Jonas, P. (2001). Rapid signaling at inhibitory synapses in a dentate gyrus interneuron network. *J. Neurosci.* 21, 2687–2698.

Becker, S., and Wojtowicz, J. M. (2007). A model of hippocampal neurogenesis in memory and mood disorders. *Trends Cogn. Sci.* 11, 70–76.

Ben-Ari, Y. (2007). GABA excites and sculpts immature neurons well before delivery: modulation by GABA of the development of ventricular progenitor cells. *Epilepsy Curr.* 7, 167–169.

Ben-Ari, Y., Gaiarsa, J. L., Tyzio, R., and Khazipov, R. (2007). GABA: a pioneer transmitter that excites immature neurons and generates primitive oscillations. *Physiol. Rev.* 87, 1215–1284.

Ben-Ari, Y., Khazipov, R., Leinekugel, X., Caillard, O., and Gaiarsa, J. L. (1997). GABAA, NMDA and AMPA receptors: a developmentally regulated 'menage a trois.' *Trends Neurosci.* 20, 523–529.

Bonaguidi, M. A., Song, J., Ming, G. L., and Song, H. (2012). A unifying hypothesis on mammalian neural stem cell properties in the adult hippocampus. *Curr. Opin. Neurobiol.* 22, 754–761.

Bucurenciu, I., Kulik, A., Schwaller, B., Frotscher, M., and Jonas, P. (2008). Nanodomain coupling between Ca2+ channels and Ca2+ sensors promotes fast and efficient transmitter release at a cortical GABAergic synapse. *Neuron* 57, 536–545.

Cabezas, C., Irinopoulou, T., Gauvain, G., and Poncer, J. C. (2012). Presynaptic but not postsynaptic GABA signaling at unitary mossy fiber synapses. *J. Neurosci.* 32, 11835–11840.

Cameron, H. A., and McKay, R. D. (2001). Adult neurogenesis produces a large pool of new granule cells in the dentate gyrus. *J. Comp. Neurol.* 435, 406–417.

Capogna, M., and Pearce, R. A. (2011). GABA A, slow: causes and consequences. *Trends Neurosci.* 34, 101–112.

Chancey, J. H., Adlaf, E., Sapp, M., Pugh, P., Wadiche, J. I., Overstreet-Wadiche, L. (2012). "GABAergic depolarization promotes excitatory synaptogenesis on adult-generated neurons. Program No. 232.09," in *Neuroscience Meeting Planner,* (New Orleans, LA: Society for Neuroscience), [online].

Chandra, D., Jia, F., Liang, J., Peng, Z., Suryanarayanan, A., Werner, D. F., et al. (2006). GABAA receptor alpha 4 subunits mediate extrasynaptic inhibition in thalamus and dentate gyrus and the action of gaboxadol. *Proc. Natl. Acad. Sci. U.S.A.* 103, 15230–15235.

Chawla, M. K., Guzowski, J. F., Ramirez-Amaya, V., Lipa, P., Hoffman, K. L., Marriott, L. K., et al. (2005). Sparse, environmentally selective expression of Arc RNA in the upper blade of the rodent fascia dentata by brief spatial experience. *Hippocampus* 15, 579–586.

Chiang, P. H., Wu, P. Y., Kuo, T. W., Liu, Y. C., Chan, C. F., Chien, T. C., et al. (2012). GABA is depolarizing in hippocampal dentate granule cells of the adolescent and adult rats. *J. Neurosci.* 32, 62–67.

Clelland, C. D., Choi, M., Romberg, C., Clemenson, G. D. J., Fragniere, A., Tyers, P., et al. (2009). A functional role for adult hippocampal neurogenesis in spatial pattern separation. *Science* 325, 210–213.

Coulter, D. A., and Carlson, G. C. (2007). Functional regulation of the dentate gyrus by GABA-mediated inhibition. *Prog. Brain Res.* 163, 235–243.

Dayer, A. G., Ford, A. A., Cleaver, K. M., Yassaee, M., and Cameron, H. A. (2003). Short-term and long-term survival of new neurons in the rat dentate gyrus. *J. Comp. Neurol.* 460, 563–572.

de Almeida, L., Idiart, M., and Lisman, J. E. (2009). The input-output transformation of the hippocampal granule cells: from grid cells to place fields. *J. Neurosci.* 29, 7504–7512.

Deisseroth, K., and Malenka, R. C. (2005). GABA excitation in the adult brain: a mechanism for excitation- neurogenesis coupling. *Neuron* 47, 775–777.

Deisseroth, K., Singla, S., Toda, H., Monje, M., Palmer, T. D., and Malenka, R. C. (2004). Excitation-neurogenesis coupling in adult neural stem/progenitor cells. *Neuron* 42, 535–552.

Deng, W., Aimone, J. B., and Gage, F. H. (2010). New neurons and new memories: how does adult hippocampal neurogenesis affect learning and memory? *Nat. Rev. Neurosci.* 11, 339–350.

Dudek, F. E., and Sutula, T. P. (2007). Epileptogenesis in the dentate gyrus: a critical perspective. *Prog. Brain Res.* 163, 755–773.

Duveau, V., Laustela, S., Barth, L., Gianolini, F., Vogt, K. E., Keist, R., et al. (2011). Spatiotemporal specificity of GABAA receptor-mediated regulation of adult hippocampal neurogenesis. *Eur. J. Neurosci.* 34, 362–373.

Encinas, J. M., and Enikolopov, G. (2008). Identifying and quantitating neural stem and progenitor cells in the adult brain. *Methods Cell Biol.* 85, 243–272.

Eriksson, P. S., Perfilieva, E., Bjork-Eriksson, T., Alborn, A. M., Nordborg, C., Peterson, D. A., et al. (1998). Neurogenesis in the adult human hippocampus. *Nat. Med.* 4, 1313–1317.

Esposito, M. S., Piatti, V. C., Laplagne, D. A., Morgenstern, N. A., Ferrari, C. C., Pitossi, F. J., et al. (2005). Neuronal differentiation in the adult hippocampus recapitulates embryonic development. *J. Neurosci.* 25, 10074–10086.

Essrich, C., Lorez, M., Benson, J. A., Fritschy, J. M., and Luscher, B. (1998). Postsynaptic clustering of major GABAA receptor subtypes requires the gamma 2 subunit and gephyrin. *Nat. Neurosci.* 1, 563–571.

Ewell, L. A., and Jones, M. V. (2010). Frequency-tuned distribution of inhibition in the dentate gyrus. *J. Neurosci.* 30, 12597–12607.

Farrant, M., and Nusser, Z. (2005). Variations on an inhibitory theme: phasic and tonic activation of GABA(A) receptors. *Nat. Rev. Neurosci.* 6, 215–229.

Felice, D., O'Leary, O. F., Pizzo, R. C., and Cryan, J. F. (2012). Blockade of the GABA(B) receptor increases neurogenesis in the ventral but not dorsal adult hippocampus: relevance to antidepressant action. *Neuropharmacology* 63, 1380–1388.

Filippov, V., Kronenberg, G., Pivneva, T., Reuter, K., Steiner, B., Wang, L. P., et al. (2003). Subpopulation of nestin-expressing progenitor cells in the adult murine hippocampus shows electrophysiological and morphological characteristics of astrocytes. *Mol. Cell. Neurosci.* 23, 373–382.

Freund, T. F., and Buzsaki, G. (1996). Interneurons of the hippocampus. *Hippocampus* 6, 347–470.

Fukuda, S., Kato, F., Tozuka, Y., Yamaguchi, M., Miyamoto, Y., and Hisatsune, T. (2003). Two distinct subpopulations of nestin-positive cells in adult mouse dentate gyrus. *J. Neurosci.* 23, 9357–9366.

Ge, S., Goh, E. L., Sailor, K. A., Kitabatake, Y., Ming, G. L., and Song, H. (2006). GABA regulates synaptic integration of newly generated neurons in the adult brain. *Nature* 439, 589–593.

Ge, S., Pradhan, D. A., Ming, G. L., and Song, H. (2007a). GABA sets the

tempo for activity-dependent adult neurogenesis. *Trends Neurosci.* 30, 1–8.

Ge, S., Yang, C. H., Hsu, K. S., Ming, G. L., and Song, H. (2007b). A critical period for enhanced synaptic plasticity in newly generated neurons of the adult brain. *Neuron* 54, 559–566.

Hayes, N. L., and Nowakowski, R. S. (2002). Dynamics of cell proliferation in the adult dentate gyrus of two inbred strains of mice. *Brain Res. Dev. Brain Res.* 134, 77–85.

Hefft, S., and Jonas, P. (2005). Asynchronous GABA release generates long-lasting inhibition at a hippocampal interneuron-principal neuron synapse. *Nat. Neurosci.* 8, 1319–1328.

Herman, M. A., and Jahr, C. E. (2007). Extracellular glutamate concentration in hippocampal slice. *J. Neurosci.* 27, 9736–9741.

Hollrigel, G. S., and Soltesz, I. (1997). Slow kinetics of miniature IPSCs during early postnatal development in granule cells of the dentate gyrus. *J. Neurosci.* 17, 5119–5128.

Houser, C. R. (2007). Interneurons of the dentate gyrus: an overview of cell types, terminal fields and neurochemical identity. *Prog. Brain Res.* 163, 217–232.

Hu, H., Martina, M., and Jonas, P. (2010). Dendritic mechanisms underlying rapid synaptic activation of fast-spiking hippocampal interneurons. *Science* 327, 52–58.

Hutcheon, B., Fritschy, J. M., and Poulter, M. O. (2004). Organization of GABA receptor alpha-subunit clustering in the developing rat neocortex and hippocampus. *Eur. J. Neurosci.* 19, 2475–2487.

Hutcheon, B., Morley, P., and Poulter, M. O. (2000). Developmental change in GABAA receptor desensitization kinetics and its role in synapse function in rat cortical neurons. *J. Physiol.* 522(Pt 1), 3–17.

Imayoshi, I., Sakamoto, M., Ohtsuka, T., Takao, K., Miyakawa, T., Yamaguchi, M., et al. (2008). Roles of continuous neurogenesis in the structural and functional integrity of the adult forebrain. *Nat. Neurosci.* 11, 1153–1161.

Jagasia, R., Steib, K., Englberger, E., Herold, S., Faus-Kessler, T., Saxe, M., et al. (2009). GABA-cAMP response element-binding protein signaling regulates maturation and survival of newly generated neurons in the adult hippocampus. *J. Neurosci.* 29, 7966–7977.

Jones, M. V., Jonas, P., Sahara, Y., and Westbrook, G. L. (2001). Microscopic kinetics and energetics distinguish GABA(A) receptor agonists from antagonists. *Biophys. J.* 81, 2660–2670.

Jung, M. W., and McNaughton, B. L. (1993). Spatial selectivity of unit activity in the hippocampal granular layer. *Hippocampus* 3, 165–182.

Karayannis, T., Elfant, D., Huerta-Ocampo, I., Teki, S., Scott, R. S., Rusakov, D. A., et al. (2010). Slow GABA transient and receptor desensitization shape synaptic responses evoked by hippocampal neurogliaform cells. *J. Neurosci.* 30, 9898–9909.

Kee, N., Teixeira, C. M., Wang, A. H., and Frankland, P. W. (2007). Preferential incorporation of adult-generated granule cells into spatial memory networks in the dentate gyrus. *Nat. Neurosci.* 10, 355–362.

Kempermann, G., Kuhn, H. G., and Gage, F. H. (1997a). More hippocampal neurons in adult mice living in an enriched environment. *Nature* 386, 493–495.

Kempermann, G., Kuhn, H. G., and Gage, F. H. (1997b). Genetic influence on neurogenesis in the dentate gyrus of adult mice. *Proc. Natl. Acad. Sci. U.S.A.* 94, 10409–10414.

Kim, W. R., Christian, K., Ming, G. L., and Song, H. (2012). Time-dependent involvement of adult-born dentate granule cells in behavior. *Behav. Brain Res.* 227, 470–479.

Klausberger, T., and Somogyi, P. (2008). Neuronal diversity and temporal dynamics: the unity of hippocampal circuit operations. *Science* 321, 53–57.

Kullmann, D. M. (2000). Spillover and synaptic cross talk mediated by glutamate and GABA in the mammalian brain. *Prog. Brain Res.* 125, 339–351.

Lagace, D. C., Whitman, M. C., Noonan, M. A., Ables, J. L., DeCarolis, N. A., Arguello, A. A., et al. (2007). Dynamic contribution of nestin-expressing stem cells to adult neurogenesis. *J. Neurosci.* 27, 12623–12629.

Laplagne, D. A., Esposito, M. S., Piatti, V. C., Morgenstern, N. A., Zhao, C., van Praag, H., et al. (2006). Functional convergence of neurons generated in the developing and adult hippocampus. *PLoS Biol.* 4:e409. doi: 10.1371/journal.pbio.0040409

Laplagne, D. A., Kamienkowski, J. E., Esposito, M. S., Piatti, V. C., Zhao, C., Gage, F. H., et al. (2007). Similar GABAergic inputs in dentate granule cells born during embryonic and adult neurogenesis. *Eur. J. Neurosci.* 25, 2973–2981.

Li, G., Bien-Ly, N., Andrews-Zwilling, Y., Xu, Q., Bernardo, A., Ring, K., et al. (2009). GABAergic interneuron dysfunction impairs hippocampal neurogenesis in adult apolipoprotein E4 knockin mice. *Cell Stem Cell* 5, 634–645.

Li, Y., Aimone, J. B., Xu, X., Callaway, E. M., and Gage, F. H. (2012). Development of GABAergic inputs controls the contribution of maturing neurons to the adult hippocampal network. *Proc. Natl. Acad. Sci. U.S.A.* 109, 4290–4295.

Liu, Y. B., Ye, G. L., Liu, X. S., Pasternak, J. F., and Trommer, B. L. (1998). GABAA currents in immature dentate gyrus granule cells. *J. Neurophysiol.* 80, 2255–2267.

LoTurco, J. J., Owens, D. F., Heath, M. J., Davis, M. B., and Kriegstein, A. R. (1995). GABA and glutamate depolarize cortical progenitor cells and inhibit DNA synthesis. *Neuron* 15, 1287–1298.

Maccaferri, G., and Lacaille, J. C. (2003). Interneuron diversity series: hippocampal interneuron classifications–making things as simple as possible, not simpler. *Trends Neurosci.* 26, 564–571.

Marin-Burgin, A., Mongiat, L. A., Pardi, M. B., and Schinder, A. F. (2012). Unique processing during a period of high excitation/inhibition balance in adult-born neurons. *Science* 335, 1238–1242.

Markwardt, S. J., Dieni, C. V., Wadiche, J. I., and Overstreet-Wadiche, L. (2011). Ivy/neurogliaform interneurons coordinate activity in the neurogenic niche. *Nat. Neurosci.* 14, 1407–1409.

Markwardt, S. J., Wadiche, J. I., and Overstreet-Wadiche, L. S. (2009). Input-specific GABAergic signaling to newborn neurons in adult dentate gyrus. *J. Neurosci.* 29, 15063–15072.

Marr, D. (1971). Simple memory: a theory for archicortex. *Philos. Trans. R. Soc. Lond. B Biol. Sci.* 262, 23–81.

Masiulis, I., Yun, S., and Eisch, A. J. (2011). The interesting interplay between interneurons and adult hippocampal neurogenesis. *Mol. Neurobiol.* 44, 287–302.

Michelson, H. B., and Wong, R. K. (1994). Synchronization of inhibitory neurones in the guinea-pig hippocampus *in vitro*. *J. Physiol.* 477, 35–45.

Miles, R., Toth, K., Gulyas, A. I., Hajos, N., and Freund, T. F. (1996). Differences between somatic and dendritic inhibition in the hippocampus. *Neuron* 16, 815–823.

Ming, G. L., and Song, H. (2011). Adult neurogenesis in the mammalian brain: significant answers and significant questions. *Neuron* 70, 687–702.

Mongiat, L. A., Esposito, M. S., Lombardi, G., and Schinder, A. F. (2009). Reliable activation of immature neurons in the adult hippocampus. *PLoS ONE* 4:e5320. doi: 10.1371/journal.pone.0005320

Mongiat, L. A., and Schinder, A. F. (2011). Adult neurogenesis and the plasticity of the dentate gyrus network. *Eur. J. Neurosci.* 33, 1055–1061.

Mozrzymas, J. W. (2004). Dynamism of GABA(A) receptor activation shapes the "personality" of inhibitory synapses. *Neuropharmacology* 47, 945–960.

Nakashiba, T., Cushman, J. D., Pelkey, K. A., Renaudineau, S., Buhl, D. L., McHugh, T. J., et al. (2012). Young dentate granule cells mediate pattern separation, whereas old granule cells facilitate pattern completion. *Cell* 149, 188–201.

Neunuebel, J. P., and Knierim, J. J. (2012). Spatial firing correlates of physiologically distinct cell types of the rat dentate gyrus. *J. Neurosci.* 32, 3848–3858.

Nusser, Z., and Mody, I. (2002). Selective modulation of tonic and phasic inhibitions in dentate gyrus granule cells. *J. Neurophysiol.* 87, 2624–2628.

Nusser, Z., Roberts, J. D., Baude, A., Richards, J. G., Sieghart, W., and Somogyi, P. (1995). Immunocytochemical localization of the alpha 1 and beta 2/3 subunits of the GABAA receptor in relation to specific GABAergic synapses in the dentate gyrus. *Eur. J. Neurosci.* 7, 630–646.

Olah, S., Fule, M., Komlosi, G., Varga, C., Baldi, R., Barzo, P., et al. (2009). Regulation of cortical microcircuits by unitary GABA-mediated volume transmission. *Nature* 461, 1278–1281.

Overstreet, L. S., Hentges, S. T., Bumaschny, V. F., de Souza, F. S., Smart, J. L., Santangelo, A. M., et al. (2004). A transgenic marker for newly born granule cells in dentate gyrus. *J. Neurosci.* 24, 3251–3259.

Overstreet, L. S., Jones, M. V., and Westbrook, G. L. (2000). Slow desensitization regulates the availability of synaptic GABA(A) receptors. *J. Neurosci.* 20, 7914–7921.

Overstreet, L. S., and Westbrook, G. L. (2001). Paradoxical reduction of synaptic inhibition by vigabatrin. *J. Neurophysiol.* 86, 596–603.

Overstreet, L. S., and Westbrook, G. L. (2003). Synapse density regulates independence at unitary inhibitory synapses. *J. Neurosci.* 23, 2618–2626.

Overstreet-Wadiche, L., Bromberg, D. A., Bensen, A. L., and Westbrook, G. L. (2005). GABAergic signaling to newborn neurons in dentate gyrus. *J. Neurophysiol.* 94, 4528–4532.

Overstreet-Wadiche, L. S., Bensen, A. L., and Westbrook, G. L. (2006). Delayed development of adult-generated granule cells in dentate gyrus. *J. Neurosci.* 26, 2326–2334.

Overstreet-Wadiche, L. S., and Westbrook, G. L. (2006). Functional maturation of adult-generated granule cells. *Hippocampus* 16, 208–215.

Owens, D. F., Liu, X., and Kriegstein, A. R. (1999). Changing properties of GABA(A) receptor-mediated signaling during early neocortical development. *J. Neurophysiol.* 82, 570–583.

Peng, Z., Hauer, B., Mihalek, R. M., Homanics, G. E., Sieghart, W., Olsen, R. W., et al. (2002). GABA(A) receptor changes in delta subunit-deficient mice: altered expression of alpha4 and gamma2 subunits in the forebrain. *J. Comp. Neurol.* 446, 179–197.

Piatti, V. C., Esposito, M. S., and Schinder, A. F. (2006). The timing of neuronal development in adult hippocampal neurogenesis. *Neuroscientist* 12, 463–468.

Pugh, P., Adlaf, E., Zhao, C. S., Markwardt, S., Gavin, C., Wadiche, J., et al. (2011). Enhanced integration of newborn neurons after neonatal insults. *Front. Neurosci.* 5:45. doi: 10.3389/fnins.2011.00045

Rajasekaran, K., Joshi, S., Sun, C., Mtchedlishvilli, Z., and Kapur, J. (2010). Receptors with low affinity for neurosteroids and GABA contribute to tonic inhibition of granule cells in epileptic animals. *Neurobiol. Dis.* 40, 490–501.

Renno-Costa, C., Lisman, J. E., and Verschure, P. F. (2010). The mechanism of rate remapping in the dentate gyrus. *Neuron* 68, 1051–1058.

Richerson, G. B., and Wu, Y. (2003). Dynamic equilibrium of neurotransmitter transporters: not just for reuptake anymore. *J. Neurophysiol.* 90, 1363–1374.

Rivera, C., Voipio, J., Payne, J. A., Ruusuvuori, E., Lahtinen, H., Lamsa, K., et al. (1999). The K+/Cl-co-transporter KCC2 renders GABA hyperpolarizing during neuronal maturation. *Nature* 397, 251–255.

Sahay, A., Scobie, K. N., Hill, A. S., O'Carroll, C. M., Kheirbek, M. A., Burghardt, N. S., et al. (2011). Increasing adult hippocampal neurogenesis is sufficient to improve pattern separation. *Nature* 472, 466–470.

Sauer, J. F., Struber, M., and Bartos, M. (2012). Interneurons provide circuit-specific depolarization and hyperpolarization. *J. Neurosci.* 32, 4224–4229.

Schmidt-Hieber, C., Jonas, P., and Bischofberger, J. (2004). Enhanced synaptic plasticity in newly generated granule cells of the adult hippocampus. *Nature* 429, 184–187.

Schweizer, C., Balsiger, S., Bluethmann, H., Mansuy, I. M., Fritschy, J. M., Mohler, H., et al. (2003). The gamma 2 subunit of GABA(A) receptors is required for maintenance of receptors at mature synapses. *Mol. Cell. Neurosci.* 24, 442–450.

Seri, B., Garcia-Verdugo, J. M., McEwen, B. S., and Alvarez-Buylla, A. (2001). Astrocytes give rise to new neurons in the adult mammalian hippocampus. *J. Neurosci.* 21, 7153–7160.

Sernagor, E., Chabrol, F., Bony, G., and Cancedda, L. (2010). GABAergic control of neurite outgrowth and remodeling during development and adult neurogenesis: general rules and differences in diverse systems. *Front. Cell. Neurosci.* 4:11. doi: 10.3389/fncel.2010.00011

Sierra, A., Encinas, J. M., Deudero, J. J., Chancey, J. H., Enikolopov, G., Overstreet-Wadiche, L. S., et al. (2010). Microglia shape adult hippocampal neurogenesis through apoptosis-coupled phagocytosis. *Cell Stem Cell* 7, 483–495.

Sloviter, R. S. (1991). Feedforward and feedback inhibition of hippocampal principal cell activity evoked by perforant path stimulation: GABA-mediated mechanisms that regulate excitability *in vivo*. *Hippocampus* 1, 31–40.

Smith, T. C., and Jahr, C. E. (2002). Self-inhibition of olfactory bulb neurons. *Nat. Neurosci.* 5, 760–766.

Snyder, J. S., Choe, J. S., Clifford, M. A., Jeurling, S. I., Hurley, P., Brown, A., et al. (2009). Adult-born hippocampal neurons are more numerous, faster maturing, and more involved in behavior in rats than in mice. *J. Neurosci.* 29, 14484–14495.

Soltesz, I., Smetters, D. K., and Mody, I. (1995). Tonic inhibition originates from synapses close to the soma. *Neuron* 14, 1273–1283.

Song, J., Zhong, C., Bonaguidi, M. A., Sun, G. J., Hsu, D., Gu, Y., et al. (2012). Neuronal circuitry mechanism regulating adult quiescent neural stem-cell fate decision. *Nature* 489, 150–154.

Staley, K. J., and Mody, I. (1992). Shunting of excitatory input to dentate gyrus granule cells by a depolarizing GABAA receptor-mediated postsynaptic conductance. *J. Neurophysiol.* 68, 197–212.

Stell, B. M., Brickley, S. G., Tang, C. Y., Farrant, M., and Mody, I. (2003). Neuroactive steroids reduce neuronal excitability by selectively enhancing tonic inhibition mediated by delta subunit-containing GABAA receptors. *Proc. Natl. Acad. Sci. U.S.A.* 100, 14439–14444.

Stone, S. S., Teixeira, C. M., Zaslavsky, K., Wheeler, A. L., Martinez-Canabal, A., Wang, A. H., et al. (2011). Functional convergence of developmentally and adult-generated granule cells in dentate gyrus circuits supporting hippocampus-dependent memory. *Hippocampus* 21, 1348–1362.

Sun, B., Halabisky, B., Zhou, Y., Palop, J. J., Yu, G., Mucke, L., et al. (2009). Imbalance between GABAergic and glutamatergic transmission impairs adult neurogenesis in an animal model of Alzheimer's disease. *Cell Stem Cell* 5, 624–633.

Sun, C., Sieghart, W., and Kapur, J. (2004). Distribution of alpha1, alpha4, gamma2, and delta subunits of GABAA receptors in hippocampal granule cells. *Brain Res.* 1029, 207–216.

Szabadics, J., Tamas, G., and Soltesz, I. (2007). Different transmitter transients underlie presynaptic cell type specificity of GABAA, slow and GABAA, fast. *Proc. Natl. Acad. Sci. U.S.A.* 104, 14831–14836.

Toni, N., Teng, E. M., Bushong, E. A., Aimone, J. B., Zhao, C., Consiglio, A., et al. (2007). Synapse formation on neurons born in the adult hippocampus. *Nat. Neurosci.* 10, 727–734.

Tozuka, Y., Fukuda, S., Namba, T., Seki, T., and Hisatsune, T. (2005). GABAergic excitation promotes neuronal differentiation in adult hippocampal progenitor cells. *Neuron* 47, 803–815.

Tyzio, R., Represa, A., Jorquera, I., Ben-Ari, Y., Gozlan, H., and Aniksztejn, L. (1999). The establishment of GABAergic and glutamatergic synapses on CA1 pyramidal neurons is sequential and correlates with the development of the apical dendrite. *J. Neurosci.* 19, 10372–10382.

Tzingounis, A. V., and Wadiche, J. I. (2007). Glutamate transporters: confining runaway excitation by shaping synaptic transmission. *Nat. Rev. Neurosci.* 8, 935–947.

van Praag, H., Kempermann, G., and Gage, F. H. (1999). Running increases cell proliferation and neurogenesis in the adult mouse dentate gyrus. *Nat. Neurosci.* 2, 266–270.

Wang, L. P., Kempermann, G., and Kettenmann, H. (2005). A subpopulation of precursor cells in the mouse dentate gyrus receives synaptic GABAergic input. *Mol. Cell. Neurosci.* 29, 181–189.

Wang, S., Scott, B. W., and Wojtowicz, J. M. (2000). Heterogenous properties of dentate granule neurons in the adult rat. *J. Neurobiol.* 42, 248–257.

Waterhouse, E. G., An, J. J., Orefice, L. L., Baydyuk, M., Liao, G. Y., Zheng, K., et al. (2012). BDNF promotes differentiation and maturation of adult-born neurons through GABAergic transmission. *J. Neurosci.* 32, 14318–14330.

Zhang, N., Wei, W., Mody, I., and Houser, C. R. (2007). Altered localization of GABA(A) receptor subunits on dentate granule cell dendrites influences tonic and phasic inhibition in a mouse model of epilepsy. *J. Neurosci.* 27, 7520–7531.

Zhang, W., Yamawaki, R., Wen, X., Uhl, J., Diaz, J., Prince, D. A., et al. (2009). Surviving hilar somatostatin interneurons enlarge, sprout axons, and form new synapses with granule cells in a mouse model of temporal lobe epilepsy. *J. Neurosci.* 29, 14247–14256.

Conflict of Interest Statement: The authors declare that the research was conducted in the absence of any commercial or financial relationships that could be construed as a potential conflict of interest.

Received: 22 October 2012; accepted: 11 December 2012; published online: 08 January 2013.

Citation: Dieni CV, Chancey JH and Overstreet-Wadiche LS (2013) Dynamic functions of GABA signaling during granule cell maturation. Front. Neural Circuits ***6****:113. doi: 10.3389/fncir.2012.00113*

frontiers in
NEURAL CIRCUITS

REVIEW ARTICLE
published: 25 February 2013
doi: 10.3389/fncir.2013.00015

Functional circuits of new neurons in the dentate gyrus

Carmen Vivar and Henriette van Praag*

Neuroplasticity and Behavior Unit, Laboratory of Neurosciences, Intramural Research Program, National Institute on Aging, National Institutes of Health, Baltimore, MD, USA

Edited by:
John Lisman, Brandeis University, USA

Reviewed by:
Perry Bartlett, University of Queensland, Australia
Michael Drew, University of Texas at Austin, USA

****Correspondence:***
Henriette van Praag, Neuroplasticity and Behavior Unit, Laboratory of Neurosciences, Biomedical Research Center, National Institute on Aging, National Institutes of Health, Suite 100, 251 Bayview Blvd., Baltimore, MD 21224, USA.
e-mail: vanpraagh@mail.nih.gov

The hippocampus is crucial for memory formation. New neurons are added throughout life to the hippocampal dentate gyrus (DG), a brain area considered important for differential storage of similar experiences and contexts. To better understand the functional contribution of adult neurogenesis to pattern separation processes, we recently used a novel synapse specific trans-neuronal tracing approach to identify the (sub) cortical inputs to new dentate granule cells (GCs). It was observed that newly born neurons receive sequential innervation from structures important for memory function. Initially, septal-hippocampal cells provide input to new neurons, including transient innervation from mature GCs as well as direct feedback from area CA3 pyramidal neurons. After about 1 month perirhinal (PRH) and lateral entorhinal cortex (LEC), brain areas deemed relevant to integration of novel sensory and environmental information, become substantial input to new GCs. Here, we review the developmental time-course and proposed functional relevance of new neurons, within the context of their unique neural circuitry.

Keywords: dentate gyrus, adult neurogenesis, rabies virus, retrograde trans-neuronal tracing, learning and memory, area CA3, lateral entorhinal cortex, pattern separation

INTRODUCTION

The hippocampus, a brain area important for the acquisition of new memories (Scoville and Milner, 1957; Squire et al., 2004), consists of three subfields: dentate gyrus (DG), area CA3 and area CA1. Information is considered to be processed from entorhinal cortex (EC) to DG, DG to CA3 pyramidal cells, and from CA3 to CA1 pyramidal cells to be ultimately stored in cortex, forming the "tri-synaptic hippocampal circuit" (Amaral and Witter, 1989). Each of these regions has specific cell types and plasticity contributing to learning and memory processes (Nakazawa et al., 2002, 2004; Gold and Kesner, 2005; Kesner, 2007). The DG is of particular interest as new dentate granule cells (GCs) are generated continuously in the adult mammalian brain (Altman and Das, 1965; Cameron and McKay, 2001; Ming and Song, 2011). Over the past decade, the maturation, integration into the hippocampal network, and the functional relevance of new GCs has been researched extensively (for review see Zhao et al., 2008; Suh et al., 2009; Deng et al., 2010; Ming and Song, 2011). Adult neurogenesis is considered important for regulation of cognition and mood (Zhao et al., 2008), and has been proposed as a mechanism underlying efficient cortical storage of new memories (Kitamura et al., 2009). It has also been suggested that new neurons contribute to pattern separation (Clelland et al., 2009; Creer et al., 2010; Guo et al., 2011; Sahay et al., 2011; Nakashiba et al., 2012), the distinct encoding of very similar events or stimuli, a function attributed to the DG (Marr, 1971; Gilbert et al., 2001; Leutgeb et al., 2007). However, until recently, relatively little was known about the specific circuitry into which the new neurons are integrated, which may provide further clues to their functional role. Using a novel combination of viral vectors (Vivar et al., 2011, 2012), we found that newborn neurons have unique afferents. In particular, new GCs receive inputs from mature GCs, a direct "back-projection" from area CA3 and predominant innervation from the lateral (LEC) rather than the medial (MEC) entorhinal cortex. LEC and MEC provide different types of information to the hippocampus (for review see Knierim et al., 2006; McNaughton et al., 2006; Lisman, 2007). Stronger input from LEC (information about external cues and context) than from MEC (spatial position information) may facilitate the role of newly born neurons in pattern separation. The potentially important role of new neurons in this process as well as the time-course of their physiological and anatomical integration into the hippocampal circuitry is the focus of this review.

METHODS RELEVANT TO ADULT NEUROGENESIS

The initial studies that suggested the adult brain could generate new neurons were largely ignored. In the 1960s Joseph Altman and colleagues used tritiated thymidine autoradiography to label dividing cells, but could not prove conclusively that these were new DG neurons rather than glia (Altman and Das, 1965). Subsequently, combined electron microscopy and tritiated thymidine labeling was used to show that labeled cells in the rat DG have ultrastructural characteristics of neurons, such as dendrites and synapses (Kaplan and Hinds, 1977). An important advance was the use of the thymidine analog, 5-bromo-2′-deoxyuridine (BrdU), which is incorporated into the genome of dividing cells, and can be combined with specific neural markers (Kuhn et al., 1996). Retroviral methods, selective for dividing cells (**Figure 1**), can be used for birth-dating, genetic marking, electron microscopy, and electrophysiology, and have provided strong evidence that newborn neurons in the adult mammalian brain are functional and synaptically integrated (van Praag et al., 2002; Carleton et al., 2003; Ming and Song, 2005). Furthermore, modulation of neurogenesis using x-irradiation, pharmacology,

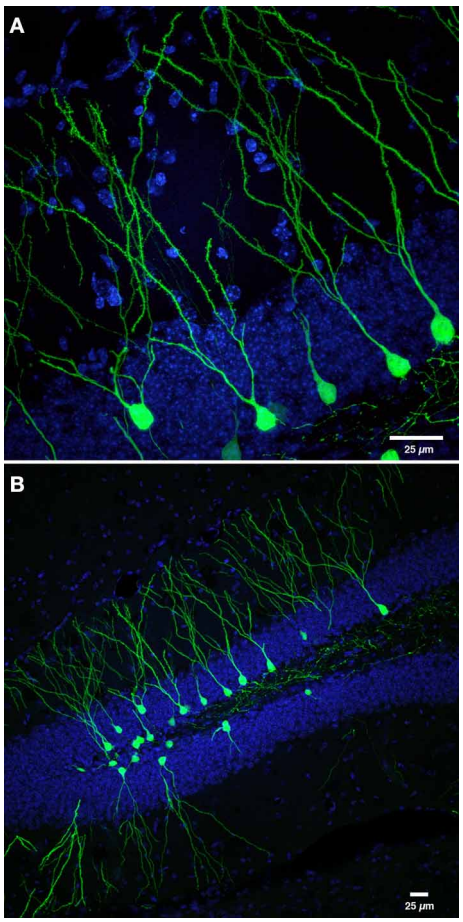

FIGURE 1 | Retroviral labeling of newborn neurons in the DG. **(A)** Photomicrograph shows retrovirally labeled newborn dentate GCs (pCAGGFP, Zhao et al., 2006) expressing green fluorescent protein (GFP) throughout the entire cell, at 42 days post-retroviral injection (dpi). **(B)** Low power overview of new neurons shown in panel **(A)**, expressing cytoplasmic GFP in the DG at 42 dpi. Nuclei are labeled with 4′-6-diaminodino-2-phenylindole (DAPI), blue. Scale bar, 25 μm.

environmental factors, and transgenic mouse models has provided important functional insights about the possible role of these new neurons in the adult brain. Reduction of neurogenesis generally results in deficient memory function whereas increased cell genesis is associated with enhanced cognition (for review see Zhao et al., 2008; Deng et al., 2010).

All of the above methods, however, do not reveal the circuitry into which the newborn GCs are integrated. Network analysis is essential for understanding how new neurons are activated, as well as comprehending the functional significance of adult neurogenesis. To overcome this limitation, we recently used a novel combination of retroviral labeling with rabies virus as a retrograde tracer (**Figures 2** and **3**). Rabies virus as a trans-neuronal circuit tracer offers several advantages over other conventional neuronal tracers (for review see Callaway, 2008; Ugolini, 2010, 2011). Rabies virus propagates by trans-neuronal transfer exclusively in retrograde direction. In particular, intracellular transport of rabies virus after replication is only directed to neuronal dendrites (Ugolini, 1995), and subsequently by retrograde trans-neuronal transfer to presynaptic terminals of higher order neurons (Callaway, 2008; Ugolini, 2010, 2011). Rabies virus propagation occurs at chemical synapses, regardless of their neurotransmitters, synaptic strength, termination site, or distance (Ugolini, 1995, 2010), but not via gap junctions (Tang et al., 1999) or cell-to-cell spread (volume transmission) (Tang et al., 1999; Ugolini, 2010). The mechanisms underlying selective retrograde transport of the rabies virus are not fully understood, however, it has been proposed that several presynaptic elements can act as rabies virus receptors, including the p75 neurotrophin receptor, the nicotinic acetylcholine receptor, and NCAM, among other, as of yet unidentified receptors. The large variety of neurons infected by rabies virus suggests that presynaptic receptors for rabies virus are ubiquitously distributed in the central nervous system (Ugolini, 2010).

Modifications of the rabies virus genome have made it possible to control synaptic spread, reduce pathogenicity, infect select cell types, and add optogenetic tools (Osakada et al., 2011). Trans-synaptic retrograde spread of rabies virus has been proposed to be critically dependent on rabies glycoprotein (Rgp; Etessami et al., 2000). Recently, a glycoprotein-deleted (ΔG) variant of the SAD-B19 strain of rabies virus (SADΔG, Mebatsion et al., 1996) in which Rgp was exchanged for a fluorophore such as green fluorescent protein (GFP) or MCherry (MCh) was developed. Providing exogenous Rgp to infected cells allows the virus to cross one synapse, enabling the selective study of infected first-order afferents (Wickersham et al., 2007a). Further specificity can be achieved by pseudotyping the ΔG rabies virus with an avian viral glycoprotein (EnvA) to selectively infect mammalian neurons modified to express the, typically foreign, avian TVA receptor (Wickersham et al., 2007b; for review see Ginger et al., 2013). Monosynaptic trans-neuronal tracing with rabies virus has been applied to analyze the properties of neural circuits in different parts of the central nervous system such as the amygdala (Haubensak et al., 2010), olfactory bulb (Arenkiel et al., 2011; Miyamichi et al., 2011), visual cortex (Wickersham et al., 2007b; Marshel et al., 2010; Rancz et al., 2011), barrel cortex (Wall et al., 2010), cerebellum (Wall et al., 2010), ventral tegmental area (Lammel et al., 2012; Watabe-Uchida et al., 2012), spinal cord (Stepien et al., 2010), and retina (Yonehara et al., 2011). Recently, Arenkiel et al. (2011) applied the EnvA-TVA methodology to identify inputs to newborn olfactory bulb neurons, the only other brain area considered to generate new neurons under basal conditions (Ming and Song, 2011). Specifically, a conditional reporter mouse was generated, harboring a Cre/LoxP-dependent allele driving cytosolic tdTomato expression upon electroporation of a plasmid containing Rgp, TVA, and Cre, which was introduced on postnatal day 2 into the lateral ventricles. Thirty days later EnvA pseudotyped rabies virus was injected to trace connections to the tdTomato, TVA and Rgp expressing cells. It was shown that early postnatal-born GCs of the olfactory bulb make synaptic connections with cortical inputs and multiple olfactory bulb cell types which could be modified by olfactory experience.

We applied the powerful EnvA-TVA tracing method to map the inputs to newborn dentate GCs by developing a selective and direct dual virus approach that can be used in wild-type

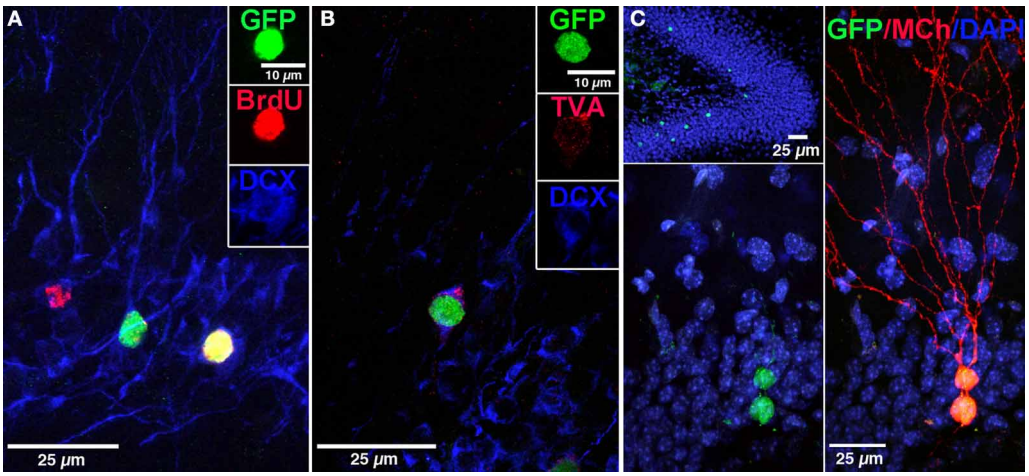

FIGURE 2 | Labeling of "starter" neural progenitor cells. **(A)** Photomicrograph showing retrovirally labeled newborn GCs (pRV-SYN-GTRgp) expressing nucleus-localized histone-tagged green fluorescent protein (hGFP), avian TVA receptor, and rabies glycoprotein under control of the synapsin promoter. Co-labeling of $hGFP^+$ cells (green), with bromodeoxyuridine (BrdU, red), and the immature neuronal marker doublecortin (DCX, blue). Insert shows a new GC expressing all three markers (yellow). **(B)** Confocal image of $hGFP^+$ cell (green) co-labeled with DCX (blue) and the TVA receptor (red). **(C)** Overview of the DG showing newborn GCs labeled with retrovirus expressing nuclear hGFP (green, top). Magnification of the GC layer shows dual virus labeled newborn "starter" cells with retrovirus expressing hGFP (green) and EnvA pseudotyped rabies virus expressing MCherry (MCh, red) at 30 dpi. Scale bar, 25 μm. Nuclei labeled with DAPI (blue). From Vivar et al. (2012); Reprinted with permission from Macmillan Publishers Ltd.: Nature Communications Copyright 2012.

animals. Monosynaptic rabies virus-mediated retrograde tracing was combined with retroviral labeling (Vivar et al., 2011, 2012). Specifically, Murine Maloney leukemia virus (MMLV) retrovirus which only infects dividing cells (Lewis and Emerman, 1994; van Praag et al., 2002) was modified to express nuclear GFP, TVA receptor and Rgp. This vector was used to label proliferating neural progenitor cells in the DG that are destined to become neurons by using the neuron-specific synapsin promoter. Double-labeling of GFP^+ cells with the immature neuronal marker doublecortin in the majority of the labeled cells at 15 days postinjection, supported the specificity of the retrovirus (**Figure 2A**). Following an interval of 21, 30, 60, or 90 days after retroviral injection during which the progenitor cells matured into GC neurons, EnvA pseudotyped rabies virus (EnvA-ΔG-MCh) was injected into the DG and mice were perfused 1 week thereafter. This rabies virus selectively infects new neurons expressing the TVA receptor, which were termed "starter cells" (**Figures 2B**,**C**). The rabies virus is then complemented with Rgp provided by the retrovirus in the new neurons. The virus crosses synapses, labeling presynaptic neurons, and because the traced cells lack Rgp, the virus does not spread any further, labeling only first order inputs (**Figure 3**). Indeed, when Rgp was deleted from the retroviral vector and subsequent infection with EnvA-ΔG-MCh was performed, double-labeled new GCs (GFP + MCh) were observed but not traced cells, indicating Rgp is required for the system to work. Altogether, this novel approach has allowed us to evaluate how the anatomy of newborn neuron circuitry changes over time and to identify the neurochemical characteristics of their specific inputs. Moreover, as rabies virus does not compromise cell viability, at least for 2 weeks after infection, characterization of the physiology and synaptic plasticity of afferent inputs can be performed (Wickersham et al., 2007a; Callaway, 2008; Vivar et al., 2012).

TIME-COURSE OF CIRCUITRY DEVELOPMENT

It is generally considered that it takes about 1 month for proliferating progenitor cells to develop into new GC neurons and that full maturation takes several months (Zhao et al., 2008). During the first month, subgranular zone neural stem cells (Type I cells) and progenitor cells (Type II, Type III) have been shown to go through stages with distinct morphological, physiological and molecular characteristics. Newborn neurons are considered to originate from Type I neural stem cells in the subgranular layer. These cells have radial processes extending into the molecular layer, are deemed relatively quiescent and express markers such as nestin, glial fibrillary acidic protein (GFAP) and Sox2. Activation of Type I neural stem cells is considered to be mediated by niche factors such as Notch or bone morphogenic protein (Lugert et al., 2010; Mira et al., 2010) and the neurotransmitter GABA (Song et al., 2012). Type I cells likely give rise to Type II progenitor cells under the influence of additional local niche factors [fibroblast growth factor-2 (Jin et al., 2003), sonic hedgehog (Lai et al., 2003), vascular endothelial growth factor (Cao et al., 2004), and Wnt7a (Qu et al., 2010)]. A subset of the cells retain neural stem cell markers (such as nestin and Sox2), whereas the remaining cells begin to differentiate along a neuronal lineage becoming NeuroD and Prox1 positive, progressing into Type III neuroblasts expressing markers such as PSA-NCAM, calretinin and doublecortin before maturing into GCs (Encinas et al., 2006; Suh et al., 2007, 2009; Lugert et al., 2010). While 1 month later these cells have the morphological and physiological characteristics of GCs, their full maturation and incorporation into functional circuits appears to be a prolonged process. Indeed, newborn neuron physiology, plasticity, and circuitry may continually evolve for at least 3 months (**Figure 4**).

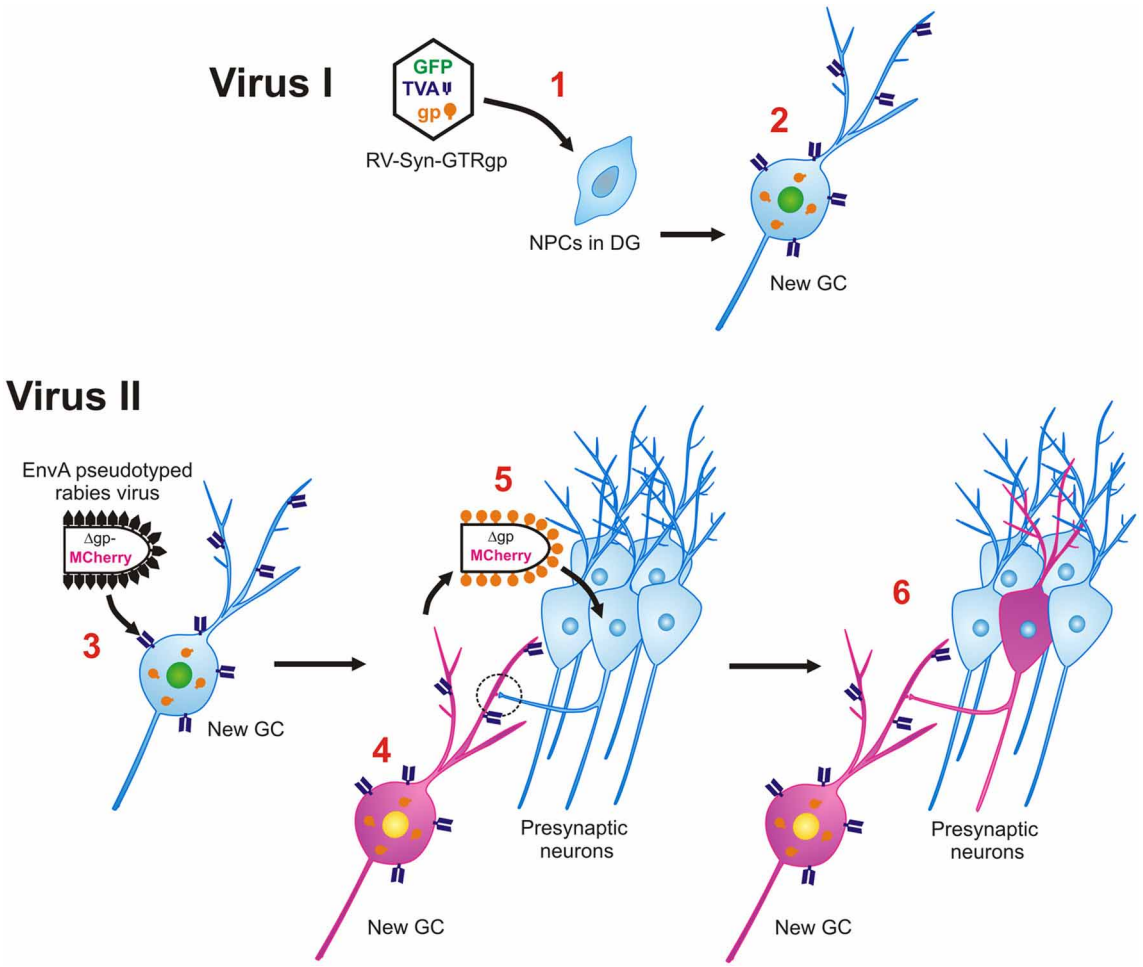

FIGURE 3 | Monosynaptic retrograde tracing of inputs to new GCs. Virus I, Retroviral labeling. 1. Retrovirus (RV-SYN-GTRgp) expressing nucleus-localized histone-tagged green fluorescent protein (hGFP), avian TVA receptor, and rabies glycoprotein (gp) under control of the synapsin promoter infect proliferating neural progenitor cells (NPCs) in the DG. **2**. The retrovirally labeled NPCs differentiate into newborn GCs over time and express hGFP, TVA and gp. **Virus II, Rabies virus. 3**. Avian envelope glycoprotein EnvA pseudotyped rabies virus, in which rabies gp was replaced with MCherry (EnvA-ΔG-MCh) is injected into the same DG at different time-points after retroviral labeling (21–90 dpi). Through interaction between EnvA glycoprotein and its receptor, TVA, pseudotyped rabies virus can selectively infect newborn GCs. **4**. EnvA-ΔG-MCh rabies virus is complemented with rabies gp provided by the retrovirus and MCherry is expressed in the cytoplasm. **5**. The rabies virus spreads trans-synaptically to presynaptic neurons connected to the new GC. **6**. Only neurons synaptically connected are labeled and express MCherry. The traced cells lack rabies gp, therefore this virus will not spread any further.

FIRST WEEK

During the first week of the maturation process, neuronal lineage-committed Type II cells begin to migrate into the inner GC layer of the DG. Initially, there are no clear dendritic or axonal processes and patch-clamp recordings indicate that the cells do not show spontaneous synaptic activity (Esposito et al., 2005). However, these cells are tonically activated by ambient GABA. Indeed, upon recording from retrovirally labeled cells 3 days after infection a tonic inward excitatory current could be selectively blocked by bicuculline, suggesting non-synaptic activation of $GABA_A$ receptors (Ge et al., 2006).

SECOND WEEK

During the second week, the cells extend spineless dendrites that reach the inner molecular layer (I-ML) 10 days after retroviral injection (dpi), and the middle molecular layer (M-ML) at 14 dpi. In addition, mossy fiber axons are estimated to begin to form synapses with pyramidal cells at 10–14 dpi (Zhao et al., 2006). The physiological properties of the cells are immature with cells firing few action potentials with a small amplitude (Esposito et al., 2005; Vivar et al., 2012). GABA continues to be depolarizing (Lo Turco and Kriegstein, 1991). However, at this time-point hilar interneurons are considered to provide synaptic input to newborn neurons (Tozuka et al., 2005; Ge et al., 2006). The depolarizing action of GABA depends on the Na-K-2Cl co-transporter (NKCC1). NKCC1 maintains high $[Cl^-]_i$ and regulates the resting membrane potential of developing neurons (Ge et al., 2006; Mejia-Gervacio et al., 2011). A recent study shows that knockdown of NKCC1 *in vivo* reduces DG progenitor cell proliferation and delays dendritic development (Young et al., 2012).

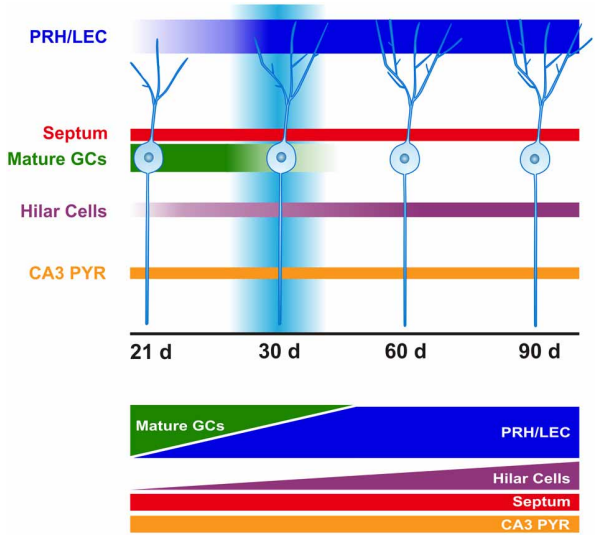

FIGURE 4 | Time course of afferent innervation of newborn GCs. Schematic representation of monosynaptic inputs to the newborn GCs at time-points evaluated (21, 30, 60, and 90 days after retroviral infection). At 21 days (d), newborn GCs mainly receive connections from mature GCs. This input gradually shifts from mature GCs to cortex following strengthening of afferents from the perirhinal (PRH) and lateral entorhinal cortex (LEC). Increased hilar cell (mossy cells and interneurons) innervation is observed over time. Convergence of excitatory afferents onto the newborn GCs around 30 days correlates with transiently enhanced new neuron excitability and plasticity. Innervation from septum and area CA3 pyramidal cells (PYR) remains constant over time.

Around this time-point, the cells go through a critical period. Indeed, more than 50% of adult born granule neurons are lost about 2 weeks into the maturation process (Cameron et al., 1993; Dayer et al., 2003). Around 14 dpi, glutamatergic signaling through NMDA receptors may be critical for the survival and integration of newborn neurons (Tashiro et al., 2006). Since the main glutamatergic input to newborn GCs from the EC develops around 1 month (Mongiat et al., 2009), innervation by ipsi- and contralateral mossy cells (Kumamoto et al., 2012) and/or mature GCs may provide the glutamatergic input critical for new cell survival. Morphological evidence for input from mature GCs to newborn GCs was substantiated by electrophysiological recordings performed at short time intervals (1–2 weeks) after viral labeling. Specifically, cells double-labeled for both vectors (retrovirus + rabies virus expressing "starter" cells) showed immature physiological characteristics, while cells with single-labeling (rabies virus only, afferent "traced" cells) exhibited properties of mature GCs in the same acute slice (Vivar et al., 2012), suggesting mature-newborn GC connectivity.

Interestingly, intra-granular connections have been observed after denervation of EC input to the DG, producing sprouting of the mossy fibers into the molecular layer. These mossy fibers form synaptic contacts with spines on proximal dendritic segments of GCs, suggesting that the lack of EC input may be compensated for by intra-granular synapses (Frotscher and Zimmer, 1983). This connectivity has been also observed after seizures or brain injury, producing the same extension of mossy fibers to the molecular layer (Buckmaster et al., 2002; Marqués-Marí et al., 2007; Murphy et al., 2011). It should be noted that seizures accelerate the integration of the new GCs, albeit with a reduction of dendritic length (Overstreet-Wadiche et al., 2006), and increase adult neurogenesis (Parent and Lowenstein, 2002). Whether this can be interpreted as brain self-repair or lead to further pathology (Parent, 2003; Pun et al., 2012; Sanchez et al., 2012) remains to be determined.

THIRD WEEK

During the third week, the cells begin to resemble mature GCs more closely. The GC dendrites reach the outer molecular layer (O-ML) with spine formation from 17 dpi onwards. In addition, mossy fiber output to area CA3 increases (Zhao et al., 2006), physiological properties are more mature and spontaneous synaptic activity is detected, indicative of synaptic input (Esposito et al., 2005; Vivar et al., 2012). Furthermore, GABA has become hyperpolarizing and excitatory glutamatergic responses are consistently observed (Ge et al., 2006; Ming and Song, 2011). The source of excitatory input, according to our observations, is mainly from mature GCs, hilar mossy cells, a direct "back-projection" from area CA3 pyramidal cells and sparse input from LEC and perirhinal cortex (PRH) (Vivar et al., 2012). Interestingly, the direct "back projection" from area CA3 pyramidal cells contrasts with the generally accepted idea that the "trisynaptic hippocampal circuit" is unidirectional, a pathway that relays information from EC to hippocampus (EC → DG → CA3 → CA1) and then to cortex (Amaral and Witter, 1989). Although the concept of a "back-projection" from area CA3 to the DG is not entirely new, it is generally considered to be indirect. Indeed, previous anatomical and physiological studies of mature GCs have provided evidence for a di-synaptic "back-projection" from CA3 to DG through hilar inhibitory interneurons and/or excitatory mossy cells (Scharfman, 2007). Our recent finding of a direct "back projection" is consistent with anatomical studies that showed that CA3 pyramidal cells axons can be found in the I-ML of the ventral DG (Li et al., 1994; Wittner et al., 2007). Indeed, the specificity of retroviral labeling for newborn neurons, combined with the selective TVA-EnvA retrograde tracing method, supports the notion of a direct "back-projection" from area CA3. However, it remains to be determined whether this connectivity is unique to newborn GCs and if so, what the potential functional consequences are. One could imagine a faster processing of information through a direct "back-projection," which may support a specific role for new neurons in physiological processing of sequential memories (Lisman, 1999) and in pattern separation (Lisman, 2011).

Substantial input from septal cells was also observed at this time. Using immunohistochemistry for GABA and ChAT, we identified inputs to new GCs as cholinergic. Our observations indicate that newborn neurons receive direct robust input from septal cholinergic cells at 21 dpi (the starting point of our study, when new GCs consistently show spontaneous postsynaptic activity), suggesting that this innervation may be important during the maturation of new neurons. Indeed, it is quite possible that new GCs receive septal cholinergic innervation at earlier developmental stages (Ide et al., 2008). Previous research has

shown that neurotoxic cholinergic forebrain lesions decrease cell proliferation and neurogenesis in the DG (Cooper-Kuhn et al., 2004; Mohapel et al., 2005), whereas activation of the cholinergic system with donezepil increases new cell survival (Kaneko et al., 2006). Both nicotinic (beta2, alpha7) and muscarinic (m1, m2, m4) acetylcholine receptors are present on the somata of immature GCs (Mohapel et al., 2005; Kaneko et al., 2006). Nicotine receptors have been implicated in cell proliferation and survival. Chronic nicotine administration (Abrous et al., 2002) and knockout of nicotinic beta2 receptors (Harrist et al., 2004) reduce hippocampal cell genesis while selective knockdown of alpha7 receptors in DG progenitors affects dendritic complexity and branching (Campbell et al., 2010). It has also been suggested that acetylcholine may have a modulating effect, by regulating excitability and network integration of newborn (olfactory bulb) neurons (Lin et al., 2010).

While rabies virus infection is almost exclusively restricted to neurons, there are electron microscopic reports of rare infection of glia cells (Matsumoto, 1963; Gosztonyi, 1994). It has been suggested that this may be indicative of inflammation associated with rabies virus administration (Marshel et al., 2010). However, rabies virus positive glial cells were associated with new neurons in the molecular layer of the DG (Vivar et al., 2012), as well as the olfactory bulb (Arenkiel et al., 2011). Immunocytochemical analysis showed that these cells express GFAP and are astrocytes. One possible explanation for an association between new GCs and astrocytes is the formation of a stem cell niche that influences the maturation of neuroblasts, similar to that observed in the subventricular zone (Lim and Alvarez-Buylla, 1999; Platel et al., 2010). Indeed, *in vitro* and *in vivo* experiments have shown that DG astrocytes support progenitor cell differentiation (Song et al., 2002; Barkho et al., 2006; Ashton et al., 2012). Interestingly, very few astrocytes were observed in the molecular layer at 3 weeks, however, an increase over time was observed, potentially associated with incremental spine density of the newborn neurons. Recent research has shown that astrocytes may express specific proteins important for the formation of excitatory synapses (Huang and Bergles, 2004; Allen et al., 2012). As the rabies virus appeared to "trace" these cells, this suggests that there may be synapse-like connections between new GCs and astrocytes. Indeed, astrocytes are considered to form synapse-like connections with the dendrites/spines of new GCs that may enhance synapse maturation and integration of new neurons (Toni and Sultan, 2011).

FOURTH WEEK

At this time-point new GC processes continue to grow. Dendritic branching and protrusions, including mushroom spines, increase. The cells now have axosomatic, axodendritic and axospinous synapses (Zhao et al., 2006; Toni et al., 2007, 2008). Concurrently, mossy fibers have formed extensive contacts with area CA3 (Zhao et al., 2006; Faulkner et al., 2008; Ide et al., 2008; Toni et al., 2008). Glutamatergic and GABAergic (slow and fast) synaptic responses are detected, and enhanced intrinsic excitability is exhibited (Esposito et al., 2005). However, the new GCs still display immature characteristics compared to mature GCs, such as higher input resistance (R_{in}) and smaller membrane capacitance (C_m) (van Praag et al., 2002; Ambrogini et al., 2004; Esposito et al., 2005; Couillard-Despres et al., 2006; Mongiat et al., 2009). At this time-point, we observed that the new GCs continue receiving synaptic input from intra-hippocampal areas, including mature GCs, CA3 pyramidal cells and hilar cells (mossy cells and interneurons). Interestingly, intra-granular connectivity was substantially reduced as compared to 21 dpi. The reduction of this connectivity may be compensated for by gradual strengthening of distal cortical input (Vivar et al., 2012). Indeed, temporary overlap of intra-granular and cortical inputs may provide a mechanistic explanation for the transiently enhanced excitability and lower threshold for induction of long-term potentiation (LTP) in new GCs (Wang et al., 2000; Schmidt-Hieber et al., 2004; Ge et al., 2007) (**Figure 4**).

The EC is the major excitatory glutamatergic input to the DG. Projections arise from the LEC, considered to integrate novel environmental information, as well as from the MEC which contains grid cells with spatial specificity (Fyhn et al., 2004). LEC and MEC projections course through the lateral (LPP) and medial (MPP) perforant pathways, toward the outer (O-ML) and M-ML of the DG, respectively (Witter, 2007). Our trans-synaptic tracing approach revealed predominant LEC and PRH rather than MEC input to new GCs, as well as some input from dorsal caudo-medial entorhinal cortex (CEnt). Stimulation of the LPP and MPP evokes synaptic responses of larger amplitude in 1 month old GCs as compared to 3-week-old GCs, consistent with the strengthening of cortical input (Mongiat et al., 2009). Interestingly, stimulation of the MPP evokes synaptic responses in the new GCs even without substantial input from the MEC. There are several further questions that arise from this observation. First, is it possible that rabies virus may not trace well to the MEC and the observed response may be due to other glutamatergic inputs? This is unlikely, as upon labeling of both immature and mature GCs with lentivirus expressing TVA, GP, and GFP, trans-synaptic tracing is observed in the MEC, indicating that the rabies virus can reach this brain area (Vivar et al., 2012). Second, is it possible that axons from the LEC, usually confined to the O-ML (Witter, 2007), cross into the M-ML and mediate the synaptic response evoked by the stimulation of the M-ML in the new GCs? This remains to be determined. Third, recent research showed that selective optogenetic activation of the MEC evokes synaptic responses in 1 month old GCs (Kumamoto et al., 2012). However, could the elicited response be indirectly mediated via a polysynaptic pathway and/or by glutamatergic spillover (volume transmission) (Kullmann and Asztely, 1998)? Indeed, rabies virus propagation occurs at chemical synapses but not via cell-to-cell spread (volume transmission) (Ugolini, 1995; Tang et al., 1999). Consistent with this assumption, we were not able to see trans-synaptic tracing from ventral tegmental area or locus coereleus, two monoaminergic (dopaminergic and noradrenergic) areas, whose signaling is mainly mediated by volume transmission (Fuxe et al., 2007; Rice and Cragg, 2008), even though it has been described that dopamine modulates the activity of new GCs in the DG (Mu et al., 2011). Therefore, synaptic input from the MEC may be mediated by glutamate spillover in the M-ML, which may also play a role in the observed unique short-term plasticity of new GCs.

Evaluation of short-term plasticity in newborn and mature GCs revealed differences in integration of LEC and MEC inputs. It is well established that LEC and MEC projections to the DG exhibit distinctive physiological properties (McNaughton, 1980; Abraham and McNaughton, 1984). Stimulation of O-ML evokes paired-pulse facilitation (PPF), characteristic of LEC input, while stimulation of the M-ML evokes pair-pulse depression (PPD), characteristic of MEC input (McNaughton, 1980). Interestingly, at 1 month, new GCs exhibit PPF following M-ML stimulation instead of PPD (Vivar et al., 2012). Our findings are consistent with studies showing that stimulation of M-ML produced PPF in putative young GCs recorded from the inner GC layer (Wang et al., 2000) and in embryonic stem cell derived neurons transplanted into DG of hippocampal slice cultures (Benninger et al., 2003). However, the mechanisms underlying this differential response are as of yet unknown and may be associated with selective (segmental) dendritic spine maturation, whereby the medial portion of the cell could be preferentially activated by glutamate spillover and the outer portion by direct synaptic contacts.

Spine density in new GCs (6 weeks after retroviral injection) shows a progressive increment by branch order (Stone et al., 2011). Full maturation of the spines in the O-ML may take 6 months (Zhao et al., 2006; Toni et al., 2007). The medial portion may develop even more slowly and therefore contain a larger proportion immature dendritic spines or filopodia. At 30 dpi new GC filopodia are preferentially associated with boutons already synapsing on a dendritic spine (Toni et al., 2007). Development of these filopodia into spines may be regulated by neurotransmission (Harris, 1999), including glutamate spillover from active synapses (Kullmann and Asztely, 1998; Richards et al., 2005), which may in turn affect short-term plasticity. In addition, differential expression of glutamate receptors in young and mature neurons may play a role. AMPA receptor density is correlated with spine (Hall and Ghosh, 2008) and GC maturation (Hagihara et al., 2011). Furthermore, NR2B-containing NMDA receptors associated with enhanced synaptic plasticity in the new GCs (Ge et al., 2007) may be differentially expressed along the medial and outer portions of the dendritic tree. Indeed, structural and biophysical properties of the dendritic tree regulate synaptic input integration and neuronal function (Cline, 2001), and these appear to differ between newborn and mature GCs. Overall, the mechanisms underlying this differential short-term plasticity are as of yet unknown and future studies will be necessary to elucidate it.

The LEC appears to play an important role in the integration and function of the newborn GCs in the mature hippocampal network, similar to observations made during early postnatal development of new GCs, when EC axons preferentially make synapses onto distal dendritic GC segments (O-ML) (Frotscher et al., 2000; Förster et al., 2006). Indeed, LEC has been previously suggested to be important for adult neurogenesis (Froc et al., 2003; Shimazu et al., 2006). Shimazu et al. (2006) showed that deletion of the *NT-3* (Neurotrophin-3) gene results reduced adult neurogenesis and spatial memory function, and is associated with impaired DG LTP induced by stimulation of the LPP but not the MPP. Similarly, LPP stimulation failed to induce LTP in aged rats (Froc et al., 2003), which correlates with the observed decline in adult neurogenesis with aging (Seki and Arai, 1995). Moreover, LEC and MEC excitotoxic lesion experiments in young adult mice showed that the synaptic responses of retrovirally labeled newborn neurons to stimulation of either the LPP or MPP after LEC or MEC lesions were differentially affected. Both mature and new GCs exhibited impaired synaptic responses evoked by LPP stimulation after LEC lesion. However, only synaptic responses evoked in mature GCs by MPP stimulation were affected by MEC lesion (Vivar et al., 2012). Altogether these observations show that newborn GCs respond preferentially to LEC input, and suggest that synaptic connectivity/integration differs between mature and newborn GCs.

TWO AND THREE MONTHS

At these time-points, new GCs continue receiving synaptic input from area CA3 pyramidal cells, hilar cells (mossy cells and interneurons) and distal cortex (PRH, LEC and CEnt) but not from mature GCs. Interestingly, hilar cell innervation increased from one to 3 months (Vivar et al., 2012). The majority of the hilar cells appear to be calretinin positive mossy cells (Blasco-Ibañez and Freund, 1997). Interestingly, recent research using a transgenic mouse model to selectively ablate these cells indicates that the net effect of mossy cells on GCs may be inhibitory rather than excitatory (Jinde et al., 2012). A smaller portion of the hilar cells were GABAergic interneurons, which expressed characteristic markers such as parvalbumin (PV), neuropeptide Y (NPY) and somatostatin (STT). In particular, NPY has been implicated in cell proliferation in the adult DG (Howell et al., 2005). In addition, recent research has shown that PV cells express TrkB receptors and may regulate newborn GC differentiation via a brain-derived neurotrophic factor (BDNF) dependent mechanism (Waterhouse et al., 2012). While interneurons are relatively few in number, these cells have an elaborate axonal arborization that forms synaptic contacts with multiple GCs (Freund and Buzsáki, 1996). The increased hilar input together with the reduction of intra-granular connectivity may lead to diminished excitability of new neurons observed during this time window (Ge et al., 2006). Even so, morphological plasticity of adult newborn neurons, for parameters such as dendritic branching and soma size, is reportedly greater than that of those born during development, at 2 and 4 months after retroviral labeling (Lemaire et al., 2012).

The distal cortical input from LEC/PRH became more robust over time. Analysis of the ratio of LEC/PRH cells to new GCs showed a strengthening of this synaptic input over 3 months after retroviral labeling. Trans-synaptic tracing from MEC was not obvious though cells were detected in the CEnt, which has both spatial and non-spatial memory processing functions (Sauvage et al., 2010). Electrophysiological recordings showed that at 60 dpi, newborn GCs still exhibit PPF. At 90 dpi, new neurons appear to begin to transition toward PPD (Vivar et al., 2012). Possibly, substantial input from MEC will develop upon complete maturation of the newborn GCs which has been suggested to take about 6 months (Toni et al., 2007). Overall, further research will be needed to elucidate how exactly the shift toward a more mature phenotype in new GCs occurs.

FUNCTIONAL SIGNIFICANCE OF ADULT NEUROGENESIS

Research into the functional significance of adult neurogenesis has hitherto mainly focused on the DG. However, it should be considered that newborn GCs do not operate in isolation but rather are part of an elaborate neural circuitry important for learning and memory that originates in the EC. The flow of information from EC is generally considered to be propagated serially by excitatory synaptic transmission to DG → CA3 → CA1 and back to EC (Amaral and Witter, 1989). While it has become increasingly clear that there are recurrent networks between these areas (Lisman, 1999; Scharfman, 2007), for new GC neurons, this wiring diagram has further selective characteristics. Our recent work shows that newly born neurons receive preferential input from the LEC, PRH, and some innervation from CEnt, as well as a direct "back-projection" from area CA3 (**Figures 4** and **5**). This unique connectivity may have important implications for understanding the role of new DG neurons in memory function.

Information from the EC relays from two major cortical inputs, the MEC and LEC (Witter, 2007; van Cauter et al., 2012). The MEC, a region that contains grid cells, conveys highly specific spatial information to the hippocampus ("where") (Fyhn et al., 2004; Hafting et al., 2005). In contrast, LEC is considered important for integration of sensory information about the environment, as well as for processing of novel object recognition and familiarity ("what") (Myhrer, 1988; Zhu et al., 1995a,b; Hargreaves et al., 2005; Lisman, 2007; Murray et al., 2007; Deshmukh and Knierim, 2011). LEC receives non-spatial information mainly from the PRH (Insausti et al., 1997; Burwell, 2000). Evidence of a direct input from PRH to DG has been controversial (Liu and Bilkey, 1997; Canning and Leung, 1999). However, our recent work shows that newborn GCs receive direct input from the PRH (Vivar et al., 2012). The PRH is important for visual discrimination and novel objection recognition (Mumby and Pinel, 1994; Bussey et al., 1999; McTighe et al., 2010; Winters et al., 2010). PRH lesions lead to impairments in visual discrimination between closely related complex stimuli (Baxter and Murray, 2001; Bussey et al., 2003; Buckley, 2005; Bartko et al., 2007). In addition, aging related changes in the PRH in rodents have been implicated in the reduced ability to distinguish between objects with overlapping features (Burke et al., 2010, 2011). Pattern separation of perceptual sensory information in cortex may facilitate similar downstream mnemonic encoding processes. Indeed, the excitatory input from PRH/LEC may play an important role in enabling the DG to further process closely related events and locations and store them in memory. Preferential input to new GCs from PRH/LEC as compared to mature GCs, which are innervated by both LEC and MEC, suggests that newborn GCs may be more "specialized" in the processing of incoming environmental information than mature GCs.

Distinct storage of information is critical for minimizing memory overlap between closely similar stimuli and events. DG neurons outnumber EC cells resulting in sparse encoding (Treves and Rolls, 1992, 1994) considered to underlie pattern separation (Gilbert et al., 2001; Leutgeb et al., 2007; McHugh et al., 2007; Bakker et al., 2008; Yassa and Stark, 2011; Yassa et al., 2011; Schmidt et al., 2012; Hunsaker and Kesner, 2013), and newborn GCs may play an important role therein. Disruption of new neuron circuitry by PRH/LEC lesions (Vivar et al., 2012) as well as knockdown of adult neurogenesis by focal x-irradiation in the DG (Clelland et al., 2009) led to deficits in fine discrimination in the

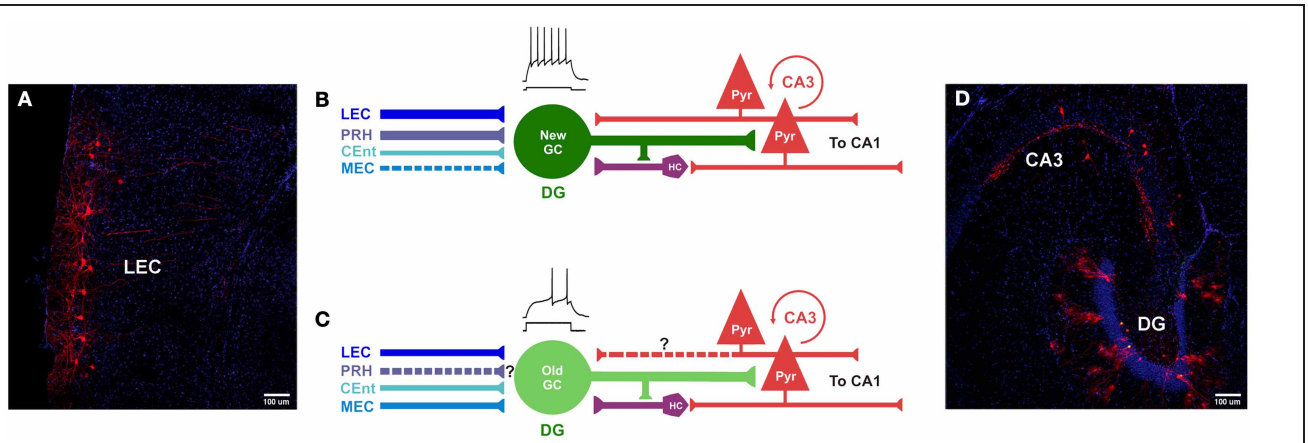

FIGURE 5 | Comparison of inputs to newborn and mature GCs. **(A–D)** Photomicrographs and models of inputs, and their hypothesized relative synaptic strengths, onto newborn and mature GCs. **(A,D)** Photomicrographs of horizontal sections (40 μm) derived from a mouse injected with retrovirus, followed by rabies virus at 30 dpi (30 dpi retrovirus + 7 dpi rabies virus). **(A)** Retrograde tracing is observed in cortical layers II/III of LEC, traced cells express MCherry (red) and nuclei are labeled with DAPI (blue). **(B)** Newborn GCs receive synaptic input from PRH, LEC and CEnt rather than from MEC. The new neurons are highly excitable, their mossy fiber outputs enable firing in area CA3 pyramidal cells. New GCs receive both direct and indirect "back-projections" from area CA3. **(C)** Inputs from LEC, CEnt and MEC converge onto mature GCs. It is unknown (?) if they receive first-order afferents from PRH. Mature GCs are less excitable and may have a weaker impact on CA3. It is unknown (?) if mature GCs receive a direct "back-projection" from CA3, but indirect connectivity via hilar cells has been reported. **(D)** Horizontal section through the hippocampus shows double-labeling of hGFP and MCherry ("starter" cells, yellow) and traced cells in the DG and area CA3 (red). Nuclei are labeled with DAPI (blue). DG, dentate gyrus; PRH, Perirhinal Cortex; PYR, pyramidal cells; HC, hilar cells; LEC, Lateral entorhinal cortex; MEC, medial entorhinal cortex; CEnt, Caudo-medial entorhinal cortex. ? Unclear whether this is a direct input.

touchscreen task. In addition, in experiments in which neurogenesis is reduced followed by testing in contextual fear conditioning paradigms or the radial arm maze provide support for a role of new neurons in fine contextual discrimination (Guo et al., 2011; Nakashiba et al., 2012; Tronel et al., 2012). Furthermore, enhancement of neurogenesis (Creer et al., 2010; Sahay et al., 2011) results in improved pattern separation. This raises the possibility that new DG neurons may process contextual rather than spatial path integration information. Consistently, research showed that reduction of neurogenesis by x-irradiation selectively affected contextual fear conditioning, but not water maze or Y-maze learning (Saxe et al., 2006). In other behavioral studies, spatial memory was found to be impaired following knockdown of adult neurogenesis (Snyder et al., 2005; Imayoshi et al., 2008; Deng et al., 2009; Jessberger et al., 2009). However, tasks evaluated may rely both on external/contextual information (such as cues on the walls of a water maze room) as well as internal navigation strategies (traversing a maze requiring location of "self"), (Lisman, 2007). As reduction or silencing of new neurons also affects area CA3 function (Niibori et al., 2012), a brain area that receives direct input from MEC grid cells and is important for spatial path integration processes (Leutgeb et al., 2007), it may be difficult to determine the precise role of new neurons based on ablation studies.

Physiological research shows that DG cells have multiple place fields throughout an environment (Leutgeb et al., 2007). Interestingly, recent research suggests these could reflect the subpopulation of newly born GCs (Neunuebel and Knierim, 2012). Furthermore, computational modeling studies (de Almeida et al., 2009) indicate that the majority of DG cells are non-functional (Lisman, 2011), as well as that adult-born neurons may become redundant after 1 month of age and "retire" early (Alme et al., 2010), suggesting that young GCs may be the DG subpopulation of cells preferentially active in encoding incoming information. Indeed, transgenic mice in which output of old GCs (mossy fibers) to area CA3 was silenced had improved or normal pattern separation between similar contexts in fear conditioning paradigms. However, when young GCs were ablated, deficits in pattern separation were observed (Nakashiba et al., 2012), suggesting that new neurons are the main functional component. Thus, mossy fiber output to area CA3 may convey contextual rather than spatial position information and may arise from new rather than from mature, relatively silent, GCs. This output may be further modulated by the transiently enhanced plasticity of newborn as compared to mature GCs (Wang et al., 2000; Schmidt-Hieber et al., 2004; Ge et al., 2007).

Interestingly, newly born GCs receive direct innervation from area CA3 (Vivar et al., 2012). It is as of yet unknown whether mature GCs receive similar feedback or only indirect "back-projections" via mossy cells and inhibitory interneurons (Scharfman, 2007). While the functional significance of direct input from area CA3 to new GCs is unclear, this finding provides further support for the notion that recurrent circuits between the DG and area CA3 are important (Hunsaker et al., 2008; Myers and Scharfman, 2011; de Almeida et al., 2012). CA3 pyramidal cells have extensive collateral connections (Marr, 1971; Ishizuka et al., 1990; O'Reilly and McClelland, 1994; Rolls, 2010) which are considered to mediate pattern completion, a process where parts of objects or events are combined into a retrievable memory (Nakazawa et al., 2002; Hunsaker and Kesner, 2013). A back-projection can play a role in pattern separation (Myers and Scharfman, 2009, 2011), as there are fewer area CA3 than DG cells. Furthermore, the ability to make fine distinctions between closely related stimuli, such as the choice between adjacent arms in a radial arm maze (Clelland et al., 2009; Guo et al., 2011), may be supported by a component of spatial information from the MEC to area CA3, and then from area CA3 directly to newborn GCs. Behavioral studies where rats sustained area CA3 lesions suggest that the DG requires area CA3 for metric spatial detection (Hunsaker et al., 2008). In addition, monosynaptic area CA3 back-projections may be important for the correction of cumulative errors in episodic and spatial memory that could arise from serial uni-directional propagation of information in the network (Lisman, 1999; Lisman et al., 2005). If so, a feedback loop between the cells that may be most active in encoding new information (adult-generated GCs) and the CA3 auto-associative network may enhance efficiency and accuracy of memory storage.

Recent imaging studies in humans support the concept that pattern separation is mediated by circuitry consisting of EC, DG and CA3 (Yassa and Stark, 2011). It should be noted that this network is particularly susceptible to aging related changes (Bevilaqua et al., 2008). Especially the input from the EC via the perforant pathway is compromised with aging (Yassa et al., 2011). It is of interest that in Alzheimer's disease patients PRH and LEC are among the first cortical regions to be affected (Hyman et al., 1984; Braak and Braak, 1991). The close association between these brain regions and adult neurogenesis may open new windows for therapeutic interventions in humans. Further research, however, is needed to better understand the functional significance of adult neurogenesis within this memory circuit.

ACKNOWLEDGMENTS

This work was supported by the National Institute on Aging, Intramural Research Program. We thank Linda R. Kitabayashi for help with preparation of the photomicrographs.

REFERENCES

Abraham, W. C., and McNaughton, N. (1984). Differences in synaptic transmission between medial and lateral components of the perforant path. *Brain Res.* 303, 251–260.

Abrous, D. N., Adriani, W., Montaron, M. F., Aurousseau, C., Rougon, G., Le Moal, M., et al. (2002). Nicotine self-administration impairs hippocampal plasticity. *J. Neurosci.* 22, 3656–3662.

Allen, N. J., Bennett, M. L., Foo, L. C., Wang, G. X., Chakraborty, C., Smith, S. J., et al. (2012). Astrocyte glypicans 4 and 6 promote formation of excitatory synapses via GluA1 AMPA receptors. *Nature* 486, 410–414.

Alme, C. B., Buzzetti, R. A., Marrone, D. F., Leutgeb, J. K., Chawla, M. K., Schaner, M. J., et al. (2010). Hippocampal granule cells opt for early retirement. *Hippocampus* 20, 1109–1123.

Altman, J., and Das, G. D. (1965). Autoradiographic and histological evidence of postnatal hippocampal neurogenesis in rats. *J. Comp. Neurol.* 124, 319–335.

Amaral, D. G., and Witter, M. P. (1989). The three-dimensional organization of the hippocampal formation: a review of

anatomical data. *Neuroscience* 31, 571–591.

Ambrogini, P., Lattanzi, D., Ciuffoli, S., Agostini, D., Bertini, L., Stocchi, V., et al. (2004). Morpho-functional characterization of neuronal cells at different stages of maturation in granule cell layer of adult rat dentate gyrus. *Brain Res.* 1017, 21–31.

Arenkiel, B. R., Hasegawa, H., Yi, J. J., Larsen, R. S., Wallace, M. L., Philpot, B. D., et al. (2011). Activity-induced remodeling of olfactory bulb microcircuits revealed by monosynaptic tracing. *PLoS ONE* 6:e29423. doi: 10.1371/journal.pone.0029423

Ashton, R. S., Conway, A., Pangarkar, C., Bergen, J., Lim, K. I., Shah, P., et al. (2012). Astrocytes regulate adult hippocampal neurogenesis through ephrin-B signaling. *Nat. Neurosci.* 15, 1399–1406.

Bakker, A., Kirwan, C. B., Miller, M., and Stark, C. E. (2008). Pattern separation in the human hippocampal CA3 and dentate gyrus. *Science* 19, 1640–1642.

Barkho, B. Z., Song, H., Aimone, J. B., Smrt, R. D., Kuwabara, T., Nakashima, K., et al. (2006). Identification of astrocyte-expressed factors that modulate neural stem/progenitor cell differentiation. *Stem Cells Dev.* 15, 407–421.

Bartko, S. J., Winters, B. D., Cowell, R. A., Saksida, L. M., and Bussey, T. J. (2007). Perceptual functions of perirhinal cortex in rats: zero-delay object recognition and simultaneous oddity discriminations. *J. Neurosci.* 27, 2548–2559.

Baxter, M. G., and Murray, E. A. (2001). Impairments in visual discrimination learning and recognition memory produced by neurotoxic lesions of rhinal cortex in rhesus monkeys. *Eur. J. Neurosci.* 13, 1228–1238.

Benninger, F., Beck, H., Wernig, M., Tucker, K. L., Brüstle, O., and Scheffler, B. (2003). Functional integration of embryonic stem cell-derived neurons in hippocampal slice cultures. *J. Neurosci.* 23, 7075–7083.

Bevilaqua, L. R., Rossato, J. I., Bonini, J. S., Myskiw, J. C., Clarke, J. R., Monteiro, S., et al. (2008). The role of the entorhinal cortex in extinction: influences of aging. *Neural Plast.* 2008:595282. doi: 10.1155/2008/595282

Blasco-Ibañez, J. M., and Freund, T. F. (1997). Distribution, ultrastructure, and connectivity of calretinin-immunoreactive mossy cells of the mouse dentate gyrus. *Hippocampus* 7, 307–320.

Braak, H., and Braak, E. (1991). Neuropathological stageing of Alzheimer-related changes. *Acta Neuropathol. (Berl.)* 82, 239–259.

Buckley, M. J. (2005). The role of the perirhinal cortex and hippocampus in learning, memory, and perception. *Q. J. Exp. Psychol. B* 58, 246–268.

Buckmaster, P. S., Zhang, G. F., and Yamawaki, R. (2002). Axon sprouting in a model of temporal lobe epilepsy create a predominantly excitatory feedback circuit. *J. Neurosci.* 22, 6650–6658.

Burke, S. N., Wallace, J. L., Hartzell, A. L., Nematollahi, S., Plange, K., and Barnes, C. A. (2011). Age-associated deficits in pattern separation functions of the perirhinal cortex: a cross-species consensus. *Behav. Neurosci.* 125, 836–847.

Burke, S. N., Wallace, J. L., Nematollahi, S., Uprety, A. R., and Barnes, C. A. (2010). Pattern separation deficits may contribute to age-associated recognition impairments. *Behav. Neurosci.* 124, 559–573.

Burwell, R. D. (2000). The parahippocampal region: corticocortical connectivity. *Ann. N.Y. Acad. Sci.* 911, 25–42.

Bussey, T. J., Muir, J. L., and Aggleton, J. P. (1999). Functionally dissociating aspects of event memory: the effects of combined perirhinal and postrhinal cortex lesions on object and place memory in the rat. *J. Neurosci.* 19, 495–502.

Bussey, T. J., Saksida, L. M., and Murray, E. A. (2003). Impairments in visual discrimination after perirhinal cortex lesions: testing 'declarative' vs. 'perceptual-mnemonic' views of perirhinal cortex function. *Eur. J. Neurosci.* 17, 649–660.

Callaway, E. M. (2008). Transneuronal circuit tracing with neurotropic viruses. *Curr. Opin. Neurobiol.* 18, 617–623.

Cameron, H. A., and McKay, R. D. (2001). Adult neurogenesis produces a large pool of new granule cells in the dentate gyrus. *J. Comp. Neurol.* 435, 406–417.

Cameron, H. A., Woolley, C. S., McEwen, B. S., and Gould, E. (1993). Differentiation of newly born neurons and glia in the dentate gyrus of the adult rat. *Neuroscience* 56, 337–344.

Campbell, N. R., Fernandes, C. C., Halff, A. W., and Berg, D. K. (2010). Endogenous signaling through alpha7-containing nicotinic receptors promotes maturation and integration of adult-born neurons in the hippocampus. *J. Neurosci.* 30, 8734–8744.

Canning, K. J., and Leung, L. S. (1999). Current source density analysis does not reveal a direct projection from perirhinal cortex to septal part of hippocampal CA1 or dentate gyrus. *Hippocampus* 9, 599–600.

Cao, L., Jiao, X., Zuzga, D. S., Liu, Y., Fong, D. M., Young, D., et al. (2004). VEGF links hippocampal activity with neurogenesis, learning and memory. *Nat. Genet.* 36, 827–835.

Carleton, A., Petreanu, L. T., Lansford, R., Alvarez-Buylla, A., and Lledo, P. M. (2003). Becoming a new neuron in the adult olfactory bulb. *Nat. Neurosci.* 6, 507–518.

Clelland, C. D., Choi, M., Romberg, C., Clemenson, G. D. Jr., Fragniere, A., Tyers, P., et al. (2009). A functional role for adult hippocampal neurogenesis in spatial pattern separation. *Science* 325, 210–213.

Cline, H. T. (2001). Dendritic arbor development and synaptogenesis. *Curr. Opin. Neurobiol.* 11, 118–126.

Cooper-Kuhn, C. M., Winkler, J., and Kuhn, H. G. (2004). Decreased neurogenesis after cholinergic forebrain lesion in the adult rat. *J. Neurosci. Res.* 77, 155–165.

Couillard-Despres, S., Winner, B., Karl, C., Lindemann, G., Schmid, P., Aigner, R., et al. (2006). Targeted transgene expression in neuronal precursors: watching young neurons in the old brain. *Eur. J. Neurosci.* 24, 1535–1545.

Creer, D. J., Romberg, C., Saksida, L. M., van Praag, H., and Bussey, T. J. (2010). Running enhances spatial pattern separation in mice. *Proc. Natl. Acad. Sci. U.S.A.* 107, 2367–2372.

Dayer, A. G., Ford, A. A., Cleaver, K. M., Yassaee, M., and Cameron, H. A. (2003). Short-term and long-term survival of new neurons in the rat dentate gyrus. *J. Comp. Neurol.* 460, 563–572.

de Almeida, L., Idiart, M., and Lisman, J. E. (2009). The input-output transformation of the hippocampal granule cells: from grid cells to place fields. *J. Neurosci.* 29, 7504–7512.

de Almeida, L., Idiart, M., and Lisman, J. E. (2012). The single place fields of CA3 cells: a two-stage transformation from grid cells. *Hippocampus* 22, 200–208.

Deng, W., Aimone, J. B., and Gage, F. H. (2010). New neurons and new memories: how does adult hippocampal neurogenesis affect learning and memory? *Nat. Rev. Neurosci.* 11, 339–350.

Deng, W., Saxe, M. D., Gallina, I. S., and Gage, F. H. (2009). Adult-born hippocampal dentate granule cells undergoing maturation modulate learning and memory in the brain. *J. Neurosci.* 29, 13532–13542.

Deshmukh, S. S., and Knierim, J. J. (2011). Representation of non-spatial and spatial information in the lateral entorhinal cortex. *Front. Behav. Neurosci.* 5:69. doi: 10.3389/fnbeh.2011.00069

Encinas, J. M., Vaahtokari, A., and Enikolopov, G. (2006). Fluoxetine targets early progenitor cells in the adult brain. *Proc. Natl. Acad. Sci. U.S.A.* 103, 8233–8238.

Esposito, M. S., Piatti, V. C., Laplagne, D. A., Morgenstern, N. A., Ferrari, C. C., Pitossi, F. J., et al. (2005). Neuronal differentiation in the adult hippocampus recapitulates embryonic development. *J. Neurosci.* 25, 10074–10086.

Etessami, R., Conzelmann, K. K., Fadai-Ghotbi, B., Natelson, B., Tsiang, H., and Ceccaldi, P. E. (2000). Spread and pathogenic characteristics of a G-deficient rabies virus recombinant: an *in vitro* and *in vivo* study. *J. Gen. Virol.* 81, 2147–2153.

Faulkner, R. L., Jang, M. H., Liu, X. B., Duan, X., Sailor, K. A., Kim, J. Y., et al. (2008). Development of hippocampal mossy fiber synaptic outputs by new neurons in the adult brain. *Proc. Natl. Acad. Sci. U.S.A.* 105, 14157–14162.

Förster, E., Zhao, S., and Frotscher, M. (2006). Laminating the hippocampus. *Nat. Rev. Neurosci.* 7, 259–267.

Freund, T. F., and Buzsáki, G. (1996). Interneurons of the hippocampus. *Hippocampus* 6, 347–470.

Froc, D. J., Eadie, B., Li, A. M., Wodtke, K., Tse, M., and Christie, B. R. (2003). Reduced synaptic plasticity in the lateral perforant path input to the dentate gyrus of aged C57BL/6 mice. *J. Neurophysiol.* 90, 32–38.

Frotscher, M., Drakew, A., and Heimrich, B. (2000). Role of afferent innervation and neuronal activity in dendritic development and spine maturation of fascia dentata granule cells. *Cereb. Cortex* 10, 946–951.

Frotscher, M., and Zimmer, J. (1983). Lesion-induced mossy fibers to the molecular layer of the rat fascia dentata: identification of postsynaptic granule cells by Golgi-EM technique. *J. Comp. Neurol.* 215, 299–311.

Fuxe, K., Dahlström, A., Höistad, M., Marcellino, D., Jansson, A., Rivera, A., et al. (2007). From the Golgi-Cajal mapping to the transmitter-based characterization

of the neuronal networks leading to two modes of brain communication: wiring and volume transmission. *Brain Res. Rev.* 55, 17–54.

Fyhn, M., Molden, S., Witter, M. P., Moser, E. I., and Moser, M. B. (2004). Spatial representation in the entorhinal cortex. *Science* 305, 1258–1264.

Ge, S., Goh, E. L., Sailor, K. A., Kitabatake, Y., Ming, G. L., and Song, H. (2006). GABA regulates synaptic integration of newly generated neurons in the adult brain. *Nature* 439, 589–593.

Ge, S., Yang, C., Hsu, K., Ming, G., and Song, H. (2007). A critical period for enhanced synaptic plasticity in newly generated neurons of the adult brain. *Neuron* 54, 559–566.

Gilbert, P. E., Kesner, R. P., and Lee, I. (2001). Dissociating hippocampal subregions: double dissociation between dentate gyrus and CA1. *Hippocampus* 11, 626–636.

Ginger, M., Haberl, M., Conzelmann, K. K., Schwarz, M. K., and Frick, A. (2013). Revealing the secrets of neuronal circuits with recombinant rabies virus technology. *Front. Neural Circuits* 7:2. doi: 10.3389/fncir.2013.00002

Gold, A. E., and Kesner, R. P. (2005). The role of the CA3 subregion of the dorsal hippocampus in spatial pattern completion in the rat. *Hippocampus* 15, 808–814.

Gosztonyi, G. (1994). Reproduction of lyssaviruses: ultrastructural composition of lyssavirus and functional aspects of pathogenesis. *Curr. Top. Microbiol. Immunol.* 187, 43–68.

Guo, W., Allan, A. M., Zong, R., Zhang, L., Johnson, E. B., Schaller, E. G., et al. (2011). Ablation of Fmrp in adult neural stem cells disrupts hippocampus-dependent learning. *Nat. Med.* 17, 559–565.

Hafting, T., Fyhn, M., Molden, S., Moser, M. B., and Moser, E. I. (2005). Microstructure of a spatial map in the entorhinal cortex. *Nature* 436, 801–806.

Hagihara, H., Ohira, K., Toyama, K., and Miyakawa, T. (2011). Expression of the AMPA receptor subunits GluR1 and GluR2 is associated with granule cell maturation in the dentate gyrus. *Front. Neurosci.* 5:100. doi: 10.3389/fnins.2011.00100

Hall, B. J., and Ghosh, A. (2008). Regulation of AMPA receptor recruitment at developing synapses. *Trends Neurosci.* 31, 82–89.

Hargreaves, E. L., Rao, G., Lee, I., and Knierim, J. J. (2005). Major dissociation between medial and lateral entorhinal input to dorsal hippocampus. *Science* 308, 1792–1794.

Harris, K. M. (1999). Structure, development, and plasticity of dendritic spines. *Curr. Opin. Neurobiol.* 9, 343–348.

Harrist, A., Beech, R. D., King, S. L., Zanardi, A., Cleary, M. A., Caldarone, B. J., et al. (2004). Alteration of hippocampal cell proliferation in mice lacking the beta 2 subunit of the neuronal nicotinic acetylcholine receptor. *Synapse* 54, 200–206.

Haubensak, W., Kunwar, P. S., Cai, H., Ciocchi, S., Wall, N. R., Ponnusamy, R., et al. (2010). Genetic dissection of an amygdala microcircuit that gates conditioned fear. *Nature* 468, 270–276.

Howell, O. W., Doyle, K., Goodman, J. H., Scharfman, H. E., Herzog, H., Pringle, A., et al. (2005). Neuropeptide Y stimulates neural precursor proliferation in the post-natal and adult dentate gyrus. *J. Neurochem.* 93, 560–570.

Huang, Y. H., and Bergles, D. E. (2004). Glutamate transporters bring competition to the synapse. *Curr. Opin. Neurobiol.* 14, 346–352.

Hunsaker, M. R., and Kesner, R. P. (2013). The operation of pattern separation and pattern completion processes associated with different attributes or domains of memory. *Neurosci. Biobehav. Rev.* 37, 36–58.

Hunsaker, M. R., Rosenberg, J. S., and Kesner, R. P. (2008). The role of the dentate gyrus, CA3a, b, and CA3c for detecting spatial and environmental novelty. *Hippocampus* 18, 1064–1073.

Hyman, B. T., Van Hoesen, G. W., Damasio, A. R., and Barnes, C. L. (1984). Alzheimer's disease: cell-specific pathology isolates the hippocampal formation. *Science* 225, 1168–1170.

Ide, Y., Fujiyama, F., Okamoto-Furuta, K., Tamamaki, N., Kaneko, T., and Hisatsune, T. (2008). Rapid integration of young newborn dentate gyrus granule cells in the adult hippocampal circuitry. *Eur. J. Neurosci.* 28, 2381–2392.

Imayoshi, I., Sakamoto, M., Ohtsuka, T., Takao, K., Miyakawa, T., Yamaguchi, M., et al. (2008). Roles of continuous neurogenesis in the structural and functional integrity of the adult forebrain. *Nat. Neurosci.* 11, 1153–1161.

Insausti, R., Herrero, M. T., and Witter, M. P. (1997). Entorhinal cortex of the rat: cytoarchitectonic subdivisions and the origin and distribution of cortical efferents. *Hippocampus* 7, 146–183.

Ishizuka, N., Weber, J., and Amaral, D. G. (1990). Organization of intrahippocampal projections originating from CA3 pyramidal cells in the rat. *J. Comp. Neurol.* 295, 580–623.

Jessberger, S., Clark, R. E., Broadbent, N. J., Clemenson, G. D. Jr., Consiglio, A., Lie, D. C., et al. (2009). Dentate gyrus-specific knockdown of adult neurogenesis impairs spatial and object recognition memory in adult rats. *Learn. Mem.* 16, 147–154.

Jin, K., Sun, Y., Xie, L., Batteur, S., Mao, X. O., Smelick, C., et al. (2003). Neurogenesis and aging: FGF-2 and HB-EGF restore neurogenesis in hippocampus and subventricular zone of aged mice. *Aging Cell* 2, 175–183.

Jinde, S., Zsiros, V., Jiang, Z., Nakao, K., Pickel, J., Kohno, K., et al. (2012). Hilar mossy cell degeneration causes transient dentate granule cell hyperexcitability and impaired pattern separation. *Neuron* 76, 1189–1200.

Kaneko, N., Okano, H., and Sawamoto, K. (2006). Role of the cholinergic system in regulating survival of newborn neurons in the adult mouse dentate gyrus and olfactory bulb. *Genes Cells* 11, 1145–1159.

Kaplan, M. S., and Hinds, J. W. (1977). Neurogenesis in the adult rat: electron microscopic analysis of light radioautographs. *Science* 197, 1092–1094.

Kesner, R. P. (2007). Behavioral functions of the CA3 subregion of the hippocampus. *Learn. Mem.* 14, 771–781.

Kitamura, T., Saitoh, Y., Takashima, N., Murayama, A., Niibori, Y., Ageta, H., et al. (2009). Adult neurogenesis modulates the hippocampus-dependent period of associative fear memory. *Cell* 139, 814–827.

Knierim, J. J., Lee, I., and Hargreaves, E. L. (2006). Hippocampal place cells: parallel input streams, subregional processing, and implications for episodic memory. *Hippocampus* 16, 755–764.

Kuhn, H. G., Dickinson-Anson, H., and Gage, F. H. (1996). Neurogenesis in the dentate gyrus of the adult rat: age-related decrease of neuronal progenitor proliferation. *J. Neurosci.* 16, 2027–2033.

Kullmann, D. M., and Asztely, F. (1998). Extrasynaptic glutamate spillover in the hippocampus: evidence and implications. *Trends Neurosci.* 21, 8–14.

Kumamoto, N., Gu, Y., Wang, J., Janoschka, S., Takemaru, K., Levine, J., et al. (2012). A role for primary cilia in glutamatergic synaptic integration of adult-born neurons. *Nat. Neurosci.* 15, 399–405.

Lai, K., Kaspar, B. K., Gage, F. H., and Schaffer, D. V. (2003). Sonic hedgehog regulates adult neural progenitor proliferation *in vitro* and *in vivo*. *Nat. Neurosci.* 6, 21–27.

Lammel, S., Lim, B. K., Ran, C., Huang, K. W., Betley, M. J., Tye, K. M., et al. (2012). Input-specific control of reward and aversion in the ventral tegmental area. *Nature* 491, 212–217.

Lemaire, V., Tronel, S., Montaron, M. F., Fabre, A., Dugast, E., and Abrous, D. N. (2012). Long-lasting plasticity of hippocampal adult-born neurons. *J. Neurosci.* 32, 3101–3108.

Leutgeb, J. K., Leutgeb, S., Moser, M. B., and Moser, E. I. (2007). Pattern separation in the dentate gyrus and CA3 of the hippocampus. *Science* 315, 961–966.

Lewis, P. F., and Emerman, M. (1994). Passage through mitosis is required for oncoretroviruses but not for the human immunodeficiency virus. *J. Virol.* 68, 510–516.

Li, X. G., Somogyi, P., Ylinen, A., and Buzsáki, G. (1994). The hippocampal CA3 network: an *in vivo* intracellular labeling study. *J. Comp. Neurol.* 339, 181–208.

Lim, D. A., and Alvarez-Buylla, A. (1999). Interaction between astrocytes and adult subventricular zone precursors stimulates neurogenesis. *Proc. Natl. Acad. Sci. U.S.A.* 96, 7526–7531.

Lin, C. W., Sim, S., Ainsworth, A., Okada, M., Kelsch, W., and Lois, C. (2010). Genetically increased cell-intrinsic excitability enhances neuronal integration into adult brain circuits. *Neuron* 65, 32–39.

Lisman, J. E. (1999). Relating hippocampal circuitry to function: recall of memory sequences by reciprocal dentate-CA3 interaction. *Neuron* 22, 233–242.

Lisman, J. E. (2007). Role of the dual entorhinal inputs to hippocampus: a hypothesis based on cue/action (non-self/self) couplets. *Prog. Brain Res.* 163, 615–625.

Lisman, J. E. (2011). Formation of the non-functional and functional pools of granule cells in the dentate gyrus: role of the neurogenesis, LTP and LTD. *J. Physiol.* 589, 1905–1909.

Lisman, J. E., Talamini, L. M., and Raffone, A. (2005). Recall of memory sequences by interaction of the dentate and CA3: a revised model of the phase precession. *Neural Netw.* 18, 1191–1201.

Liu, P., and Bilkey, D. K. (1997). Current source density analysis of the potential evoked in

hippocampus by perirhinal cortex stimulation. *Hippocampus* 7, 389–396.

Lo Turco, J. J., and Kriegstein, A. R. (1991). Clusters of coupled neuroblasts in embryonic neocortex. *Science* 252, 563–566.

Lugert, S., Basak, O., Knuckles, P., Haussler, U., Fabel, K., Götz, M., et al. (2010). Quiescent and active hippocampal neural stem cells with distinct morphologies respond selectively to physiological and pathological stimuli and aging. *Cell Stem Cell* 6, 445–456.

Marqués-Marí, A. I., Nacher, J., Crespo, C., Gutièrrez-Mecinas, M., Martínez-Guijarro, F. J., and Blasco-Ibáñez, J. M. (2007). Loss of input from the mossy cells blocks maturation of newly generated granule cells. *Hippocampus* 17, 510–524.

Marr, D. (1971). Simple memory: a theory for archicortex. *Proc. R. Soc. Lond. B Biol. Sci.* 262, 23–81.

Marshel, J. H., Mori, T., Nielsen, K. J., and Callaway, E. M. (2010). Targeting single neuronal networks for gene expression and cell labeling *in vivo*. *Neuron* 67, 562–574.

Matsumoto, S. (1963). Electron microscope studies of rabies virus in mouse brain. *J. Cell Biol.* 19, 565–591.

McHugh, T. J., Jones, M. W., Quinn, J. J., Balthasar, N., Coppari, R., Elmquist, J. K., et al. (2007). Dentate gyrus NMDA receptors mediate rapid pattern separation in the hippocampal network. *Science* 317, 94–99.

McNaughton, B. L. (1980). Evidence for two physiologically distinct perforant pathways to the fascia dentata. *Brain Res.* 199, 1–19.

McNaughton, B. L., Battaglia, F. P., Jensen, O., Moser, E. I., and Moser, M. B. (2006). Path integration and the neural basis of the 'cognitive map'. *Nat. Rev. Neurosci.* 7, 663–678.

McTighe, S. M., Cowell, R. A., Winters, B. D., Bussey, T. J., and Saksida, L. M. (2010). Paradoxical false memory for objects after brain damage. *Science* 330, 1408–1410.

Mebatsion, T., Konig, M., and Conzelmann, K. K. (1996). Budding of rabies virus particles in the absence of the spike glycoprotein. *Cell* 84, 941–951.

Mejia-Gervacio, S., Murray, K., and Lledo, P. M. (2011). NKCC1 controls GABAergic signaling and neuroblast migration in the postnatal forebrain. *Neural Dev.* 6:4. doi: 10.1186/1749-8104-6-4

Ming, G. L., and Song, H. (2005). Adult neurogenesis in the mammalian central nervous system. *Annu. Rev. Neurosci.* 28, 223–250.

Ming, G. L., and Song, H. (2011). Adult neurogenesis in the mammalian brain: significant answers and significant questions. *Neuron* 70, 687–702.

Mira, H., Andreu, Z., Suh, H., Lie, D. C., Jessberger, S., Consiglio, A., et al. (2010). Signaling through BMPR-IA regulates quiescence and long-term activity of neural stem cells in the adult hippocampus. *Cell Stem Cell* 7, 78–89.

Miyamichi, K., Amat, F., Moussavi, F., Wang, C., Wickersham, I., Wall, N. R., et al. (2011). Cortical representation of olfactory input by trans-synaptic tracing. *Nature* 472, 191–196.

Mohapel, P., Leanza, G., Kokaia, M., and Lindvall, O. (2005). Forebrain acetylcholine regulates adult hippocampal neurogenesis and learning. *Neurobiol. Aging* 26, 939–946.

Mongiat, L. A., Espósito, M. S., Lombardi, G., and Schinder, A. F. (2009). Reliable activation of immature neurons in the adult hippocampus. *PLoS ONE* 4:e5320. doi: 10.1371/journal.pone.0005320

Mu, Y., Zhao, C., and Gage, F. H. (2011). Dopaminergic modulation of cortical inputs during maturation of adult-born dentate granule cells. *J. Neurosci.* 31, 4113–4123.

Mumby, D. G., and Pinel, J. P. (1994). Rhinal cortex lesions and object recognition in rats. *Behav. Neurosci.* 108, 11–28.

Murphy, B. L., Pun, R. Y., Yin, H., Faulkner, C. R., Loepke, A. W., and Danzer, S. C. (2011). Heterogeneous integration of adult-generated granule cells into the epileptic brain. *J. Neurosci.* 31, 105–117.

Murray, E. A., Bussey, T. J., and Saksida, L. M. (2007). Visual perception and memory: a new view of medial temporal lobe function in primates and rodents. *Annu. Rev. Neurosci.* 30, 99–122.

Myers, C. E., and Scharfman, H. E. (2009). A role for hilar cells in pattern separation in the dentate gyrus: a computational approach. *Hippocampus* 19, 321–337.

Myers, C. E., and Scharfman, H. E. (2011). Pattern separation in the dentate gyrus: a role for the CA3 backprojection. *Hippocampus* 21, 1190–1215.

Myhrer, T. (1988). The role of medial and lateral hippocampal perforant path lesions and object distinctiveness in rats' reaction to novelty. *Physiol. Behav.* 42, 371–377.

Nakashiba, T., Cushman, J. D., Pelkey, K. A., Renaudineau, S., Buhl, D. L., McHugh, T. J., et al. (2012). Young dentate granule cells mediate pattern separation, whereas old granule cells facilitate pattern completion. *Cell* 149, 188–201.

Nakazawa, K., McHugh, T. J., Wilson, M. A., and Tonegawa, S. (2004). NMDA receptors, place cells and hippocampal spatial memory. *Nat. Rev. Neurosci.* 5, 361–372.

Nakazawa, K., Quirk, M. C., Chitwood, R. A., Watanabe, M., Yeckel, M. F., Sun, L. D., et al. (2002). Requirement for hippocampal CA3 NMDA receptors in associative memory recall. *Science* 297, 211–218.

Neunuebel, J. P., and Knierim, J. J. (2012). Spatial firing correlates of physiologically distinct cell types of the rat dentate gyrus. *J. Neurosci.* 32, 3848–3858.

Niibori, Y., Yu, T. S., Epp, J. R., Akers, K. G., Josselyn, S. A., and Frankland, P. W. (2012). Suppression of adult neurogenesis impairs population coding of similar contexts in hippocampal CA3 region. *Nat. Commun.* 3:1253. doi: 10.1038/ncomms2261

O'Reilly, R. C., and McClelland, J. L. (1994). Hippocampal conjunctive encoding, storage, and recall: avoiding a trade-off. *Hippocampus* 4, 661–682.

Osakada, F., Mori, T., Cetin, A. H., Marshel, J. H., Virgen, B., and Callaway, E. M. (2011). New rabies virus variants for monitoring and manipulating activity and gene expression in defined neural circuits. *Neuron* 71, 617–631.

Overstreet-Wadiche, L. S., Bromberg, D. A., Bensen, A. L., and Westbrook, G. L. (2006). Seizures accelerate functional integration of adult-generated granule cells. *J. Neurosci.* 26, 4095–4103.

Parent, J. M. (2003). Injury-induced neurogenesis in the adult mammalian brain. *Neuroscientist* 9, 261–272.

Parent, J. M., and Lowenstein, D. H. (2002). Seizure-induced neurogenesis: are more new neurons good for an adult brain? *Prog. Brain Res.* 135, 121–131.

Platel, J. C., Dave, K. A., Gordon, V., Lacar, B., Rubio, M. E., and Bordey, A. (2010). NMDA receptors activated by subventricular zone astrocytic glutamate are critical for neuroblast survival prior to entering a synaptic network. *Neuron* 65, 859–872.

Pun, R. Y., Rolle, I. J., Lasarge, C. L., Hosford, B. E., Rosen, J. M., Uhl, J. D., et al. (2012). Excessive activation of mTOR in postnatally generated granule cells is sufficient to cause epilepsy. *Neuron* 75, 1022–1034.

Qu, Q., Sun, G., Li, W., Yang, S., Ye, P., Zhao, C., et al. (2010). Orphan nuclear receptor TLX activates Wnt/beta-catenin signalling to stimulate neural stem cell proliferation and self-renewal. *Nat. Cell Biol.* 12, 31–40. sup pp 1–9.

Rancz, E. A., Franks, K. M., Schwarz, M. K., Pichler, B., Schaefer, A. T., and Margrie, T. W. (2011). Transfection via whole-cell recording *in vivo*: bridging single-cell physiology, genetics and connectomics. *Nat. Neurosci.* 14, 527–532.

Rice, M. E., and Cragg, S. J. (2008). Dopamine spillover after quantal release: rethinking dopamine transmission in the nigrostriatal pathway. *Brain Res. Rev.* 58, 303–313.

Richards, D. A., Mateos, J. M., Hugel, S., de Paola, V., Caroni, P., Gähwiler, B. H., et al. (2005). Glutamate induces the rapid formation of spine head protrusions in hippocampal slice cultures. *Proc. Natl. Acad. Sci. U.S.A.* 102, 6166–6171.

Rolls, E. T. (2010). A computational theory of episodic memory formation in the hippocampus. *Behav. Brain Res.* 215, 180–196.

Sahay, A., Scobie, K. N., Hill, A. S., O'Carroll, C. M., Kheirbek, M. A., Burghardt, N. S., et al. (2011). Increasing adult hippocampal neurogenesis is sufficient to improve pattern separation. *Nature* 472, 466–470.

Sanchez, R. M., Ribak, C. E., and Shapiro, L. A. (2012). Synaptic connections of hilar basal dendrites of dentate granule cells in a neonatal hypoxia model of epilepsy. *Epilepsia* 53(Suppl. 1), 98–108.

Sauvage, M. M., Beer, Z., Ekovich, M., Ho, L., and Eichenbaum, H. (2010). The caudal medial entorhinal cortex: a selective role in recollection-based recognition memory. *J. Neurosci.* 30, 15695–15699.

Saxe, M. D., Battaglia, F., Wang, J. W., Malleret, G., David, D. J., Monckton, J. E., et al. (2006). Ablation of hippocampal neurogenesis impairs contextual fear conditioning and synaptic plasticity in the dentate gyrus. *Proc. Natl. Acad. Sci. U.S.A.* 103, 17501–17506.

Scharfman, H. E. (2007). The CA3 "backprojection" to the dentate gyrus. *Prog. Brain Res.* 163, 627–637.

Schmidt, B., Marrone, D. F., and Markus, E. J. (2012). Disambiguating the similar: the dentate gyrus and pattern separation. *Behav. Brain Res.* 226, 56–65.

Schmidt-Hieber, C., Jonas, P., and Bischofberger, J. (2004). Enhanced synaptic plasticity in newly generated granule cells of the adult hippocampus. *Nature* 429, 184–187.

Scoville, W. B., and Milner, B. (1957). Loss of recent memory after bilateral hippocampal lesions. *J. Neurol. Neurosurg. Psychiatry* 20, 11–21.

Seki, T., and Arai, Y. (1995). Age-related production of new granule cells in the adult dentate gyrus. *Neuroreport* 6, 2479–2482.

Shimazu, K., Zhao, M., Sakata, K., Akbarian, S., Bates, B., Jaenisch, R., et al. (2006). NT-3 facilitates hippocampal plasticity and learning and memory by regulating neurogenesis. *Learn. Mem.* 13, 307–315.

Snyder, J. S., Hong, N. S., McDonald, R. J., and Wojtowicz, J. M. (2005). A role for adult neurogenesis in spatial long-term memory. *Neuroscience* 130, 843–852.

Song, H., Stevens, C. F., and Gage, F. H. (2002). Astroglia induce neurogenesis from adult neuronal stem cells. *Nature* 417, 39–44.

Song, J., Zhong, C., Bonaguidi, M. A., Sun, G. J., Hsu, D., Gu, Y., et al. (2012). Neuronal circuitry mechanism regulating adult quiescent neural stem-cell fate decision. *Nature* 489, 150–154.

Squire, L. R., Stark, C. E. L., and Clark, R. E. (2004). The medial temporal lobe. *Annu. Rev. Neurosci.* 27, 279–306.

Stepien, A. E., Tripodi, M., and Arber, S. (2010). Monosynaptic rabies virus reveals premotor network organization and synaptic specificity of cholinergic partition cells. *Neuron* 68, 456–472.

Stone, S. S., Teixeira, C. M., Devito, L. M., Zaslavsky, K., Josselyn, S. A., Lozano, A. M., et al. (2011). Stimulation of entorhinal cortex promotes adult neurogenesis and facilitates spatial memory. *J. Neurosci.* 31, 13469–13484.

Suh, H., Consiglio, A., Ray, J., Sawai, T., D'Amour, K. A., and Gage, F. H. (2007). *In vivo* fate analysis reveals the multipotent and self-renewal capacities of Sox2+ neural stem cells in the adult hippocampus. *Cell Stem Cell* 1, 515–528.

Suh, H., Deng, W., and Gage, F. H. (2009). Signaling in adult neurogenesis. *Annu. Rev. Cell Dev. Biol.* 25, 253–275.

Tang, Y., Rampin, O., Giuliano, F., and Ugolini, G. (1999). Spinal and brain circuits to motoneurons of the bulbospongiosus muscle: retrograde transneuronal tracing with rabies virus. *J. Comp. Neurol.* 414, 167–192.

Tashiro, A., Sandler, V. M., Toni, N., Zhao, C., and Gage, F. H. (2006). NMDA-receptor-mediated, cell-specific integration of new neurons in adult dentate gyrus. *Nature* 442, 929–933.

Toni, N., Laplagne, D. A., Zhao, C., Lombardi, G., Ribak, C. E., Gage, F. H., et al. (2008). Neurons born in the adult dentate gyrus form functional synapses with target cells. *Nat. Neurosci.* 11, 901–907.

Toni, N., and Sultan, S. (2011). Synaptic formation on adult-born hippocampal neurons. *Eur. J. Neurosci.* 33, 1062–1068.

Toni, N., Teng, E. M., Bushong, E. A., Aimone, J. B., Zhao, C., Consiglio, A., et al. (2007). Synapse formation on neurons born in the adult hippocampus. *Nat. Neurosci.* 10, 727–734.

Tozuka, Y., Fukuda, S., Namba, T., Seki, T., and Hisatsune, T. (2005). GABAergic excitation promotes neuronal differentiation in adult hippocampal progenitor cells. *Neuron* 47, 803–815.

Treves, A., and Rolls, E. T. (1992). Computational constraints suggest the need for two distinct input systems to the hippocampal CA3 network. *Hippocampus* 2, 189–199.

Treves, A., and Rolls, E. T. (1994). Computational analysis of the role of the hippocampus in memory. *Hippocampus* 4, 374–391.

Tronel, S., Belnoue, L., Grosjean, N., Revest, J. M., Piazza, P. V., Koehl, M., et al. (2012). Adult-born neurons are necessary for extended contextual discrimination. *Hippocampus* 22, 292–298.

Ugolini, G. (1995). Specificity of rabies virus as a transneuronal tracer of motor networks: transfer from hypoglossal motoneurons to connected second-order and higher order central nervous system cell groups. *J. Comp. Neurol.* 356, 457–480.

Ugolini, G. (2010). Advances in viral transneuronal tracing. *J. Neurosci. Methods* 194, 2–20.

Ugolini, G. (2011). Rabies virus as a transneuronal tracer of neuronal connections. *Adv. Virus Res.* 79, 165–202.

van Cauter, T., Camon, J., Alvernhe, A., Elduayen, C., Sargolini, F., and Save, E. (2012). Distinct roles of medial and lateral entorhinal cortex in spatial cognition. *Cereb. Cortex* 23, 451–459.

van Praag, H., Schinder, A. F., Christie, B. R., Toni, N., Palmer, T. D., and Gage, F. H. (2002). Functional neurogenesis in the adult hippocampus. *Nature* 415, 1030–1034.

Vivar, C., Choi, J., Callaway, E. M., Gage, F. H., Suh, H., and van Praag, H. (2011). Afferent input integrates newborn dentate granule cells into the existing adult network. *Soc. Neurosci. Abstr.* 30.15.

Vivar, C., Potter, M. C., Choi, J., Lee, J. Y., Stringer, T. P., Callaway, E. M., et al. (2012). Monosynaptic inputs to new neurons in the dentate gyrus. *Nat. Commun.* 3:1107. doi: 10.1038/ncomms2101

Wall, N. R., Wickersham, I. R., Cetin, A., De La Parra, M., and Callaway, E. M. (2010). Monosynaptic circuit tracing *in vivo* through Cre-dependent targeting and complementation of modified rabies virus. *Proc. Natl. Acad. Sci. U.S.A.* 107, 21848–21853.

Wang, S., Scott, B. W., and Wojtowicz, J. M. (2000). Heterogeneous properties of dentate granule neurons in the adult rat. *J. Neurobiol.* 42, 248–257.

Watabe-Uchida, M., Zhu, L., Ogawa, S. K., Vamanrao, A., and Uchida, N. (2012). Whole-brain mapping of direct inputs to midbrain dopamine neurons. *Neuron* 74, 858–873.

Waterhouse, E. G., An, J. J., Orefice, L. L., Baydyuk, M., Liao, G. Y., Zheng, K., et al. (2012). BDNF promotes differentiation and maturation of adult-born neurons through GABAergic transmission. *J. Neurosci.* 32, 14318–14330.

Wickersham, I. R., Lyon, D. C., Barnard, R. J., Mori, T., Finke, S., Conzelmann, K. K., et al. (2007a). Monosynaptic restriction of transsynaptic tracing from single, genetically target neurons. *Neuron* 53, 639–647.

Wickersham, I. R., Finke, S., Conzelmann, K. K., and Callaway, E. M. (2007b). Retrograde neuronal tracing with a deletion-mutant rabies virus. *Nat. Methods* 4, 47–49.

Winters, B. D., Saksida, L. M., and Bussey, T. J. (2010). Implications of animal object memory research for human amnesia. *Neuropsychologia* 48, 2251–2261.

Witter, M. P. (2007). The perforant path: projections from the entorhinal cortex to the dentate gyrus. *Prog. Brain Res.* 163, 43–61.

Wittner, L., Henze, D. A., Záborszky, L., and Buzsáki, G. (2007). Three-dimensional reconstruction of the axon arbor of a CA3 pyramidal cell recorded and filled *in vivo*. *Brain Struct. Funct.* 212, 75–83.

Yassa, M. A., Mattfeld, A. T., Stark, S. M., and Stark, C. E. (2011). Age-related memory deficits linked to circuit-specific disruptions in the hippocampus. *Proc. Natl. Acad. Sci. U.S.A.* 108, 8873–8878.

Yassa, M. A., and Stark, C. E. (2011). Pattern separation in the hippocampus. *Trends Neurosci.* 34, 515–525.

Yonehara, K., Balint, K., Noda, M., Nagel, G., Bamberg, E., and Roska, B. (2011). Spatially asymmetric reorganization of inhibition establishes a motion-sensitive circuit. *Nature* 469, 407–410.

Young, S. Z., Taylor, M. M., Wu, S., Ikeda-Matsuo, Y., Kubera, C., and Bordey, A. (2012). NKCC1 knockdown decreases neuron production through GABAA-regulated neural progenitor proliferation and delays dendrite development. *J. Neurosci.* 32, 13630–13638.

Zhao, C., Deng, W., and Gage, F. H. (2008). Mechanisms and functional implications of adult neurogenesis. *Cell* 132, 645–660.

Zhao, C., Teng, E. M., Summers, R. G. Jr., Ming, G. L., and Gage, F. H. (2006). Distinct morphological stages of dentate granule neuron maturation in the adult mouse hippocampus. *J. Neurosci.* 26, 3–11.

Zhu, X. O., Brown, M. W., McCabe, B. J., and Aggleton, J. P. (1995a). Effects of the novelty or familiarity of visual stimuli on the expression of the immediate early gene c-fos in rat brain. *Neuroscience* 69, 821–829.

Zhu, X. O., Brown, M. W., and Aggleton, J. P. (1995b). Neuronal signalling of information important to visual recognition memory in rat rhinal and neighbouring cortices. *Eur. J. Neurosci.* 7, 753–765.

Conflict of Interest Statement: The authors declare that the research was conducted in the absence of any commercial or financial relationships that could be construed as a potential conflict of interest.

Received: 12 October 2012; accepted: 23 January 2013; published online: 25 February 2013.

Citation: Vivar C and van Praag H (2013) Functional circuits of new neurons in the dentate gyrus. Front. Neural Circuits 7:15. doi: 10.3389/fncir.2013.00015

frontiers in
NEURAL CIRCUITS

METHODS ARTICLE
published: 16 November 2012
doi: 10.3389/fncir.2012.00083

Toward a full-scale computational model of the rat dentate gyrus

Calvin J. Schneider*, Marianne Bezaire and Ivan Soltesz

Department of Anatomy and Neurobiology, University of California Irvine, Irvine, CA, USA

Edited by:
Peter Jonas, Institute of Science and Technology (IST) Austria, Austria

Reviewed by:
Nicholas T. Carnevale, Yale University School of Medicine, USA
Nelson Spruston, Howard Hughes Medical Institute, USA

****Correspondence:***
Calvin J. Schneider, Department of Anatomy and Neurobiology, University of California, 139 Irvine Hall, Irvine, CA 92697, USA.
e-mail: calvinjs@uci.edu

Recent advances in parallel computing, including the creation of the parallel version of the NEURON simulation environment, have allowed for a previously unattainable level of complexity and detail in neural network models. Previously, we published a functional NEURON model of the rat dentate gyrus with over 50,000 biophysically realistic, multicompartmental neurons, but network simulations could only utilize a single processor. By converting the model to take advantage of parallel NEURON, we are now able to utilize greater computational resources and are able to simulate the full-scale dentate gyrus, containing over a million neurons. This has eliminated the previous necessity for scaling adjustments and allowed for a more direct comparison to experimental techniques and results. The translation to parallel computing has provided a superlinear speedup of computation time and dramatically increased the overall computer memory available to the model. The incorporation of additional computational resources has allowed for more detail and elements to be included in the model, bringing the model closer to a more complete and accurate representation of the biological dentate gyrus. As an example of a major step toward an increasingly accurate representation of the biological dentate gyrus, we discuss the incorporation of realistic granule cell dendrites into the model. Our previous model contained simplified, two-dimensional dendritic morphologies that were identical for neurons of the same class. Using the software tools L-Neuron and L-Measure, we are able to introduce cell-to-cell variability by generating detailed, three-dimensional granule cell morphologies that are based on biological reconstructions. Through these and other improvements, we aim to construct a more complete full-scale model of the rat dentate gyrus, to provide a better tool to delineate the functional role of cell types within the dentate gyrus and their pathological changes observed in epilepsy.

Keywords: computational model, dentate gyrus, parallel, morphology, variability

INTRODUCTION

The dentate gyrus network model was developed to study the role of the circuit alterations present in the epileptic dentate gyrus (Santhakumar et al., 2005; Dyhrfjeld-Johnsen et al., 2007) and has been used to make predictions for the existence of non-random microcircuits in epilepsy (Morgan and Soltesz, 2008). The network model has also been used in other studies on topics such as epilepsy (Thomas et al., 2009, 2010), paired-pulse inhibition (Jedlicka et al., 2010), excitability (Winkels et al., 2009; Jedlicka et al., 2011), computational modeling software (Gleeson et al., 2007), and in the construction of a CA1 model (Cutsuridis et al., 2010). Of particular note is the use of the model to test improvements to the NEURON simulation environment (Migliore et al., 2006; Hines and Carnevale, 2008; Hines et al., 2008a,b). The network simulations performed in the studies listed above have exclusively used the smaller 1:2000 scale model (Santhakumar et al., 2005), in part due to the increased time associated with simulating the 1:20 scale model, with a reported 35–70 h per simulation (Dyhrfjeld-Johnsen et al., 2007).

The creation of parallel NEURON and the speedup obtained during tests on the 1:2000 scale model (Migliore et al., 2006) have provided a means to not only make the recent model more accessible to researchers, but to also remove the limitations on the size and complexity of the computational model. The results presented in this study represent the next step in model development, expanding the size and scope of the model. The results from the translation of the 1:20 scale model from a serial to parallel implementation are described, as well as the enlargement of the model to the full size of the rat dentate gyrus. Through the cooperation of two software tools, the complexity of the model can be increased with the generation of variable and realistic dendritic morphology for the sample case of granule cells. These model improvements reflect a significant advancement toward a realistic full-scale computational model.

MATERIALS AND METHODS

All simulations, virtual neuron generation, and analysis were performed on the UCI Broadcom Distributed Unified Cluster

(BDUC) or a PC running Ubuntu Linux. Data analysis and plotting were performed using Python 2.7.1.

DENTATE GYRUS NETWORK SIMULATIONS

All network simulations were performed using NEURON 7.0 (Hines and Carnevale, 1997). NEURON was configured to run in parallel on the Linux BDUC cluster with Openmpi 1.4.3, as shown previously (Hines and Carnevale, 2008). The serial version of the 1:20 scale model is freely available at ModelDB (http://senselab.med.yale.edu/modeldb/ShowModel.asp?model=124513). The serial version of the dentate model was translated to a parallel implementation using strategies described elsewhere (Migliore et al., 2006; Hines and Carnevale, 2008). This involved assigning each cell a global identifier, so that even though a cell is only created on one host, all other hosts are still be able to refer to that cell. Each cell was then associated with its own random number generator for creating connections which uses a seed that is dependent on its global identifier. The dentate model NEURON code has also been rewritten with an emphasis on modularization and explanatory commenting in order to increase its adaptability and accessibility for the general neuroscience community.

The 1:20 scale parallel model was constructed in accordance with the serial model from previous studies (Dyhrfjeld-Johnsen et al., 2007; Morgan and Soltesz, 2008). Multicompartmental models for granule cells, mossy cells, basket cells, and hilar cells with axonal projections to the perforant path (HIPP) were taken from the original 1:2000 scale model (Santhakumar et al., 2005). These are the numerically dominant cell types found in the dentate gyrus. The single-cell models contained ionic currents dependent on the given cell type, including sodium, fast- and slow-delayed rectifier potassium, A-type potassium, I_h, L, N, and T-type calcium, and calcium-dependent potassium currents. The ionic currents in the cell models were previously tuned to match the passive and active properties observed experimentally for each cell type (Santhakumar et al., 2005). Connectivity was based on a highly realistic, data-driven structural model (Dyhrfjeld-Johnsen et al., 2007), and the probability of making a connection between two cells was increased fivefold to account for the reduced size of the network. The two elements of the injured model (hilar cell loss and mossy fiber sprouting) were simulated at 80% of their maximum values, as this value produced maximal epileptiform activity in the network model and corresponds to the level of mossy cell survival observed in human temporal lobe epilepsy (Blumcke et al., 2000; Gabriel et al., 2004). Perforant path stimulation was simulated through simultaneous input to 5000 granule cells (10%), 10 mossy cells (3.3%), and 50 basket cells (10%) located in the middle lamella of the model dentate gyrus at 5 ms from the start of the simulation.

The full-scale model eliminated previous scaling adjustments that were required by the smaller network size. The number of cells was the same as estimated to be in the dentate gyrus in the rat (for a detailed description, see Dyhrfjeld-Johnsen et al., 2007), with 1,000,000 granule cells, 30,000 mossy cells, 10,000 basket cells, and 12,000 HIPP cells evenly distributed along the septotemporal axis. Hilar cell loss and mossy fiber sprouting were again simulated at 80% of their maximum. The peak conductance for sprouted granule cell synapses was reduced from 1.0 to 0.5 nS, the original estimate based on experimental data (Molnar and Nadler, 1999). Synaptic conductances for connections from granule cells to both inhibitory cell types were reduced by a factor of two to avoid depolarization block, as done previously (Dyhrfjeld-Johnsen et al., 2007). Perforant path stimulation was simulated through simultaneous input to 10,000 granule cells (1%), 20 mossy cells (0.33%), and 100 basket cells (1%), which corresponds to stimulation of 1/10th of the middle lamella of the model dentate gyrus.

RECONSTRUCTIONS

Digital reconstructions of dendritic trees were obtained from 19 granule cells labeled *in vivo* in the rat dentate gyrus (Buckmaster, 2012). The three-dimensional Neurolucida reconstructions were corrected for shrinkage in the transverse (1.06X) and depth (1.96X) planes based on previous estimates (Buckmaster and Dudek, 1999) using Neurolucida software (MicroBrightfield, Williston, VT). Reconstruction files were converted from .DAT to .ASC format for compatibility with morphological analysis.

ANALYSIS AND GENERATION OF DENDRITIC MORPHOLOGY

The creation of realistic dendritic morphologies was performed using two freely available software programs: L-Measure and L-Neuron. Morphological parameters from granule cell reconstructions and generated virtual neurons were extracted using L-Measure v4.0 software (Scorcioni et al., 2008). L-Measure is available at http://cng.gmu.edu:8080/Lm/. Virtual dendritic trees were generated using L-Neuron v1.08 (Ascoli and Krichmar, 2000), available at http://krasnow1.gmu.edu/cn3/L-Neuron/index.htm. The L-Neuron program was executed with the Hillman/PK dendritic growth algorithm (Ascoli et al., 2001), and outputs were generated in Southampton Archive format (.swc) for compatibility with L-Measure analysis.

The parameters utilized by the dendritic growth algorithm, referred to as basic parameters, were extracted from the granule cell reconstructions as raw values. Extracted basic parameter distributions were then incorporated into L-Neuron using one or more of the statistical distributions allowed in L-Neuron: gamma, normal, uniform, and constant value distributions. Many of the basic parameters are compatible and can thus be directly incorporated into L-Neuron from L-Measure. The definitions for some basic parameters, however, are different between L-Neuron and L-Measure, which can be modified to create congruency. For example, L-Neuron generates terminal dendritic branches by creating an interbifurcation segment and then attaching a terminal segment, whereas L-Measure analyzes the two segments as a single branch. This creates a discrepancy between the distribution input for L-Neuron and the distribution for generated outputs measured with L-Measure for parameters such as the path length of the terminal branch. Adjustments were made to the L-Neuron input to maximize the overlap between the basic parameter distributions extracted from generated virtual neurons and those extracted from reconstructions. As a result, L-Neuron creates morphologies that have similar basic parameters, including the path length of terminal branches noted above, as the sample

reconstructions. For statistical tests, the outputs for the constant value distributions in L-Neuron were set to their intended values due to minor deviations imposed in the L-Neuron program.

Morphological parameters not used in the dendritic growth algorithm, known as emergent parameters, were used to compare virtual and real neurons, as well as to filter for biologically realistic virtual granule cells. Scalar emergent parameters summarize a morphological characteristic in a single value, whereas distribution emergent parameters show the dependence of one parameter on another. The scalar and distribution emergent parameters used in this study were largely taken from a previous study using L-Neuron (Ascoli et al., 2001). The scalar emergent parameters used were total dendritic length, number of bifurcations, surface area, average path distance to dendritic tips, average Euclidean distance to tips, maximum Euclidean distance to tips, maximum branch order, partition asymmetry, transverse spread, and longitudinal spread. The transverse and longitudinal spreads were used instead of height, width, and depth in order to provide an orientation-independent measure of the three-dimensional extent of dendritic trees. Transverse spread was defined as the maximum distance in the xy plane between dendritic tips, while longitudinal spread was the maximum distance in the z plane. Generated virtual neurons were selected if they fell within two standard deviations of the mean for all emergent parameters except surface area. Assuming a normal distribution, this theoretically includes more than 95% of the granule cell population. The two standard deviation limit for surface area would have allowed for unrealistic values that were lower than the allowed length, so the constraint was changed to 1.65 standard deviations (theoretically more than 90% of granule cells).

RESULTS

PARALLELIZATION OF THE 1:20 SCALE MODEL

Previous implementations of the rat dentate gyrus network model were scaled down from the biological dentate gyrus because they were limited to the use of a single processor. The creation of parallel NEURON (Migliore et al., 2006) dramatically increased the computational resources available to network simulations. Increasing the number of processors for the 1:2000 scale model has been shown to produce a superlinear speedup of the overall runtime when tested on several different parallel computing systems (Migliore et al., 2006). Using the principles detailed in that conversion, the more recent 1:20 scale dentate gyrus model (Dyhrfjeld-Johnsen et al., 2007; Morgan and Soltesz, 2008) was translated for compatibility with parallel NEURON. Because the granule cells in the control model network only fire sparsely as in the biological dentate gyrus (Morgan and Soltesz, 2008), the "injured" model, which contains several of the experimentally observed changes in epilepsy and displays epilepsy-related hyperactivity, was used in order to generate network activity for the parallel implementation. The general network topology of the dentate gyrus model is depicted in **Figure 1A**. The superlinear speedup from previous studies was also observed with the 1:20 scale model for up to the 90 processors tested, as shown in **Figure 1B**. The superlinear quality, instead of a purely linear result, is thought to be due to the more efficient use of a processor's memory (Migliore et al., 2006). The use of 90 processors decreased the overall runtime from 11.0 h to 6.8 min for 300 ms of model network activity. The granule cell activity for parallel model simulations is shown in **Figure 1C**. The model network connectivity and activity were identical for all parallel simulations regardless of the number of processors used.

The conversion to a parallel implementation makes the construction of a full-scale dentate gyrus computational model feasible. The increased availability of computational resources provided by parallel computing addresses the two main limiting factors to model network size: runtime and memory capacity. To construct the full-scale model, the number of cells and the connectivity of the 1:20 scale model were modified to be in agreement with the previous dentate gyrus structural model (Dyhrfjeld-Johnsen et al., 2007). The full-scale model contained over 1,000,000 cells and over 470,000,000 connections when simulated with the 80% injured model. The full-scale simulation shown in **Figure 2** was performed on 150 processors, required ∼220 GB of RAM, and was completed in 11.1 h. The reverberating network activity seen in previous scaled down injured models is observed in the full-scale network, shown for each cell type in **Figure 2A**. The granule cell activity spreads throughout the network and persists for the entire simulation time of 1 s. A voltage trace recorded from a granule cell demonstrates the realistic firing pattern of the model granule cells, shown in **Figure 2B**. The model, as explained above, represents a dentate gyrus from the epileptic rat brain with 80% hilar cell loss and heavy mossy fiber sprouting. The model depicted in **Figure 2**, while data-driven, still omits many of the changes known to occur in epilepsy, with hilar interneuron axon sprouting as one example (Zhang et al., 2009), as well as several other features, e.g., some interneuronal subtypes, gap junctions, short-term plasticity, etc. These features will need to be incorporated into the model in the future.

CREATING VARIABILITY IN DENDRITIC MORPHOLOGY

Due to the additional computational resources provided by parallel computing, the complexity of the dentate gyrus model can be expanded just as with the network size. The single cell models are one of the previously simplified aspects of the model that can be improved, such as the single granule cell model. The current granule cell model [introduced in Santhakumar et al. (2005) for the 1:2000 model and also used in Dyhrfjeld-Johnsen et al. (2007) for the 1:20 model] contains nine cylindrical compartments with the diameter of the dendrites constant throughout the dendrites, based on a previous computational model (Aradi and Holmes, 1999). In addition, the morphology and biophysics are equivalent for every granule cell in the network, so that the 1:20 scale model contains 50,000 identical simplified granule cells. The introduction of realistic morphology and cell-to-cell variability would greatly improve the complexity of the network model and can be achieved using two freely available software tools: L-Measure (Scorcioni et al., 2008) and L-Neuron (Ascoli and Krichmar, 2000).

The general strategy for virtual neuron generation was to use morphological parameters extracted from granule cell reconstructions to create realistic virtual neurons that are as much as possible indistinguishable from the reconstructed cells. Basic morphological parameters required by the L-Neuron dendritic

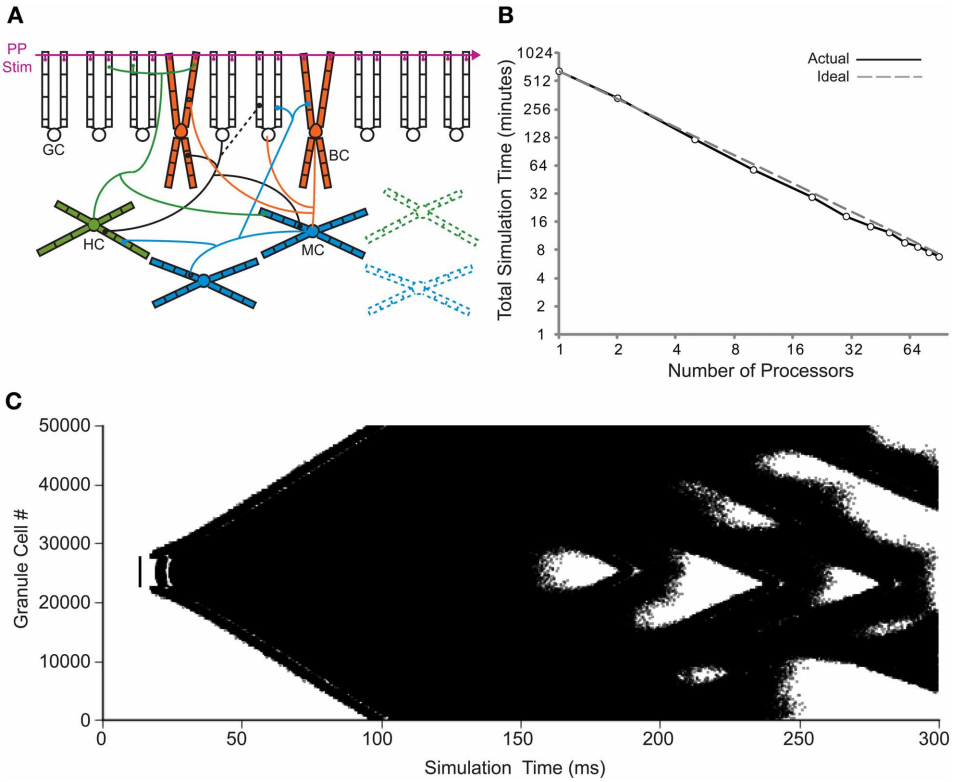

FIGURE 1 | Translation to parallel NEURON. (A) Basic network connectivity of the dentate model. A depiction of the dendritic structure, connectivity, and location of synapses for the four cell types is shown. Note that the septo-temporal extent of the axons is also incorporated into the model (see Dyhrfjeld-Johnsen et al., 2007) but is not illustrated here. In the injured model, HIPP cells and mossy cells are lost, while granule cells synapse onto other granule cells (changes are represented by dashed lines). GC, granule cell; BC, basket cell; HC, HIPP cell; MC, mossy cell; and PP Stim, perforant path stimulation. **(B)** Runtime of 80% injured network simulations versus the number of processors for actual and ideal scaling. **(C)** Granule cell activity for the parallel 1:20 scale model. Each dot represents a single granule cell spike.

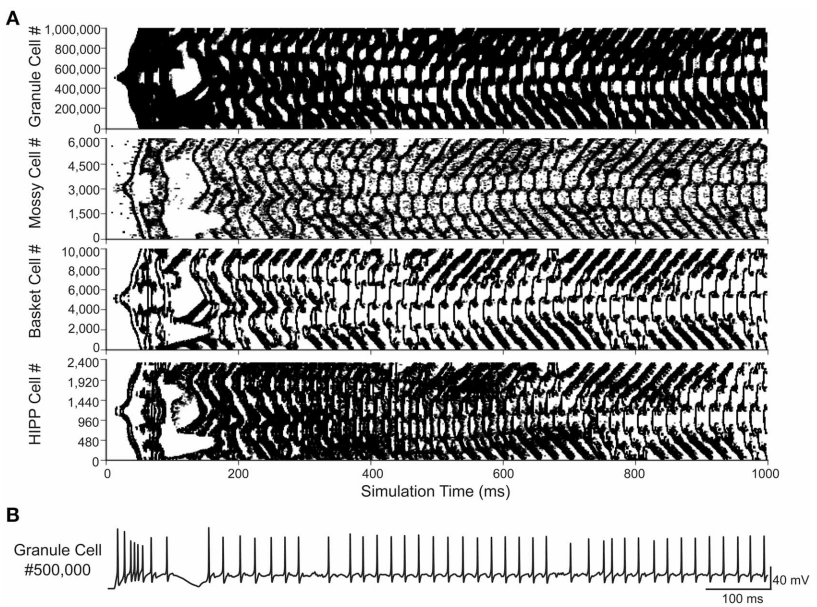

FIGURE 2 | Full-scale dentate gyrus simulation. (A) Activity for each of the four cell types in the 80% injured model. Each dot represents a single spike. **(B)** Voltage trace from the simulation shown in **(A)** for granule cell #500,000.

growth algorithm were extracted from granule cell reconstructions using L-Measure and are listed in **Figure 3**. The extracted parameter distributions were incorporated into L-Neuron to generate virtual dendritic trees with the same basic parameters as the experimental reconstructions. There was no significant difference between real and virtual granule cell basic parameter distributions (**Figure 3**; $p > 0.05$, two-sample Kolmogorov–Smirnov test). The L-Neuron program thus creates granule cell dendritic trees with similar basic parameters to those seen in granule cells in the biological dentate gyrus. However, the basic parameter distributions used in L-Neuron have a high degree of variability, and it has been noted by previous studies (Ascoli et al., 2001; Donohue et al., 2002) that virtual dendrites generated with L-Neuron have an excessive degree of variability when compared with sample dendrites. Accordingly, generated dendrites will not necessarily be biologically realistic nor produce a representative population. To counteract the excessive variability, the high degree of variability in L-Neuron inputs is still allowed, but the outputs are filtered to select for only those morphologies that are representative of the experimental reconstructions. A population can then be constructed from these biologically realistic morphologies that have a similar degree of variability as the sample set of reconstructions.

The generated granule cells were filtered based on scalar emergent parameters that are not used in the dendritic growth algorithm, such as the total dendritic length of the cell. Constraints involving variability up to two standard deviations for most emergent parameters allowed for values beyond those measured from the sample reconstructions, but restricted generated neurons to only those that have biologically realistic values. The virtual granule cells were then chosen to match a Gaussian or Poisson distribution for the total dendritic length, number of bifurcations, and surface area, shown in **Figure 4A**, to create a representative and distributed population. The virtual granule cell population

Basic Parameter	Description	Probability Distribution	KS p-value
bif_ampl_remote	Angle between a bifurcation point and the ends of the two daughter branches	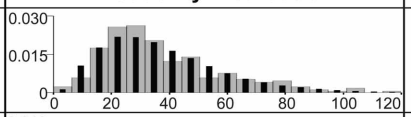	0.61
ibf_branch_pathlength	Length of interbifurcation branches (μm)	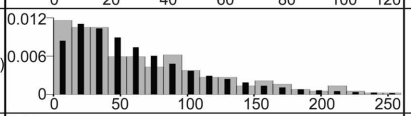	0.27
term_branch_ pathlength	Length between the last bifurfaction in a branch and the terminal tip (μm)	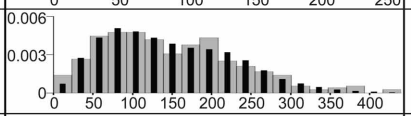	0.93
contraction	Ratio between the Euclidean distance and the path length of a branch	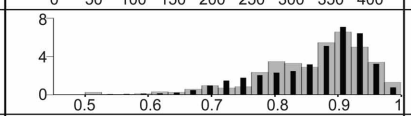	0.29
PK_classic	Poliko constant modifying Rall's law, with Rall Power set to 1.5	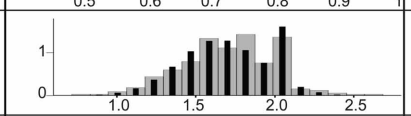	0.28
HillmanThreshold	Weighted average between 50% of father and 25% of daughter diameters for terminal bifurcation (μm)	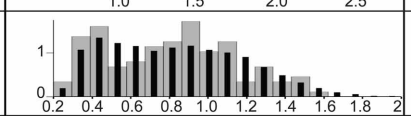	0.51
Daughter_Ratio	Ratio between larger and smaller branch diameters at bifurcation	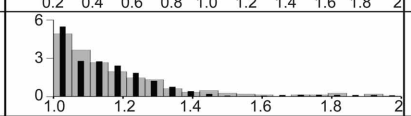	0.35
Taper_2	Length-independent percent of decrease in diameter	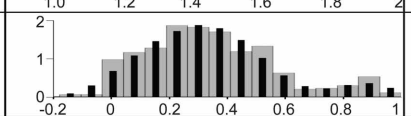	0.38
Stem_Diameter	Starting diameter for dendritic tree (μm)	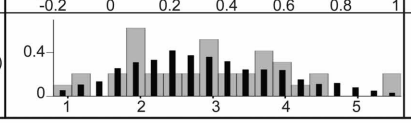	0.96

FIGURE 3 | Basic parameter distributions are matched in order to generate virtual granule cells. The basic parameters extracted from L-Measure and incorporated into L-Neuron are listed with their definitions. For more information see the L-Measure website listed in Materials and Methods. The probability distributions are plotted as probability density versus the basic parameter value for experimental reconstructions (gray bars) and 10,000 generated virtual neurons (black bars), and the *p*-value for the two-sample Kolmogorov–Smirnov test for the overlap of these distributions is shown.

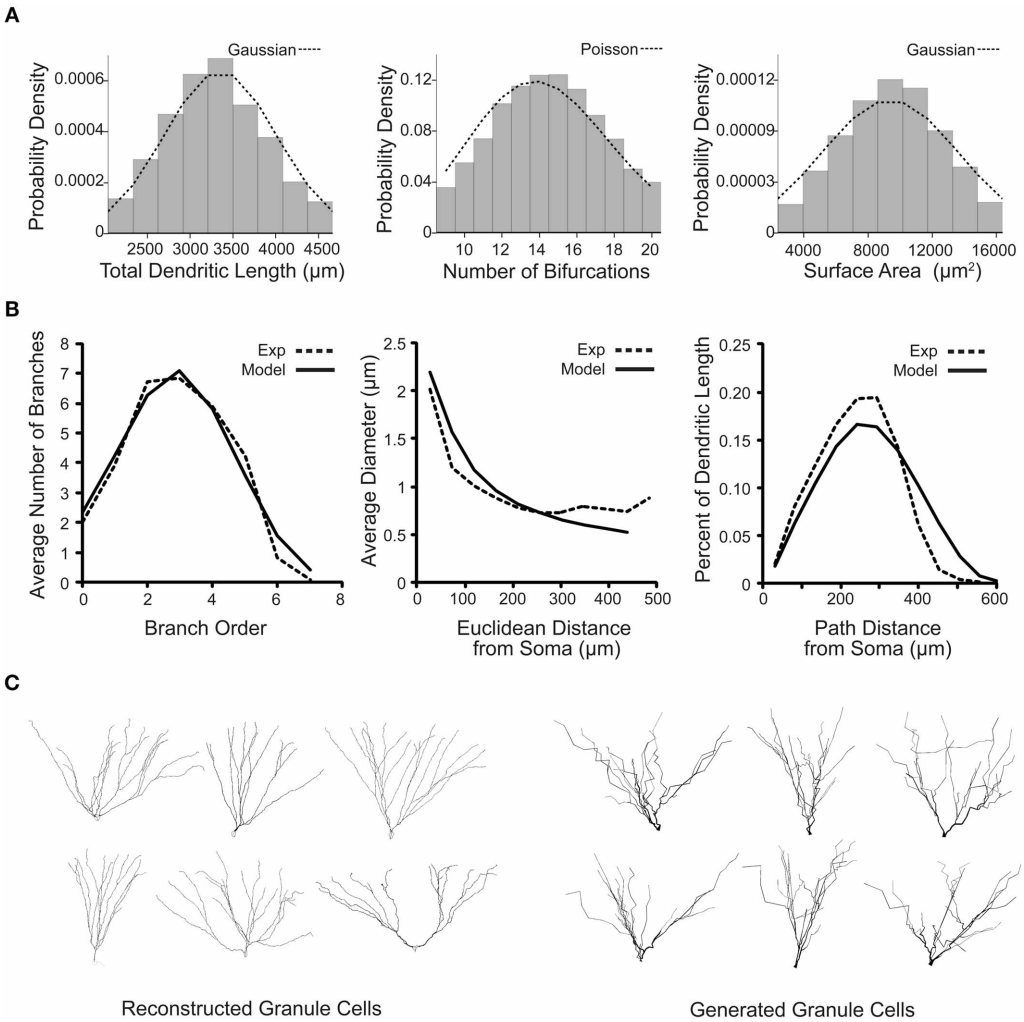

FIGURE 4 | Emergent parameter distributions demonstrate the creation of variable and realistic virtual granule cells of the dentate gyrus. (A) Probability distributions for several scalar emergent parameters of 100,000 generated granule cells. Distributions for total dendritic length, number of bifurcations, and surface area are shown with their ideal respective truncated Gaussian and Poisson probability density functions. **(B)** Distribution emergent parameters for real (dashed line) and 10,000 generated (solid line) neurons. **(C)** Sample reconstructed and generated dentate granule neurons, visualized in NEURON.

and granule cell reconstructions were also compared using distribution emergent parameters that examine the relationship between two parameters. The distribution emergent parameters shown in **Figure 4B** demonstrate that the generated granule cells are nearly indistinguishable from the reconstructed cells. This method of constraining and selecting virtual dendrites allows a small set of experimental reconstructions to be amplified to create a realistic and distributed population of granule cells. A sample of real and virtual granule cells is shown in **Figure 4C**. The dendritic trees can be improved by adding tropism to increase the curvature and smoothness of the dendrites, but the overall structures for real and generated neurons are statistically indistinguishable.

DISCUSSION

The model development presented in this study reflects a significant advancement in bridging the gap between the biological dentate gyrus and the dentate gyrus network model. The speedup conferred by parallel computing makes the 1:20 scale model more accessible for use with even a small computing cluster by reducing the time required for simulations, and the additional computational resources enable the model to be implemented at full scale. These full-scale simulations are advantageous in that they remove the scaling adjustments made for smaller models, and values determined experimentally can now be directly incorporated into the model. The computational model thus becomes a more effective complement to experimental techniques.

The additional computational resources also allow for the complexity of the network to be increased to provide a greater level of accuracy, including at the level of single cells. The inherent cooperation between morphological analysis with L-Measure and generation with L-Neuron provides a means by which to amplify a small sample of reconstructed cells into a distributed

virtual population. The availability of detailed reconstructions is ever-growing, such as through the Neuromorpho.org database (Ascoli et al., 2007), so the tools and principles used in this study can be applied to other cell types within the dentate gyrus. The potential covariance of morphological parameters, however, is not considered in this study. Similarly, the inter-dependence of physiological parameters will also need to be addressed, especially with a functional model, given previous insights (Golowasch et al., 2002). The introduction of realistic morphology expands the network from a two-dimensional structure that is dominated by a linear strip to a three-dimensional model that allows for cells to be distributed in space and throughout layers. This ability gives rise to the possibility of making more direct comparisons to the experimental literature, through concepts such as taking a virtual slice of the model.

The incorporation of realistic morphology can be used in concert with experimentation on the passive and active properties of dentate gyrus neurons to create accurate and variable neurons. Recent studies using a combination of experimental methods and computational modeling have described the dynamics of action potential initiation (Schmidt-Hieber and Bischofberger, 2010) and dendritic integration (Schmidt-Hieber et al., 2007; Krueppel et al., 2011) for dentate granule cells. Generated functional models will need to possess the documented characteristics of granule cells in these studies, such as axonal action potential initiation and a similar level of dendritic attenuation of backpropagating action potentials. In addition, the passive and active properties (e.g., resting membrane potential, action potential threshold, etc.) will be compared to literature values, similar to the development of our previous single cell model (Santhakumar et al., 2005). The improvement of single cell models is not reserved only to principal cells, as the properties of fast-spiking basket cells determined through experiment and modeling (Hu et al., 2010; Norenberg et al., 2010), for example, can be incorporated into a more accurate basket cell model. Through these improvements and the resources conferred by parallel NEURON, the computational model of the rat dentate gyrus can reflect a previously unattainable size and accuracy in order to approach a more complete model of the biological dentate gyrus.

ACKNOWLEDGMENTS

The authors would like to thank Michael Hines for assistance with translating the NEURON code, Sridevi Polavaram for assistance with L-Neuron and L-Measure, and Harry Mangalam for assistance with the BDUC cluster. This work was supported by NSF DGE-0808392 to Marianne Bezaire and NASA NNX10AD59G and NIH grant NS74432 to Ivan Soltesz.

REFERENCES

Aradi, I., and Holmes, W. R. (1999). Role of multiple calcium and calcium-dependent conductances in regulation of hippocampal dentate granule cell excitability. *J. Comput. Neurosci.* 6, 215–235.

Ascoli, G. A., Donohue, D. E., and Halavi, M. (2007). NeuroMorpho.Org: a central resource for neuronal morphologies. *J. Neurosci.* 27, 9247–9251.

Ascoli, G. A., and Krichmar, J. L. (2000). L-Neuron: a modeling tool for the efficient generation and parsimonious description of dendritic morphology. *Neurocomputing* 32, 1003–1011.

Ascoli, G. A., Krichmar, J. L., Scorcioni, R., Nasuto, S. J., and Senft, S. L. (2001). Computer generation and quantitative morphometric analysis of virtual neurons. *Anat. Embryol. (Berl.)* 204, 283–301.

Blumcke, I., Suter, B., Behle, K., Kuhn, R., Schramm, J., Elger, C. E., et al. (2000). Loss of hilar mossy cells in Ammon's horn sclerosis. *Epilepsia* 41(Suppl. 6), S174–S180.

Buckmaster, P. S. (2012). Mossy cell dendritic structure quantified and compared with other hippocampal neurons labeled in rats *in vivo*. *Epilepsia* 53(Suppl. 1), 9–17.

Buckmaster, P. S., and Dudek, F. E. (1999). *In vivo* intracellular analysis of granule cell axon reorganization in epileptic rats. *J. Neurophysiol.* 81, 712–721.

Cutsuridis, V., Cobb, S., and Graham, B. P. (2010). Encoding and retrieval in a model of the hippocampal CA1 microcircuit. *Hippocampus* 20, 423–446.

Donohue, D. E., Scorcioni, R., and Ascoli, G. A. (2002). "Generation and description of neuronal morphology using L-Neuron: a case study," in *Computational Neuroanatomy: Principles and Methods,* ed G. A. Ascoli (Totowa, NJ: Humana), 49–70.

Dyhrfjeld-Johnsen, J., Santhakumar, V., Morgan, R. J., Huerta, R., Tsimring, L., and Soltesz, I. (2007). Topological determinants of epileptogenesis in large-scale structural and functional models of the dentate gyrus derived from experimental data. *J. Neurophysiol.* 97, 1566–1587.

Gabriel, S., Njunting, M., Pomper, J. K., Merschhemke, M., Sanabria, E. R., Eilers, A., et al. (2004). Stimulus and potassium-induced epileptiform activity in the human dentate gyrus from patients with and without hippocampal sclerosis. *J. Neurosci.* 24, 10416–10430.

Gleeson, P., Steuber, V., and Silver, R. A. (2007). neuroConstruct: a tool for modeling networks of neurons in 3D space. *Neuron* 54, 219–235.

Golowasch, J., Goldman, M. S., Abbott, L. F., and Marder, E. (2002). Failure of averaging in the construction of a conductance-based neuron model. *J. Neurophysiol.* 87, 1129–1131.

Hines, M. L., and Carnevale, N. T. (1997). The NEURON simulation environment. *Neural Comput.* 9, 1179–1209.

Hines, M. L., and Carnevale, N. T. (2008). Translating network models to parallel hardware in NEURON. *J. Neurosci. Methods* 169, 425–455.

Hines, M. L., Eichner, H., and Schurmann, F. (2008a). Neuron splitting in compute-bound parallel network simulations enables runtime scaling with twice as many processors. *J. Comput. Neurosci.* 25, 203–210.

Hines, M. L., Markram, H., and Schurmann, F. (2008b). Fully implicit parallel simulation of single neurons. *J. Comput. Neurosci.* 25, 439–448.

Hu, H., Martina, M., and Jonas, P. (2010). Dendritic mechanisms underlying rapid synaptic activation of fast-spiking hippocampal interneurons. *Science* 327, 52–58.

Jedlicka, P., Deller, T., and Schwarzacher, S. W. (2010). Computational modeling of GABAA receptor-mediated paired-pulse inhibition in the dentate gyrus. *J. Comput. Neurosci.* 29, 509–519.

Jedlicka, P., Hoon, M., Papadopoulos, T., Vlachos, A., Winkels, R., Poulopoulos, A., et al. (2011). Increased dentate gyrus excitability in neuroligin-2-deficient mice *in vivo*. *Cereb. Cortex* 21, 357–367.

Krueppel, R., Remy, S., and Beck, H. (2011). Dendritic integration in hippocampal dentate granule cells. *Neuron* 71, 512–528.

Migliore, M., Cannia, C., Lytton, W. W., Markram, H., and Hines, M. L. (2006). Parallel network simulations with NEURON. *J. Comput. Neurosci.* 21, 119–129.

Molnar, P., and Nadler, J. V. (1999). Mossy fiber-granule cell synapses in the normal and epileptic rat dentate gyrus studied with minimal laser photostimulation. *J. Neurophysiol.* 82, 1883–1894.

Morgan, R. J., and Soltesz, I. (2008). Nonrandom connectivity of the epileptic dentate gyrus predicts a major role for neuronal hubs in seizures. *Proc. Natl. Acad. Sci. U.S.A.* 105, 6179–6184.

Norenberg, A., Hu, H., Vida, I., Bartos, M., and Jonas, P. (2010). Distinct nonuniform cable properties optimize rapid and efficient activation of fast-spiking GABAergic interneurons. *Proc. Natl. Acad. Sci. U.S.A.* 107, 894–899.

Santhakumar, V., Aradi, I., and Soltesz, I. (2005). Role of mossy fiber sprouting and mossy cell loss in

hyperexcitability: a network model of the dentate gyrus incorporating cell types and axonal topography. *J. Neurophysiol.* 93, 437–453.

Schmidt-Hieber, C., and Bischofberger, J. (2010). Fast sodium channel gating supports localized and efficient axonal action potential initiation. *J. Neurosci.* 30, 10233–10242.

Schmidt-Hieber, C., Jonas, P., and Bischofberger, J. (2007). Subthreshold dendritic signal processing and coincidence detection in dentate gyrus granule cells. *J. Neurosci.* 27, 8430–8441.

Scorcioni, R., Polavaram, S., and Ascoli, G. A. (2008). L-Measure: a web-accessible tool for the analysis, comparison and search of digital reconstructions of neuronal morphologies. *Nat. Protoc.* 3, 866–876.

Thomas, E. A., Reid, C. A., and Petrou, S. (2010). Mossy fiber sprouting interacts with sodium channel mutations to increase dentate gyrus excitability. *Epilepsia* 51, 136–145.

Thomas, E. A., Reid, C. A., Berkovic, S. F., and Petrou, S. (2009). Prediction by modeling that epilepsy may be caused by very small functional changes in ion channels. *Arch. Neurol.* 66, 1225–1232.

Winkels, R., Jedlicka, P., Weise, F. K., Schultz, C., Deller, T., and Schwarzacher, S. W. (2009). Reduced excitability in the dentate gyrus network of betaIV-spectrin mutant mice *in vivo*. *Hippocampus* 19, 677–686.

Zhang, W., Yamawaki, R., Wen, X., Uhl, J., Diaz, J., Prince, D. A., et al. (2009). Surviving hilar somatostatin interneurons enlarge, sprout axons, and form new synapses with granule cells in a mouse model of temporal lobe epilepsy. *J. Neurosci.* 29, 14247–14256.

Conflict of Interest Statement: The authors declare that the research was conducted in the absence of any commercial or financial relationships that could be construed as a potential conflict of interest.

Received: 01 September 2012; paper pending published: 24 September 2012; accepted: 27 October 2012; published online: 16 November 2012.

Citation: Schneider CJ, Bezaire M and Soltesz I (2012) Toward a full-scale computational model of the rat dentate gyrus. Front. Neural Circuits ***6****:83. doi: 10.3389/fncir.2012.00083*

frontiers in
NEURAL CIRCUITS

ORIGINAL RESEARCH ARTICLE
published: 26 April 2013
doi: 10.3389/fncir.2013.00081

Unveiling the metric structure of internal representations of space

***Federico Stella*[1]*, *Erika Cerasti*[2] *and Alessandro Treves*[1]**

[1] *Neuroscience, SISSA, Trieste, Italy*
[2] *Department of Human Physiology and Pharmacology, Università "La Sapienza", Rome, Italy*

Edited by:
Peter Jonas, Institute of Science and Technology Austria, Austria

Reviewed by:
Leonard Maler, University of Ottawa, Canada
Peter Jonas, Institute of Science and Technology Austria, Austria
Jozsef Csicsvari, Institute of Science and Technology Austria, Austria

***Correspondence:**
Federico Stella, LIMBO Lab, Neuroscience, SISSA, Via Bonomea 265, Trieste 34136, Italy.
e-mail: fstella@sissa.it

How are neuronal representations of space organized in the hippocampus? The self-organization of such representations, thought to be driven in the CA3 network by the strong randomizing input from the Dentate Gyrus, appears to run against preserving the topology and even less the exact metric of physical space. We present a way to assess this issue quantitatively, and find that in a simple neural network model of CA3, the average topology is largely preserved, but the local metric is loose, retaining e.g., 10% of the optimal spatial resolution.

Keywords: spatial representations, place cells, CA3, decoding, neural network, information theory, metric space

INTRODUCTION

CA3 neurons in rodents develop their selectivity for certain portions of any new environment (O'Keefe and Dostrovsky, 1971; Wilson and McNaughton, 1993) through an ongoing unsupervised learning process, probably driven by the dentate gyrus (Treves and Rolls, 1992; Leutgeb et al., 2007) which is random in nature and which generates a non-trivial mapping between the external input (the position of the animal in that environment) and the response of individual cells. The position, the shape and the number of the fields developed by each CA3 cell are thus not captured by any simple rule of organization (Park et al., 2011). This is true also for non-spatial stimuli, which are most probably deposited in the hippocampal memory store in a similar fashion (Komorowski et al., 2009; Naya and Suzuki, 2011; Tort et al., 2011). Also in this case, we expect neurons to develop random profiles of activation to stimulus features, spanning random regions of feature space (Quiroga et al., 2005).

What is specific about physical space, and makes it different from other correlates of neuronal activity, is its intrinsic topographical structure. A set of spatial stimuli are naturally endowed with a canonical topology and with a continuous metric, defined by the relative position of locations in the environment. These stimuli thus span a multi-dimensional manifold, which, in the typical experimental situation of a recording box, is two-dimensional and Euclidean. How "spatial" is the internal representation generated in CA3? How much of the external metric is preserved inside the brain? (Samsonovich and McNaughton, 1997; Stringer et al., 2002; McNaughton et al., 2006).

One may pretend to ignore the real-world metric, and study the metric of the virtual manifold established by the patterns of neuronal activity with which physical space has been associated (Muller and Stead, 1996; Muller et al., 1996). How? In CA3 the movements of an animal traversing an environment elicit, on repeated trials, a distribution of responses which one can use to define distances between pairs of locations (Brown et al., 1998; Deneve et al., 1999; Averbeck et al., 2006), in terms e.g., of the mean overlaps in the corresponding distributions of population vectors, and one can analyze the overall structure of such pair-wise distances in geometric terms.

Ideally a faithful mapping of space should produce isometric representations, i.e., whose relationships mirror the relationships induced in real space by the Euclidean metric (Curto and Itskov, 2008). Such an ideal mapping is, however, unfeasible with any finite neuronal population, even more so with a random self-organization process (Tsodyks and Sejnowski, 1995; Hamaguchi et al., 2006; Papp et al., 2007; Roudi and Treves, 2008). But how to assess the degree of deviation from isometricity?

Spatial representations in CA3 depend, of course, not just on the physical structure of external space but also on how it is *perceived* by the animal, and on the effective dimensionality of the representation, as spanned by animal behavior (Hayman et al., 2011; Ulanovsky and Moss, 2011). Distant locations might be seen as similar or confused altogether, irrelevant dimensions might be ignored, e.g., on a linear track, the relative distance between locations might be distorted, not all the locations might be assigned a representation in the population, etc. In a word, the Euclidean nature of external space may be altered arbitrarily. To start with, it is useful, however, to remove such arbitrariness and consider a model situation in which there is nothing but the Euclidean metric of physical space to be represented, through self-organization. This is what we set out to do in this study. While in a companion paper (Cerasti and Treves, under review) we focus on characterizing the local smoothness of these representations, and how it scales with the size of the network, here we aim to quantify their metric content.

In Treves (1997), and later papers, e.g., Treves et al. (1998), Ciaramelli et al. (2006), and Lauro-Grotto et al. (2007), a *metric content* index was introduced in order to characterize the amount of perceived metric in the representation of a discrete set of stimuli, such as faces. It was shown empirically that such metric content index is almost invariant as one varies the sample of cells used to assess the representation. Thus, it approaches the role of an objective or intrinsic measure, insensitive to the procedure used to extract it (e.g., how many and which cells are recorded in a particular experiment). Can a similar descriptor be applied to the representation of real space?

Although physical space is low dimensional, each spatial variable can span during everyday behavior a small or large interval along any of the dimensions and, crucially, can do so continuously. To actually define a set of distinct locations, for data analysis, one has in practice to discretize space in a finite number of bins and to assign to each of them a reference population vector, resulting from averaging over the activity expressed when in that bin (the actual procedure to perform this average can vary). One would want these bins to be as small as possible, to retain part of the continuity compromised by the binning. On the other hand, any refinement of the bin resolution leads unavoidably to a low sampling problem.

This "curse of dimensionality" (Golomb et al., 1997; Panzeri et al., 2007) (where the dimensionality referred to is not of space itself, but of multiple locations in space) limits the current feasibility of the metric content analysis of a set of real, experimental data. The length of a recording session necessary to properly sample the distribution of population vectors tends to be prohibitive. One may, however, turn to computer simulations, which can be as long as needed, to produce the data necessary for the analysis.

MATERIALS AND METHODS

BASIC MODEL

The model we consider is, as in Cerasti and Treves (under review) an extended version of the one used in our previous study (Cerasti and Treves, 2010), where the firing rate of a CA3 pyramidal cell, η_i, was determined, as the one informative component, by the firing rates $\{\beta\}$ of DG granule cells, which feed into it through mossy fiber (MF) connections. The model used for the neuron was a simple threshold-linear unit (Treves, 1990), so that the firing of the unit results from an activating current (which includes several non-informative components) and is compared to a threshold:

$$\eta_i(\vec{x}) = g\left[\sum_j c_{ij}^{\mathrm{MF}} J_{ij}^{\mathrm{MF}} \beta_j(\vec{x}) + \tilde{\delta}_i - \tilde{T}\right]^+ \qquad (1)$$

where g is a gain factor, while $[\cdot]^+$ equals the sum inside the brackets if positive in value, and zero if negative. The effect of the current threshold for activating a cell, along with the effect of inhibition, and other non-informative components, are summarized into a single subtractive term, with a mean value across CA3 cells expressed as $\tilde{T}$, and a deviation from the mean for each particular cell i as $\tilde{\delta}_i$, which acts as a sort of noise; threshold and inhibition, in fact, while influencing the mean activity of the network, are supposed to have a minor influence on the coding properties of the system. In the earlier reduced model, however, $\tilde{T}$ and $\tilde{\delta}_i$ also included the effect of other cells in CA3, through RC connections, and that of the perforant path, both regarded as unspecific inputs—this based on the assumption that information is driven into a new CA3 representation solely by MF inputs.

In Cerasti and Treves (under review) and in this study, instead, since we are interested in the ability of the RC system (Amaral et al., 1990; van Strien et al., 2009) to express spatial representations, we separate out the RC contribution, and redefine $\tilde{T}$ and $\tilde{\delta}_i$ into T and δ_i—which sum the remaining unspecific inputs, including the perforant path, not analyzed here:

$$\eta_i(\vec{x}) = g\left[\sum_j c_{ij}^{\mathrm{MF}} J_{ij}^{\mathrm{MF}} \beta_j(\vec{x}) + \sum_k c_{ik}^{\mathrm{RC}} J_{ik}^{\mathrm{RC}} \eta_k(\vec{x}) + \delta_i - T\right]^+ \qquad (2)$$

Connections between cells are indicated by the fixed binary matrices $\{c^{MF}\}$, $\{c^{RC}\}$, whose non-zero elements (which take value 1) represent the existence of anatomical synapses between two cells. The synaptic efficacies are instead indicated by the matrices of weights $\{J^{MF}\}$, $\{J^{RC}\}$, whose elements are allowed to take positive values. The notation is chosen to minimize differences with our previous analysis of other components of the hippocampal system (e.g., Treves, 1990; Kropff and Treves, 2008).

The perforant path inputs from Entorhinal Cortex are not explicitly included in the model, in line with the hypothesis that they relay the cue that initiates the retrieval of a previously stored representation, and have no role in the storage of a new representation and in defining the properties of the attractors in CA3. This perspective has been theoretically described in (Treves and Rolls) and has found experimental support (Lassalle et al., 2000; Lee and Kesner, 2004).

The firing rates of the various populations are all assumed to depend on the spatial position $\vec{x}$ of the animal; and the time scale considered for evaluating the firing rate is of order the theta period, about 100 ms, so the finer temporal dynamics over shorter time scales is neglected. To be precise, in the simulations, we take a time step to correspond to 125 ms of real time, or a theta period, during which the simulated rat moves 2.5 cm, thus at a speed of 20 cm/s. This is taken to be an average over a virtual exploratory session, familiarizing with a new environment.

THE STORAGE OF NEW REPRESENTATIONS

The important novel ingredient that was introduced by (Cerasti and Treves, 2010), and that makes the difference from previous models of self-organizing recurrent networks, is a realistic description of the patterns of firing in the inputs, i.e., in the dentate gyrus. As the virtual rat explores the new environment, the activity $\beta_j(\vec{x})$ of DG unit j is determined by the position $\vec{x}$ of the animal, according to the expression:

$$\beta_j(\vec{x}) = \sum_{k=0}^{Q_j} \beta_0 e^{-(\vec{x}-\vec{x}_{jk})^2/2\sigma_f^2} \qquad (3)$$

The firing rate of the granule cells is then a combination of Q_j Gaussian functions, resulting in "bumps," or fields in the firing map of the environment, centered at random points $\vec{x}_{jk}$. The environment is taken to have size A, and the fields are defined as all having the same effective size $\pi(\sigma_f)^2$ and height β_0. Q_j, which indicates the multiplicity of fields of DG cell j, is drawn from a Poisson distribution:

$$P(Q_j) = \frac{q^{Q_j}}{Q_j!} e^{-q} \tag{4}$$

with mean value q, which roughly fits the data reported by Leutgeb et al. According to the same experimental data, we assume that only a randomly selected fraction $p_{DG} << 1$ (here set at $p_{DG} = 0.033$) of the granule cells are active in a given environment. Hence population activity is sparse, but the firing map of individual active granule units need not be sparse [it would only be sparse if $q\pi(\sigma_f)^2/A << 1$, which we do not assume to be always the case].

The activity of DG units determines the probability distribution for the firing rate of any given CA3 pyramidal unit, once the connectivity level between the two layer has been fixed: $\left\{C_{ij}^{\mathrm{MF}}\right\} = 0, 1$ with $P\left(C_{ij}^{\mathrm{MF}} = 1\right) = \frac{C^{\mathrm{MF}}}{N_{DG}} \equiv c^{\mathrm{MF}}$. In agreement with experimental data, we set $C^{MF} = 50$, a value in the range of the ones providing an optimal information transmission from DG to CA3 (Cerasti and Treves, 2010). The MF synaptic weights are set to be uniform in value, $J_{ij}^{\mathrm{MF}} \equiv J$, and similarly $J_{ij}^{\mathrm{RC}} \equiv J_0^{\mathrm{RC}}$ initially. Subsequently, during the learning phase, RC weights are modified according to the simulated learning process and under the influence of the input coming from the MF connections. Following the simplified hypothesis that the MFs carry all the information to be stored without contributing anything to the retrieval process, which is left to the recurrent collateral, MF weights are kept fixed to their initial values J; note that we have found, in our earlier study that MF connections appear to be inadequate, even when associatively plastic, to support retrieval of spatial representation (Cerasti and Treves, 2010).

The connectivity among CA3 cells is given by the matrix $\left\{C_{ij}^{\mathrm{RC}}\right\} = 0, 1$ with $P\left(C_{ij}^{\mathrm{RC}} = 1\right) = \frac{C^{\mathrm{RC}}}{N_{CA3}} \equiv c^{\mathrm{RC}}$, where $C^{RC} = 900$ in most simulations. The activity of the network is regulated by the constraint we impose on its mean and on its sparsity a_{CA3}, i.e., the fraction of the CA3 units firing significantly at each position, which is an important parameter affecting memory retrieval [(Treves, 1990); more precisely, $a_{\mathrm{CA3}} = \langle\eta_i\rangle^2/\langle\eta_i^2\rangle$]. Here we set the sparsity of each representations as $a_{CA3} = 0.1$, in broad agreement with experimental data (Papp et al., 2007), and at each time step we regulate the threshold T accordingly, to fulfill such requirement, while keeping the mean activity $\langle\eta_i\rangle = 0.1$ by adjusting the gain g.

RECURRENT COLLATERAL PLASTICITY

During the learning phase, the activity of CA3 is driven by DG inputs, and RC connections contribute through weights uniformly set to their initial value J_0^{RC}. While the virtual rat explores the environment, RC weights are allowed to change according to an associative "Hebbian" learning rule, such that the total change in the synaptic weights is given as a sum of independent terms

$$\Delta J_{ij}^{\mathrm{RC}}(t) = \gamma\eta_i(t)\left(\eta_j(t) - \Lambda_j(t)\right) \tag{5}$$

where $\Delta J_{ij}(t)$ indicates the variation of the connection weight between cells i and j occurring at a given time step t, η_i, and η_j are the postsynaptic and presynaptic firing rate, while γ is the learning rate. This associative learning rule includes the contribution of a trace, Λ, of the recent past activity of the presynaptic cell, defined as

$$\Lambda_j(t) = \frac{1}{\tau}\sum_{t_s=1}^{\tau}\eta_j(t - t_s) \tag{6}$$

where τ is taken equal to 14 time steps (1750 ms). RC weights are forced to be non-negative, so they are reset to zero each time they become negative. Moreover, the total of the synaptic weights afferent to a single postsynaptic CA3 cell is normalized at the end of the learning process, so that $\sum_{j=1}^{C^{\mathrm{RC}}} J_{ij}^{\mathrm{RC}} = 1$ per each CA3 cell. In words, the synaptic plasticity on recurrent connections allows the system to store the information about the current environment conveyed by MF inputs; such information is expressed in the form of place-like patterns of activity in CA3 units, and the Hebb-like learning rule strengthens the connections between units that show overlapping fields.

THRESHOLD SETTING IN CA3

CA3 units fire according to Equation (2), with the threshold T hypothesized to serve to adjust the sparsity a_{CA3} of CA3 activity to its required value. The sparsity is defined as

$$a_{\mathrm{CA3}} = \left(\sum_i \eta_i(\vec{x})\right)^2 \Big/ \sum_i \eta_i^2(\vec{x}) \tag{7}$$

and it is set to $a_{CA3} = 0.1$. This implies that the activity of the CA3 cell population is under tight inhibitory control.

SIMULATIONS

The mathematical model described above was simulated with a network of 45,000 DG units and 1500 CA3 units. A virtual rat explores a continuous two dimensional space, intended to represent a 1 sqm square environment but realized as a torus, with periodic boundary conditions. In each time step (of 125 ms) the virtual rat moves 2.5 cm in a direction similar to the direction of the previous time step, with a small amount of noise.

Before and during the learning session, all recurrent connections weights take the same value J_0^{RC}; after the learning phase, they take the values resulting from the sum of all modifications occurred during the session, and described by Equation (5), with learning rate γ. The trajectory of the virtual rat during the learning session is a random path, extended over a time long enough for it to effectively visit repeatedly all possible locations in space: 10,000 time steps to cover the entire environment. This is taken to correspond to about 20 min of exploration in real time. Such synaptic modifications start to have an effect on the CA3 firing rate only at the end of the

learning session, when the RC weights are updated to their new values.

After the learning phase for the CA3 network, we run a training phase for our decoding algorithm, during which we build the so called activity templates (Rolls and Treves, 2011): the environment is discretized in a grid of 8×8 locations and to each of these bins we associate a reference population vector. This reference vector for a bin is obtained averaging the activity of the network in all the time steps that the rat spends in that bin during a simulation of 100,000 time steps.

Subsequently a test phase is run. This time the rat is left wandering on a random trajectory through the environment and at each time step the activity generated in the network is compared to the templates previously defined. The dynamics is analyzed when the input coming from the DG units is either on, to characterize externally driven representation, or turned off, to characterize instead memory driven attractors (Wills et al., 2005; Colgin et al., 2010). The noise level we use is kept very low ($\delta = 0.002$), as we are more interested to probe the microstructure of the spatial representation rather than to test its robustness. To have a roughly even coverage of the surface of the environment and to produce a sufficient number of visits to each one of the locations in which it is divided, simulations are run for 400,000 time steps (nearly 35 h of virtual rat time).

For simulations without DG direct input, aimed at describing attractor properties, in each step of the virtual rat trajectory, activity is allowed to reverberate for 15 time steps; with a full DG input during the first one, an input reduced to 1/3 during the second, and to 0 for the remaining 13 time steps. The final configuration attained by the system after this interval is then observed and the rat is moved to the next position and the procedure is repeated.

ANALYSIS AND RESULTS

GLOBAL METRIC

What does the global structure of the CA3 representation generated in our simulations look like? One may start addressing this question by using the most comprehensive measure of activity in the network. In our simulations, templates are generated using the entirety of the cells and averaging their activity over the spatial extent of the relative bin. They are the fingerprints of the representation of the environment contained in CA3. Templates are vectors in a high-dimensional space, namely the number of dimensions corresponds to the number of units in the network, 1500 in the simulations we use for the analysis. To visualize the configuration of these vectors and their arrangement, one should use some procedure to reduce their dimensionality and to produce a readable picture. One can use the correlation between the vectors associated to different positions to construct a *similarity matrix* containing the relative distance of all the vector pairs. Multidimensional scaling (MDS) uses this similarity matrix to assign positions to the templates in a Euclidean space of a specified dimension (in our case, 3-dimensional), so as to best preserve the ordering of the distances in the distance matrix. One can then directly compare the configuration obtained from the algorithm to the topology of the external environment, which, in the case of our simulations that make use of periodic boundary conditions, is a two-dimensional torus.

In fact, also configurations produced by a metric MDS [Sammon algorithm (Sammon Jr), Stress = 0.04] tend to have a torus-like topology (**Figure 1**). The global properties of the model CA3 representation thus faithfully reproduce those of external space, at least in terms of average templates. This assessment, however, is only qualitative and it misses finer details that may hide at different levels of resolution. The actual responses of the network while the animal is traversing the environment are averaged away in building the templates. Moreover a measure based on the activity of the whole population does not provide indications as to the distribution of information sampled, in practice, from the few neurons which can be recorded simultaneously, leaving doubts as to whether such a global measure has any experimental relevance. We are then left with the problem of constructing a synthetic description of the representation that comprises information on its local properties, as gauged by observing a few units at a time.

DECODING

To quantitatively assess the features of a neural representation of any set of stimuli we can rely on some standard procedures (Quian Quiroga and Panzeri, 2009). Decoding the spike trains emitted by a population of neurons, when one (s) of a set of stimuli is presented, means applying an algorithm that estimates, given the current spike train and those previously recorded in response to each stimulus, the likelihood for each (s') of the possible stimuli to be the current one. The stimulus for which the likelihood is maximal is the stimulus predicted on the basis of the chosen decoding algorithm. One repeats this all the times s is the current stimulus, to generate a table $P(s' \mid s)$. The decoded stimulus is not necessarily the correct one, and a first measure of the nature of the representation is just the fraction of correct

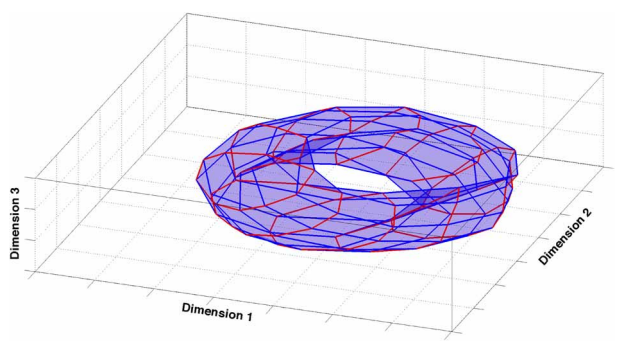

FIGURE 1 | Multidimensional scaling analysis. The figure shows the 3-dimensional configuration of template vectors based on pairwise correlations obtained by multidimensional scaling [Sammon criterion (Sammon, 1969)], applied to the spatial representation produced by the model CA3 network. The configuration closely reproduces the original similarity matrix (Stress = 0.04). Red and blue lines correspond to orthogonal directions in the external environment.

hits in the table, $\sum_s P(s \mid s)P(s)$, where $P(s \mid s)$ are just the diagonal elements of the confusion matrix. A more complex, yet more complete, measure is given by the mutual information I

$$I = \sum_{r,s} P(r, s) \log_2 \frac{P(r, s)}{P(r)P(s)} \tag{8}$$

which also reflects the distribution of errors, and thus provides further insight on the way the stimuli are encoded (Rolls and Treves). These two quantities, percent correct and mutual information, depend on the pool of neurons used to perform the decoding, and most crucially on the size of this pool. More cells obviously allow for better decoding.

The two quantities are not completely independent, as there are mutual constraints between them. At the same time, one does not completely define the other: given a certain percent correct there is a possible range of information values that depends on the way errors are distributed among incorrect locations. At one extreme, when there is no overlap between the representations of different stimuli, we expect errors to be distributed at chance: the "distance" between any pair of stimuli is maximal and effectively the same, and no non-trivial metric can be defined. Conversely, any non-uniform overlap influences the way errors are produced. The more the distribution of errors deviates from being flat, the more the representation contains overlapping and interfering elements.

THE SPATIAL CONFUSION MATRIX

During the test phase of our simulations, at each time step, the firing vector of a set of CA3 units is compared to all the templates recorded at each position in the 8×8 grid, for the same sample, in a test trial (these are the template vectors). The comparison is made by calculating the Euclidean distance between the current vector and each template, and the position of the closest template is taken to be the decoded position at that time step, for that sample. This procedure applies to our spatial analysis what has been termed maximum likelihood Euclidean distance decoding (where the distance between population vectors should not be confused with the distance between locations in the environment). The frequency of each pair of decoded and real positions are compiled in a so-called "confusion matrix." Should decoding "work" perfectly, in the sense of always detecting the correct position in space of the virtual rat, the confusion matrix would be the identity matrix. The confusion matrix is thus $L^2 \times L^2$ (64×64 for our simulations) and its dimension grows very fast when increasing the number of bins, requiring a prohibitively longer number of time steps to properly fill all its entries.

The confusion matrix gives us the value of the percent correct and of the mutual information. The size of the sample is then varied to describe the dependence of these quantities on the number of cells in the pool. We used samples of up to 256 units, a number which can be compared with the total population in our CA3 network, 1500 units.

METRIC CONTENT

For a given percent correct (f_{cor}) there is in general, in a non-spatial paradigm, a certain range of possible amounts of information contained in the confusion matrix. Ideally the information should be comprised between a minimum value

$$I_{\min} = \log_2 S + f_{\text{cor}} \log_2 f_{\text{cor}} + (1 - f_{\text{cor}}) \log_2 (1 - f_{\text{cor}}) - (1 - f_{\text{cor}}) \log_2 (S - 1) \tag{9}$$

(where S is the number of elements in the stimulus set) corresponding to an even distribution of errors among all the possible stimuli, while the maximum is attained when all the errors are concentrated on a single incorrect stimulus

$$I_{\max_{\text{bias}}} = \log_2 S + f_{\text{cor}} \log_2 f_{\text{cor}} + (1 - f_{\text{cor}}) \log_2 (1 - f_{\text{cor}}) \tag{10}$$

However, this maximum corresponds to a systematic misclassification of the current location by the network. It might therefore be reasonable to assume that our system is an unbiased classifier, which implies that incorrect stimuli can at most be chosen as frequently as the correct one, and reformulate the previous maximum in the following terms

$$I_{\max} = \log_2 S + \log_2 f_{\text{cor}} \tag{11}$$

The metric content index can then be defined, in such a non-spatial paradigm, as

$$\lambda = \frac{I - I_{\min}}{I_{\max} - I_{\min}} \tag{12}$$

This is the measure considered in our previous studies. With this choice, though, we wouldneglect the intrinsic topological structure of spatial information. In fact, the high correlation existing between the representations of neighboring locations constrains the distribution of errors. We need to distinguish between errors originating from random correlations in the representation of distant, unrelated locations, and errors emerging form the continuity of the representation. The latter can be considered as structural to the representation and they are expected to be present around the correct location even in the case of optimal decoding, but with limited spatial resolution.

FULL AND REDUCED MATRIX

The confusion matrix conveys information which is location-specific: we know for each of the locations how it was decoded during the test phase. The appearance of a typical example of these location-specific matrices shows how a decoding approach reveals characteristics of the representation otherwise overseen (**Figure 2A**). Far from being close to the real position, the decoded positions appear to be distributed in multiple locations over the environment, often far away from the correct spot. The pattern of distribution of decoding probability depends on the choice of the sampled neurons, and on the size of the sample, and it seems to lack any regular principle of organization.

If any regularity in the distribution of errors across positions exists, we can try to reveal it by extracting the translational invariant component of this distribution. By deriving a

position-averaged version of the matrix (**Figure 2B**), we construct a simplified matrix $Q_{(x-x0)}$, which averages over all decoding events with the same vector displacement between actual ($x0$) and decoded (x) positions. $Q_{(x-x0)}$ is easily constructed on the torus we have used in all simulations, and it is only L × L, much smaller than the complete confusion matrix.

The two procedures, given that the simplified matrix is obtained just by averaging the full confusion matrix after a row translation, might be expected to yield similar measures, but this is not the case (Cerasti and Treves, 2010). In fact the amount of information that can be extracted from the reduced matrix is significantly inferior to that of the full matrix, even if the difference decreases as the sample of neurons gets larger (**Figure 3A**). The discrepancy between the two measures reflects the presence of a distribution of errors which is not translational invariant. The distribution found in the reduced matrix instead represents the performance of the system when the effects of specific firing configurations are averaged away. Being quasi-randomly distributed, the errors of the complete matrix average out and produce a smooth, radially decreasing distribution around the central, correct position in the reduced matrix (**Figure 2B**). We are thus able to extract the average error dependence on the distance between two points, regardless of their specific position. The reduced matrix is the expression of the overlaps induced by the external metric of space together with the continuity of the internal place field representation.

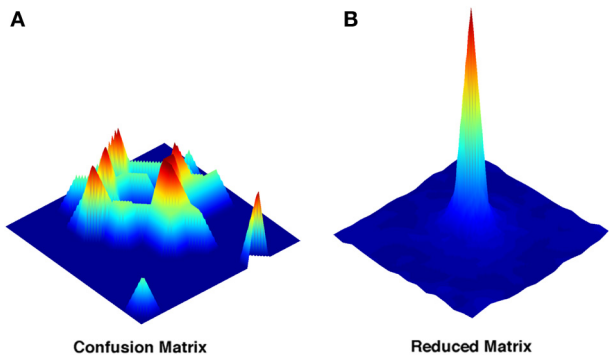

FIGURE 2 | Representative examples of the full and of the reduced confusion matrix. (A) Decoding probability distribution for a single location extracted from the complete confusion matrix. **(B)** Decoding probability distribution obtained from the reduced matrix. Both are obtained with a sample size of $N = 4$. Color coding just reflects the relative heights of the points in the probability distributions.

All the quantities of interest, the information contained in the full and reduced matrix and the percent correct, have a dependence on the sample size which can be fit rather precisely by a sigmoid function. The function we use to fit the information is

$$I_{\text{fit}} = \frac{I_{\text{sat}}}{1 + (n_0/n)^b} \tag{13}$$

where n is the number of units in the decoding sample and I_{sat}, n, and b are the fit parameters. An analogous form is used for the percent correct,

$$f_{\text{cor}_{\text{fit}}} = f_{\text{cor}_{\text{min}}} + \frac{f_{\text{cor}_{\text{max}}} - f_{\text{cor}_{\text{min}}}}{1 + (n_0/n)^b} \tag{14}$$

The change in the convexity of the data is particularly evident when using a log scale for the number of unit in the sample (**Figures 3A**,**B**).

THE METRIC INDUCED BY AN ACTIVE DG

We can use the information contained in the reduced matrix to separate the effects of the external metric on the CA3

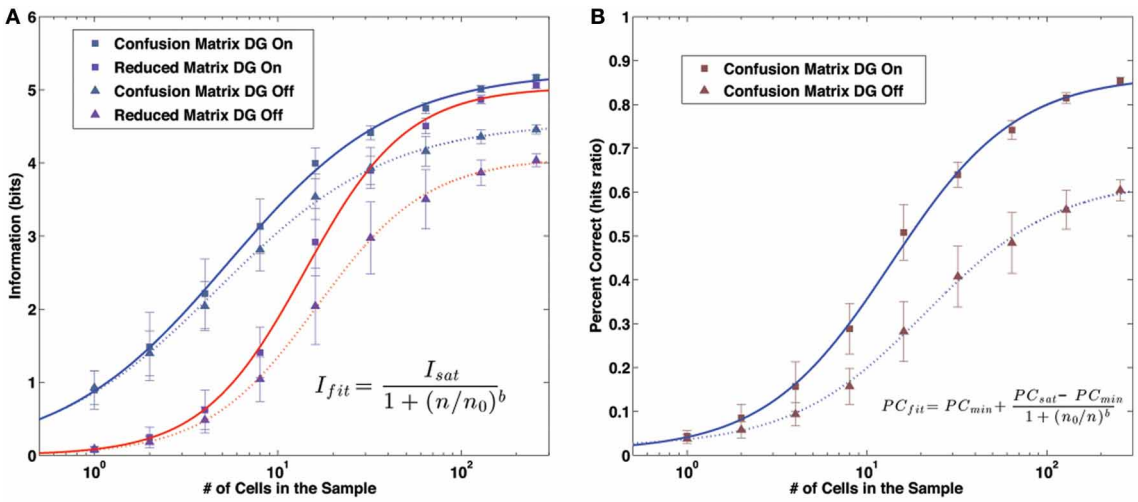

FIGURE 3 | Information and Percent Correct dependence on sample size. (A) Information values. Markers: model data. Lines: fit curves. Gray markers/blue lines: information content of the confusion matrix. Purple markers/red lines: information content of the reduced matrix. Square markers/solid lines: results with the DG input active. Triangular markers/dashed lines: results without the DG input. **(B)** Percent Correct values. Markers: model data. Lines: fit curves, as in **(A)**.

representation from the other sources of correlation. For this aim, the condition with the active DG is better suited, as we consider the original map imposed by the external input, before the modifications induced by the storage, which will be described in the following section.

If we fit the distribution of values in the reduced matrix with a Gaussian we can extract the parameters describing the distance dependence of the errors, namely the height of the central peak (*pc*), the width of the distribution (*w*) and the total volume below the distribution (*a*). They correspond, respectively, to the number of correct hits, the spread of errors around the central location and to the proportion of decoding steps associated with a single location. These parameters depend on the sample size (**Figure 4**): a larger sample corresponds to a higher peak of the Gaussian (corresponding to an increase in the percent correct), to a lower standard deviation around the mean and to a higher total volume. It should be noted, however, that the observed width *w* bundles together the distribution of outright errors and the spread of correct but spatially imprecise responses.

A non-zero standard deviation σ, which can then be regarded as a component of the width *w*, expresses the difference between decoding a set of spatial stimuli and decoding a non-spatial one.

We can use this measure of the structural confusion between locations of the environment to reformulate our measure of metric content for the case of spatial information. We can argue that given a certain percent correct, the minimal information would be obtained when the decoding distribution corresponds to a Gaussian of width σ and total volume *a* centered on the correct location, plus the remaining $(1 - a)$ evenly distributed on all the spatial bins. Analogously the maximal information attainable would correspond to the situation in which $1/a$ Gaussians of the same shape sit on the same number of different locations (one of them, of course, should be placed on the correct one). Indeed this is a first maximum, and it corresponds to the maximal unbiased information defined above for the non-spatial case.

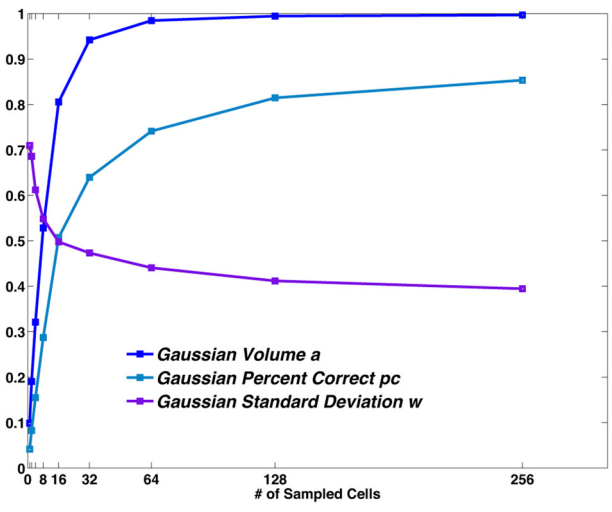

FIGURE 4 | The Gaussian distribution parameters vs. sample size. The values obtained from the fit of the central bump of the reduced matrix, are plotted for different sample sizes. *Pc* and *a* are probabilities. *w* is measured in spatial bin units (each bin is 12.5 cm in size).

For the spatial case, however, these minimum and maximum information values largely reflect simply the definition of the reduced and full confusion matrix. They tell us about the procedure used in the analysis more than about the representations being analyzed. We can, however, go further, as we can also extract the limit toward the discrete case for our model, attained when the spatial resolution is optimal, i.e., the spatial code is precise, spatially exact. By sending the standard deviation σ to zero, in the limit, and by replacing the Gaussian distribution with a single peak of height *a* located in the central spot, we retrieve the situation in which, in the absence of errors due to fluctuations in the topology, only the "retrieval" (i.e., identification) of a certain location is taken into account. This upper maximum does not differ from the previous one in terms of the number of different locations erroneously decoded as the correct one, but it modifies the way in which individual decoded locations are distributed around them. Of course all the conditions between these two extremes can be obtained, using an intermediate value of the standard deviation.

We can then define a spatial descriptor of the metric content applicable to spatial representations, as

$$\chi = 1 - \frac{\sigma}{w} \tag{15}$$

Note that $\chi = 0$ implies that the entire width of the Gaussian in the reduced confusion matrix is due to the poor spatial resolution, as decoding has a standard deviation $\sigma = w$; $\chi = 1$ instead implies that decoding is spatially exact, and the apparent width w emerges entirely from averaging the errors in the full confusion matrix. We can call χ the metric resolution index.

We can see where the data we generated with our simulations sit in relation these three reference curves (**Figure 5A**). For simplicity and clarity, instead of the original data we will use the fit curves we previously calculated. For each sample size, the parameters of the fit define the two maxima (lowest and highest dark blue dashed curves for $\chi = 0$ and $\chi = 1$, respectively) and the minimum (dark red dashed line) for the information, and we can compare then with the actual value of the simulated network, both the value extracted from the complete confusion matrix (blue solid line), and the value coming from the reduced one (**Figure 5A**, red solid line). Both series of values appear to sit on a curve of constant metric resolution. The metric resolution expressed by the complete confusion matrix is just above the one defined by our "first maximum" curve, in fact it sits roughly at $\chi = 0.1$. This corresponds to having a matrix in which there are essentially no randomly distributed errors, while those associated with specific locations are spread out locally, with resolution $\sigma = 0.9$ w.

As expected, the form of the reduced matrix is quite different. It belongs to a complete different category: here the errors are almost entirely randomly distributed, with the exception of those giving rise to the central bump.

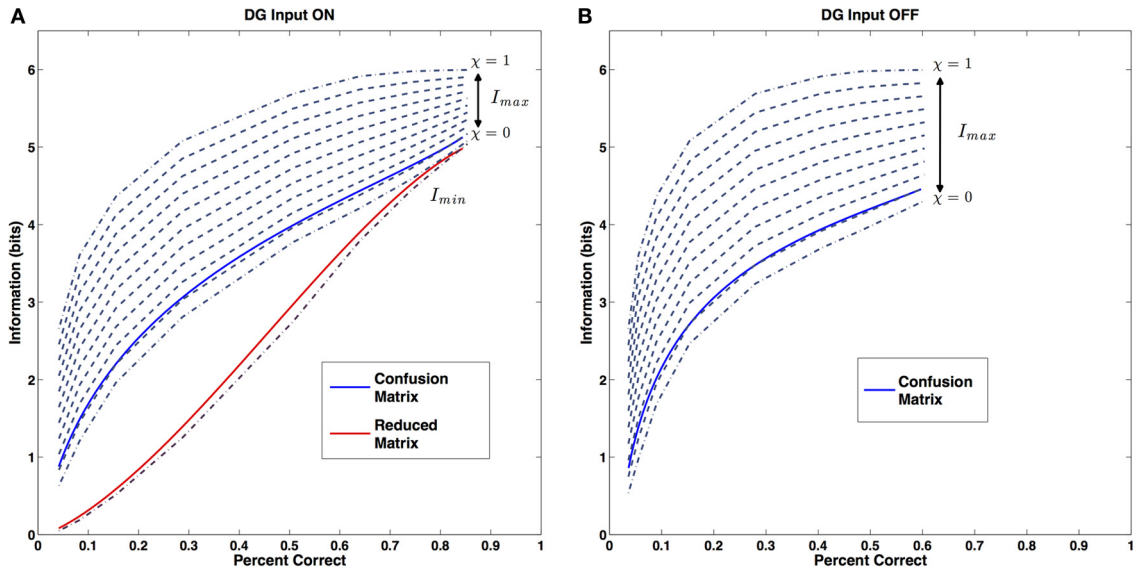

FIGURE 5 | Metric Resolution. (A) Metric resolution of the CA3 representation generated with the external DG input. Blue solid line: information content of the confusion matrix (close to $\chi \sim 0.1$). Red solid line: information content of the reduced matrix. Dark red dashed line: theoretical minimum for the information. Dark blue dashed lines: theoretical maxima of the information for progressively decreasing values of the error dispersion. **(B)** Metric resolution of the CA3 representation based on the internal collateral activity only (also close to $\chi \sim 0.1$). Color code, same as **(A)**. Only the metric resolution of the full confusion matrix is shown.

This measure of metric resolution, thus, extends the previous, non-spatial notion of metric content, and captures the qualitatively different nature of the information expressed by the two different types of matrices, full and reduced. It allows us to shed light on the way spatial information is encoded in a CA3-like network by quantifying the presence and the relative importance of the different sources of confusion present in the system. Moreover it indicates that the nature of the confusion is an invariant of the spatial code expressed by the network and it does not depend on the size of the sample of cells used for the decoding.

DRIFT

One may ask how the procedure previously described applies to the other condition, in which the DG input is removed. As already shown by Cerasti and Treves (2010) the removal of the external drive causes a major drop in the information about the position of the rat retrievable from the system (also shown in the figure). This drop comes with a parallel decrease in the percent correct obtained by the system (**Figure 3B**). This effect has been extensively described by Cerasti and Treves (in preparation) and has to do with what there has been called "drift."

The main effect of storing a map in CA3 is to reduce the number of positions stably represented by the system. After initializing the network in a certain configuration, the activity reverberated in the collaterals modifies this initial pattern and drives it to another, stable point of the configuration space. Eventually, when the final population vector is used to decode the rat position, the outcome will not correspond to the real position. Note that this effect is not due to fast noise, which is kept very low or even absent in the simulations, nor to the use of a limited sample of units: it persists even when the whole population is used in the decoding. Moreover such drift is completely deterministic: at every presentation of the same position, the trajectory of the system's "relaxation" is the same. The size of the distance between the real position and the one decoded after drifting varies for different location of the environment. Its average depends on the number of units in the network.

METRIC RESOLUTION WITHOUT DG INPUT

The main effect of drift on our analysis is to introduce a systematic bias in the decoding of some of the positions in the environment. Since we discretize space in bins of side L, every time drift crosses bin boundaries, the decoded position will belong to a neighboring bin. Not all the points in the same bin are decoded as belonging to another bin, however, some of them will be assigned correctly, while those who are not may move in different directions to different neighboring bins.

This phenomenon introduces a series of non-negligible effects in our measure. It undermines one of the fundamental assumptions of the approach, the unbiased nature of the decoding. In many cases, in those locations where the drift is strong enough, the maximum of the decoding matrix will be associated to an incorrect bin. Moreover it invalidates the use of the reduced matrix to extract information about the distribution of errors around the correct location. Being limited in space, the bump obtained in the reduced matrix is a combination of metric errors and of neighboring bins reached by the drift. This makes the parameters of the bump very unreliable and of little use.

It turns out, however, that the effects of drift can be effectively accommodated in the analysis. To estimate the metric content of the representation generated without the contribution of the

external input we follow the same procedure used in the "DG On" condition with a single modification. We calculate the minimal and maximal information levels as in the previous case, using the same parameters extracted from the previous fits and therefore still coming from the reduced matrix of the "DG On" case. The only adjustment we introduce is to impose that each of the $1/a$ bumps present in the confusion matrix is transformed to a combination of two adjacent Gaussian bumps, with the same width of the original, but half of the height. In this way the amount a of hits associated with the location is preserved but the drift away from (some of) the locations comprised in the bin is taken into account. This solution is an average of the effects present at different locations in the environment, as in some of them no drift is taking place, while in others the phenomenon is present with different strengths and a variable number of directions.

The result proves that this simple procedure captures very well the effects of drift on the properties of the representation and justifies the 2-bump choice. As shown in **Figure 5B**, the data sits on a curve of constant metric resolution, which happens to coincide with the one expressed in the previous condition.

The calculation of the metric resolution offers insights on the characteristics of this representation. In fact it shows how, factoring out the drift phenomenon, the representation expressed by the recurrent collaterals alone appears to have the very same metric properties as the one obtained with the active contribution of the DG. For each sample size, the distribution of errors around the central location is indeed the same, as are the number of locations erroneously chosen by the decoding algorithm. As in the previous case, no portion of the errors is allocated randomly. This consistency is noteworthy as we applied a method adapted, in the previous study, to a completely different set of data, where both the information and the percent correct values are drastically different. The metric content analysis shows a remarkable persistence of the relationship between these two quantities, even when the external input is removed.

DISCUSSION

The ability of the hippocampus to operate as a cognitive map and to successfully guide spatial behavior (Morris et al., 1982) lies in the amount of information about the external environment that can be stored and retrieved from its representations (Battaglia and Treves, 1998; Kali and Dayan, 2000). In particular one would expect that the global topography expressed by these representations, the set of relationships existing among the patterns of activation associated with the different points of the environment, should reflect the one which the animal actually experiences (Curto and Itskov, 2008; Dabaghian et al., 2012). If we imagine an internal observer trying to decode the position of the rat, and the structure of the environment in which it is moving, only relying on the sequence of units that get activated in the hippocampus, similarities between the population vectors would be the most probable criteria to infer the geometrical location of points traversed at different times, or to predict the existence of traversable routes (Gupta et al., 2010; Dragoi and Tonegawa, 2011).

In fact we observe that the topology realized by the averaged activity of our network actually reproduces the torus in which the virtual rat of our simulations is moving. From such a coarse-scale perspective, a CA3 representation is a true reconstruction of the metric the rat is experiencing. Within minor deviations, the correlation between two average population vectors is a good estimate of the distance of the two locations over which their individual population vectors were recorded.

But does such a general approach capture all the variability expressed by the network during its normal operation? We actually find that at a finer scale, the structure of a CA3 spatial representation is richer than it appears at the coarser scale. The difference we observe, between the information content of the full confusion matrix and its reduced version, is telling us about other, non-metric sources of correlation between different parts of the representation. This difference appears when decoding is based on limited samples of network units, but the effects persist up to substantial sizes of the sample, and one should also consider the experimental impracticality of a decoding procedure based on the whole population.

To quantify the properties of the finer aspects of the spatial representation we propose the use of an index, the metric resolution that like the metric content used earlier with non-spatial stimuli, combines the measures of information and percent correct, which are obtained from a confusion matrix. The index allows for an assessment of the metric in the internal representation of space. The measure of metric resolution is applied to our model of a CA3 network in two different regimes, when driven by an external input coming from DG, and when this external input is absent and the active representation is solely an expression of the activity reverberating in the collateral connections. In both cases we find that the metric resolution of the representation is roughly constant, at a value $\chi \sim 0.1$, when the size of the sample is varied, and that the same combination of metric and non-metric structure is present in the confusion matrix generated from these different samples. The metric resolution measure tells us that the self-organizing process has generated an internal representation of space, in the model, which is consistent with external space but has limited metricity, i.e., limited spatial resolution, close to the minimum amount possible (which would yield $\chi = 0.0$).

We acknowledge the possible dependence of the results on the size of the network that represents the real CA3. Although a network of 1500 units is significantly smaller than the actual rodent hippocampus, in some respects it can produce representations which faithfully reproduce the characteristics of the ones experimentally observed (Cerasti and Treves). Moreover the difference in size is less extreme if one regards the real CA3 network as comprised of partially independent sub-modules. The fact that metric content, in our model system, is independent of sample size and of the mode of operation (whether or not externally driven) is an indication of the robustness of this measure.

The errors in decoding that do not depend on the similarity in the representation due to close distance, might be seen as hindering the proper operation of the hippocampal memory system, by introducing ambiguities in the reconstruction of the external space. But another possibility is that these "holes"

in the consistency of the representation offer the hippocampus a handle to introduce non-spatial elements of information in the representation itself (Wood et al., 2000; Leutgeb et al., 2005; Singer et al., 2010; Eichenbaum et al., 2012).

Thus the metric content analysis reinforces the suggestion (Cerasti and Treves, submitted) that the CA3 network, with its effectively random drive from the Dentate Gyrus, might be best adapted to serve a memory function, rather than to produce faithful representations of space.

ACKNOWLEDGMENTS

Research supported in part by the EU SPACEBRAIN project and in part by the EU GRIDMAP project. Extensive discussions with colleagues in both collaborations are gratefully acknowledged.

REFERENCES

Amaral, D., Ishizuka, N., and Claiborne, B. (1990). Neurons, numbers and the hippocampal network. *Prog. Brain Res.* 83, 1–11.

Averbeck, B., Latham, P., and Pouget, A. (2006). Neural correlations, population coding and computation. *Nat. Rev. Neurosci.* 7, 358–366.

Battaglia, F. P., and Treves, A. (1998). Attractor neural networks storing multiple space representations: a model for hippocampal place fields. *Phys. Rev. E.* 58, 7738.

Brown, E., Frank, L., Tang, D., Quirk, M., and Wilson, M. (1998). A statistical paradigm for neural spike train decoding applied to position prediction from ensemble firing patterns of rat hippocampal place cells. *J. Neurosci.* 18, 7411–7425.

Cerasti, E., and Treves, A. (2010). How informative are spatial CA3 representations established by the dentate gyrus? *PLoS Comput. Biol.* 6:e1000759. doi: 10.1371/journal.pcbi.1000759

Ciaramelli, E., Lauro-Grotto, R., and Treves, A. (2006). Dissociating episodic from semantic access mode by mutual information measures: evidence from aging and Alzheimer's disease. *J. Physiol. Paris* 100, 142–153.

Colgin, L., Leutgeb, S., Jezek, K., Leutgeb, J., Moser, E., McNaughton, B., et al. (2010). Attractor-map versus autoassociation based attractor dynamics in the hippocampal network. *J. Neurophysiol.* 104, 35–50.

Curto, C., and Itskov, V. (2008). Cell groups reveal structure of stimulus space. *PLoS Comput. Biol.* 4:e1000205. doi: 10.1371/journal.pcbi.1000205

Dabaghian, Y., Memoli, F., Frank, L., and Carlsson, G. (2012). A topological paradigm for hippocampal spatial map formation using persistent homology. *PLoS Comput. Biol.* 8:e1002581. doi: 10.1371/journal.pcbi.1002581

Deneve, S., Latham, P., and Pouget, A. (1999). Reading population codes: a neural implementation of ideal observers. *Nat. Neurosci.* 2, 740–745.

Dragoi, G., and Tonegawa, S. (2011). Preplay of future place cell sequences by hippocampal cellular assemblies. *Nature* 469, 397–401.

Eichenbaum, H., Sauvage, M., Fortin, N., Komorowski, R., and Lipton, P. (2012). Towards a functional organization of episodic memory in the medial temporal lobe. *Neurosci. Biobehav. Rev.* 36, 1597–1608.

Golomb, D., Hertz, J., Panzeri, S., Treves, A., and Richmond, B. (1997). How well can we estimate the information carried in neuronal responses from limited samples? *Neural Comput.* 9, 649–665.

Gupta, A., Van Der Meer, M. A., Touretzky, D., and Redish, A. (2010). Hippocampal replay is not a simple function of experience. *Neuron* 65, 695–705.

Hamaguchi, K., Hatchett, J., and Okada, M. (2006). Analytic solution of neural network with disordered lateral inhibition. *Phys. Rev. E Stat. Nonlin. Soft Matter Phys.* 73:51104. doi: 10.1103/PhysRevE.73.051104

Hayman, R., Verriotis, M., Jovalekic, A., Fenton, A., and Jeffery, K. (2011). Anisotropic encoding of three-dimensional space by place cells and grid cells. *Nat. Neurosci.* 14, 1182–1188.

Kali, S., and Dayan, P. (2000). The involvement of recurrent connections in area CA3 in establishing the properties of place fields: a model. *J. Neurosci.* 20, 7463–7477.

Komorowski, R., Manns, J., and Eichenbaum, H. (2009). Robust conjunctive item-place coding by hippocampal neurons parallels learning what happens where. *J. Neurosci.* 29, 9918–9929.

Kropff, E., and Treves, A. (2008). The emergence of grid cells: intelligent design or just adaptation? *Hippocampus* 18, 1256–1269.

Lassalle, J., Bataille, T., and Halley, H. (2000). Reversible inactivation of the hippocampal mossy fiber synapses in mice impairs spatial learning, but neither consolidation nor memory retrieval, in the Morris navigation task. *Neurobiol. Learn. Mem.* 73, 243–257.

Lauro-Grotto, R., Ciaramelli, E., Piccini, C., and Treves, A. (2007). Differential impact of brain damage on the access mode to memory representations: an information theoretic approach. *Eur. J. Neurosci.* 26, 2702–2712.

Lee, I., and Kesner, R. (2004). Encoding versus retrieval of spatial memory: double dissociation between the dentate gyrus and the perforant path inputs into CA3 in the dorsal hippocampus. *Hippocampus* 14, 66–76.

Leutgeb, J., Leutgeb, S., Moser, M.-B., and Moser, E. (2007). Pattern separation in the dentate gyrus and CA3 of the hippocampus. *Science* 315, 961–966.

Leutgeb, S., Leutgeb, J., Barnes, C., Moser, E., McNaughton, B., and Moser, M.-B. (2005). Independent codes for spatial and episodic memory in hippocampal neuronal ensembles. *Science* 309, 619–623.

McNaughton, B., Battaglia, F., Jensen, O., Moser, E., and Moser, M.-B. (2006). Path integration and the neural basis of the 'cognitive map'. *Nat. Rev. Neurosci.* 7, 663–678.

Morris, R., Garrud, P., Rawlins, J., and O'Keefe, J. (1982). Place navigation impaired in rats with hippocampal lesions. *Nature* 297, 681–683.

Muller, R., and Stead, M. (1996). Hippocampal place cells connected by Hebbian synapses can solve spatial problems. *Hippocampus* 6, 709–719.

Muller, R., Stead, M., and Pach, J. (1996). The hippocampus as a cognitive graph. *J. Gen. Physiol.* 107, 663–694.

Naya, Y., and Suzuki, W. (2011). Integrating what and when across the primate medial temporal lobe. *Science* 333, 773–776.

O'Keefe, J., and Dostrovsky, J. (1971). The hippocampus as a spatial map. Preliminary evidence from unit activity in the freely-moving rat. *Brain Res.* 34, 171–175.

Panzeri, S., Senatore, R., Montemurro, M., and Petersen, R. (2007). Correcting for the sampling bias problem in spike train information measures. *J. Neurophysiol.* 98, 1064–1072.

Papp, G., Witter, M., and Treves, A. (2007). The CA3 network as a memory store for spatial representations. *Learn. Mem.* 14, 732–744.

Park, E., Dvorak, D., and Fenton, A. (2011). Ensemble place codes in hippocampus: CA1, CA3, and dentate gyrus place cells have multiple place fields in large environments. *PLoS ONE* 6:e22349. doi: 10.1371/journal.pone.0022349

Quian Quiroga, R., and Panzeri, S. (2009). Extracting information from neuronal populations: information theory and decoding approaches. *Nat. Rev. Neurosci.* 10, 173–185.

Quiroga, R., Reddy, L., Kreiman, G., Koch, C., and Fried, I. (2005). Invariant visual representation by single neurons in the human brain. *Nature* 435, 1102–1107.

Rolls, E., and Treves, A. (2011). The neuronal encoding of information in the brain. *Prog. Neurobiol.* 95, 448–490.

Roudi, Y., and Treves, A. (2008). Representing where along with what information in a model of a cortical patch. *PLoS Comput. Biol.* 4:e1000012. doi: 10.1371/journal.pcbi.1000012

Sammon, J. W. Jr. (1969). A nonlinear mapping for data structure analysis. *IEEE Transact. Comput.* 100, 401–409.

Samsonovich, A., and McNaughton, B. (1997). Path integration and cognitive mapping in a continuous attractor neural network model. *J. Neurosci.* 17, 5900–5920.

Singer, A., Karlsson, M., Nathe, A., Carr, M., and Frank, L. (2010). Experience-dependent development of coordinated hippocampal spatial activity representing the similarity of related locations. *J. Neurosci.* 30, 11586–11604.

Stringer, S., Trappenberg, T., Rolls, E., and De Araujo, I. (2002). Self-organizing continuous attractor networks and path integration: one-dimensional models of head direction cells. *Network* 13, 217–242.

Tort, A., Komorowski, R., Kopell, N., and Eichenbaum, H. (2011).

A mechanism for the formation of hippocampal neuronal firing patterns that represent what happens where. *Learn. Mem.* 18, 718–727.

Treves, A. (1990). Graded-response neurons and information encodings in autoassociative memories. *Phys. Rev. A* 42, 2418–2430.

Treves, A. (1997). On the perceptual structure of face space. *BioSystems* 40, 189–196.

Treves, A., Georges-Francois, P., Panzeri, S., Robertson, R. G., and Rolls, E. T. (1998). "The metric content of spatial views as represented in the primate hippocampus," in *Neural Circuits and Networks, NATO ASI Series F, Computer and Systems Sciences*. Vol 167, eds V. Torre and J. Nicholls (Berlin: Springer-Verlag), 239–247.

Treves, A., and Rolls, E. (1992). Computational constraints suggest the need for two distinct input systems to the hippocampal CA3 network. *Hippocampus* 2, 189–199.

Tsodyks, M., and Sejnowski, T. (1995). Associative memory and hippocampal place cells. *Int. J. Neural Syst.* 6, 81–86.

Ulanovsky, N., and Moss, C. (2011). Dynamics of hippocampal spatial representation in echolocating bats. *Hippocampus* 21, 150–161.

van Strien, N., Cappaert, N., and Witter, M. (2009). The anatomy of memory: an interactive overview of the parahippocampal-hippocampal network. *Nat. Rev. Neurosci.* 10, 272–282.

Wills, T., Lever, C., Cacucci, F., Burgess, N., and O'Keefe, J. (2005). Attractor dynamics in the hippocampal representation of the local environment. *Science* 308, 873–876.

Wilson, M., and McNaughton, B. (1993). Dynamics of the hippocampal ensemble code for space. *Science* 261, 1055–1058.

Wood, E., Dudchenko, P., Robitsek, R., and Eichenbaum, H. (2000). Hippocampal neurons encode information about different types of memory episodes occurring in the same location. *Neuron* 27, 623–633.

Conflict of Interest Statement: The authors declare that the research was conducted in the absence of any commercial or financial relationships that could be construed as a potential conflict of interest.

Received: 08 December 2012; accepted: 10 April 2013; published online: 26 April 2013.

Citation: Stella F, Cerasti E and Treves A (2013) Unveiling the metric structure of internal representations of space. Front. Neural Circuits 7:81. doi: 10.3389/fncir.2013.00081

frontiers in
NEURAL CIRCUITS

REVIEW ARTICLE
published: 18 February 2013
doi: 10.3389/fncir.2013.00017

Structural plasticity in the dentate gyrus- revisiting a classic injury model

Julia V. Perederiy and Gary L. Westbrook*

Vollum Institute, Oregon Health and Science University, Portland, OR, USA

Edited by:
Peter Jonas, Institute of Science and Technology, Austria

Reviewed by:
John Lisman, Brandeis University, USA
Michael Frotscher, University Medical Center Hamburg-Eppendorf, Germany

***Correspondence:**
Gary L. Westbrook, Vollum Institute, Oregon Health and Science University, 3181 SW Sam Jackson Park Road, Portland, OR 97210, USA.
e-mail: westbroo@ohsu.edu

The adult brain is in a continuous state of remodeling. This is nowhere more true than in the dentate gyrus, where competing forces such as neurodegeneration and neurogenesis dynamically modify neuronal connectivity, and can occur simultaneously. This plasticity of the adult nervous system is particularly important in the context of traumatic brain injury or deafferentation. In this review, we summarize a classic injury model, lesioning of the perforant path, which removes the main extrahippocampal input to the dentate gyrus. Early studies revealed that in response to deafferentation, axons of remaining fiber systems and dendrites of mature granule cells undergo lamina-specific changes, providing one of the first examples of structural plasticity in the adult brain. Given the increasing role of adult-generated new neurons in the function of the dentate gyrus, we also compare the response of newborn and mature granule cells following lesioning of the perforant path. These studies provide insights not only to plasticity in the dentate gyrus, but also to the response of neural circuits to brain injury.

Keywords: perforant path lesion, adult neurogenesis, dentate gyrus, reactive synaptogenesis

PLASTICITY IN THE ADULT BRAIN

The ability of the mammalian brain to change with experience is perhaps its most important feature. At the organismal level, the positive (adaptive) benefits of experience-dependent changes underlie our abilities to learn, speak multiple languages, ride a bicycle and so on. However, equally important are enduring negative (maladaptive) effects that are associated with experience-dependent changes including benign habits as well as more disruptive conditions such as anxiety, post-traumatic stress, and drug addiction. In both cases, these changes are manifested at the level of circuits and individual neurons as a reordering of gene expression profiles, synaptic strength, and circuit connectivity. Reorganization reflects the adaptation of the network to a changing environment, either encoding new information or compensating for injury-induced degeneration. Reorganization following a brain injury inevitably perturbs the dynamic equilibrium, which can affect many aspects of neuronal structure and function including intrinsic neuronal properties, synaptic interactions, and connectivity within and between networks. The cellular and molecular landscape can impose limits on plasticity and regenerative capacity of the adult brain.

A variety of injury models have been used to examine the response of the brain such as crush injuries to peripheral nerves, cortical stab wounds, and spinal cord injury (SCI) models. For example, SCI models have been extensively examined for factors that limit the growth of axons following damage or transection (Akbik et al., 2012; Tuszynski and Steward, 2012). Here we focus on the perforant path lesion, a brain injury model that interrupts the main excitatory input to the dentate gyrus of the hippocampus. This model has the experimental advantages of a highly laminated structure and allows analysis of not only the axonal response to injury, but also changes in dendrite morphology and synaptic reorganization. This classic lesion provided some of the first evidence for structural plasticity following injury in the CNS, and also provides an opportunity to examine the injury response of some of the most highly plastic neurons in the brain, adult-generated newborn granule cells. Because perforant path axons are lesioned at a site remote from the dentate, this model is particularly useful to evaluate axonal sprouting from other pathways terminating in the dentate gyrus. Prior results indicate that axonal sprouting occurs, but only in a lamina-specific manner. There are also compensatory changes in dendritic structure and dendritic spines on the post-synaptic mature granule cells, including an initial reduction in dendritic complexity and spine counts, followed by a limited recovery, presumably based on axonal sprouting. Recent studies with adult-generated granule cells indicate that these cells are highly dynamic following denervation, surprisingly developing dendritic spines in the denervated zone in the absence of functional input. These latter studies suggest that a unique post-lesion environment affects development of dendritic spines and new synapses in deafferented laminae. Before discussing the insights gained from the perforant path lesion model, we first highlight features of neuronal and non-neuronal plasticity that drive adaptive and maladaptive changes in brain circuits.

SYNAPTIC AND DENDRITIC PLASTICITY IN THE INJURED BRAIN

It is well known that synaptic and dendritic plasticity occur in sensory systems following deprivation, and in motor systems following disuse (Hickmott and Steen, 2005; Hofer et al., 2006). However, spines and dendrites also undergo dynamic functional and structural changes following acute injury or

neurodegeneration. These changes fall into several categories including retraction of dendritic arbors following loss of inputs, compensatory increases in dendritic arbors in domains of afferent inputs unaffected by the injury, transient changes in spine densities, and alterations in the types or shapes of dendritic spines. For example, dendritic reorganization occurs after ischemia (Hosp and Luft, 2011), but the degree of remodeling depends on the proximity of dendrites to the site of infarction. Brown et al. (2010) reported a dendritic retraction following ischemic injury in cortex adjacent to the infarct, but compensatory dendritic outgrowth away from the site of injury. On the other hand, Mostany and Portera-Cailliau (2011) saw only dendritic pruning at cells in peri-infarct cortex. Dendritic spine density is also sensitive to ischemia (Brown et al., 2008) and SCI (Kim et al., 2006), both of which lead to a reduction in spine density and elongation of the remaining spines, albeit at different time scales. Because spine elongation is associated with synaptogenesis, the underlying mechanisms for these changes are in many cases thought to be sensitive to injury-induced alterations in network activity. For example, the intense neuronal activity associated with kainate-induced seizures triggers beading of dendrites and subsequent loss of spines (Drakew et al., 1996; Zeng et al., 2007). However, brief seizure activity can also trigger more "physiological" responses, such as the induction LTP in CA3 pyramidal neurons (Ben-Ari and Gho, 1988). This dichotomy suggests that network responses to injury are likely to be context-specific, and may reflect exaggerations of the normal adaptive responses to stimuli (**Figure 1**).

SPROUTING AND THE AXONAL RESPONSE TO INJURY

Axons can also reorganize following injury, although the extent of regeneration varies. In the peripheral nervous system, regenerating axons can grow long distances and re-innervate their targets, thus leading to functional recovery. However, regenerating axons in the central nervous system are often unable to penetrate the lesion, thus limiting long-range axonal outgrowth. Perhaps most extensively studied examples are experimental models of SCI, in which cut or damaged axons of the corticospinal tract form retraction bulbs and eventually move away from the lesion site, unable to penetrate the gliotic scar (Hill et al., 2001; Fitch and Silver, 2008). However, if the transection is incomplete, sprouting of uninjured axons, as well as cortical reorganization can lead to partial functional recovery following injury (Raineteau and Schwab, 2001; Maier and Schwab, 2006). The difference in the capacity for axonal regeneration in the peripheral and central nervous systems reflects differences in intrinsic neuronal properties (Liu et al., 2011) and in post-injury changes in the extracellular environment (Giger et al., 2010). Whereas degenerating material in the peripheral nervous system is effectively cleared following injury (Chen et al., 2007; Bosse, 2012), these processes are much

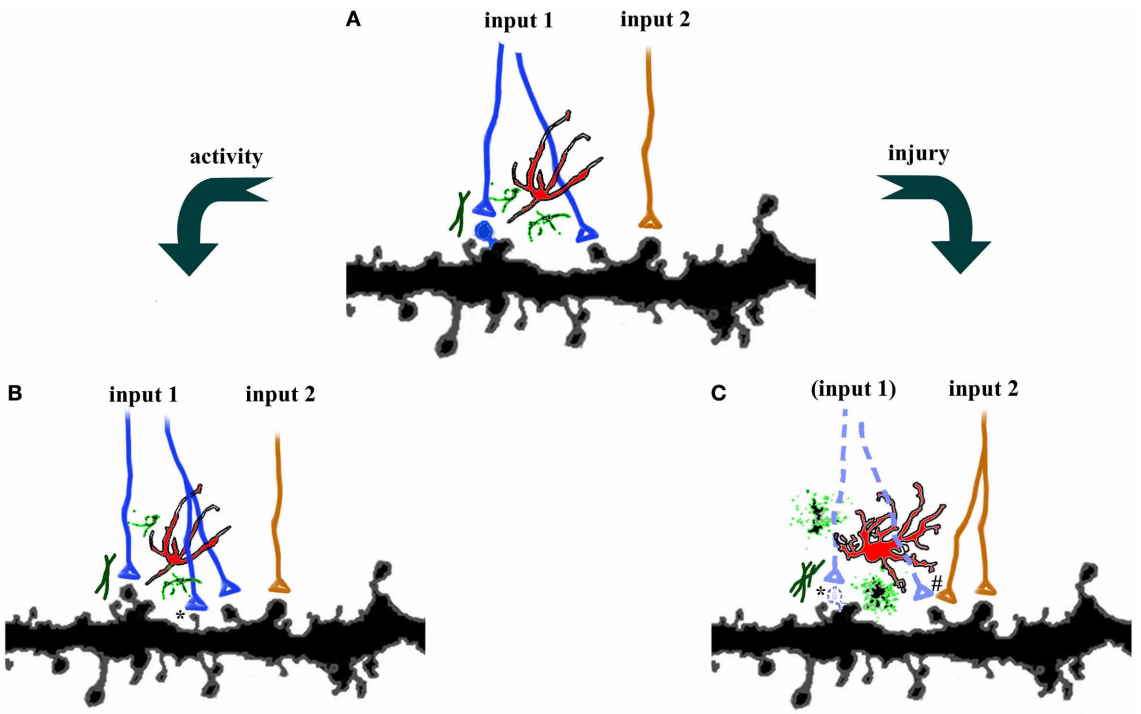

FIGURE 1 | Plasticity in the central nervous system. (A) Axons from two different pathways synapse onto spines on the same dendrites. Each synapse is surrounded by astrocytes (red), microglia (green), and extracellular matrix. **(B)** Increases in activity, such as occur during learning, can strengthen connections by axonal sprouting (blue) as well as formation of new filopodia and dendritic spines (*). Adjacent afferents, surrounding glia, and extracellular matrix are relatively unaffected. **(C)** Disruption of afferents, such as following injury, leads to degeneration of damaged axons (dotted lines), activation of astrocytes, microglia, and extracellular matrix, as well as retraction of dendritic spines (*). Compensatory sprouting of undamaged afferents from another brain region (orange) can form new synapses, including contacts with denervated spines (#).

slower in the central nervous system (Vargas and Barres, 2007; Giger et al., 2010), and may thus interfere with reinnervation of deafferented target areas. Axonal structural plasticity may also be maladaptive following injury, as can occur in the brain of patients with temporal lobe epilepsy. Following seizures, mossy fiber axons sprout recurrent collaterals that synapse onto granule cell dendrites in the inner molecular layer, thereby increasing excitatory connectivity within the dentate gyrus (Sutula and Dudek, 2007). Such structural reorganization can lead to an imbalance between excitation and inhibition in the circuit, which may underlie recurrent seizures.

GLIAL AND EXTRACELLULAR RESPONSE TO BRAIN INJURY

Glial cells are intimately involved in function and plasticity of the healthy adult brain, however, their contribution to recovery following injury is even more striking. Brain and spinal cord trauma, neurodegeneration, ischemia, and infection, all stimulate morphological and molecular changes in surrounding astrocytes, often referred to as reactive gliosis. Depending on the triggering mechanism and its duration, the glial response can promote or inhibit recovery (**Figure 2**; Sofroniew, 2009). For example, during mild insults to the CNS, such as the immune reaction that follows a viral infection or as occurs in areas distant to a lesion site, astrocytes hypertrophy but remain tiled (**Figure 2B**; Wilhelmsson et al., 2006). In such cases, tissue reorganization is minimal and reactive astrogliosis resolves within a few weeks. However, following more severe CNS insults such as major trauma, stroke, or neurodegeneration, astrocytes proliferate, acquire expansive reactive morphology, and their processes extend beyond their original borders (Sofroniew and Vinters, 2010). The resulting dense network of newly proliferated astrocytes can recruit other cell types, including fibromeningeal cells and microglia, resulting in the formation of a permanent and impenetrable glial scar (**Figure 2C**). Reactive astrogliosis has traditionally been viewed as maladaptive because gliosis can contribute to glutamate toxicity (Takano et al., 2005), generation of seizures (Jansen et al., 2005; Tian et al., 2005), inflammation (Brambilla et al., 2005), and chronic pain (Milligan and Watkins, 2009). Furthermore, the glial scar can inhibit axonal regrowth (Silver and Miller, 2004). Although experimental interference with glial scar formation can increase axonal regeneration, it can also increase lesion size and diminish functional recovery (Sofroniew, 2009). The latter suggests that the presence of reactive astrocytes, depending on the context, can have positive effects on neuronal reorganization by stabilizing the extracellular ion balance, reducing seizure likelihood, and dampening excitotoxicity (Rothstein et al., 1996; Koistinaho et al., 2004; Swanson et al., 2004).

An important product of glial cells, the extracellular matrix (ECM), surrounds the synapse (Dityatev et al., 2006, 2010b) and is instrumental in synaptic plasticity both in the healthy and injured brain (Dityatev and Fellin, 2008; Dityatev et al., 2010a; Frischknecht and Gundelfinger, 2012). For example, astrocyte-derived ECM components, such as thrombospondins, initiate synaptic development (Christopherson et al., 2005; Xu et al., 2010) as well as regulate synaptic plasticity (Eroglu, 2009). In addition, inactive perisynaptic matrix metalloproteases are transiently activated following induction of LTP in the hippocampus (Nagy et al., 2006; Bozdagi et al., 2007). Because ECM

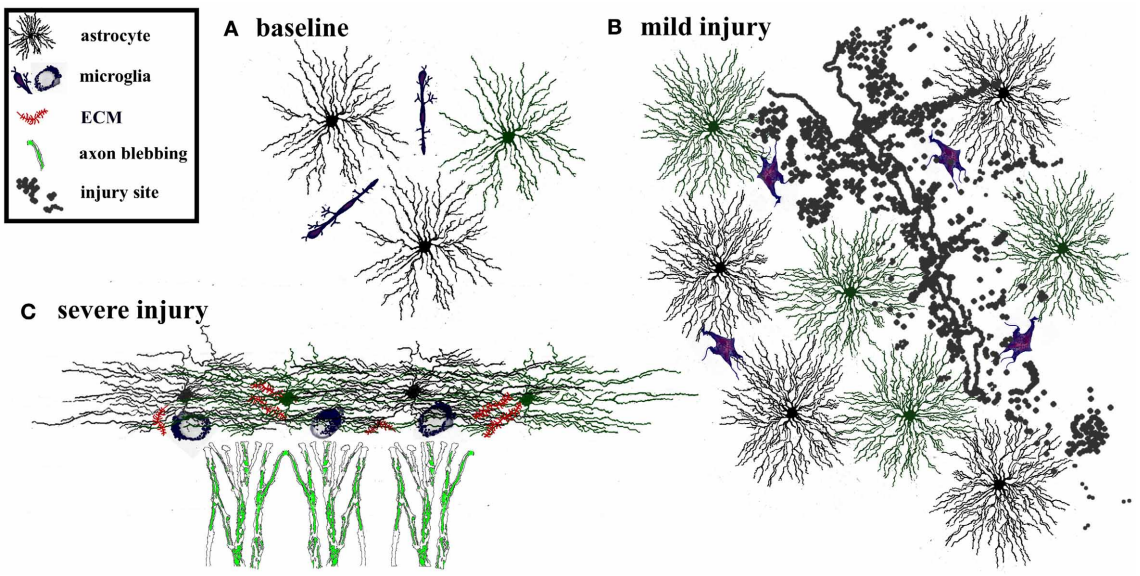

FIGURE 2 | Adaptive and maladaptive glial changes following injury. The degree of astrogliosis depends on the severity of injury. **(A)** Glia and extracellular matrix at baseline. Astrocytes are tiled, i.e., their processes do not overlap with neighboring astrocytes. Microglia are interspersed throughout the region. **(B)** Mild injury triggers activation of microglia and astrocytes. Astrocytes and microglia increase in size and acquire more complex process morphology, but astrocytes maintain their tiled formation. This response is considered adaptive because it limits the spread of degeneration away from the site of injury, dampens excitotoxicity, and promotes tissue regeneration. Such glial activation typically resolves within a few weeks after a mild, transient injury. **(C)** In contrast severe injury causes reactive astrocytes to invade neighboring domains, recruit reactive microglia, and increases secretion of extracellular molecules. This results in formation of a persistent glial scar that can be impenetrable to sprouting axons.

components originate from glia, activation of astrocytes following injury can affect expression of ECM molecules and thus post-injury neuroplasticity. Like the astroglial response, these molecules can have a dual role in recovery. For example, chondroitin sulfate proteoglycan expression is beneficial in containing the size of a lesion, but a few days later can inhibit axonal growth (Zuo et al., 1998; Galtrey and Fawcett, 2007). Likewise, matrix metalloproteinases have a positive effect on reactive synaptogenesis when transiently upregulated (Falo et al., 2006), but persistent and widespread MMP expression leads to regression of dendritic spines, degeneration of synapses and neuronal apoptosis (Falo et al., 2006; Huntley, 2012). The complexity of the glial and ECM response underscores both the potential for, and the limitations of, repair and regeneration following brain injury.

PERFORANT PATH LESION AS A MODEL OF POST-INJURY PLASTICITY IN THE ADULT BRAIN

ADVANTAGES OF MODEL

Lesioning of the perforant path was one of the first models to document injury-induced plasticity in the adult brain. This lesion of the major excitatory input into the dentate gyrus affects the trisynaptic hippocampal circuit, disrupting the distinctly unidirectional progression of excitatory activity arriving from other brain regions (Knowles, 1992). Because the entorhinal lesion site is distant from the dentate gyrus, local degenerative/inflammatory effects at the lesion site can be easily separated from the regenerative effects of post-lesion circuit reorganization. The simple cyto- and fiber architecture and lamination pattern of the dentate gyrus also provides an experimental advantage because the lesion affects only one of many afferent fiber systems. Each afferent input terminates in a specific lamina of the molecular layer (Hjorth-Simonsen and Jeune, 1972) and each is functionally and molecularly distinct (Leranth and Hajszan, 2007). This diversity allows a comparison of heterotypic and homotypic sprouting post-lesion (Ramirez, 2001), as the balance of these inputs may have a role in functional recovery.

POST-LESION CIRCUIT REORGANIZATION—AXONS

Afferents to the dentate gyrus have diverse origins and neurotransmitter phenotypes that converge on the hippocampus (**Figure 3**, left panel). Glutamatergic inputs to the outer two-thirds of the dentate molecular layer include the entorhinodentate perforant path (Hjorth-Simonsen and Jeune, 1972; van Groen et al., 2003) and a weak species-specific commissural projection from the contralateral entorhinal cortex (van Groen et al., 2002; Deller et al., 2007). Glutamatergic input to the inner molecular layer consists of the mossy cell axons from the commissural/associational (C/A) collaterals (Gottlieb and Cowan, 1973; Soriano and Frotscher, 1994). These excitatory synaptic inputs are complemented by cholinergic, GABAergic, noradrenergic, dopaminergic, and serotonergic projections that terminate throughout the molecular layer (Leranth and Hajszan, 2007). Because the entorhinodentate projection is the largest glutamatergic afferent fiber system, a perforant path lesion severs the

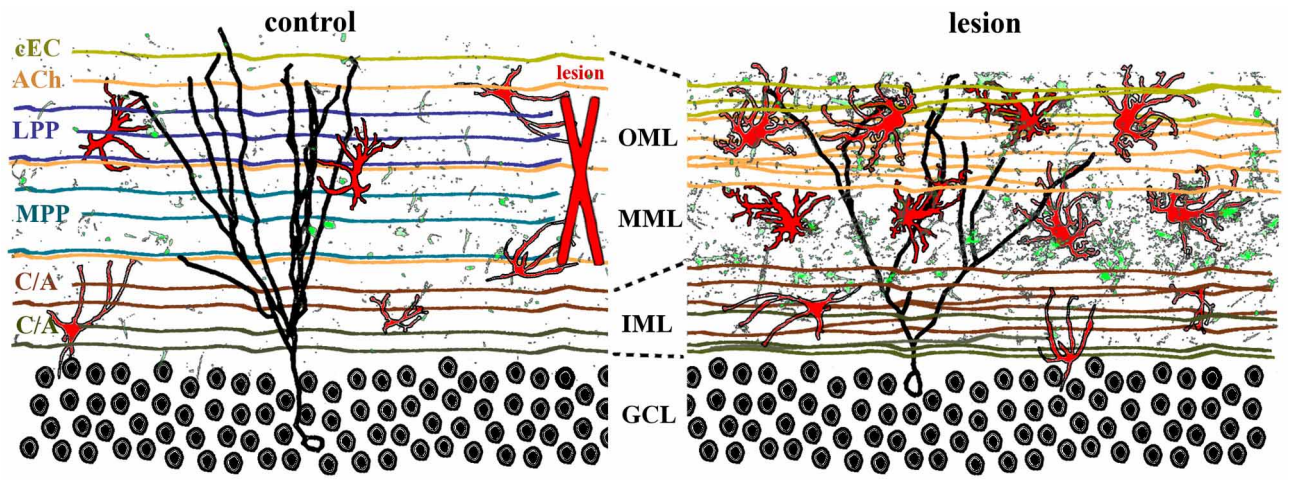

FIGURE 3 | Lamina-specific axon sprouting and reactive gliosis following perforant path lesion. The molecular layer of the adult dentate gyrus is a highly laminated structure with afferent inputs segregated based on their origin and neurotransmitter phenotype. All afferent axons form either symmetrical or asymmetrical synapses with mature granule cells (black traces) in a lamina-specific manner. **Left panel**: the inner molecular layer (IML) is occupied by the glutamatergic commissural/associational fibers (C/A) that arise from mossy cells in the ipsi- or contralateral hilus. The middle and outer molecular layer (MML, OML) are occupied predominantly by the glutamatergic perforant path (MPP, LPP), which originates in the ipsilateral entorhinal cortex. In rats (but not in mice), there is also a crossed glutamatergic projection from the contralateral entorhinal cortex (cEC) that terminates in the outermost molecular layer (OML). Cholinergic axons (ACh) from the septal nuclei/diagonal band of Broca are interspersed throughout the molecular layer, as are astrocytes (red) and quiescent microglia (green). **Right panel**: lesion of the entorhinal cortex (red X, left panel) transects both medial and lateral perforant path, thus eliminating the majority of excitatory input into the dentate gyrus. Degeneration of these axons induces lamina-specific sprouting of the remaining septohippocampal (ACh), commissural/associational (C/A), and crossed entorhino-dentate (cEC) afferents. In the rat, the contralateral entorhino-dentate projection (cEC) partially restores excitatory innervation of the mature granule cells (black trace), however, their dendritic length and complexity are still reduced. The microglia (green) and astrocytes (red) become "activated" following lesion, but this response is limited to the deafferented zone. Note the expansion of the inner molecular layer and shrinkage of the outer layers.

majority of excitatory innervation in the dentate gyrus, thus effectively denervating the outer two-thirds of the molecular layer and vacating 80–90% of all synapses in that region (Matthews et al., 1976a; Steward and Vinsant, 1983). Such degeneration of excitatory synapses triggers compensatory axonal sprouting that is lamina-specific (Frotscher et al., 1997) and can be either homo- or heterotypic, depending on the neurotransmitter involved. Sprouting of other glutamatergic axons, defined as homotypic to the perforant path, includes the weak entorhinodentate projection from the contralateral, non-lesioned entorhinal cortex that normally terminates in the deafferented region (Steward et al., 1973; Steward, 1976; Cotman et al., 1977; Deller et al., 1996a), and the glutamatergic component of the commissural/associational fiber system that normally terminates in the inner molecular layer (Gall and Lynch, 1981; Deller et al., 1996b). Although homotypic reactive sprouting can partially replace lost synapses in the denervated zone (Marrone et al., 2004), the degree of excitatory reinnervation is species-specific (van Groen et al., 2002; Del Turco et al., 2003; Deller et al., 2007). Homotypic sprouting also can partially restore postsynaptic function (Reeves and Steward, 1988) as well as ameliorate some behavioral deficits (Ramirez, 2001).

Lesion of the perforant path also triggers reactive heterotypic sprouting of non-glutamatergic afferents such as the cholinergic septodentate projection. Sprouting of this fiber system was initially detected as an increase in acetylcholinesterase (AChE) staining in the denervated zone (**Figure 4**; Lynch et al., 1972; Nadler et al., 1977a,b). The width of the AChE band was subsequently correlated with the extent of the lesion and the time course of reorganization (Zimmer et al., 1986; Steward, 1992), and therefore has been used as a marker for the extent and completeness of a perforant path lesion. Although the increase in AChE staining density in the denervated region has been corroborated (Vuksic et al., 2011), it remains uncertain whether this increase indicates actual cholinergic sprouting or is a consequence of post-lesion tissue shrinkage (Phinney et al., 2004). Perforant path lesions also cause sprouting of GABAergic C/A axons (Deller et al., 1995) as well as trigger receptor reorganization and new inhibitory synapse formation on mature granule cells (Simbürger et al., 2000, 2001). In combination with a decrease in glutamatergic innervation, these results suggest that lesions of the perforant path can alter the excitation/inhibition balance in the dentate gyrus (Clusmann et al., 1994), which can potentially complicate functional recovery. However, heterotypic sprouting may also serve an adaptive purpose in post-lesion circuit reorganization by reinnervating vacated synapses and thus preventing or delaying transsynaptic cell death.

POST-LESION CIRCUIT REORGANIZATION—DENDRITES/SPINES

Interruption of the perforant path denervates one of the main inputs to the principal neurons in the adult dentate gyrus—the mature granule cells. These cells are part of the trisynaptic hippocampal circuit, with their dendrites receiving afferent input from the entorhinal cortex and other brain regions; and their axons forming the mossy fibers that synapse with pyramidal cells in CA3. The two subdivisions of the perforant path, medial and lateral, synapse with mature granule cell dendrites in the middle and outer molecular layers, respectively (Hjorth-Simonsen and Jeune, 1972; van Groen et al., 2003). Following a perforant path lesion, these axons degenerate (Matthews et al., 1976a), thus eliminating the majority of excitatory input onto dendritic segments in the outer two-thirds of the molecular layer (**Figure 3**).

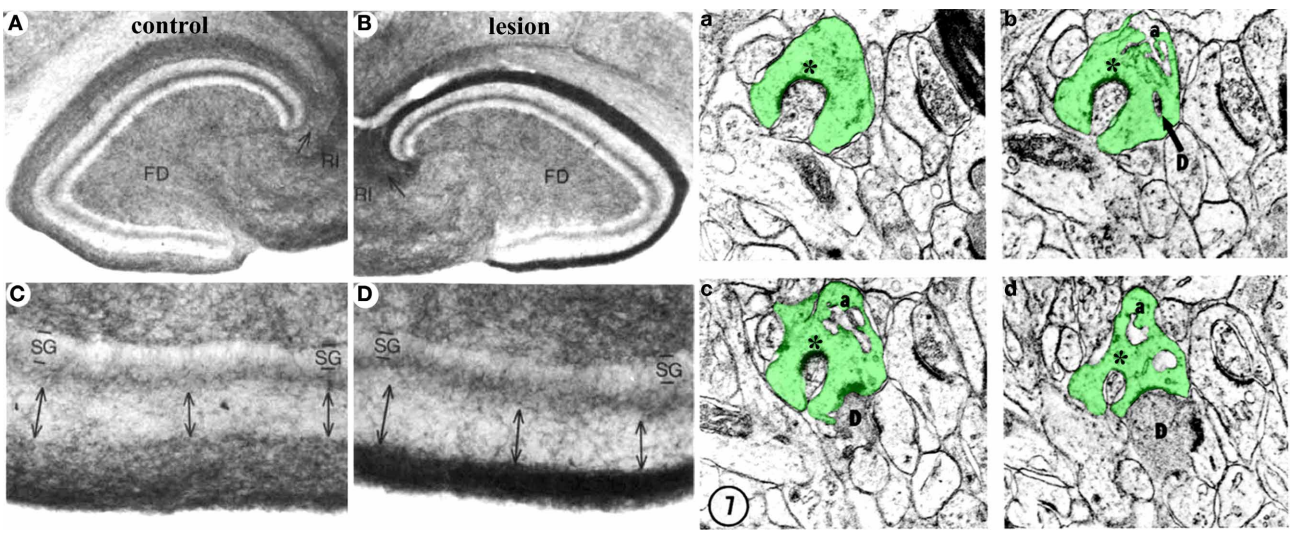

FIGURE 4 | Structural plasticity following perforant path lesions. Left panels (modified from Steward and Messenheimer, 1978): Mature cat hippocampus histochemically stained for acetyl cholinesterase (AChE) activity at 60 days post-lesion. The density of AChE is dramatically increased in the denervated outer molecular layer (**A,B,** top right, dark band), consistent with sprouting of the cholinergic septohippocampal axons following lesion. Also note that the thickness of the inner molecular layer is increased due to sprouting of the glutamatergic commissural/associational fibers (**C,D,** bottom right, double arrows). **Right panels** (modified from Matthews et al., 1976b): Ultrastructural evidence for synaptic regeneration in the denervated zone at 60 days post-lesion in the mature rat. Serial sections through a complex spine (a,b,c,d, green) show synaptic contacts with a degenerating bouton "D" as well as with a regenerating axon "*." a = spine apparatus.

The loss of excitatory input initiates a series of morphological and functional changes in the post-synaptic mature granule cells. Dendrites retract, resulting in less complex dendritic arbors in the denervated region (Caceres and Steward, 1983; Diekmann et al., 1996; Schauwecker and McNeill, 1996; Vuksic et al., 2011). Distal dendritic segments are progressively lost for periods up to 90 days post-lesion, with some recovery by 180 days post-lesion. However, the recovery most likely reflects the extension of existing dendrites, rather than formation of new branches (Vuksic et al., 2011). Similarly, the density of dendritic spines—the post-synaptic targets of the entorhinodentate projection—is significantly reduced following lesion, but only in the deafferented zone (Parnavelas et al., 1974; Vuksic et al., 2011). Surprisingly there is relatively little data assessing the functional state of the dentate gyrus circuit following such lesions. However, spontaneous neural activity in mature granule cells post-lesion appears to transiently decrease immediately following lesion, then gradually returns to pre-lesion levels by 8 days (Reeves and Steward, 1988). The source of this activity presumably reflects reorganization of synaptic inputs that follows excitatory reinnervation by sprouting afferents.

POST-LESION GLIAL AND EXTRACELLULAR MATRIX (ECM) RESPONSE

Post-lesion structural reorganization in the adult dentate gyrus is influenced by the post-injury dynamics of the extracellular environment. Reactive gliosis following perforant path lesion is both rapid and sustained, and is considered adaptive in this context. Gliosis serves to clear degenerating debris, to maintain laminar borders, and to aid reactive synaptogenesis in the deafferented region. For example, microglia proliferate and acquire reactive morphology within 3 days post-lesion and return to baseline by day 10 (Hailer et al., 1999). However, activation of astrocytes in the denervated zone is delayed relative to microglia and persists for at least 30 days post-lesion (Hailer et al., 1999). Together, microglia and astrocytes participate in phagocytosis of degenerating axons (Bechmann and Nitsch, 2000) and may regulate axon sprouting and reactive synaptogenesis (Gage et al., 1988; Ullian et al., 2004). The efficiency of phagocytosis following injury, especially of degenerating myelinated axons, generally correlates with the degree of regeneration in the CNS (Neumann et al., 2009). Because the glial response is limited to the denervated lamina with relatively little reactive gliosis in the inner molecular layer, this lamina-specific reaction may underlie the lack of sprouting across laminar borders into the denervated zone. Reactive gliosis also triggers changes in the extracellular matrix, which may affect the maintenance of laminar borders following lesion. For example, tenascin-C (Deller et al., 1997) and chondroitin sulfate proteoglycans (Haas et al., 1999) are secreted by reactive astrocytes following perforant path lesion. Both these factors affect axon outgrowth during development as well as following injury (Bovolenta and Fernaud-Espinosa, 2000; Bartus et al., 2012). Similarly, reactive astrocytes can secrete thrombospondins or matrix metalloproteases (Christopherson et al., 2005; Warren et al., 2012), which can provide a scaffold for lesion-induced synaptogenesis (Deller et al., 2001; Mayer et al., 2005).

In summary, lesion of the perforant path eliminates the main excitatory input in the outer two-thirds of the dentate molecular layer, thus partially denervating dendrites of mature granule cells. This lesion illustrates both the potential for regeneration in the CNS, but also some of the limits. Within 2 weeks post-lesion, remaining afferent homo- and heterotypic systems can sprout, but the laminar borders largely limit reorganization of axons and synaptic terminals. Changes in the composition of the extracellular matrix, triggered by degenerating perforant path axons and reactive gliosis, are a major contributing factor in this regard.

ADULT-GENERATED NEWBORN NEURONS AND THE RESPONSE TO BRAIN INJURY

Plasticity of neuronal circuits occurs in the adult mammalian brain and is particularly intriguing in the form of adult neurogenesis (Lledo et al., 2006). The dentate gyrus of the hippocampal formation harbors a continuously proliferating population of granule cells precursors, some of which mature over several weeks and become functionally indistinguishable from mature granule cells in the dentate gyrus (van Praag et al., 2002; Overstreet-Wadiche and Westbrook, 2006; Ge et al., 2008). In contrast to mature granule cells, newborn neurons have enhanced synaptic plasticity (Ambrogini et al., 2004; Schmidt-Hieber et al., 2004), suggesting that they may have distinct roles in normal hippocampal function as well as following injury.

PROLIFERATION OF ADULT-GENERATED NEURONS FOLLOWING INJURY

Proliferation of newborn neurons in the dentate gyrus is highly sensitive to environmental and endogenous signals, such as learning, exercise, or severe stress (van Praag et al., 1999; Overstreet et al., 2004; Tashiro et al., 2007). Interestingly, increases in proliferation also occur in various animal models of ischemia, epilepsy, and traumatic brain injury (Liu et al., 1998; Parent, 2003; Jessberger et al., 2005; Lichtenwalner and Parent, 2006; Parent, 2007; Kernie and Parent, 2010). Depending on the stimulus, increased proliferation of neuronal precursors can be adaptive and has therefore been targeted as a potential therapeutic avenue (Magavi et al., 2000; Mitchell et al., 2004; DeCarolis and Eisch, 2010). However, proliferation can also be maladaptive. For example, following seizures, newborn neurons can proliferate and disperse throughout the granule cell layer as well as ectopically in the hilus (Scharfman et al., 2000; Parent et al., 2006; Koyama et al., 2012). Ectopic cells in the hilus show enhanced excitability and fire synchronously with aberrantly reorganized mossy fibers (Scharfman et al., 2000), thus potentially contributing to epileptogenesis (Parent, 2007; Koyama et al., 2012; but see also Buckmaster and Lew, 2011). However, abnormal migration of mature granule cells (without accompanying neurogenesis) has also been reported following seizures induced by intrahippocampal kainic acid (Heinrich et al., 2006), suggesting that both proliferation and dispersion are context-specific. Interestingly proliferation of neuronal precursors is also stimulated by a unilateral lesion of the perforant path, which removes the major input to the dentate gyrus and thus might be expected to reduce neuronal activity in granule cells. A dramatic increase in new granule neurons can be observed in the ipsilateral dentate gyrus at 14 days post-lesion (**Figure 5**, green cells; Perederiy et al., 2013).

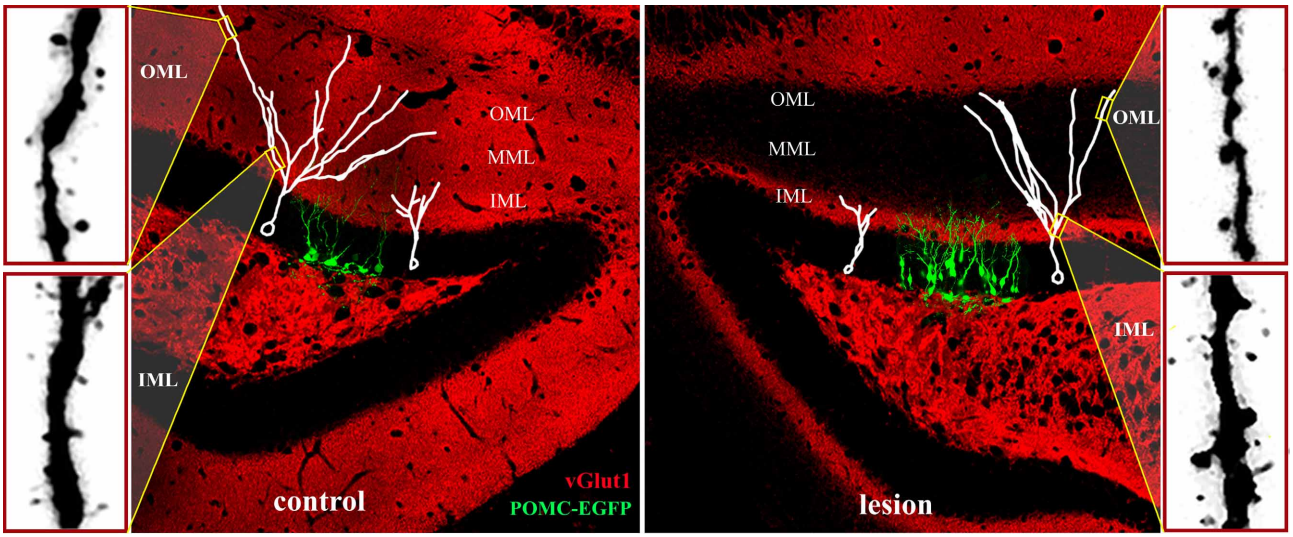

FIGURE 5 | Adult neurogenesis and synaptic integration following perforant path lesion. Data montage of dorsal hippocampus in mature mouse. **Left panel:** The morphology of 14-day-old newborn granule cells (POMC-EGFP, green), and typical maturation of newborn granule cells (white traces) shown at 14- (white cell at right in panel) and 21- (white cell at left in panel) days post-mitosis. At 14 days, dendritic arbors are limited to the inner molecular layer (IML) and lack spines, whereas dendrites of 21-day-old granule penetrate the middle (MML) and outer (OML) molecular layers and develop spines. Typical dendritic spine densities are shown at far left for the inner (IML) and outer (OML) molecular layers. **Right panel:** Unilateral perforant path lesion increases proliferation of newborn granule cells (POMC-EGFP, 14 days post-mitosis) and reduces their dendritic outgrowth (white traces). Traces of 14- (left trace) and 21- (right trace) day-old granule cells shown at 14- (left) and 21- (right) days post-lesion, respectively. Dendritic length and complexity are reduced relative to those of newborn granule cells in the contralateral hemisphere (left panel). At 21 days post-lesion *de novo* spine formation in 21-day old granule cells (far right panels) is decreased in the deafferented zone (OML), but increased in the intact inner molecular layer (IML). Note the dramatically reduced staining for a marker for glutamatergic axons (vGlut1, red) at 21 days post-lesion in the middle and outer molecular layers illustrating the absence of excitatory inputs in the denervated zone.

DENDRITIC MATURATION OF NEWBORN GRANULE CELLS

Newly-differentiated neurons in the first 1–2 weeks post-mitosis (Kempermann et al., 2004), have a distinct morphology with small cell bodies, a primary dendrite that is confined to the inner molecular layer, and an immature axon that has reached the CA3 region (Overstreet et al., 2004). Although newborn neurons in the first 1–2 weeks post-mitosis express glutamate receptors, they have yet to make synaptic contact with perforant path axons. Instead, these cells receive depolarizing GABAergic inputs (Ambrogini et al., 2004; Ge et al., 2006), consistent with a trophic role for GABA in neuronal development (Owens and Kriegstein, 2002). Over the subsequent 2 weeks, newborn granule cells extend their dendrites to the middle and outer molecular layers, develop dendritic spines, and are innervated by the glutamatergic perforant path (van Praag et al., 2002; Overstreet-Wadiche and Westbrook, 2006). This stereotyped maturation process provides an ideal opportunity to examine how newborn neurons in the adult dentate gyrus develop in the absence of their main excitatory input from the perforant path. Specifically, one can follow a cohort of new neurons labeled on the day of the injury as they extend processes and form synapses in the weeks following the injury, in this case lesion of the perforant path. As discussed above, this is a dynamic period of extracellular changes and circuit reorganization. At 14 days after a unilateral perforant path lesion—the time of maximal sprouting and reactive synaptogenesis in the deafferented molecular layer—newly developed dendrites on newborn neurons have extended into the intact inner molecular layer. However, their total dendritic length is shorter than dendrites in the contralateral hemisphere (**Figure 5**, right panel; Perederiy et al., 2013). By 21 days post-lesion, dendrites of 21-day-old neurons have penetrated into the deafferented zone, but the overall dendritic length and complexity are reduced. The dendritic complexity deficit is most pronounced in the distal segments, which at 21 days normally would be contacted by perforant path afferents. The reduced complexity of the dendritic arbor on newborn neuron post-injury is similar in degree to the post-lesion retraction of distal dendritic segments in mature cells (Vuksic et al., 2011).

LAMINA-SPECIFIC DEVELOPMENT OF DENDRITIC SPINES FOLLOWING LESION

Although dendritic arbors are reduced in total length and complexity, 21-day-old granule cells in the adult mouse develop dendritic spines in the denervated zone. This is surprising because mice have no detectable entorhino-dentate projection from the contralateral hemisphere (van Groen et al., 2002; Del Turco et al., 2003; Deller et al., 2007). Thus, the spines develop in the apparent absence of functional presynaptic input (**Figure 5**, red stain/vGlut1). Dendritic spine density, however, is lower than that in the contralateral hemisphere. The newly formed spines in the denervated outer molecular layer have postsynaptic densities, but typically lack a functional apposing presynaptic terminal (Perederiy et al., 2013). What signal substitutes for the presynaptic terminal as these new dendritic spines appear in

the denervated zone remains a mystery. One possibility is that the post-lesion environment surrounding distal dendrites provides molecular signals that substitute for glutamatergic axons in the formation of dendritic spines. The overall reduction in spine density in the denervated zone is comparable between dendrites of newborn and mature granule neurons. However, newly formed dendrites in the ipsilateral inner molecular layer show a dramatic increase in spine density relative to those in the contralateral hemisphere (**Figure 5**, lower far right panel), whereas spine density on mature granule cells is unaffected in this region (Vuksic et al., 2011; Perederiy et al., 2013). The increase in spine density in the inner molecular layer may reflect the enhanced synaptic plasticity of newborn neurons relative to mature granule cells. Immature granule cells in the normal dentate gyrus exhibit decreased LTP induction thresholds at 2–3 weeks and increased LTP amplitudes at 4–6 weeks, which can be observed even with sparse glutamatergic innervation (Schmidt-Hieber et al., 2004; Ge et al., 2007; Lemaire et al., 2012). These observations indicate that newborn neurons are preferentially targeted by sprouting axons in the intact inner molecular layer and suggest that newborn granule cells may be more responsive during circuit reorganization than mature granule cells. Such post-lesion innervation of new dendrites by sprouting homotypic axons may provide a sufficient amount of excitatory input to ensure functional integration and survival of newborn granule cells, thus partially compensating for the degenerated perforant path.

LIMITS OF PLASTICITY

The perforant path model serves as an example of CNS plasticity that incorporates many features of the injury response. Neuroplasticity in the adult brain is a complex process that involves all aspects of the neural circuit—axonal sprouting and terminal bouton turnover, reorganization of dendrites and spines, activity-dependent modulation of synaptic strength, as well as adult neurogenesis. The dynamic nature of the adult brain gives hope for endogenous repair following injury, however, the limits of neuroplasticity must be recognized in order to optimize medical treatments. Following perforant path lesion, newborn neurons showed a greater degree of structural plasticity than mature granule cells by accommodating sprouting axons in the inner molecular layer. However, circuit-appropriate reinnervation of denervated targets is essential for functional recovery, and this aspect of recovery has yet to be fully explored. For example, following ischemic lesions, newborn neurons from the expanded ipsilateral SVZ can replenish cells lost in the striatum by migrating in chains toward the site of infarction, where they differentiate into medium spiny neurons (Arvidsson et al., 2002; Parent et al., 2002). Interestingly, migration of these cells can persist for at least 1 year after stroke (Kokaia et al., 2006), suggesting that repair mechanisms can remain active long after the insult. Some evidence shows that newly differentiated neurons in the striatum grow dendrites, form synapses, and have spontaneous post-synaptic activity, indicative of functional integration (Hou et al., 2008). However, whether these cells receive appropriate inputs is unknown (Burns et al., 2009). The importance of appropriate reinnervation is perhaps best exemplified by stem cell therapy following SCI. Although promising (Bareyre, 2008; Coutts and Keirstead, 2008), grafting of neural progenitor cells around the lesion site can trigger aberrant axonal sprouting and subsequent pain hypersensitivity in the forepaw (Hofstetter et al., 2005). This issue potentially may be resolved by creating a favorable environment for stem cell maturation and functional integration, including axon guidance molecules, growth factors, and, if necessary, immune suppressors (Liu et al., 2003; Williams and Lavik, 2009). The lamina-specific reorganization following perforant path lesion suggests that effective circuit regeneration and functional recovery will require a rebalancing of the glial response and the extracellular environment, to allow new axons to find their appropriate targets and to provide a permissive scaffold for synaptogenesis.

ACKNOWLEDGMENTS

This work was supported by NIH Grant MH46613 to Gary L. Westbrook and an institutional core imaging grant from NIH (P30 NS06180).

REFERENCES

Akbik, F., Cafferty, W. B., and Strittmatter, S. M. (2012). Myelin associated inhibitors: a link between injury-induced and experience-dependent plasticity. *Exp. Neurol.* 235, 43–52.

Ambrogini, P., Lattanzi, D., Ciuffoli, S., Agostini, D., Bertini, L., Stocchi, V., et al. (2004). Morpho-functional characterization of neuronal cells at different stages of maturation in granule cell layer of adult rat dentate gyrus. *Brain Res.* 1017, 21–31.

Arvidsson, A., Collin, T., Kirik, D., Kokaia, Z., and Lindvall, O. (2002). Neuronal replacement from endogenous precursors in the adult brain after stroke. *Nat. Med.* 8, 963–970.

Bareyre, F. M. (2008). Neuronal repair and replacement in spinal cord injury. *J. Neurol. Sci.* 265, 63–72.

Bartus, K., James, N. D., Bosch, K. D., and Bradbury, E. J. (2012). Chondroitin sulphate proteoglycans: key modulators of spinal cord and brain plasticity. *Exp. Neurol.* 235, 5–17.

Bechmann, I., and Nitsch, R. (2000). Involvement of non-neuronal cells in entorhinal-hippocampal reorganization following lesions. *Ann. N.Y. Acad. Sci.* 911, 192–206.

Ben-Ari, Y., and Gho, M. (1988). Long-lasting modification of the synaptic properties of rat CA3 hippocampal neurones induced by kainic acid. *J. Physiol.* 404, 365–384.

Bosse, F. (2012). Extrinsic cellular and molecular mediators of peripheral axonal regeneration. *Cell Tissue Res.* 349, 5–14.

Bovolenta, P., and Fernaud-Espinosa, I. (2000). Nervous system proteoglycans as modulators of neurite outgrowth. *Prog. Neurobiol.* 61, 113–132.

Bozdagi, O., Nagy, V., Kwei, K. T., and Huntley, G. W. (2007). *In vivo* roles for matrix metalloproteinase-9 in mature hippocampal synaptic physiology and plasticity. *J. Neurophysiol.* 98, 334–344.

Brambilla, R., Bracchi-Ricard, V., Hu, W. H., Frydel, B., Bramwell, A., Karmally, S., et al. (2005). Inhibition of astroglial nuclear factor kB reduces inflammation and improves functional recovery after spinal cord injury. *J. Exp. Med.* 202, 145–156.

Brown, C. E., Boyd, J. D., and Murphy, T. H. (2010). Longitudinal *in vivo* imaging reveals balanced and branch-specific remodeling of mature cortical pyramidal dendritic arbors after stroke. *J. Cereb. Blood Flow Metab.* 30, 783–791.

Brown, C. E., Wong, C., and Murphy, T. H. (2008). Rapid morphologic plasticity of peri-infarct dendritic spines after focal ischemic stroke. *Stroke* 39, 1286–1291.

Buckmaster, P. S., and Lew, F. H. (2011). Rapamycin suppresses mossy fiber sprouting but not seizure frequency in a mouse model of temporal lobe epilepsy. *J. Neurosci.* 31, 2337–2347.

Burns, T. C., Verfaillie, C. M., and Low, W. C. (2009). Stem cells

for ischemic brain injury: a critical review. *J. Comp. Neurol.* 515, 125–144.

Caceres, A., and Steward, O. (1983). Dendritic reorganization in the denervated dentate gyrus of the rat following entorhinal cortical lesions: a Golgi and electron microscopic analysis. *J. Comp. Neurol.* 214, 387–403.

Chen, Z. L., Yu, W. M., and Strickland, S. (2007). Peripheral regeneration. *Annu. Rev. Neurosci.* 30, 209–233.

Christopherson, K. S., Ullian, E. M., Stokes, C. C., Mullowney, C. E., Hell, J. W., Agah, A., et al. (2005). Thrombospondins are astrocyte-secreted proteins that promote CNS synaptogenesis. *Cell* 120, 421–433.

Clusmann, H., Nitsch, R., and Heinemann, U. (1994). Long lasting functional alterations in the rat dentate gyrus following entorhinal cortex lesion: a current source density analysis. *Neuroscience* 61, 805–815.

Cotman, C., Gentry, C., and Steward, O. (1977). Synaptic replacement in the dentate gyrus after unilateral entorhinal lesion: electron microscopic analysis of the extent of replacement of synapses by the remaining entorhinal cortex. *J. Neurocytol.* 6, 455–464.

Coutts, M., and Keirstead, H. S. (2008). Stem cells for the treatment of spinal cord injury. *Exp. Neurol.* 209, 368–377.

DeCarolis, N. A., and Eisch, A. J. (2010). Hippocampal neurogenesis as a target for the treatment of mental illness: a critical evaluation. *Neuropharmacology* 58, 884–893.

Deller, T., Del Turco, D., Rappert, A., and Bechmann, I. (2007). Structural reorganization of the dentate gyrus following entorhinal denervation: species differences between rat and mouse. *Prog. Brain Res.* 163, 501–528.

Deller, T., Frotscher, M., and Nitsch, R. (1995). Morphological evidence for the sprouting of inhibitory commissural fibers in response to the lesion of the excitatory entorhinal input to the rat dentate gyrus. *J. Neurosci.* 15, 6868–6878.

Deller, T., Frotscher, M., and Nitsch, R. (1996a). Sprouting of crossed entorhinodentate fibers after a unilateral entorhinal lesion: anterograde tracing of fiber reorganization with *Phaseolus vulgaris*-leucoagglutinin (PHAL). *J. Comp. Neurol.* 365, 42–55.

Deller, T., Nitsch, R., and Frotscher, M. (1996b). Layer-specific sprouting of commissural fibres to the rat fascia dentata after unilateral entorhinal cortex lesion: a *Phaseolus vulgaris* leucoagglutinin tracing study. *Neuroscience* 71, 651–660.

Deller, T., Haas, C. A., and Frotscher, M. (2001). Sprouting in the hippocampus after entorhinal cortex lesion is layer- specific but not translaminar: which molecules may be involved? *Restor. Neurol. Neurosci.* 19, 159–167.

Deller, T., Haas, C. A., Naumann, T., Joester, A., Faissner, A., and Frotscher, M. (1997). Upregulation of astrocyte-derived tenascin-C correlates with neurite outgrowth in the rat dentate gyrus after unilateral entorhinal cortex lesion. *Neuroscience* 81, 829–846.

Del Turco, D., Woods, A. G., Gebhardt, C., Phinney, A. L., Jucker, M., Frotscher, M., et al. (2003). Comparison of commissural sprouting in the mouse and rat fascia dentata after entorhinal cortex lesion. *Hippocampus* 13, 685–699.

Diekmann, S., Ohm, T. G., and Nitsch, R. (1996). Long-lasting transneuronal changes in rat dentate granule cell dendrites after entorhinal cortex lesion. A combined intracellular injection and electron microscopy study. *Brain Pathol.* 6, 205–215.

Dityatev, A., and Fellin, T. (2008). Extracellular matrix in plasticity and epileptogenesis. *Neuron Glia Biol.* 4, 235–247.

Dityatev, A., Frischknecht, R., and Seidenbecher, C. I. (2006). Extracellular matrix and synaptic functions. *Results Probl. Cell Differ.* 43, 69–97.

Dityatev, A., Schachner, M., and Sonderegger, P. (2010a). The dual role of the extracellular matrix in synaptic plasticity and homeostasis. *Nat. Rev. Neurosci.* 11, 735–746.

Dityatev, A., Seidenbecher, C. I., and Schachner, M. (2010b). Compartmentalization from the outside: the extracellular matrix and functional microdomains in the brain. *Trends Neurosci.* 33, 503–512.

Drakew, A., Müller, M., Gähwiler, B. H., Thompson, S. M., and Frotscher, M. (1996). Spine loss in experimental epilepsy: quantitative light and electron microscopic analysis of intracellularly stained CA3 pyramidal cells in hippocampal slice cultures. *Neuroscience* 70, 31–45.

Eroglu, C. (2009). The role of astrocyte-secreted matricellular proteins in central nervous system development and function. *J. Cell Commun. Signal.* 3, 167–176.

Falo, M. C., Fillmore, H. L., Reeves, T. M., and Phillips, L. L. (2006). Matrix metalloproteinase-3 expression profile differentiates adaptive and maladaptive synaptic plasticity induced by traumatic brain injury. *J. Neurosci. Res.* 84, 768–781.

Fitch, M. T., and Silver, J. (2008). CNS injury, glial scars, and inflammation: inhibitory extracellular matrices and regeneration failure. *Exp. Neurol.* 209, 294–301.

Frischknecht, R., and Gundelfinger, E. (2012). The brain's extracellular matrix and its role in synaptic plasticity. *Adv. Exp. Med. Biol.* 970, 153–171.

Frotscher, M., Heimrich, B., and Deller, T. (1997). Sprouting in the hippocampus is layer-specific. *Trends Neurosci.* 20, 218–223.

Gage, F. H., Olejniczak, P., and Armstrong, D. M. (1988). Astrocytes are important for sprouting in the septohippocampal circuit. *Exp. Neurol.* 102, 2–13.

Gall, C., and Lynch, G. (1981). Fiber architecture of the dentate gyrus following ablation of the entorhinal cortex in rats of different ages: evidence for two forms of axon sprouting in the immature brain. *Neuroscience* 6, 903–910.

Galtrey, C. M., and Fawcett, J. W. (2007). The role of chondroitin sulfate proteoglycans in regeneration and plasticity in the central nervous system. *Brain Res. Rev.* 54, 1–18.

Ge, S., Goh, E. L., Sailor, K. A., Kitabatake, Y., Ming, G. L., and Song, H. (2006). GABA regulates synaptic integration of newly generated neurons in the adult brain. *Nature* 439, 589–593.

Ge, S., Sailor, K. A., Ming, G. L., and Song, H. (2008). Synaptic integration and plasticity of new neurons in the adult hippocampus. *J. Physiol.* 586, 3759–3765.

Ge, S., Yang, C. H., Hsu, K. S., Ming, G. L., and Song, H. (2007). A critical period for enhanced synaptic plasticity in newly generated neurons of the adult brain. *Neuron* 54, 559–566.

Giger, R. J., Hollis, E. R. I. I., and Tuszynski, M. H. (2010). Guidance molecules in axon regeneration. *Cold Spring Harb. Perspect. Biol.* 2:a001867. doi: 10.1101/cshperspect.a001867

Gottlieb, D. I., and Cowan, W. M. (1973). Autoradiographic studies of the commissural and ipsilateral association connection of the hippocampus and detentate gyrus of the rat. I. The commissural connections. *J. Comp. Neurol.* 149, 393–422.

Haas, C. A., Rauch, U., Thon, N., Merten, T., and Deller, T. (1999). Entorhinal cortex lesion in adult rats induces the expression of the neuronal chondroitin sulfate proteoglycan neurocan in reactive astrocytes. *J. Neurosci.* 19, 9953–9963.

Hailer, N. P., Grampp, A., and Nitsch, R. (1999). Proliferation of microglia and astrocytes in the dentate gyrus following entorhinal cortex lesion: a quantitative bromodeoxyuridine-labelling study. *Eur. J. Neurosci.* 11, 3359–3364.

Heinrich, C., Nitta, N., Flubacher, A., Müller, M., Fahrner, A., Kirsch, M., et al. (2006). Reelin deficiency and displacement of mature neurons, but not neurogenesis, underlie the formation of granule cell dispersion in the epileptic hippocampus. *J. Neurosci.* 26, 4701–4713.

Hickmott, P. W., and Steen, P. A. (2005). Large-scale changes in dendritic structure during reorganization of adult somatosensory cortex. *Nat. Neurosci.* 8, 140–142.

Hill, C. E., Beattie, M. S., and Bresnahan, J. C. (2001). Degeneration and sprouting of identified descending supraspinal axons after contusive spinal cord injury in the rat. *Exp. Neurol.* 171, 153–169.

Hjorth-Simonsen, A., and Jeune, B. (1972). Origin and termination of the hippocampal perforant path in the rat studied by silver impregnation. *J. Comp. Neurol.* 144, 215–232.

Hofer, S. B., Mrsic-Flogel, T. D., Bonhoeffer, T., and Hübener, M. (2006). Lifelong learning: ocular dominance plasticity in mouse visual cortex. *Curr. Opin. Neurobiol.* 16, 451–459.

Hofstetter, C. P., Holmström, N. A., Lilja, J. A., Schweinhardt, P., Hao, J., Spenger, C., et al. (2005). Allodynia limits the usefulness of intraspinal neural stem cell grafts; directed differentiation improves outcome. *Nat. Neurosci.* 8, 346–353.

Hosp, J. A., and Luft, A. R. (2011). Cortical plasticity during motor learning and recovery after ischemic stroke. *Neural Plast.* 2011:871296. doi: 10.1155/2011/871296

Hou, S. W., Wang, Y. Q., Xu, M., Shen, D. H., Wang, J. J., Huang, F., et al. (2008). Functional integration of newly generated neurons into striatum after cerebral ischemia in the adult rat brain. *Stroke* 39, 2837–2844.

Huntley, G. W. (2012). Synaptic circuit remodelling by matrix metalloproteinases in health and disease. *Nat. Rev. Neurosci.* 13, 743–757.

Jansen, L. A., Uhlmann, E. J., Crino, P. B., Gutmann, D. H., and Wong, M. (2005). Epileptogenesis and reduced inward rectifier potassium current in tuberous sclerosis complex-1-deficient astrocytes. *Epilepsia* 46, 1871–1880.

Jessberger, S., Römer, B., Babu, H., and Kempermann, G. (2005). Seizures induce proliferation and dispersion of doublecortin-positive hippocampal progenitor cells. *Exp. Neurol.* 196, 342–351.

Kempermann, G., Jessberger, S., Steiner, B., and Kronenberg, G. (2004). Milestones of neuronal development in the adult hippocampus. *Trends Neurosci.* 27, 447–452.

Kernie, S. G., and Parent, J. M. (2010). Forebrain neurogenesis after focal Ischemic and traumatic brain injury. *Neurobiol. Dis.* 37, 267–274.

Kim, B. G., Dai, H. N., McAtee, M., Vicini, S., and Bregman, B. S. (2006). Remodeling of synaptic structures in the motor cortex following spinal cord injury. *Exp. Neurol.* 198, 401–415.

Knowles, W. D. (1992). Normal anatomy and neurophysiology of the hippocampal formation. *J. Clin. Neurophysiol.* 9, 252–263.

Koistinaho, M., Lin, S., Wu, X., Esterman, M., Koger, D., Hanson, J., et al. (2004). Apolipoprotein E promotes astrocyte colocalization and degradation of deposited amyloid-beta peptides. *Nat. Med.* 10, 719–726.

Kokaia, Z., Thored, P., Arvidsson, A., and Lindvall, O. (2006). Regulation of stroke-induced neurogenesis in adult brain—recent scientific progress. *Cereb. Cortex* 16(Suppl 1), i162–i167.

Koyama, R., Tao, K., Sasaki, T., Ichikawa, J., Miyamoto, D., Muramatsu, R., et al. (2012). GABAergic excitation after febrile seizures induces ectopic granule cells and adult epilepsy. *Nat. Med.* 18, 1271–1278.

Lemaire, V., Tronel, S., Montaron, M. F., Fabre, A., Dugast, E., and Abrous, D. N. (2012). Long-lasting plasticity of hippocampal adult-born neurons. *J. Neurosci.* 32, 3101–3108.

Leranth, C., and Hajszan, T. (2007). Extrinsic afferent systems to the dentate gyrus. *Prog. Brain Res.* 163, 63–84.

Lichtenwalner, R. J., and Parent, J. M. (2006). Adult neurogenesis and the ischemic forebrain. *J. Cereb. Blood Flow Metab.* 26, 1–20.

Liu, C. Y., Apuzzo, M. L., and Tirrell, D. A. (2003). Engineering of the extracellular matrix: working toward neural stem cell programming and neurorestoration–concept and progress report. *Neurosurgery* 52, 1154–1165.

Liu, J., Solway, K., Messing, R. O., and Sharp, F. R. (1998). Increased neurogenesis in the dentate gyrus after transient global ischemia in gerbils. *J. Neurosci.* 18, 7768–7778.

Liu, K., Tedeschi, A., Park, K. K., and He, Z. (2011). Neuronal intrinsic mechanisms of axon regeneration. *Annu. Rev. Neurosci.* 34, 131–152.

Lledo, P. M., Alonso, M., and Grubb, M. S. (2006). Adult neurogenesis and functional plasticity in neuronal circuits. *Nat. Rev. Neurosci.* 7, 179–193.

Lynch, G., Matthews, D. A., Mosko, S., Parks, T., and Cotman, C. (1972). Induced acetylcholinesterase-rich layer in rat dentate gyrus following entorhinal lesions. *Brain Res.* 42, 311–318.

Magavi, S. S., Leavitt, B. R., and Macklis, J. D. (2000). Induction of neurogenesis in the neocortex of adult mice. *Nature* 405, 951–955.

Maier, I. C., and Schwab, M. E. (2006). Sprouting, regeneration and circuit formation in the injured spinal cord: factors and activity. *Philos. Trans. R. Soc. Lond. B Biol. Sci.* 361, 1611–1634.

Marrone, D. F., LeBoutillier, J. C., and Petit, T. L. (2004). Comparative analyses of synaptic densities during reactive synaptogenesis in the rat dentate gyrus. *Brain Res.* 996, 19–30.

Matthews, D. A., Cotman, C., and Lynch, G. (1976a). An electron microscopic study of lesion-induced synaptogenesis in the dentate gyrus of the adult rat. I. Magnitude and time course of degeneration. *Brain Res.* 115, 1–21.

Matthews, D. A., Cotman, C., and Lynch, G. (1976b). An electron microscopic study of lesion-induced synaptogenesis in the dentate gyrus of the adult rat. II. Reappearance of morphologically normal synaptic contacts. *Brain Res.* 115, 23–41.

Mayer, J., Hamel, M. G., and Gottschall, P. E. (2005). Evidence for proteolytic cleavage of brevican by the ADAMTSs in the dentate gyrus after excitotoxic lesion of the mouse entorhinal cortex. *BMC Neurosci.* 6:52. doi: 10.1186/1471-2202-6-52

Milligan, E. D., and Watkins, L. R. (2009). Pathological and protective roles of glia in chronic pain. *Nat. Rev. Neurosci.* 10, 23–36.

Mitchell, B. D., Emsley, J. G., Magavi, S. S., Arlotta, P., and Macklis, J. D. (2004). Constitutive and induced neurogenesis in the adult mammalian brain: manipulation of endogenous precursors toward CNS repair. *Dev. Neurosci.* 26, 101–117.

Mostany, R., and Portera-Cailliau, C. (2011). Absence of large-scale dendritic plasticity of layer 5 pyramidal neurons in peri-infarct cortex. *J. Neurosci.* 31, 1734–1738.

Nadler, J. V., Cotman, C. W., and Lynch, G. S. (1977a). Histochemical evidence of altered development of cholinergic fibers in the rat dentate gyrus following lesions. I. Time course after complete unilateral entorhinal lesion at various ages. *J. Comp. Neurol.* 171, 561–587.

Nadler, J. V., Cotman, C. W., Paoletti, C., and Lynch, G. S. (1977b). Histochemical evidence of altered development of cholinergic fibers in the rat dentate gyrus following lesions. II. Effects of partial entorhinal and simultaneous multiple lesions. *J. Comp. Neurol.* 171, 589–604.

Nagy, V., Bozdagi, O., Matynia, A., Balcerzyk, M., Okulski, P., Dzwonek, J., et al. (2006). Matrix metalloproteinase-9 is required for hippocampal late-phase long-term potentiation and memory. *J. Neurosci.* 26, 1923–1934.

Neumann, H., Kotter, M. R., and Franklin, R. J. (2009). Debris clearance by microglia: an essential link between degeneration and regeneration. *Brain* 132, 288–295.

Overstreet, L. S., Hentges, S. T., Bumaschny, V. F., de Souza, F. S., Smart, J. L., Santangelo, A. M., et al. (2004). A transgenic marker for newly born granule cells in dentate gyrus. *J. Neurosci.* 24, 3251–3259.

Overstreet-Wadiche, L. S., and Westbrook, G. L. (2006). Functional maturation of adult-generated granule cells. *Hippocampus* 16, 208–215.

Owens, D. F., and Kriegstein, A. R. (2002). Is there more to GABA than synaptic inhibition? *Nat. Rev. Neurosci.* 3, 715–727.

Parent, J. M. (2003). Injury-induced neurogenesis in the adult mammalian brain. *Neuroscientist* 9, 261–272.

Parent, J. M. (2007). Adult neurogenesis in the intact and epileptic dentate gyrus. *Prog. Brain Res.* 163, 529–540.

Parent, J. M., Elliott, R. C., Pleasure, S. J., Barbaro, N. M., and Lowenstein, D. H. (2006). Aberrant seizure-induced neurogenesis in experimental temporal lobe epilepsy. *Ann. Neurol.* 59, 81–91.

Parent, J. M., Vexler, Z. S., Gong, C., Derugin, N., and Ferriero, D. M. (2002). Rat forebrain neurogenesis and striatal neuron replacement after focal stroke. *Ann. Neurol.* 52, 802–813.

Parnavelas, J. G., Lynch, G., Brecha, N., Cotman, C. W., and Globus, A. (1974). Spine loss and regrowth in hippocampus following deafferentation. *Nature* 248, 71–73.

Perederiy, J. V., Luikart, B. W., Washburn, E. K., Schnell, E., and Westbrook, G. L. (2013). Neural injury alters proliferation and integration of adult-generated neurons in the dentate gyrus. *J. Neurosci.* (in press).

Phinney, A. L., Calhoun, M. E., Woods, A. G., Deller, T., and Jucker, M. (2004). Stereological analysis of the reorganization of the dentate gyrus following entorhinal cortex lesion in mice. *Eur. J. Neurosci.* 19, 1731–1740.

Raineteau, O., and Schwab, M. E. (2001). Plasticity of motor systems after incomplete spinal cord injury. *Nat. Rev. Neurosci.* 2, 263–273.

Ramirez, J. J. (2001). The role of axonal sprouting in functional reorganization after CNS injury: lessons from the hippocampal formation. *Restor. Neurol. Neurosci.* 19, 237–262.

Reeves, T. M., and Steward, O. (1988). Changes in the firing properties of neurons in the dentate gyrus with denervation and reinnervation: implications for behavioral recovery. *Exp. Neurol.* 102, 37–49.

Rothstein, J. D., Dykes-Hoberg, M., Pardo, C. A., Bristol, L. A., Jin, L., Kunci, R. W., et al. (1996). Knockout of glutamate transporters reveals a major role for astroglial transport in excitotoxicity and clearance of glutamate. *Neuron* 16, 675–686.

Scharfman, H. E., Goodman, J. H., and Sollas, A. L. (2000). Granule-like neurons at the hilar/CA3 border after status epilepticus and their synchrony with area CA3 pyramidal cells: functional implications of seizure-induced neurogenesis. *J. Neurosci.* 20, 6144–6158.

Schauwecker, P. E., and McNeill, T. H. (1996). Dendritic remodeling of dentate granule cells following a combined entorhinal cortex/fimbria fornix lesion. *Exp. Neurol.* 141, 145–153.

Schmidt-Hieber, C., Jonas, P., and Bischofberger, J. (2004). Enhanced synaptic plasticity in newly generated granule cells of the adult hippocampus. *Nature* 429, 184–187.

Silver, J., and Miller, J. H. (2004). Regeneration beyond the glial scar. *Nat. Rev. Neurosci.* 5, 146–156.

Simbürger, E., Plaschke, M., Fritschy, J. M., and Nitsch, R. (2001).

Localization of two major GABA(A) receptor subunits in the dentate gyrus of the rat and cell type-specific up-regulation following entorhinal cortex lesion. *Neuroscience* 102, 789–803.

Simbürger, E., Plaschke, M., Kirsch, J., and Nitsch, R. (2000). Distribution of the receptor-anchoring protein gephyrin in the rat dentate gyrus and changes following entorhinal cortex lesion. *Cereb. Cortex* 10, 422–432.

Sofroniew, M. V. (2009). Molecular dissection of reactive astrogliosis and glial scar formation. *Trends Neurosci.* 32, 638–647.

Sofroniew, M. V., and Vinters, H. V. (2010). Astrocytes: biology and pathology. *Acta Neuropathol.* 119, 7–35.

Soriano, E., and Frotscher, M. (1994). Mossy cells of the rat fascia dentata are glutamate-immunoreactive. *Hippocampus* 4, 65–69.

Steward, O. (1976). Reinnervation of dentate gyrus by homologous afferents following entorhinal cortical lesions in adult rats. *Science* 194, 426–428.

Steward, O. (1992). Signals that induce sprouting in the central nervous system: sprouting is delayed in a strain of mouse exhibiting delayed axonal degeneration. *Exp. Neurol.* 118, 340–351.

Steward, O., Cotman, C. W., and Lynch, G. S. (1973). Re-establishment of electrophysiologically functional entorhinal cortical input to the dentate gyrus deafferented by ipsilateral entorhinal lesions: innervation by the contralateral entorhinal cortex. *Exp. Brain Res.* 18, 396–414.

Steward, O., and Messenheimer, J. A. (1978). Histochemical evidence for a postlesion reorganization of cholinergic afferents in the hippocampal formation of the mature cat. *J. Comp. Neurol.* 178, 697–710.

Steward, O., and Vinsant, S. L. (1983). The process of reinnervation in the dentate gyrus of the adult rat: a quantitative electron microscopic analysis of terminal proliferation and reactive synaptogenesis. *J. Comp. Neurol.* 214, 370–386.

Sutula, T. P., and Dudek, F. E. (2007). Unmasking recurrent excitation generated by mossy fiber sprouting in the epileptic dentate gyrus: an emergent property of a complex system. *Prog. Brain Res.* 163, 541–563.

Swanson, R. A., Ying, W., and Kauppinen, T. M. (2004). Astrocyte influences on ischemic neuronal death. *Curr. Mol. Med.* 4, 193–205.

Takano, T., Kang, J., Jaiswal, J. K., Simon, S. M., Lin, J. H., Yu, Y., et al. (2005). Receptor-mediated glutamate release from volume sensitive channels in astrocytes. *Proc. Natl. Acad. Sci. U.S.A.* 102, 16466–16471.

Tashiro, A., Makino, H., and Gage, F. H. (2007). Experience-specific functional modification of the dentate gyrus through adult neurogenesis: a critical period during an immature stage. *J. Neurosci.* 27, 3252–3259.

Tian, G. F., Azmi, H., Takano, T., Xu, Q., Peng, W., Lin, J., et al. (2005). An astrocytic basis of epilepsy. *Nat. Med.* 11, 973–981.

Tuszynski, M. H., and Steward, O. (2012). Concepts and methods for the study of axonal regeneration in the CNS. *Neuron* 74, 777–791.

Ullian, E. M., Christopherson, K. S., and Barres, B. A. (2004). Role for glia in synaptogenesis. *Glia* 47, 209–216.

van Groen, T., Kadish, I., and Wyss, J. M. (2002). Species differences in the projections from the entorhinal cortex to the hippocampus. *Brain Res. Bull.* 57, 553–556.

van Groen, T., Miettinen, P., and Kadish, I. (2003). The entorhinal cortex of the mouse: organization of the projection to the hippocampal formation. *Hippocampus* 13, 133–149.

van Praag, H., Kempermann, G., and Gage, F. H. (1999). Running increases cell proliferation and neurogenesis in the adult mouse dentate gyrus. *Nat. Neurosci.* 2, 266–270.

van Praag, H., Schinder, A. F., Christie, B. R., Toni, N., Palmer, T. D., and Gage, F. H. (2002). Functional neurogenesis in the adult hippocampus. *Nature* 415, 1030–1034.

Vargas, M. E., and Barres, B. A. (2007). Why is Wallerian degeneration in the CNS so slow? *Annu. Rev. Neurosci.* 30, 153–179.

Vuksic, M., Del Turco, D., Vlachos, A., Schuldt, G., Müller, C. M., Schneider, G., et al. (2011). Unilateral entorhinal denervation leads to long-lasting dendritic alterations of mouse hippocampal granule cells. *Exp. Neurol.* 230, 176–185.

Warren, K. M., Reeves, T. M., and Phillips, L. L. (2012). MT5-MMP, ADAM-10, and N-cadherin act in concert to facilitate synapse reorganization after traumatic brain injury. *J. Neurotrauma.* 29, 1922–1940.

Wilhelmsson, U., Bushong, E. A., Price, D. L., Smarr, B. L., Phung, V., Terada, M., et al. (2006). Redefining the concept of reactive astrocytes as cells that remain within their unique domains upon reaction to injury. *Proc. Natl. Acad. Sci. U.S.A.* 103, 17513–17518.

Williams, C. A., and Lavik, E. B. (2009). Engineering the CNS stem cell microenvironment. *Regen. Med.* 4, 865–877.

Xu, J., Xiao, N., and Xia, J. (2010). Thrombospondin 1 accelerates synaptogenesis in hippocampal neurons through neuroligin 1. *Nat. Neurosci.* 13, 22–24.

Zeng, L. H., Xu, L., Rensing, N. R., Sinatra, P. M., Rothman, S. M., and Wong, M. (2007). Kainate seizures cause acute dendritic injury and actin depolymerization *in vivo*. *J. Neurosci.* 27, 11604–11613.

Zimmer, J., Laurberg, S., and Sunde, N. (1986). Non-cholinergic afferents determine the distribution of the cholinergic septohippocampal projection: a study of the AChE staining pattern in the rat fascia dentata and hippocampus after lesions, X-irradiation, and intracerebral grafting. *Exp. Brain Res.* 64, 158–168.

Zuo, J., Hernandez, Y. J., and Muir, D. (1998). Chondroitin sulfate proteoglycan with neurite-inhibiting activity is up-regulated following peripheral nerve injury. *J. Neurobiol.* 34, 41–54.

Conflict of Interest Statement: The authors declare that the research was conducted in the absence of any commercial or financial relationships that could be construed as a potential conflict of interest.

Received: 23 November 2012; paper pending published: 10 December 2012; accepted: 27 January 2013; published online: 18 February 2013.

Citation: Perederiy JV and Westbrook GL (2013) Structural plasticity in the dentate gyrus- revisiting a classic injury model. Front. Neural Circuits 7:17. doi: 10.3389/fncir.2013.00017